

Revised Bedrock Topography and Characterization of Quaternary Sediments in the Fort McMurray Region, Northeastern Alberta

AER/AGS Report 101

Revised Bedrock Topography and Characterization of Quaternary Sediments in the Fort McMurray Region, Northeastern Alberta

D.J. Utting and L.D. Andriashek

Alberta Energy Regulator
Alberta Geological Survey

December 2020

©Her Majesty the Queen in Right of Alberta, 2020
ISBN 978-1-4601-4515-9

The Alberta Energy Regulator / Alberta Geological Survey (AER/AGS), its employees and contractors make no warranty, guarantee or representation, express or implied, or assume any legal liability regarding the correctness, accuracy, completeness or reliability of this publication. Any references to proprietary software and/or any use of proprietary data formats do not constitute endorsement by AER/AGS of any manufacturer's product.

If you use information from this publication in other publications or presentations, please acknowledge the AER/AGS. We recommend the following reference format:

Utting, D.J. and Andriashek, L.D. (2020): Revised bedrock topography and characterization of Quaternary sediments in the Fort McMurray region, northeastern Alberta; Alberta Energy Regulator / Alberta Geological Survey, AER/AGS Report 101, 171 p.

Published December 2020 by:

Alberta Energy Regulator
Alberta Geological Survey
4th Floor, Twin Atria Building
4999 – 98th Avenue
Edmonton, AB T6B 2X3
Canada

Tel: 780.638.4491
Fax: 780.422.1459
Email: AGS-Info@aer.ca
Website: www.ags.aer.ca

Contents

Acknowledgements.....	ix
Abstract.....	x
1 Introduction.....	1
2 Study Area.....	1
2.1 Physiography.....	1
2.2 Bedrock Geology.....	2
2.3 Cenozoic and Quaternary Geology.....	3
2.3.1 Buried Bedrock Valleys and Channels.....	4
2.3.2 Quaternary History.....	4
2.3.3 Glaciotectonism.....	5
2.4 Previous Quaternary Stratigraphic Studies.....	8
3 Methodology.....	10
4 Results.....	11
4.1 Nature of Bedrock Contact.....	11
4.1.1 Contact Type I: Sharp Till-Bedrock Interface.....	11
4.1.2 Contact Type II: Glaciogenic Deformation of Bedrock Interface.....	12
4.1.3 Contact Type III: Water-Laid Sediments at the Sediment-Bedrock Interface.....	13
4.2 Establishing the Bedrock Contact from Geophysical Logs.....	13
4.3 Glaciotectonically Displaced and Transported Bedrock (Rafts) within the Quaternary Succession.....	17
4.4 Delineation of Bedrock Valleys and Channels.....	24
4.5 Compilation of Bedrock Top Picks and Bedrock Topography.....	24
4.6 Till Composition, Differentiation, and Correlation.....	29
4.6.1 Representative Core: SUNCOR FIREBAG 10-31-94-5W4.....	29
4.6.2 Representative Core: CVE TLK A12 FIREBAG 12-12-95-3W4.....	32
5 Quaternary Stratigraphic Domains.....	32
5.1 Muskeg Mountain Domain.....	33
5.2 Firebag River Domain.....	37
5.3 Steepbank Plain Domain.....	38
5.4 MacKay Plain Domain.....	38
5.5 Firebag Hills Domain.....	42
5.6 Dover and Kearl Lake Plains Domain.....	45
6 Summary.....	45
7 References.....	47
Appendix 1 – Core and Drill Cutting Descriptions.....	50
Core Descriptions.....	51
Quaternary Sediments Examined in Drill Cuttings.....	164

Tables

Table 1. Quaternary stratigraphic units in the Cold Lake area, Alberta.....	9
Table 2. Stratigraphic units in Athabasca Oil Sands Area.....	9
Table 3. Till units in the Waterways and Bitumount map areas.....	9
Table 4. Correlation coefficients for selected elements, comparing analysis from X-ray fluorescence and inductively coupled plasma–mass spectrometry geochemical analyses.....	29
Table 5. Possible correlations between till units in core SUNCOR FIREBAG 10-31-94-5W4 and previous stratigraphic nomenclature.....	34
Table 6. Examined cores that did not contain Quaternary sediments.....	163

Figures

Figure 1. Geographic and physiographic features in the study area, northeastern Alberta.....	2
Figure 2. Three-dimensional rendering of the bedrock geology in the study area, northeastern Alberta.....	3
Figure 3. Thalwegs of buried bedrock valleys and channels within the study area, northeastern Alberta. ..	5
Figure 4. Location of Alberta Geological Survey studies and general location of surface tills and formations	6
Figure 5. LiDAR image of the Fort Hills area with shaded relief, northeastern Alberta.....	7
Figure 6. Location of coreholes with cores that were examined in this study, northeastern Alberta.	10
Figure 7. Locations of coreholes with three types of bedrock contacts in cores, northeastern Alberta.	12
Figure 8. Core with sharp contact between till and bedrock.....	13
Figure 9. Core of disturbed or contorted shale beneath the bedrock contact.....	14
Figure 10. Silt overlying oil sand in corehole IMP 12-23-99-4W4.	15
Figure 11. Example of logs where sandy till overlies Clearwater Formation shale.....	16
Figure 12. Example of logs where till rests on Grand Rapids Formation siltstone.....	18
Figure 13. Example of logs where till containing a high content of bitumen becomes progressively less concentrated up-hole from the contact with oil sand	19
Figure 14. Location of coreholes with displaced bedrock (rafts) evident in cores, northeastern Alberta...	20
Figure 15. Example of bedrock raft shown in core logs	21
Figure 16. Displaced siltstone overlying dark grey till in corehole TLK FIREBAG 10-4-96-4W4.....	22
Figure 17. a) LiDAR image with shaded relief of the area previously interpreted to be a glacial tear fault, northeastern Alberta. b) West to east cross-section in the area previously interpreted to be a glacial tear fault.....	23
Figure 18. Airborne electromagnetic surveys used to update the Andriashek (2019) bedrock valley and channel thalweg map, northeastern Alberta	25
Figure 19. West-east cross-section across the Alder channel on the MacKay Plain, northeastern Alberta	26
Figure 20. Locations of bedrock top picks, northeastern Alberta	27
Figure 21. a) Bedrock topography and b) sediment thickness maps of the study area, northeastern Alberta	28
Figure 22. Logs for corehole SUNCOR FIREBAG 10-31-94-5W4.....	30
Figure 23. Logs for corehole CVE TLK A12 FIREBAG 12-12-95-3W4	31
Figure 24. Similarity in appearance of unit 3 and unit 2 tills within CVE TLK A12 FIREBAG 12-12-95- 3W4 core	33
Figure 25. Map of Quaternary stratigraphic domains within the study area, northeastern Alberta	34
Figure 26. South-north cross-section centred at corehole SUNCOR FIREBAG 10-31-94-5W4 on Muskeg Mountain, northeastern Alberta.....	35
Figure 27. Location of SUNCOR FIREBAG 10-31-94-5W4 corehole in relation to glacial ice-flow patterns on Muskeg Mountain, northeastern Alberta	36
Figure 28. Section of bitumen-rich glacial sand overlying pink stratified sediments above grey till along Firebag River, northeastern Alberta.....	37
Figure 29. Location of Firebag River section and cross-sections D–D' and F–F' in relation to glacial ice- flow patterns, northeastern Alberta	39
Figure 30. West-east cross-section north of the Firebag River on the Embarras Plain, northeastern Alberta	40
Figure 31. West-east cross-section in the Steepbank Plain domain highlighting the occurrence of sand resting on sandstone of the Grand Rapids Formation, northeastern Alberta.....	41
Figure 32. Example of sandy surface till in the Firebag Hills domain in core IMP 07 OV FIREBAG 7-1- 99-4W4.....	42
Figure 33. Logs for corehole IMP 07 OV FIREBAG 7-1-99-4W4 in the Firebag Hills domain	43

Figure 34. North-south cross-section on the Johnson Lake Plain and Firebag Hills, northeastern Alberta	44
Figure 35. Logs for well UTS FT HILLS 15-15-98-9W4	51
Figure 36. Photograph of core interval from well UTS FT HILLS 15-15-98-9W4.....	52
Figure 37. Photograph of core interval from well UTS FT HILLS 15-15-98-9W4.....	53
Figure 38. Litholog for well FHEC OBSP-20 FT HILLS 15-17-98-9W4.....	54
Figure 39. Photograph of core interval from well FHEC OBSP-20 FT HILLS 15-17-98-9W4.....	55
Figure 40. Photograph of core interval from well FHEC OBSP-20 FT HILLS 15-17-98-9W4.....	56
Figure 41. Logs for well CNRL C12-241 HORIZON 8-13-98-12W4	57
Figure 42. Photograph of core interval from well CNRL C12-241 HORIZON 8-13-98-12W4.....	58
Figure 43. Logs for well CNRL C12-239 HORIZON 10-20-98-11W4	59
Figure 44. Photograph of core interval from well CNRL C12-239 HORIZON 10-20-98-11W4.....	60
Figure 45. Logs for well SILVERBIRCH 2-5-101-7W4.....	61
Figure 46. Logs for well SILVERBIRCH 2-15-100-11W4.....	62
Figure 47. Logs for well SILVERBIRCH 2-33-100-11W4.....	63
Figure 48. Photograph of core interval from well SILVERBIRCH 2-33-100-11W4.....	64
Figure 49. Logs for well SCL JP213-CR6049 JACKPINE 13-19-96-8W4	65
Figure 50. Logs for well PC 12 DOVER 14-7-93-12W4	66
Figure 51. Photograph of core interval from well PC 12 DOVER 14-7-93-12W4	67
Figure 52. Log for well SUNCOR FIREBAG 10-23-93-5W4	68
Figure 53. Log for well SUNCOR LEWIS 9-23-92-07W4.....	69
Figure 54. Photograph of core interval from well SUNCOR LEWIS 9-23-92-07W4.....	70
Figure 55. Log for well IMP OIL RES V M68 ASPEN 2-24-93-7W4	71
Figure 56. Photograph of core interval from well IMP OIL RES V M68 ASPEN 2-24-93-7W4.....	72
Figure 57. Logs for well SUNCOR FIREBAG 10-31-94-5W4.....	73
Figure 58. Photograph of core interval from well SUNCOR FIREBAG 10-31-94-5W4.....	74
Figure 59. Photograph of core interval from well SUNCOR FIREBAG 10-31-94-5W4.....	75
Figure 60. Photograph of core interval from well SUNCOR FIREBAG 10-31-94-5W4.....	76
Figure 61. Logs for well SUNCOR OB150 FIREBAG 14-34-94-6W4	77
Figure 62. Logs for well SUNCOR FIREBAG 5-3-95-6W4.....	78
Figure 63. Photograph of core interval from well SUNCOR FIREBAG 5-3-95-6W4.....	79
Figure 64. Logs for well SUNCOR OB182 FIREBAG 1-9-95-6W4	80
Figure 65. Photograph of core interval from well SUNCOR OB182 FIREBAG 1-9-95-6W4	81
Figure 66. Photograph of core interval from well SUNCOR OB182 FIREBAG 1-9-95-6W4	82
Figure 67. Logs for well SUNCOR FIREBAG 7-32-95-6W4.....	83
Figure 68. Logs for well HUSKY SUNRISE 7-2-96-6W4.....	84
Figure 69. Photograph of core interval from well HUSKY SUNRISE 7-2-96-6W4.....	85
Figure 70. Photograph of core interval from well HUSKY SUNRISE 7-2-96-6W4.....	86
Figure 71. Logs for well SUNCOR FIREBAG 10-4-96-5W4.....	87
Figure 72. Photograph of core interval from well SUNCOR FIREBAG 10-4-96-5W4.....	88
Figure 73. Photograph of core interval from well SUNCOR FIREBAG 10-4-96-5W4.....	89
Figure 74. Logs for well SUNCOR FIREBAG 12-28-96-5W4.....	90
Figure 75. Photograph of core interval from well SUNCOR FIREBAG 12-28-96-5W4.....	91
Figure 76. Photograph of core interval from well SUNCOR FIREBAG 12-28-96-5W4.....	92
Figure 77. Logs for well SUNCOR FIREBAG 12-33-96-5W4.....	93
Figure 78. Photograph of core interval from well SUNCOR FIREBAG 12-33-96-5W4.....	94
Figure 79. Logs for well TLK 10-31-95-4W4	95
Figure 80. Photograph of core interval from well TLK 10-31-95-4W4.	96
Figure 81. Log for well CVE TLK FIREBAG 10-5-96-4W4.....	97
Figure 82. Photograph of core interval from well CVE TLK FIREBAG 10-5-96-4W4	98
Figure 83. Logs for well TLK 10-11-96-4W4	99

Figure 84. Photograph of core interval from well TLK 10-11-96-4W4	100
Figure 85. Logs for well TLK FIREBAG 10-4-96-4W4	101
Figure 86. Photograph of core interval from well TLK FIREBAG 10-4-96-4W4	102
Figure 87. Photograph of core interval from well TLK FIREBAG 10-4-96-4W4	103
Figure 88. Logs for well CVE TLK 9-31-95-3W4	104
Figure 89. Photograph of core interval from well CVE TLK 9-31-95-3W4	105
Figure 90. Photograph of core interval from well CVE TLK 9-31-95-3W4	106
Figure 91. Logs for well CVE TLK 11-32-95-3W4	107
Figure 92. Logs for well CVE TLK A2 FIREBAG 2-27-95-3W4	108
Figure 93. Photograph of core interval from well CVE TLK A2 FIREBAG 2-27-95-3W4	109
Figure 94. Logs for well CVE TLK ST1 FIREBAG 12-29-95-3W4	110
Figure 95. Photograph of core interval from well CVE TLK ST1 FIREBAG 12-29-95-3W4.....	111
Figure 96. Logs for well CVE TLK D12 FIREBAG 12-21-95-3W4	112
Figure 97. Photograph of core interval from well CVE TLK D12 FIREBAG 12-21-95-3W4	113
Figure 98. Logs for well CVE TLK C2 FIREBAG 2-14-95-3W4.	114
Figure 99. Photograph of core interval from well CVE TLK C2 FIREBAG 2-14-95-3W4.....	115
Figure 100. Logs for well CVE TLK A12 FIREBAG 12-10-95-3W4	116
Figure 101. Photograph of core interval from well CVE TLK A12 FIREBAG 12-10-95-3W4	117
Figure 102. Logs for well OQI SASK WALLACE CREEK 10-18-96-2W4.	118
Figure 103. Photograph of core interval from well OQI SASK WALLACE CREEK 10-18-96-2W4	119
Figure 104. Logs for well Shell 8 ATHAE OV 5-26-95-1W4	120
Figure 105. Photograph of core interval from well Shell 8 ATHAE OV 5-26-95-1W4.....	121
Figure 106. Logs for well CVE TLK A12 FIREBAG 12-12-95-3W4	122
Figure 107. Photograph of core interval from well CVE TLK A12 FIREBAG 12-12-95-3W4	123
Figure 108. Logs for well CVE TLK B10 FIREBAG 10-11-95-3W4.....	124
Figure 109. Photograph of core interval from well CVE TLK B10 FIREBAG 10-11-95-3W4.....	125
Figure 110. Photograph of core interval from well CVE TLK B10 FIREBAG 10-11-95-3W4.....	126
Figure 111. Logs for well CVE TLK B12 FIREBAG 12-11-95-3W4.....	127
Figure 112. Photograph of core interval from well CVE TLK B12 FIREBAG 12-11-95-3W4.....	128
Figure 113. Logs for well CVE TLK FIREBAG 2-27-94-3W4.	129
Figure 114. Photograph of core interval from well CVE TLK FIREBAG 2-27-94-3W4	130
Figure 115. Logs for well CVE TLK A13 FIREBAG 13-30-94-2W4.	131
Figure 116. Logs for well SHELL 11 ATHAE OV 11-31-97-1W4	132
Figure 117. Logs for well SILVERBIRCH AUDET 12-12-98-3W4	133
Figure 118. Logs for well IMP 1024302 FIREBAG 13-23-98-4W4.....	134
Figure 119. Logs for well IMP 07 OV FIREBAG 7-1-99-4W4	135
Figure 120. Photograph of core interval from well IMP 07 OV FIREBAG 7-1-99-4W4	136
Figure 121. Logs for well IMP 1024327 FIREBAG 13-11-99-4W4.....	137
Figure 122. Logs for well IMP 3-23-99-4W4.....	138
Figure 123. Logs for well IMP 12-23-99-4W4.....	139
Figure 124. Photograph of core interval from well IMP 12-23-99-4W4.....	140
Figure 125. Logs for well IMP 1-31-99-4W4.....	141
Figure 126. Logs for well IMP 1-34-99-4W4.....	142
Figure 127. Logs for well VCI FIREBAG EAST 6-21-99-5W4.....	143
Figure 128. Logs for well VCI FIREBAG EAST 7-22-99-5W4.....	144
Figure 129. Photograph of core interval from well VCI FIREBAG EAST 7-22-99-5W4	145
Figure 130. Logs for well VCI FIREBAG EAST 3-25-99-5W4	146
Figure 131. Photograph of core interval from well VCI FIREBAG EAST 3-25-99-5W4	147
Figure 132. Logs for well SYNENCO 06-603 FIREBAG 3-33-99-6W4.....	148
Figure 133. Photograph of core interval from well SYNENCO 06-603 FIREBAG 3-33-99-6W4.....	149
Figure 134. Logs for well SUNCOR AUDET 1-18-98-6W4	150

Figure 135. Photograph of core interval from well SUNCOR AUDET 1-18-98-6W4	151
Figure 136. Logs for well SUNCOR AUDET 8-7-98-6W4	152
Figure 137. Photograph of core interval from well SUNCOR AUDET 8-7-98-6W4	153
Figure 138. Logs for well SUNCOR AUDET 9-15-98-6W4	154
Figure 139. Photograph of core interval from well SUNCOR AUDET 9-15-98-6W4	155
Figure 140. Photograph of core interval from well SUNCOR AUDET 9-15-98-6W4	156
Figure 141. Logs for well SUNCOR DW22 FIREBAG 13-3-95-6W4	157
Figure 142. Photograph of core interval from well SUNCOR DW22 FIREBAG 13-3-95-6W4	158
Figure 143. Logs for well SUNCOR FIREBAG 9-19-95-5W4.....	159
Figure 144. Photograph of core interval from well SUNCOR FIREBAG 9-19-95-5W4.....	160
Figure 145. Logs for well IMP 12-1-100-4W4.....	161
Figure 146. Logs for well FHEC FT HILLS 7-5-98-9W4.....	162
Figure 147. Portion of log at bedrock contact in well SHELL 16 ATHAE OV 10-16-98-2W4	164
Figure 148. Drill cuttings from well SHELL 16 ATHAE OV 10-16-98-2W4	165
Figure 149. Portion of logs at bedrock contact in well SHELL 19 ATHAE OV 13-11-99-1W4.....	166
Figure 150. Drill cuttings from well SHELL 19 ATHAE OV 13-11-99-1W4.....	167
Figure 151. Portion of logs from well SHELL 18 ATHAE OV 2-3-99-1W4	168
Figure 152. Drill cuttings from well SHELL 18 ATHAE OV 2-3-99-1W4.....	169
Figure 153. Portion of logs from well SHELL 15 ATHAE OV 1-13-98-1W4	170
Figure 154. Drill cuttings from well SHELL 15 ATHAE OV 1-13-98-1W4.....	171

Acknowledgements

We appreciate Steve Pawley's (Alberta Geological Survey) assistance with the core descriptions at the Alberta Energy Regulator's Core Research Centre. This report was improved by discussions and reviews by Steve Pawley, Lisa Atkinson, and Matt Grobe (Alberta Geological Survey). The X-ray fluorescence analysis on the core was completed by Graham Smerek (Alberta Geological Survey).

Abstract

This report is a summary of geological investigations in the Fort McMurray region to update the bedrock topography, delineate the buried valleys and channels that have incised the bedrock surface, and characterize the Quaternary sediments. Completion of these tasks included the examination of 55 cores that intersect the sediment-bedrock contact and comparing these core descriptions with the associated geophysical logs to develop criteria for identifying the bedrock top. These criteria were applied to the interpretation of geophysical logs from wells without core in the area, which led to the stratigraphic delineation of over 2900 new bedrock top picks.

During core analysis, complexities were identified such as the nature of the sediment-bedrock contact and how the contact varies with different sediment and bedrock types. Examination of cores revealed three types of sediment-bedrock contact including 1) sharp till-bedrock interface; 2) glaciogenic deformation of the bedrock interface; and 3) water-laid sediments at the sediment-bedrock interface. This report includes representative geophysical logs and cores that illustrate each contact type as well as the specific difficulties related to picking the bedrock top based on the underlying bedrock formation (i.e., Clearwater, Grand Rapids, or McMurray formation).

New work from this study along with compiled information from previous work was used to generate an updated bedrock topography map. From this map, areas of thick sediments (up to 200 m) are evident, particularly on the northern side of Muskeg Mountain and the Firebag Hills. To better characterize the sedimentary succession resting on bedrock, two representative cores were selected for detailed analysis and description. From these data, five till units were discerned and tentatively correlated with previously identified tills and ice-flow events.

Six geographic domains with different Quaternary stratigraphic sequences were delineated in this study. The Muskeg Mountain domain, in the central part of the study area, is typified by a thick sequence of multiple fine-grained tills capped by sandy till. To the north, the Firebag Hills domain is also composed of thick till sequences with sandy till overlying fine-grained till. In the area near the confluence of the Firebag River with the Athabasca River (Firebag River domain), glaciofluvially reworked McMurray Formation oil sand rests on pink clay-rich sediments thought to relate to deposition in a proglacial lake impounded by the Fort Hills ice flow. Although not well defined due to a paucity of data, the Steepbank Plain domain, south of Muskeg Mountain, is characterized by an extensive buried sand deposit, which is overlain by till containing rafts of bedrock. The bedrock surface in the MacKay Plain domain in the southwestern part of the study area has been incised by channels that may have both a subaerial and subglacial origin. Here, channel-fill stratified sediments are overlain by a thin cover of till. Similarly, the lowland flanking both sides of the Athabasca River (Dover and Kearl Lake plains domain) has also been incised by subglacial channels, and overlying sediments include channel-fill stratified sediments and rafts of bedrock. These six domains might be used as a basis for hydrogeological or other subsurface studies in the area.

1 Introduction

This report is a summary of investigations to update the bedrock topography and characterize the Quaternary sediments in the Fort McMurray region. The ability to define the sediment-bedrock interface and to map the distribution, nature, and thickness of overlying Quaternary deposits is needed to support economic and regulatory decisions on issues such as caprock thickness, distribution of buried potable aquifers, and the potential for migration of production fluids into near-surface aquifers. This study expands upon previous work in the area (Andriashek and Atkinson, 2007), which included mapping the bedrock topography, the thickness of Quaternary deposits, and the distribution of sand-filled buried bedrock valleys and channels from geotechnical borehole data, water well records, and oil and gas well logs. This updated study covers 35 000 km² and is based on information from thousands of more recently drilled boreholes as well as detailed examination of hundreds of metres of well core.

From core examination, suite of criteria was developed to map and identify the top of bedrock and characterize the Quaternary deposits by interpreting geophysical logs from wells without core across the study area, with a particular focus on the in situ oil sands area. An update to the bedrock topography map with thousands of bedrock top picks from geophysical logs reveals areas of thick sediments (up to 200 m), areas of thin cover bisected by buried channels incised into bedrock, and abundant evidence of glacially thrust material.

Based on detailed examination of the cores and interpretation of the geophysical well logs, the sediments resting on bedrock were characterized and the study area was divided into domains with similar Quaternary stratigraphic characteristics. These domains define areas where similar deposits might be expected, which can be used as a basis for hydrogeological or other subsurface studies in the area.

2 Study Area

2.1 Physiography

The 30 000 km² study area in northeastern Alberta (Figure 1) comprises several major physiographic elements that are defined on the basis of regional differences in elevation and drainage characteristics (Pettapiece, 1986). A prominent feature in the central part of the study area is Muskeg Mountain, which rises more than 370 m above the lowest regions of the study area. Elevation within Muskeg Mountain ranges from 450 to 670 metres above sea level (m asl; Figure 1) and the similarly prominent Firebag Hills, to the east and northeast, range from 480 to 640 m asl. In the north and northeast, low-lying topographic elements form the Firebag and Johnson Lake plains, which have surface elevations ranging from 350 to 470 m asl. The Embarras, Dover, and Kearl Lake plains to the west separate Muskeg Mountain from the highest upland in the study area, the eastern flank of the Birch Mountains, which has a maximum elevation of 870 m asl and rises about 550 m above the lowest parts of the region. The area south of Muskeg Mountain includes the Steepbank and Garson plains, and to the southwest are the Algar and Brule plains. The area is bisected by the generally northward-flowing Athabasca River, which has a confluence with the westward-flowing Clearwater River in the Fort McMurray area. Other significant drainages include the High Hill, Steepbank, Muskeg, Firebag, MacKay, Dover, and Ells rivers. The study area includes the surface mineable oil sands area along the banks of the Athabasca River and part of the in situ oil sands area.

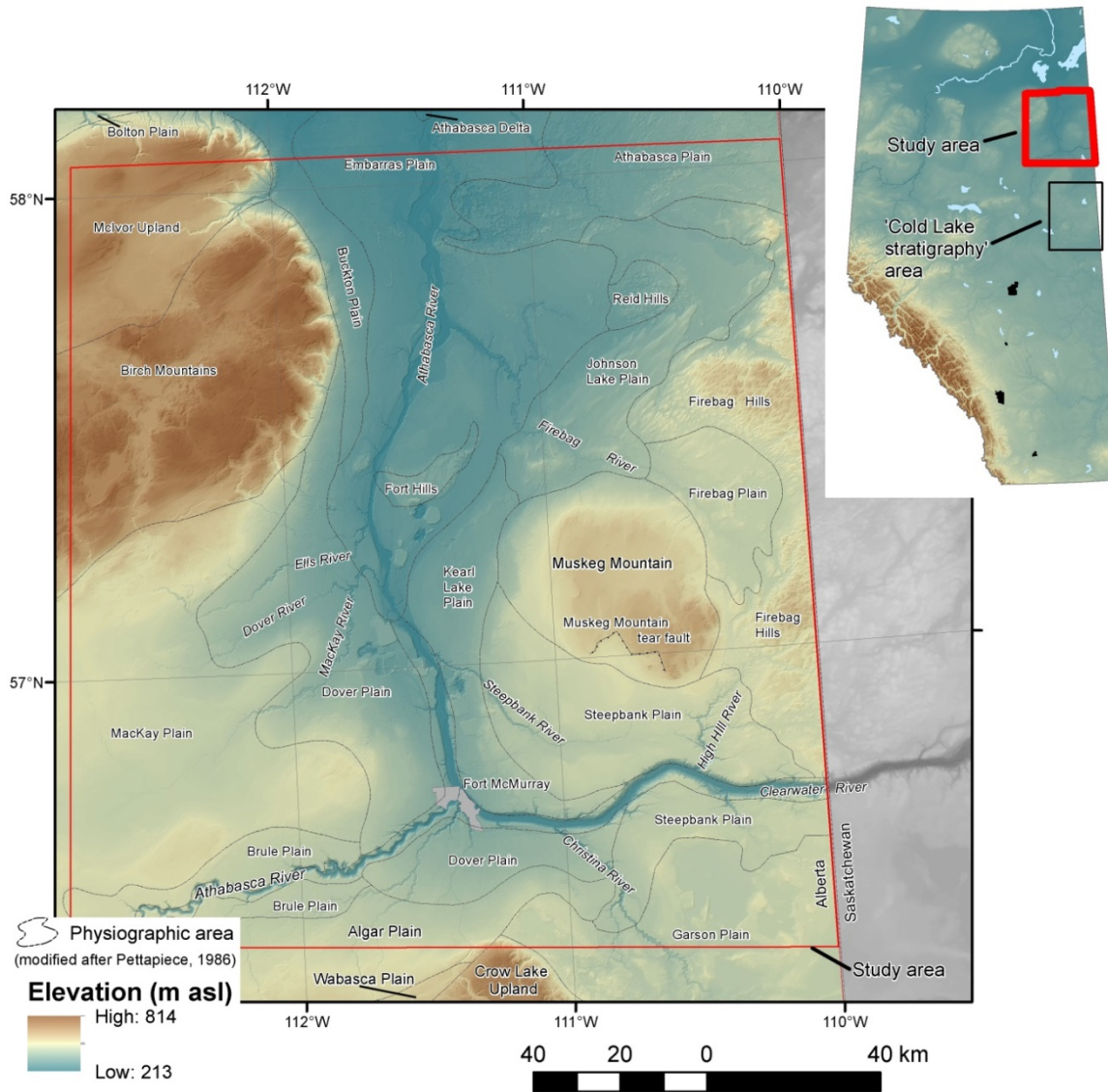


Figure 1. Geographic and physiographic features in the study area, northeastern Alberta, shown on a bare-earth LiDAR (light detection and ranging) digital elevation model image. Inset map shows the area where the ‘Cold Lake stratigraphy’ was developed by Andriashek and Fenton (1989) in relation to the area investigated in this report.

2.2 Bedrock Geology

Precambrian basement (Canadian Shield) igneous and metamorphic rocks underlie the study area and outcrop in the northeastern portion of the study area. Resting unconformably on these rocks are Devonian carbonates (including shale, limestone, and dolostone), which dip gently to the southwest (Figure 2; Hauck et al., 2017; Alberta Geological Survey, 2019). These rocks are exposed in river cuts along the Athabasca and Firebag rivers. Nested within these units are halite and anhydrite beds of the Prairie Evaporite Formation, rocks that are prone to dissolution resulting in localized karst features (Hauck et al., 2017), such as relict and active sinkholes (Haug et al., 2014). The upper surface of the Devonian carbonates is defined by the sub-Cretaceous unconformity, a basin-wide erosional surface. The unconformity is characterized by landforms such as the northwest-trending Assiniboia paleovalley, as well as karst collapse/dissolution features (Jackson, 1984; Leckie and Smith, 1992).

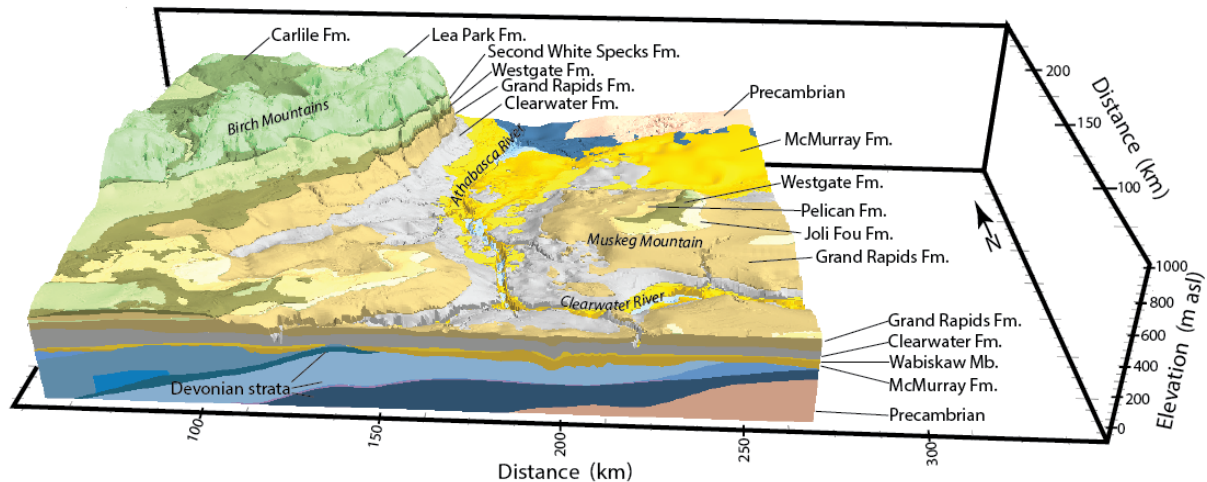


Figure 2. Three-dimensional rendering of the bedrock geology in the study area, northeastern Alberta (modified after Alberta Geological Survey, 2019). Sediment units above bedrock are not shown. Rivers and physiographic elements are italicized. Vertical exaggeration is 1:50.

Cretaceous clastic sedimentary rocks that comprise the McMurray, Clearwater, and Grand Rapids formations of the Mannville Group sit unconformably on Devonian strata (Alberta Geological Survey, 2019). The underlying topography influenced deposition of the McMurray Formation with paleoflow to the northwest within the Assiniboia paleovalley. Channels within the McMurray Formation are represented by packages of bitumen-saturated quartzose sandstone with intervening fine-grained shale and siltstone (Hein and Cotterill, 2006). The overlying Clearwater Formation represents a marine transgression into the area, and is composed primarily of shale and siltstone (Hayes et al., 1994). In some areas the lower Clearwater Formation includes the Wabiskaw Member, a glauconite-bearing shale and sandstone (Haug et al., 2014). As sea level lowered, barrier islands and coastal plain complexes formed over the area, with the deposition of various channel sand units and intervening fine-grained silt and shale, which constitute the Grand Rapids Formation (Cant and Abrahamson, 1997).

The Grand Rapids Formation is overlain by dominantly marine sedimentary rocks of the Colorado Group, composed of the Joli Fou, Pelican, Westgate, Fish Scales, Second White Specks, and Carlile formations (Leckie et al., 1994). The Joli Fou Formation represents a transgression over much of the province, and is composed mostly of shale. An erosional contact is represented by sandstone and siltstone (possibly reworked Grand Rapids Formation deposits) of the overlying Pelican Formation. The Pelican Formation, in turn, is overlain by the Westgate Formation, which is also primarily shale (Leckie et al., 1994). This is overlain by the Fish Scales Formation, consisting of fine-grained sandstone, siltstone, and shale with a high organic content and abundant fish fossils; phosphorite nodules occur in places. Overlying this is the Second White Specks Formation, another primarily shale unit, which contains abundant white coccoliths. The Carlile Formation is a siltstone and shale unit, with some sideritic concretions (Prior et al., 2013). The Colorado Group is overlain by the Lea Park Formation, another shale-dominated formation.

Because all of the above-described formations rest on the shield and dip to the southwest, their eastern edges rise to either subcrop or outcrop, forming the bedrock surface in the northeastern part of the province (Figure 2).

2.3 Cenozoic and Quaternary Geology

During the Cenozoic, fluvial erosion occurred across the study area's landscape, forming broad lowlands. This incision was interrupted during the Quaternary with the onset of glaciation. The region was glaciated at least once during the Late Wisconsinan glaciation by the Laurentide Ice Sheet. At its farthest advance

hundreds of kilometres to the west, the Laurentide Ice Sheet coalesced with the Cordilleran Ice Sheet emanating from the Rocky Mountains (Roed, 1975; Atkinson et al., 2016; Utting et al., 2016). Fluvial and glacial processes played a dominant role in shaping the bedrock topography and depositing the sediments resting on bedrock.

2.3.1 Buried Bedrock Valleys and Channels

Fluvial erosion not only eroded broad smooth benches but, depending on the type of erosional event, also incised into the bedrock. Andriashek and Atkinson (2007) defined two types of fluvially incised features: buried bedrock valleys and channels. When infilled and covered with surficial sediments, these buried bedrock valleys and channels have no surface expression; however, they are important to identify because of the potential for a thinned underlying caprock, and for coarse sediments that host potable aquifers (Andriashek and Atkinson, 2007). Buried bedrock valleys (McMurray, Clearwater, High Hill, Pemmican, south Pemmican, Pine, Thickwood, Spruce, Stony, Inglis, Ruth, Christina, Athabasca; Figure 3) represent features interpreted to have been eroded during preglacial drainage, and are typically broad with shallow valley walls. Conversely, buried channels (Fort Hills, Telephone Lake, Alder, Kearn, Lower Kearn, Lewis, Clarke, Willow, Birch; Figure 3) are thought to have been eroded by meltwater during glaciation, and are deeper (greater depth-to-width ratio) with steep channel walls. Some bedrock valleys may have been reoccupied during glaciation, blurring the distinction between the valleys and channels. The trace of the lowest point of bedrock valleys and channels is referred to as the thalweg. Maps typically show thalwegs as line features, but the width of the incised feature may vary along its length as a function of the type of erosional event that created the feature.

2.3.2 Quaternary History

During the Quaternary, the study area was probably glaciated several times. Each glaciation would have included an advance phase, when the ice margin approached the area (likely from the north or northeast) and blocked drainage, resulting in the development of a glacial lake. As the ice advanced farther, the area would have been completely covered with ice. The ice would have flowed in various directions, based on topography as well as the configuration of the ice sheet and basal conditions, which would have changed with time. Major shifts in ice-flow patterns would have occurred, leaving a pattern of cross-cutting landforms parallel to the ice flow, like drumlins and flutings, on the landscape (Ó Cofaigh et al., 2010; Norris, 2019). These ice-flow shifts, in part, would have led to surface till characteristics that change laterally depending on the ice-flow phase that deposited the till (Ross et al., 2009). Vertical changes in lithological properties of tills can also be expected from these shifting ice-flow directions. Thus tills with different lithological properties can be deposited during the same glaciation, by different ice-flow events. However, unconformities between till units (typically represented by oxidized contacts) suggest periods of subaerial exposure between deposition of the tills (Andriashek and Barendregt, 2017). As a result, tills of differing properties may or may not represent different glaciations. Some portions of present-day uplands represent areas of thick surficial (primarily till) deposits, rather than bedrock remnants (Figure 4) and may be composed of tills of differing properties based on the ice-flow event that deposited them.

As ice retreated across the province, it blocked regional drainage and proglacial lakes formed along the ice margin (Utting and Atkinson, 2019). These proglacial lakes may have led to instabilities in the ice-flow patterns triggering rapid ice flow and potential readvances (i.e., surges). Likewise, proglacial lakes may have also encouraged rapid retreat of the ice margin by marginal melt and ice sheet calving. In the study area, glacial Lake McMurray formed when the ice margin was approximately at the Fort Hills physiographic region, with the lake filling the lowlands to the south to an elevation of approximately 580 m asl (Utting and Atkinson, 2019). This margin may have fluctuated in part due to the presence of this lake. As this ice margin retreated from the Fort Hills area, glacial Lake McMurray drained. Subsequently, glacial Lake Agassiz flooded the area and is thought to have drained catastrophically along the Clearwater and Athabasca rivers into glacial Lake McConnell, which lay to the north (Fisher and Smith, 1994; Woywitka et al., 2017; Utting and Atkinson, 2019).

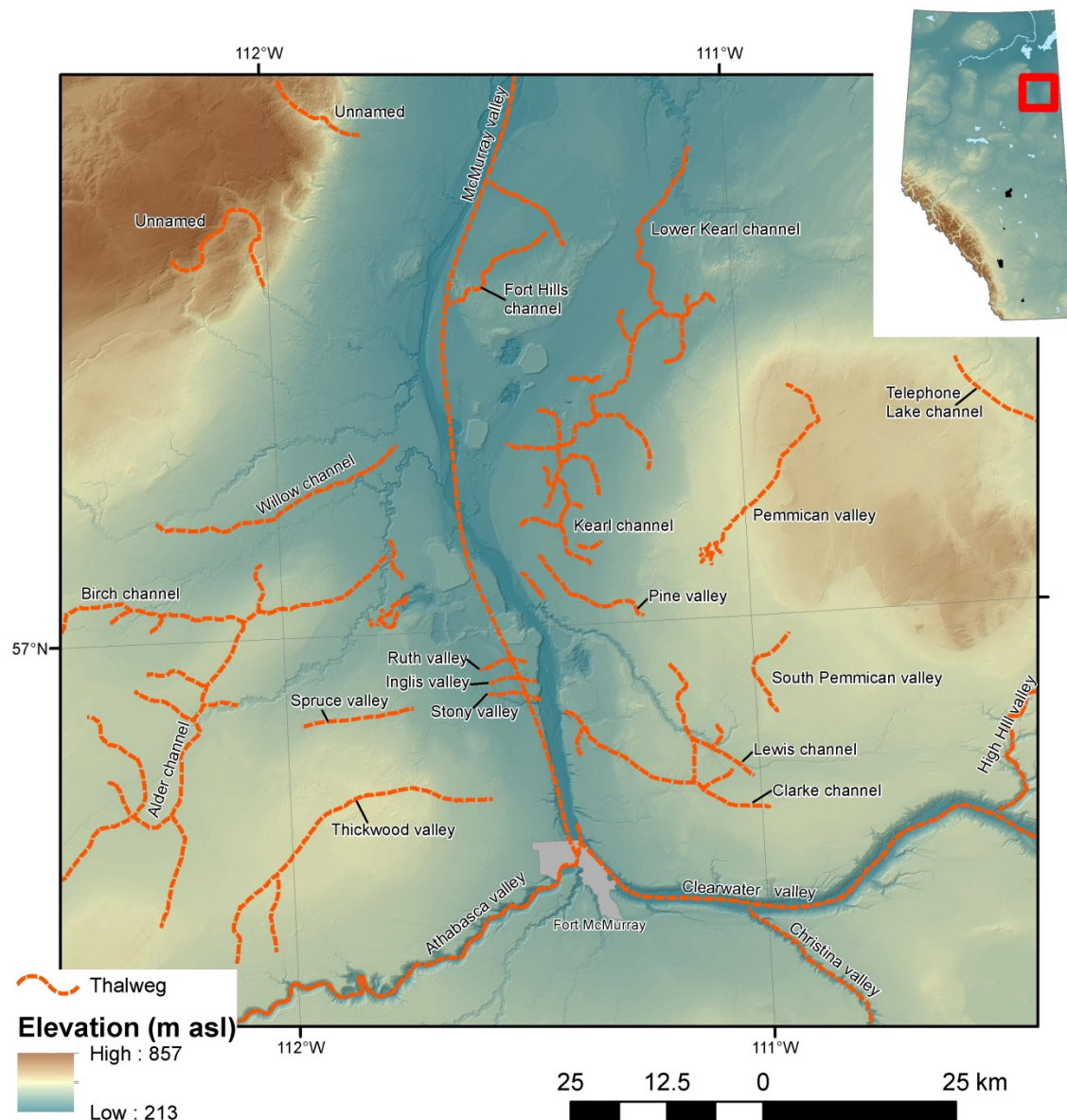


Figure 3. Thalwegs of buried bedrock valleys and channels within the study area, northeastern Alberta (Andriashek, 2019), shown on a bare-earth LiDAR (light detection and ranging) digital elevation model image. Bedrock valleys are considered preglacial in origin, whereas channels were formed subglacially. The thalweg is the lowest point of these fluviably incised features.

2.3.3 Glaciotectonism

During glaciation, the overriding glacial ice deformed and/or displaced the basal material of sediments or bedrock in a process referred to as glaciotectonism. This process may have been restricted to the few centimetres to metres near the glacial-bed contact, or may have plucked and thrust tens of metres of material, either creating landforms or modifying buried sediment sequences.

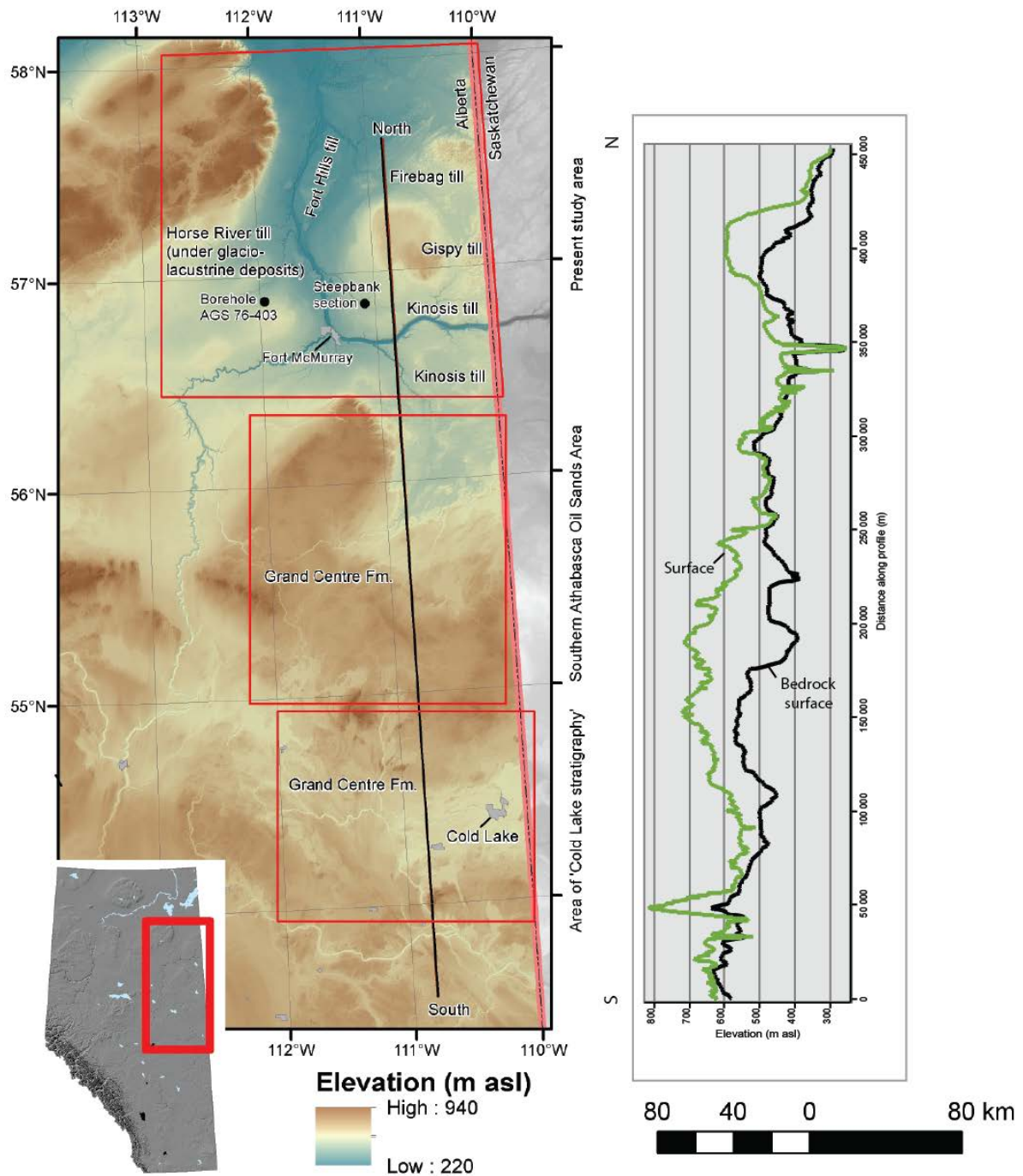


Figure 4. Location of Alberta Geological Survey studies and general location of surface tills and formations, shown on a bare-earth LiDAR (light detection and ranging) digital elevation model image. Profile shows general thickness of Quaternary sediments over bedrock across these regions. Note the general thickening of Quaternary sediments in the area of the upland in the southern Athabasca Oil Sands Area (Andriashek and Fenton, 1989) and in the 'Cold Lake stratigraphy' area (Andriashek, 2003).

Previous work by Andriashek and Atkinson (2007) reported geomorphic evidence of glaciotectonism, including a feature called the Muskeg Mountain tear fault (Figure 1) and the Fort Hills–McClelland Lake hill-hole pair (Figure 5). On the southern side of the Muskeg Mountain, four rectilinear, 6 km long, 20–30 m high scarps are visible. Based on comparisons with similar features in bedrock (e.g., Andriashek and Fenton, 1989), Andriashek and Atkinson (2007) interpreted the features as a glacial tear-fault quarry zone, which resulted from ice flow to the south and a failure occurring along the contact of the Grand Rapids Formation and underlying Clearwater Formation shale.

McClelland Lake and the adjacent Fort Hills were interpreted by Andriashek and Atkinson (2007) as a hill-hole pair that was later dissected by fluvial erosion (Figure 5). Material was glacially quarried to form the lake, and was thrust and stacked to form the Fort Hills (Andriashek and Atkinson, 2007). The hills have arcuate surface features, possibly representing evidence of shear planes related to this thrusting process (Figure 5). Moran et al. (1980) suggest hill-hole pairs are formed when blocks of material are plucked by a glacier advancing over frozen ground. The presence of frozen ground is thought to result in increased basal porewater pressures in the underlying, unfrozen, saturated sediments, resulting in the overlying frozen material to fail rather than the ice to deform (Moran et al., 1980).

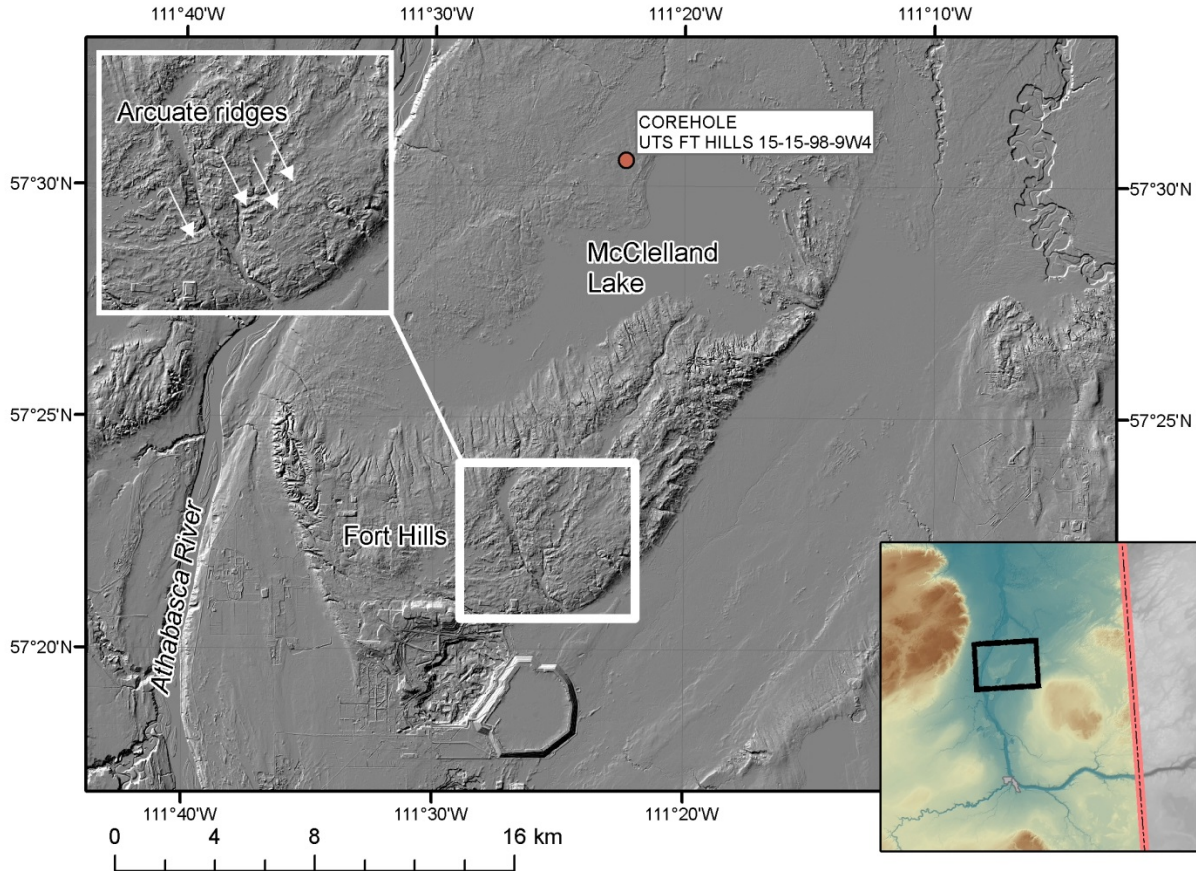


Figure 5. LiDAR (light detection and ranging) image of the Fort Hills area with shaded relief, northeastern Alberta. The hill is interpreted as composed of glacially thrust material, quarried from the McClelland Lake area (Andriashek and Atkinson, 2007). The core from the well adjacent to McClelland Lake (UTS FT HILLS 15-15-98-9W4) exhibits the thickest interval of glacially deformed bedrock (>10 m) of all the cores examined.

Displaced bedrock within the Quaternary succession of the study area, reported by Andriashek and Atkinson (2007), was likely plucked by and transported within the ice (Atkinson et al., 2013). Glaciotectonism was also invoked to explain the inclined tops of correlative units in geophysical logs from the subsurface on the northern flank of Muskeg Mountain. These were thought by Andriashek and Atkinson (2007) to be quarried blocks that were thrust as imbricate slabs, similar to those in the Cold Lake area (Andriashek et al., 1999).

2.4 Previous Quaternary Stratigraphic Studies

To understand the Quaternary stratigraphic sequences in the Fort McMurray region, two previous Alberta Geological Survey (AGS) stratigraphic studies south of the study area were assessed for the potential continuity of the till units and their correlation with units in the north (Figure 4). Andriashek and Fenton (1989) developed a stratigraphy for east-central Alberta based on regional mapping in the Cold Lake area (Figures 1 and 4). They acquired auger samples at 1 m depth intervals and submitted them for grain size and carbonate content analysis. The results were paired with geophysical logs and criteria for characterizing Quaternary deposits were developed, allowing for the interpretation of logs from wells without core over a broader area. This allowed for the identification of mappable Quaternary stratigraphic units (Table 1). The ‘Cold Lake stratigraphy’ was expanded northwards to the southern Athabasca Oil Sands Area (Figure 4) by Andriashek (2003) based on the examination of seven cores that were paired with geophysical logs, which led to the interpretation of logs from wells without core. Again, the interpretation of the geophysical logs allowed mapping of these units over a larger study area, but with some limitations as many of the geophysical logs were from oil and gas wells and did not have log information collected to surface.

The ‘Cold Lake stratigraphy’ includes a basal sand (Empress Formation) that, if present, is overlain by multiple tills and may be separated by intervening stratified sediments, or in some cases oxidized sediment profiles. The oxidized profiles were inferred by Andriashek and Fenton (1989) to be buried paleosurfaces or weathered horizons, and thus represented periods of nonglaciation in between the deposition of the till sheets (Andriashek, 2003). Andriashek and Barendregt (2017) used magnetostratigraphy to determine that the lowest (oldest) till in the succession (Bronson Lake Formation; Table 1) was reversely magnetized, suggesting it predates the Late Wisconsinan, whereas the overlying ~30–150 m of till and stratified sediments was normally magnetized.

Although multiple tills were identified in the subsurface in the Cold Lake area, previous work in the Fort McMurray study area (Figure 1) delineated only surface tills. Three surface tills were identified by McPherson and Kathol (1977; Table 2). Differences in these tills were primarily attributed to their geographic distribution, with textural and geochemical differences correlated to ice-flow events. Three different surface tills were also identified by Bayrock (1971, 1974; Table 3). Similarities in the till units described by McPherson and Kathol (1977) and Bayrock (1971, 1974), as well as the congruent distributions and stratigraphic positions, means that some of the till units defined separately in those studies can likely be considered equivalent. This study attempted to determine similarities in these till units, and determine their distribution in the subsurface using geophysical logs and core.

Table 1. Quaternary stratigraphic units in the Cold Lake area, Alberta (modified from Andriashek and Fenton, 1989; Andriashek and Barendregt, 2017).

Period	Epoch	Age	Stratigraphic Unit	Material/Description	
Quaternary	Holocene	<14 ka	Recent surficial sediments		
	Late Pleistocene	~35 ka	Grand Centre Fm.	Till	
			Sand River Fm.	Stratified sediments / glaciofluvial sand	
			Marie Creek Fm.	Till (carbonate rich)	
	Early and Middle Pleistocene	~126 ka	~780 ka	Ethel Lake Fm.	Stratified sediments / glaciolacustrine silt and clay
				Bonnyville Fm.	Till with relatively high quartz (limited carbonate) content
				Muriel Lake Fm.	Stratified sediments / glaciofluvial sand and gravel
				Bronson Lake Fm.	Clayey till and clay (reverse magnetization)
				Empress Fm.	
	Neogene			Unit 3	Glacial sand and gravel
			Unit 2	Silt and clay	
			Unit 1	Preglacial sand and gravel	

Table 2. Stratigraphic units in Athabasca Oil Sands Area (McPherson and Kathol, 1977).

Unit	Distribution	Description
Fort Hills till	Absent from higher areas, interpreted to relate to 'Fort Hills ice', a local glacial readvance	Dark grey till with pink lenses, silt loam matrix (18% sand), high percentage of carbonate grains in coarse fraction
Lower stratified sediments	Area between Fort Hills and Firebag River	Silt and clay; pink and grey glaciolacustrine
Firebag till		Surface till for much of the area
Unnamed till	Section on Steepbank River (Figure 4) and borehole on MacKay Plain (AGS 76-403; Figure 4). Overlain by glaciolacustrine sediments or Firebag till.	Till is dark grey; silty to sandy loam matrix (56% sand), low percentage of carbonate in matrix

Table 3. Till units in the Waterways and Bitumount map areas, NTS 74D, E (Bayrock, 1971, 1974).

Unit	Distribution	Description
Gipsy till	Eastern boundary, and glacially streamlined areas north of Muskeg Mountain	Grain size similar to outwash (i.e., >90% sand)
Kinosis till	North and south of the Clearwater River	Equal parts sand-silt-clay in matrix
Horse River till	Underlies glaciolacustrine deposits, or is exposed at surface on the Thickwood Hills	Clayey matrix

3 Methodology

In order to develop a suite of criteria to differentiate Quaternary deposits from underlying bedrock strata, core and geophysical logs were examined over the interval of the bedrock contact. Even though thousands of cores have been collected by the petroleum industry in the region, most were collected from bedrock strata and do not span the sediment-bedrock interface. However, 55 cores were examined in which Quaternary sediments were present and the top of bedrock could be defined. The coreholes are located primarily in the central part of the study area and on the northern flank of Muskeg Mountain (Figure 6). Cores with Quaternary sediments and bedrock were located by comparing the depth of bedrock from the previous bedrock topography model by Andriashek and Atkinson (2007) with information on the depths of coring from the Alberta Energy Regulator's Core Research Centre (CRC) files. Cores were visually examined, photographed, and described at the CRC (Appendix 1). At a few sites, coring was initiated well above the bedrock top and a thick Quaternary succession was available to examine. At most sites, coring started only a few metres above the bedrock contact, but at least revealed details of the nature of the bedrock contact.

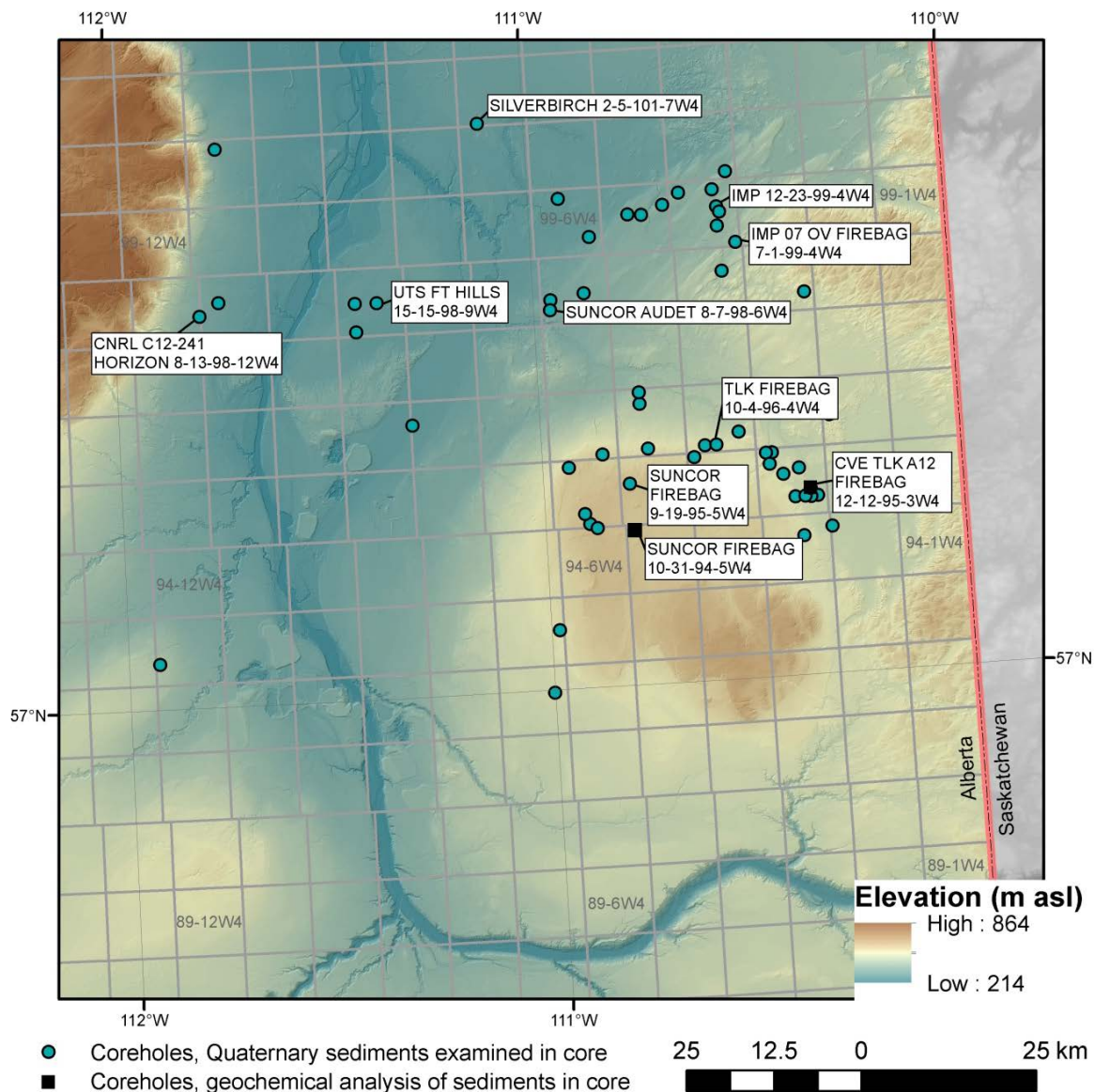


Figure 6. Location of coreholes with cores that were examined in this study, northeastern Alberta.

From the examination of core, criteria were developed to identify the bedrock top from geophysical logs. These criteria were then applied to geophysical logs from wells without core. All of these log picks (over 2900) were used to update the bedrock topography map of the Fort McMurray study area (see Section 4.5). To incorporate the geometry of some newly defined buried channels into the southwestern part of the bedrock topography map, synthetic points were created along an outline interpreted from airborne electromagnetic (EM) imagery (Dawson et al., 2018). Elevation values for these points were estimated from surrounding wells where control data existed.

To characterize and potentially correlate tills to regionally identified stratigraphic units, cores from two wells (SUNCOR FIREBAG 10-31-94-5W4, CVE TLK A12 FIREBAG 12-12-95-3W4) were selected for geochemical and grain size analysis. The X-ray fluorescence (XRF) analysis was completed using a handheld Thermo Scientific™ Niton™ XL3t 955 Ultra analyzer on intact core (i.e., whole sediment) at a spacing of approximately 0.7 m, depending on core recovery, preferentially avoiding large clasts in till. More typical geochemical analysis (inductively coupled plasma–mass spectrometry [ICP-MS]) was completed on the silt–clay fraction by Bureau Veritas Commodities Canada Ltd. (Vancouver, British Columbia). Grain size analysis was completed by wet/dry sieve analysis by Core Laboratories Ltd. (Calgary, Alberta) on the same samples as submitted for ICP-MS analysis.

4 Results

From the examination of core (Appendix 1), some complexities of the nature of the bedrock contact were identified, particularly how the contact varies over different bedrock types. During the course of this work, evidence of glaciotectonism of the bedrock surface and glaciotectonically displaced bedrock was identified.

Awareness of these complexities, combined with the log criteria, informed the picking of the bedrock top in over 2900 wells. These bedrock top picks from geophysical logs were complemented by the location of buried channels interpreted from airborne EM surveys (Dawson et al., 2018). These data, compiled with previous work, were used to generate a revised bedrock topography map for the region. Some areas of thick sediments were identified, and two representative cores were selected for detailed analysis and description in order to better characterize the sedimentary succession resting on bedrock.

4.1 Nature of Bedrock Contact

Examination of cores revealed three types of sediment–bedrock contacts: 1) sharp till–bedrock interface; 2) glaciogenic deformation of bedrock interface; and 3) water-laid sediments at the sediment–bedrock interface. Representative geophysical logs and cores provide illustrations of each type of contact and the specific difficulties relating to picking the bedrock top on different bedrock formations (e.g., Clearwater, Grand Rapids, or McMurray formation).

4.1.1 Contact Type I: Sharp Till–Bedrock Interface

Sharp contacts between till and bedrock were observed in eight cores. The bedrock is McMurray Formation oil sand in five of these cores, and shale in the remaining three cores. Geographically, the cores with sharp contacts with underlying oil sand are located north of Muskeg Mountain (Figure 1), and cores with shale are located to the south and southwest. In one of the cores (CNRL C12-241 HORIZON 8-13-98-12W4; Figure 7), the contact is also well defined by an oxidized bedrock surface (Figure 8), which is interpreted to be a preserved weathered surface. Elsewhere, for example south of the study area (Andriashek and Fenton, 1989; Andriashek, 2003), oxidized horizons on the surfaces of buried tills and geochemical anomalies have been interpreted as the remnants of weathered horizons. The oxidized horizon, and the lack of deformation features, suggests that there was little to no glacial erosion of the bedrock in the area of this well (northwest of Muskeg Mountain) prior to burial by glaciogenic sediments.

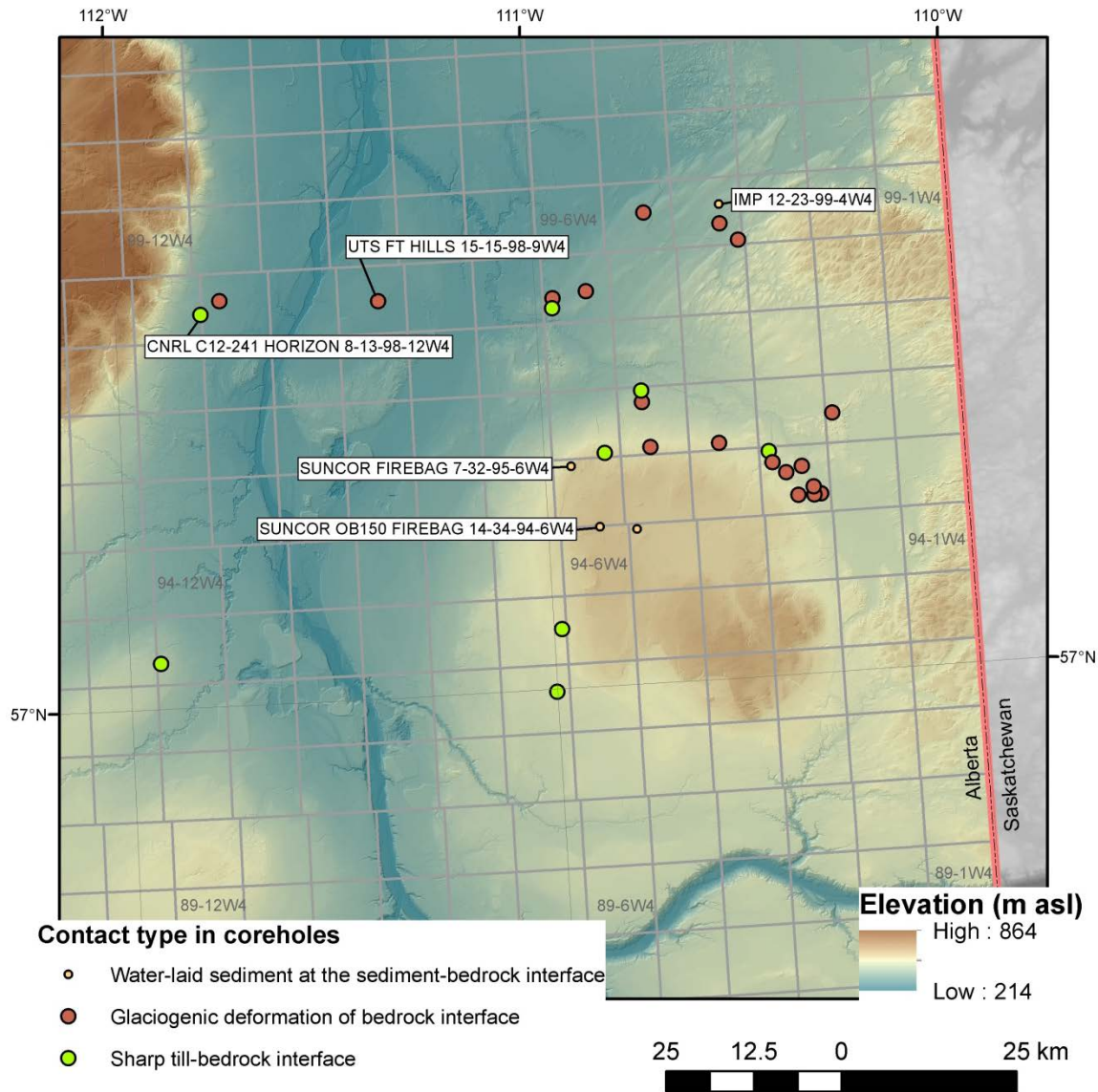


Figure 7. Locations of coreholes with three types of bedrock contacts in cores, northeastern Alberta.

Interestingly, no glacially deformed oil sand was observed in any of the cores. The absence of distortion/deformation may be a result of better internal matrix drainage and dissipation of stress, and/or greater competency of oil sand (Phillips et al., 2017) compared to shale. Alternatively, deformation is harder to observe in core with oil sand because deformation and fractures may have been annealed, making the core appear more homogeneous.

4.1.2 Contact Type II: Glaciogenic Deformation of Bedrock Interface

Cores in which deformed bedrock underlies till all occur on the northern flank of Muskeg Mountain (n=18). The depth of deformation is generally limited to less than 1 m in most of these sites (n=17). In core UTS FT HILLS 15-15-98-9W4 (Figure 7), to the north of the Fort Hills (Figure 1), deformation depth exceeded 10 m in shale (Figure 9).

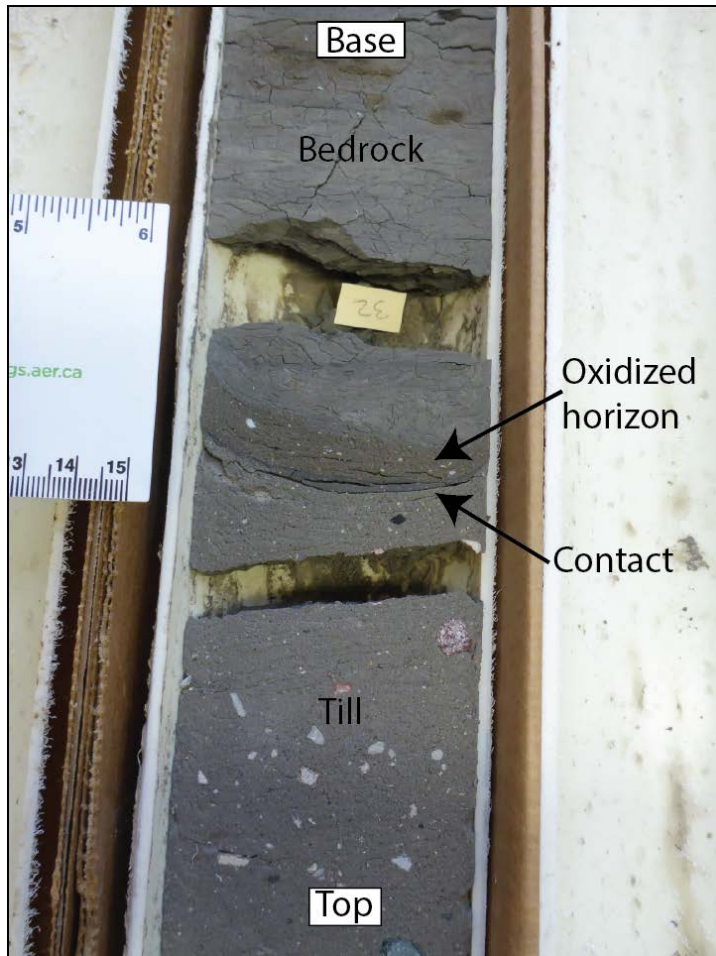


Figure 8. Core with sharp contact between till and bedrock. The upper portion of the bedrock appears oxidized. Top of photo is bottom of core (corehole CNRL C12-241 HORIZON 8-13-98-12W4, 31.60–32.50 m depth, 312.0–311.1 m asl, see Figure 7 for corehole location).

4.1.3 Contact Type III: Water-Laid Sediments at the Sediment-Bedrock Interface

In one core (IMP 12-23-99-4W4; Figure 7), silt overlies bedrock (Figure 10) and is overlain by till. Because of its stratigraphic position underlying the first till in the succession in the corehole, the silt can be classified as Empress Formation unit 2 (Table 1), and potentially relates to an advance-phase ice-dammed glacial lake. Whereas two other wells (SUNCOR FIREBAG 7-32-95-6W4, SUNCOR OB150 FIREBAG 14-34-94-6W4) contain sand and cobbles above the bedrock contact; both are likely glaciofluvial in origin and therefore interpreted as Empress Formation unit 3 (Table 1).

4.2 Establishing the Bedrock Contact from Geophysical Logs

Criteria for selecting the bedrock top from geophysical logs differ depending on the nature of the underlying bedrock formation (Figure 2) and the character of the overlying Cenozoic (inferred as Quaternary-aged) sediments. Generally, if a subcrop of Clearwater Formation shale is overlain by sandy Quaternary sediments (i.e., sandy till, sand, or gravel) the contact is relatively easy to pick on the gamma-ray log, with sandier sediments having lower gamma-ray values, which results in a shift to the left on the log (Figure 11). There is typically a corresponding, but opposite, shift in the neutron porosity log (Figure 11). This type of contact is also similar for fine-grained till over shale, as the till is generally coarser than the shale.

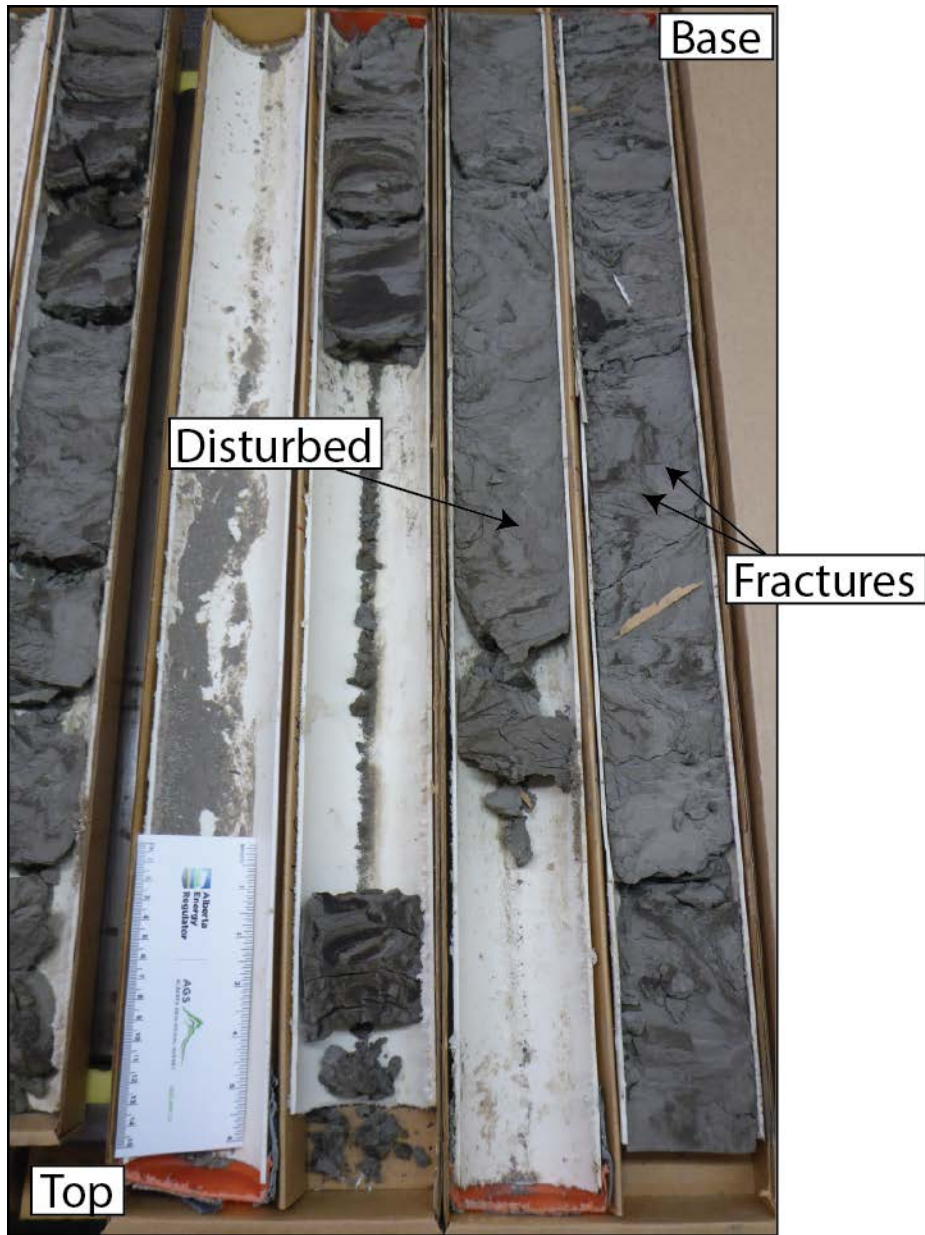


Figure 9. Core of disturbed or contorted shale beneath the bedrock contact (not shown). Note convolutions in bedding and displacement along fractures (corehole UTS FT HILLS 15-15-98-9W4, 57.0–63.3 m depth, 245.3–239.0 m asl, see Figure 7 for corehole location).

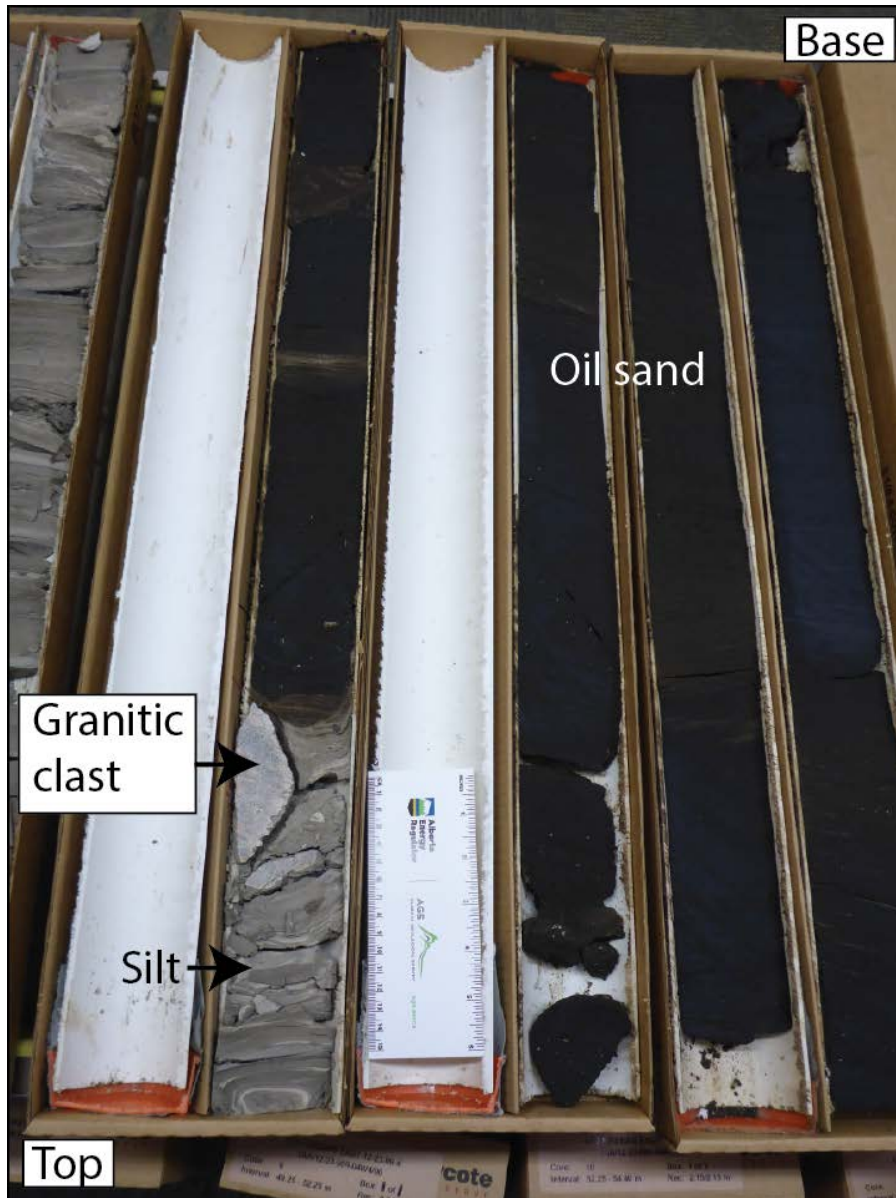


Figure 10. Silt overlying oil sand in corehole IMP 12-23-99-4W4 (52.0–55.0 m depth, 345.6–342.6 m asl, see Figure 7 for corehole location). The silt looks similar to siltstone, however, there are two granitic clasts near the bedrock contact. If this contact is in place, a glaciolacustrine origin for the silt is suggested, with the clasts being dropstones. Alternatively, if the material is siltstone, the presence of the clasts suggests the siltstone is glaciotectonically displaced.

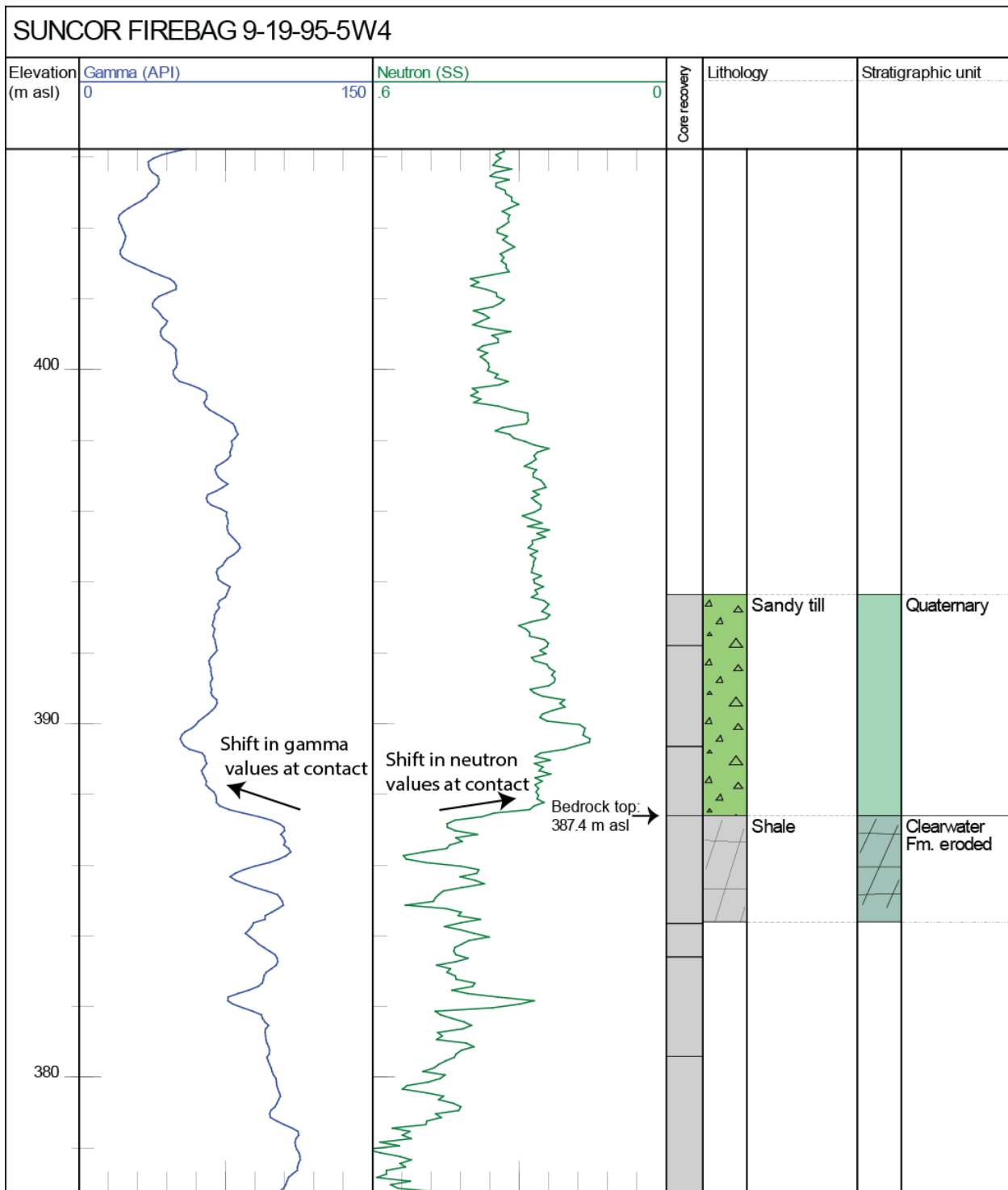


Figure 11. Example of logs where sandy till overlies Clearwater Formation shale (corehole SUNCOR FIREBAG 9-19-95-5W4, see Figure 6 for corehole location). Note shift to lower gamma-ray values (to the left) and lower neutron porosity values (to the right) at the till-bedrock contact. Litholog determined from examination of core. Abbreviations: Gamma, gamma-ray; Neutron, neutron porosity; SS, sandstone units.

Picking the contact becomes more difficult where coarse Quaternary sediments (i.e., sand, gravel, or very sandy till) overlie the Grand Rapids and McMurray formations, both of which are dominantly sandstone interspersed with siltstone and shale units. Shifts in gamma-ray logs can reflect siltstone and shale in the bedrock, however, they could also be reflecting interbedded silt and sandy till in the Quaternary succession. Hence, a gamma-ray log may not be as effective for picking the contact at the tops of these bedrock formations. However, where the top of the Grand Rapids or McMurray formation has been well-established in core, a strong shift to lower neutron porosity values (normally reported as a shift to the right) is typically well defined at the contact with the overlying Quaternary sediments (Figure 12). The shift in neutron porosity values at the bedrock contact to lower values in the Quaternary (shift to right) likely relates to the looser or less compacted nature of the Quaternary sediments, and a decrease in the volume of water-filled pores.

The presence of a strong shift in the neutron porosity log was useful for picking the bedrock top, with some exceptions. For example, because of a progressively decreasing concentration of comminuted local bedrock in the till matrix up-hole from the contact, a gradual, rather than abrupt, shift in the neutron porosity log (Figure 13) can be observed.

4.3 Glaciotectonically Displaced and Transported Bedrock (Rafts) within the Quaternary Succession

Examination of core to determine the bedrock top revealed some cores contain material that appears similar to bedrock but has Quaternary sediments beneath. This material is interpreted to be glaciotectonically displaced and transported bedrock (or rafts of bedrock). One of the processes of glaciotectonism is plucking and thrusting or displacing the substrate, either bedrock or previously deposited glaciogenic sediments. In the study area, this process resulted in numerous blocks of bedrock being plucked and transported by glacial processes, and these rafts are now preserved within the Quaternary succession (Andriashek and Atkinson, 2007).

In this study, bedrock rafts were observed in 14 cores (Figure 14). These are represented on neutron porosity logs by a shift to higher values (i.e., shift to the left; Figure 15), similar to that seen with in situ bedrock. Rafts range in thickness from 1 to 7 m. The rafts have near-horizontal to gently inclined geometries (Figure 16). In some cases, rafts could only be identified by the presence of a thin (0.1–3 m) diamict layer that separates displaced bedrock from in situ bedrock. Without observing this in core, it is reasonable to conclude that these thin beds of Quaternary sediments would not be evident on geophysical logs, and that the top of the bedrock raft would therefore be mistakenly interpreted as the top of in situ bedrock.

It is interpreted that glacial plucking of the substrate has also played a role in the origin of some features on the landscape. This includes the Muskeg Mountain tear fault, a geomorphic feature interpreted by Andriashek and Atkinson (2007) to have formed by glacial quarrying along the contact between the Clearwater and Grand Rapids formations on the southern flank of Muskeg Mountain. Applying the criteria presented in this report for picking the bedrock top, it is apparent that if this is indeed a glacial tear fault, then quarrying must have occurred completely within Quaternary sediments and not along a deeper interface between bedrock formations (Figure 17). The stratigraphic evidence shows that the bedrock top forms a generally planar surface on the south side of Muskeg Mountain, and is overlain by more than 100 m of Quaternary sediments on the upland adjacent to the scarp. A 1–2 km wide bench (Figure 17), which flanks the southern side of Muskeg Mountain, is overlain by 10–15 m of sediments on the same bedrock surface. Quarrying appears to have extended to a depth of only 40–50 m from the surface of the upland, which would place the failure zone well within the Quaternary succession. This implies that bedrock rafts located to the south of Muskeg Mountain (cf. Andriashek and Atkinson, 2007) must be sourced from another location farther up-ice.

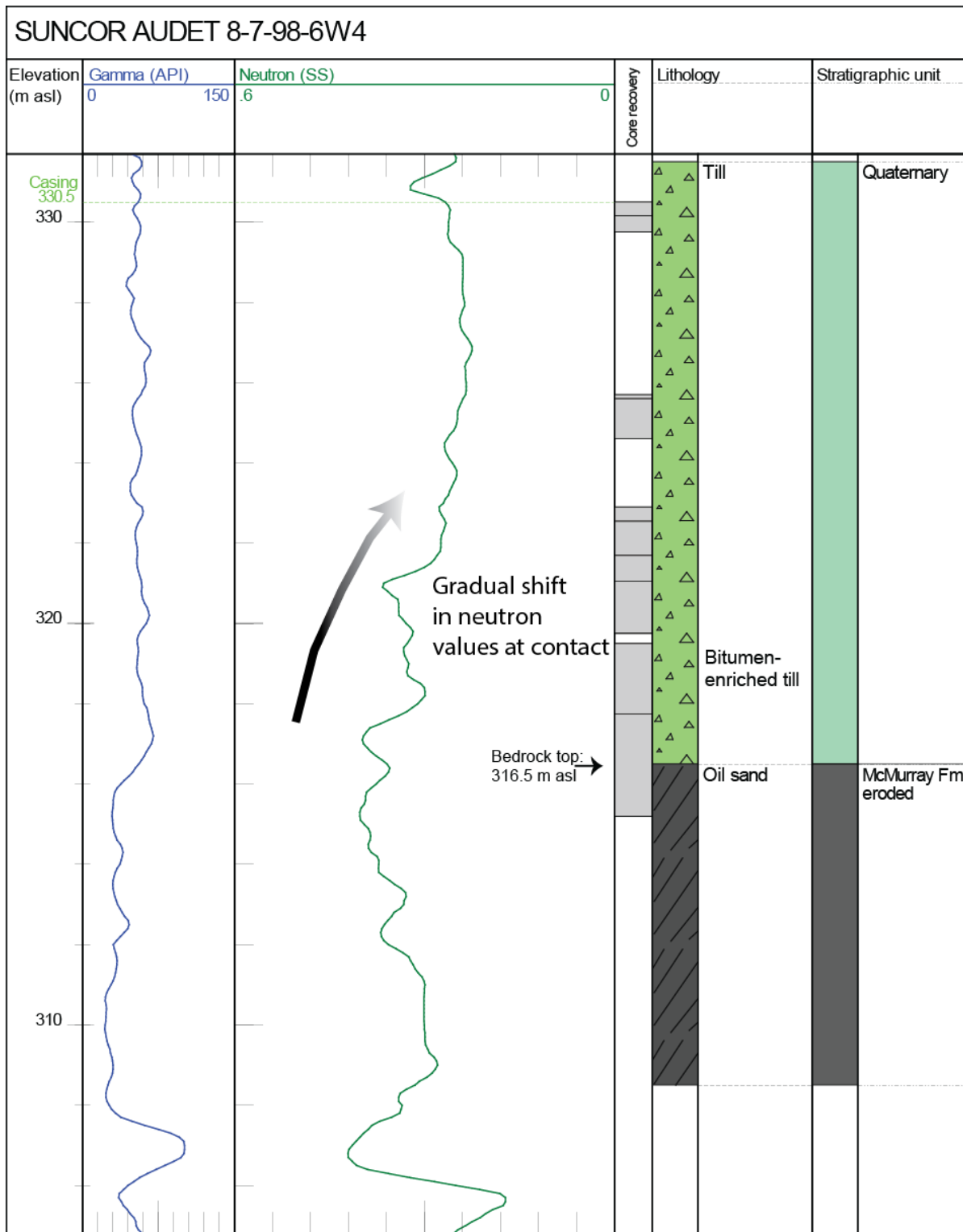


Figure 13. Example of logs where till containing a high content of bitumen becomes progressively less concentrated up-hole from the contact with oil sand (corehole SUNCOR AUDET 8-7-98-6W4, see Figure 6 for corehole location). Rather than an abrupt shift in the neutron porosity curve, the shift is more gradual as the concentration of bitumen in the till matrix decreases up-hole. Litholog determined from examination of core. Abbreviations: Gamma, gamma-ray; Neutron, neutron porosity; SS, sandstone units.

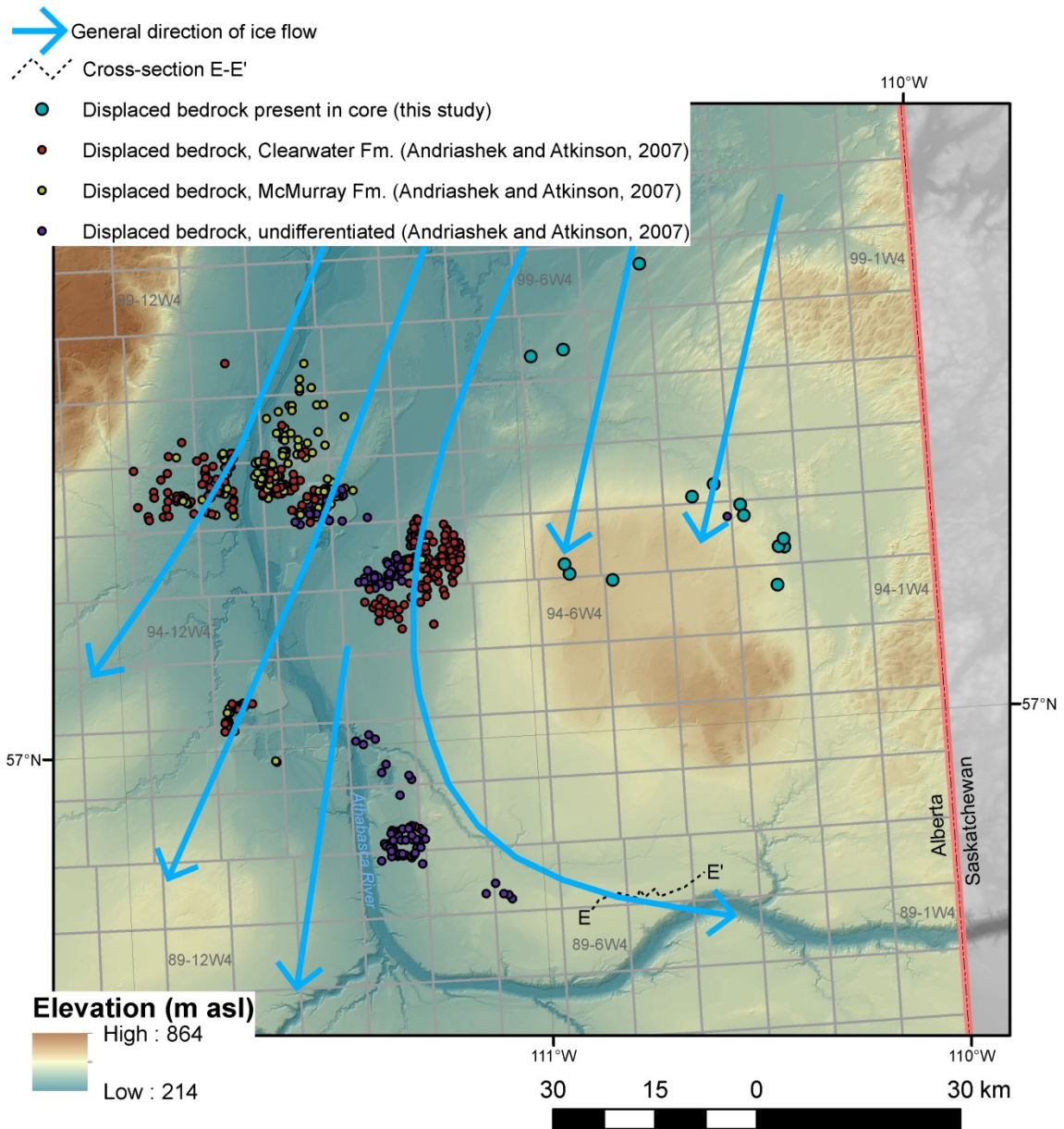


Figure 14. Location of coreholes with displaced bedrock (rafts) evident in cores, determined by this study and by Andriashek and Atkinson (2007), northeastern Alberta. Cross-section E-E' (Figure 31) indicates location of coreholes with logs that reflect displaced bedrock.

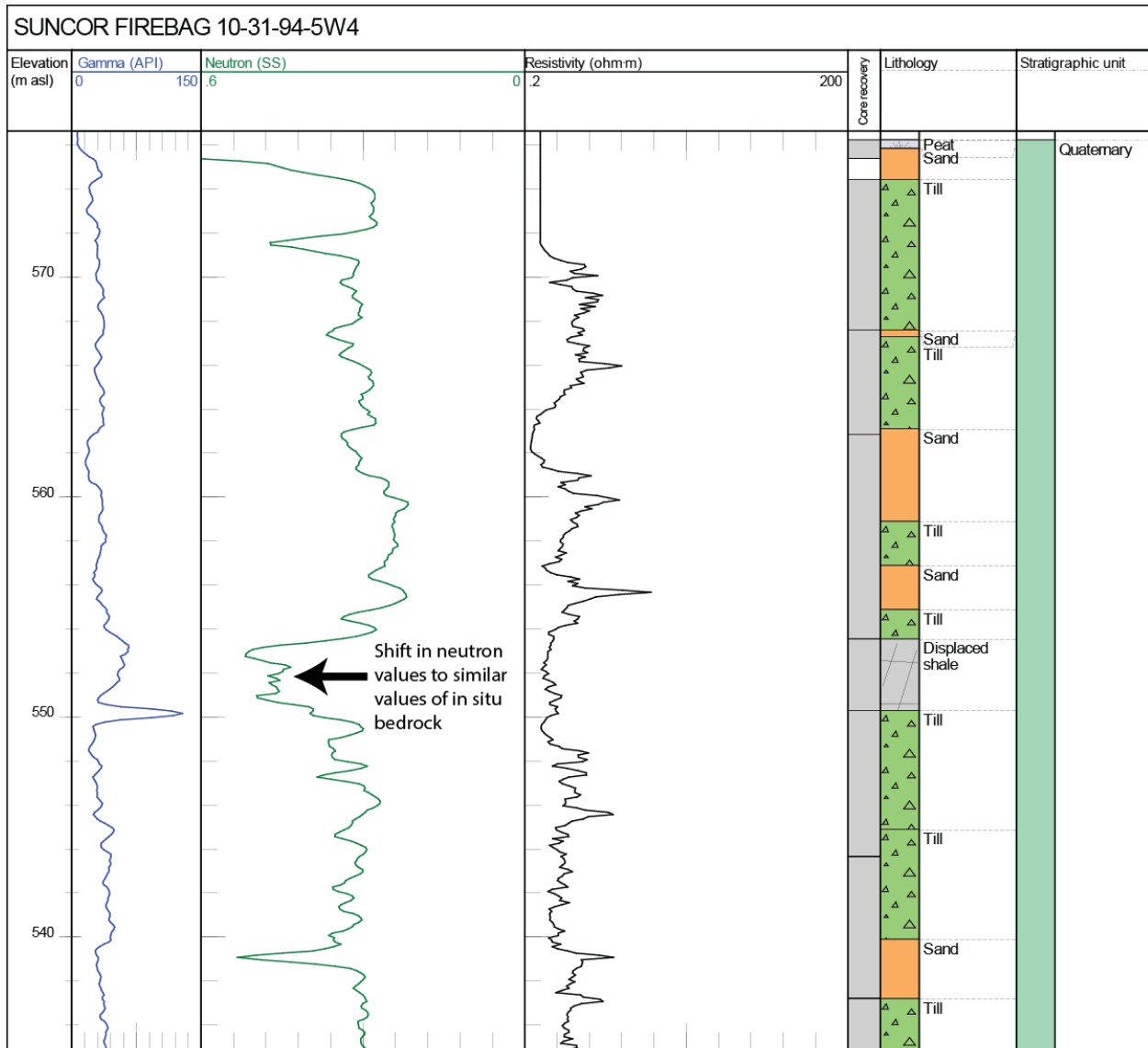


Figure 15. Example of bedrock raft (glacially displaced shale) shown in core logs (SUNCOR FIREBAG 10-31-94-5W4, see Figure 6 for corehole location). Note that the neutron porosity log shifts to higher values (to the left) for the entire thickness of the raft. Litholog determined from examination of core. Abbreviations: Gamma, gamma-ray; Neutron, neutron porosity; SS, sandstone units.

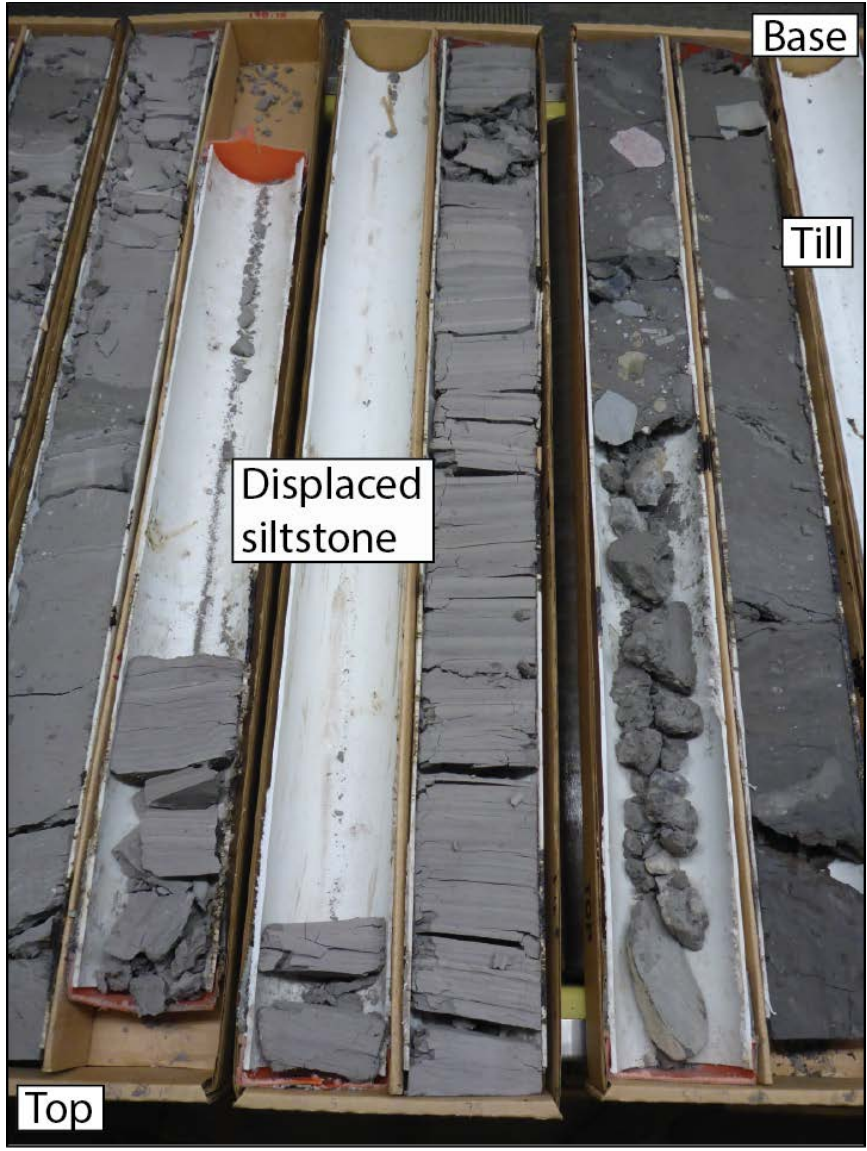


Figure 16. Displaced siltstone overlying dark grey till in corehole TLK FIREBAG 10-4-96-4W4 (176.5–182.0 m depth, 347.0–341.5 m asl, see Figure 6 for corehole location).

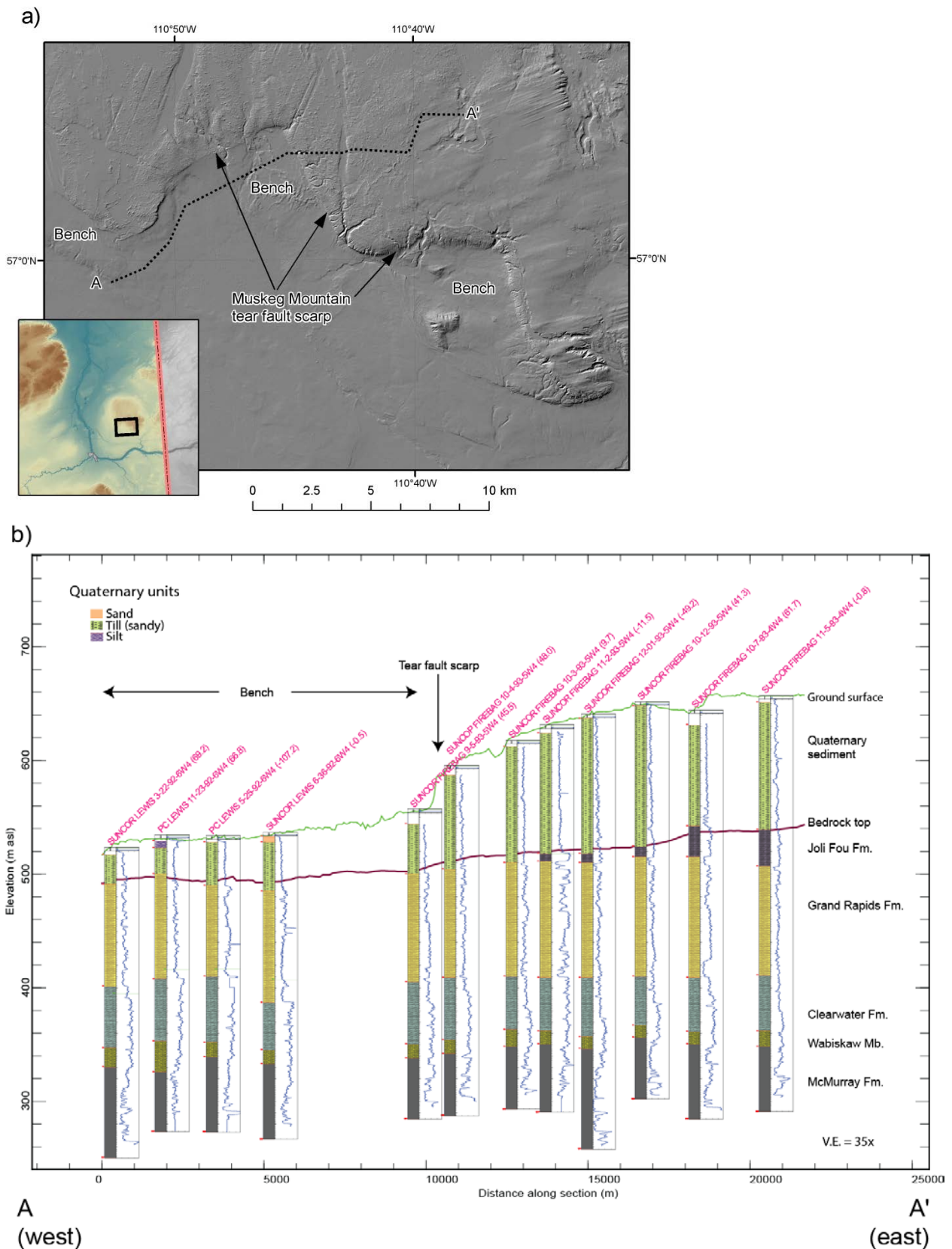


Figure 17. a) LiDAR (light detection and ranging) image with shaded relief of the area previously interpreted to be a glacial tear fault (Andriashek and Atkinson, 2007), northeastern Alberta. **b)** West to east cross-section in the area previously interpreted to be a glacial tear fault (Andriashek and Atkinson, 2007). Note the scarp is approximately 40–50 m in relief, and is interpreted here to occur completely within Quaternary sediments. A 1–2 km wide bench wraps around the southern flank of Muskeg Mountain, and is covered with 10–15 m of sediments. Location of the cross-section is also shown on Figure 27. The number in parentheses following the core name is the distance (in metres) the well is offset from the cross-section line. Abbreviation: V.E., vertical exaggeration.

4.4 Delineation of Bedrock Valleys and Channels

Even with the high density of oil and gas wells in the study area, bedrock valleys and channels may be difficult to locate from borehole data as some are relatively narrow features (hundreds of metres wide), and typically have no surface expression as they are buried by surficial sediments. They are important to delineate because they contain coarse sediments that may potentially form aquifers, which can be important sources of potable water in the region (Andriashek and Atkinson, 2007). Furthermore, depending on the depth of erosion, caprock might be thinned to an extent that compromises safe and efficient recovery of bitumen using steam-enhanced recovery methods.

Previously identified bedrock valleys and channels were located from the interpretation of geophysical logs and numerous geotechnical borehole records from the surface mineable oil sands area (Andriashek and Atkinson, 2007). More recently, airborne electromagnetic (EM) surveys (Dawson et al., 2018) have identified new fluvially incised features (bedrock valleys and channels) in the MacKay Plain, which enables updates to previously mapped fluvially incised features in the region (Andriashek, 2001; Figure 18). For example, the formerly mapped Birch and Willow channels (Andriashek, 2001; Andriashek and Atkinson, 2007) were found to be more extensive than previously defined.

Dawson et al. (2018) defined another new fluvially incised feature, named here the Alder channel, which trends north for about 60 km across the MacKay Plain (Figure 18). Based on log interpretation and shown in cross-section (Figure 19), the Alder channel is interpreted to have been formed by separate erosional events. The flanks of this channel are shallower than the central part of the channel and overlain by till. These are interpreted as multiple-aged terraces of a previously eroded valley originally formed by subaerial drainage before the last glaciation. In contrast to the flanks, the central part of the incised system is defined by a relatively steep-walled channel, suggesting it may have had a glacial meltwater origin, possibly even subglacial. This deeply incised central channel is filled with sand to the elevation of the base of the first bedrock terrace (Figure 19). Based in part on the deep incision, this central channel is interpreted to be subglacial in origin and that subglacial drainage was routed along a pre-existing valley, at least for some period of time. Similarly, Andriashek (2003) interpreted the nearby Birch channel (Figure 18) as subglacial in origin because it is deeply incised (up to 80 m) into the highest part of the bedrock surface, has a low gradient, has a hanging wall geometry at its eastern end, and contains coarse sediments.

In addition to linear highly resistive features interpreted as channels, broad nonlinear areas on the airborne imagery appear highly resistive at, or near, the surface. Based on the thin cover of Quaternary sediments in the area and the subdued topography, these areas are interpreted as sandy bedrock of the Pelican or Grand Rapids formation, which subcrop near the land surface. For example, in the Thickwood Hills (near the Thickwood valley), a 200 km² area of apparently highly resistive material corresponds spatially to the subcrop distribution of the underlying Pelican Formation (Figure 18; Alberta Geological Survey, 2019). Likewise, the larger highly resistive area in the northwestern part of the survey (800 km²; Figure 18) may relate to the near-surface sandier bedrock of the Grand Rapids Formation.

4.5 Compilation of Bedrock Top Picks and Bedrock Topography

Bedrock top picks from geophysical logs (using the criteria defined above), outlines of bedrock channels from the EM surveys, as well as data from previous studies (Kupsch and Olson, 2006; Andriashek and Atkinson, 2007) and environmental assessments (Teck Resources Limited, 2016) were compiled for the study area (Figure 20; Utting, 2020a). These data were subsequently incorporated into an update of the provincial-scale bedrock topography and sediment thickness maps (Figure 21a and b; Alberta Geological Survey, 2020a, b).

These data sources, in addition to the Andriashek and Atkinson (2007) study, enabled mapping of the bedrock surface eastward, to cover all of Muskeg Mountain to the Saskatchewan border, and northward to cover the Firebag Hills and areas beyond the 58th parallel. Furthermore, the incorporation of bedrock channels interpreted from the EM surveys (Dawson et al., 2018) means that the orientation and depth of channels in the western part of the study area are likely more accurate than those mapped in previous studies.

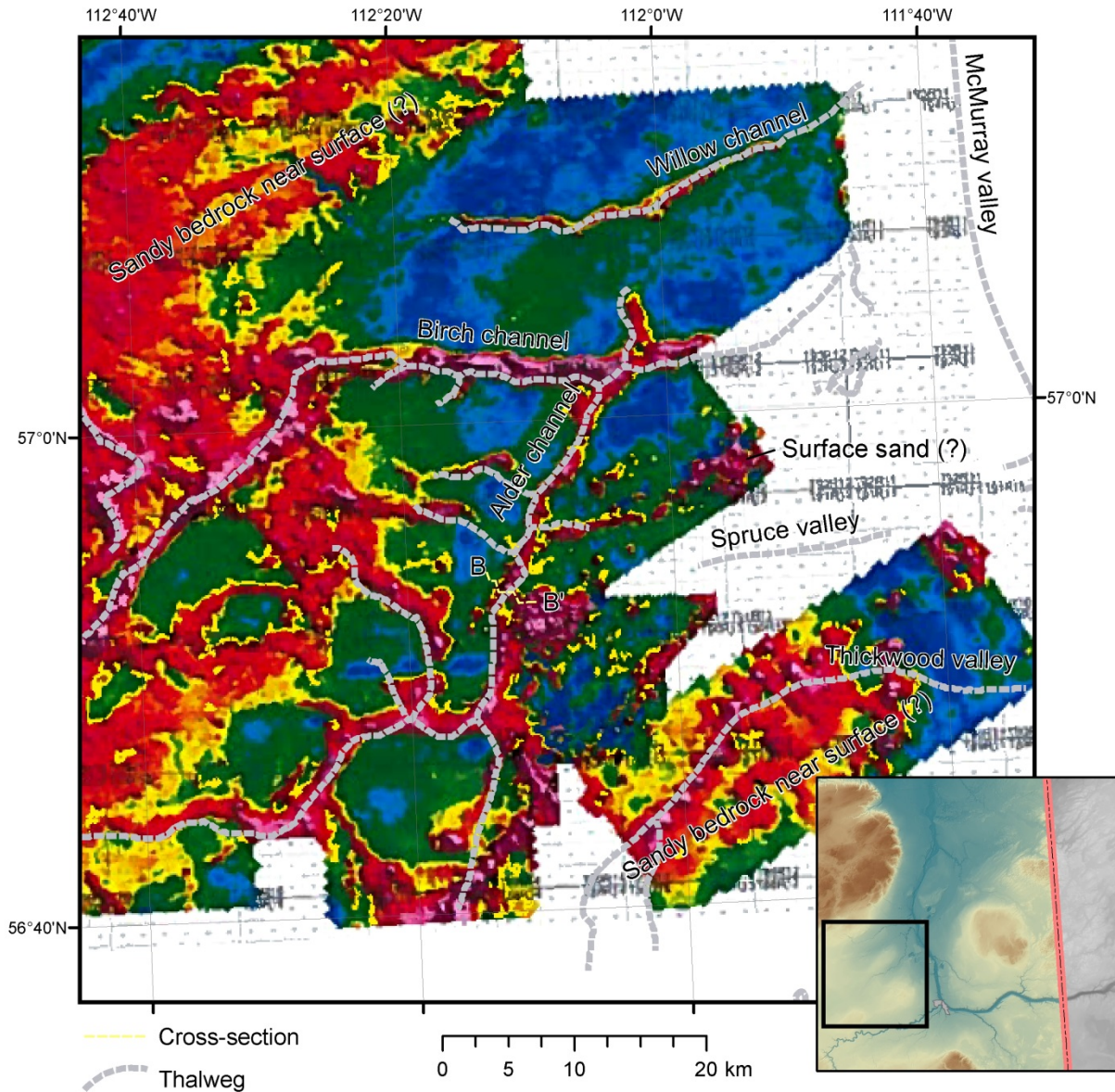


Figure 18. Airborne electromagnetic (EM) surveys (modified after Dawson et al., 2018) used to update the Andriashek (2019) bedrock valley and channel thalweg map (modified from Andriashek, 2019), northeastern Alberta. Pink and red are more resistive compared to blue and green, and are interpreted to be material that is sandier than the surrounding material.

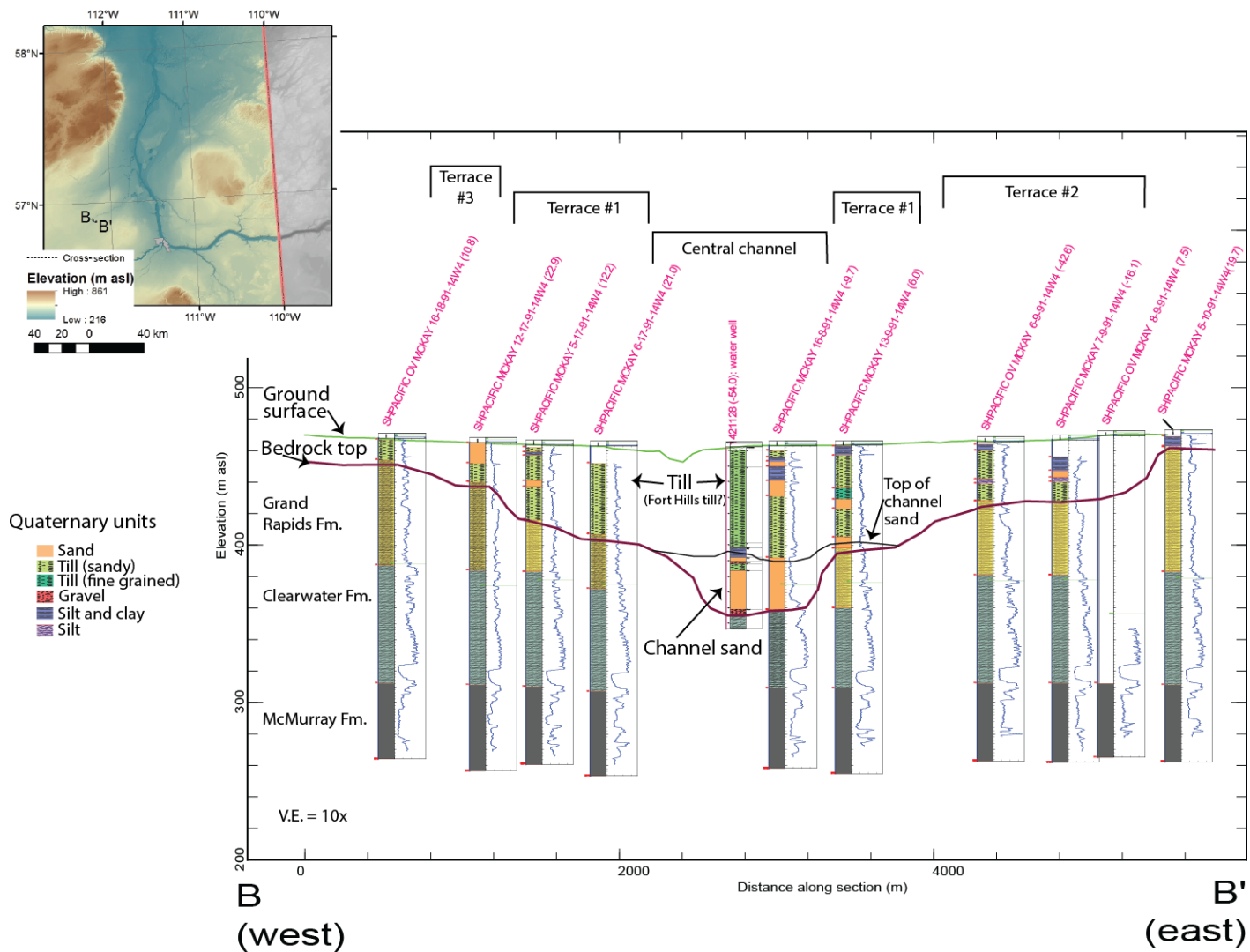


Figure 19. West-east cross-section across the Alder channel on the MacKay Plain, northeastern Alberta. Note the central channel is flanked by terraces overlain by till, and the deepest part of the channel contains ~15 m of sand at the base. Location of the cross-section is also shown on Figure 18. The number in parentheses following the core name is the distance (in metres) the well is offset from the cross-section line. Abbreviation: V.E., vertical exaggeration.

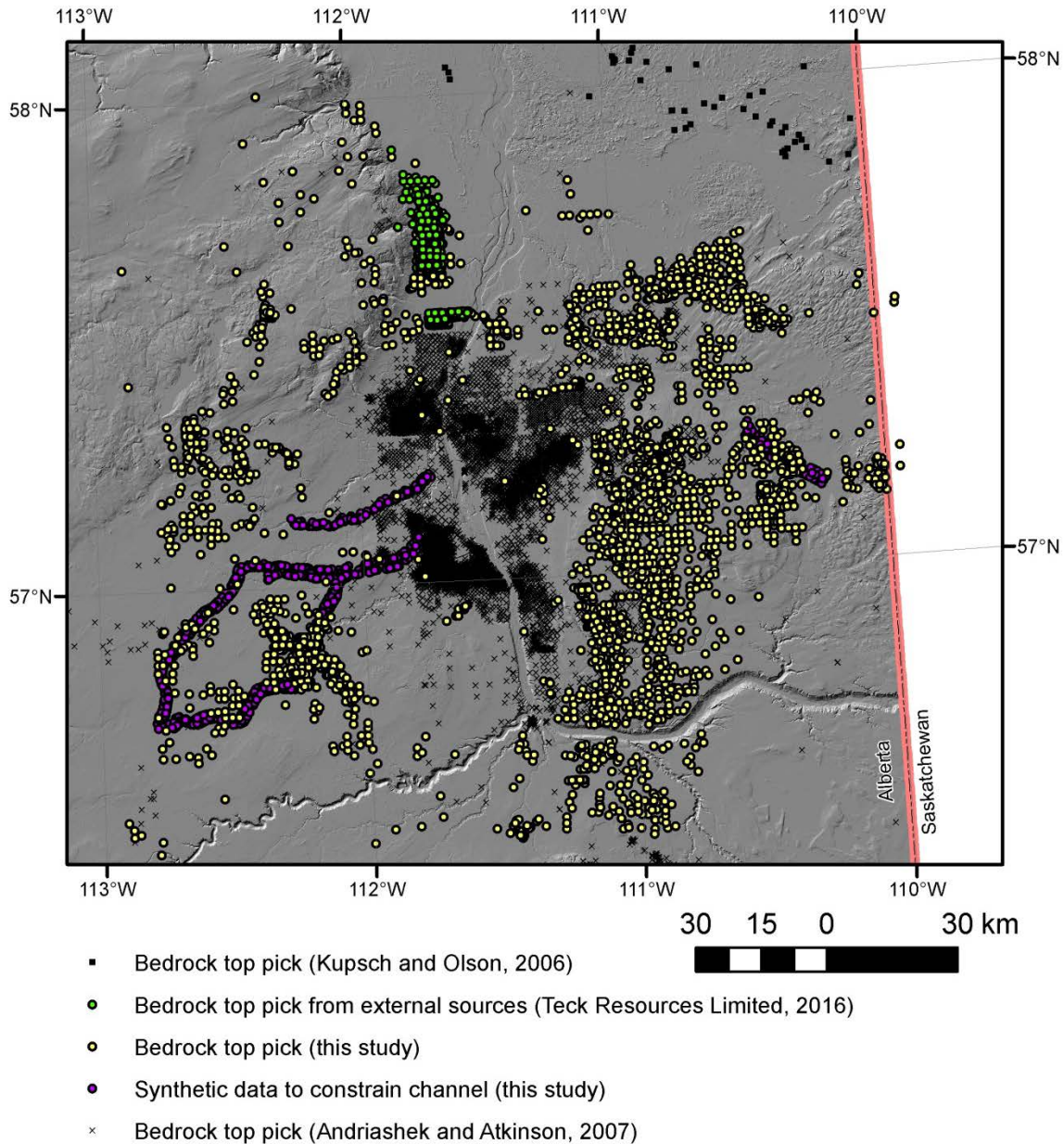


Figure 20. Locations of bedrock top picks, northeastern Alberta. Note the increase in new picks eastward (yellow symbol), since the Andriashek and Atkinson (2007) study, as well as the addition of synthetic picks (purple symbol) to incorporate the bedrock channels. Background is a LiDAR (light detection and ranging) image with shaded relief.

A sediment thickness map (Figure 21b), derived by subtracting values in a digital elevation model (DEM) of the bedrock surface from those in a ground surface DEM, highlights those areas of thickest sediment, including the northern portion of Muskeg Mountain and the Firebag Hills. In these areas, sediments overlying bedrock reaches over 200 m. Conversely, areas of thin sediment are found in the southern portion of Muskeg Mountain, as well as within much of the lowland areas flanking the Athabasca River, with the exception of the area east of Fort McMurray (the Steepbank Plain), the Fort Hills, and the area north of the Firebag River. Thick sediment is also observed within the incised channels on the MacKay, Dover, and Kearl Lake plains.

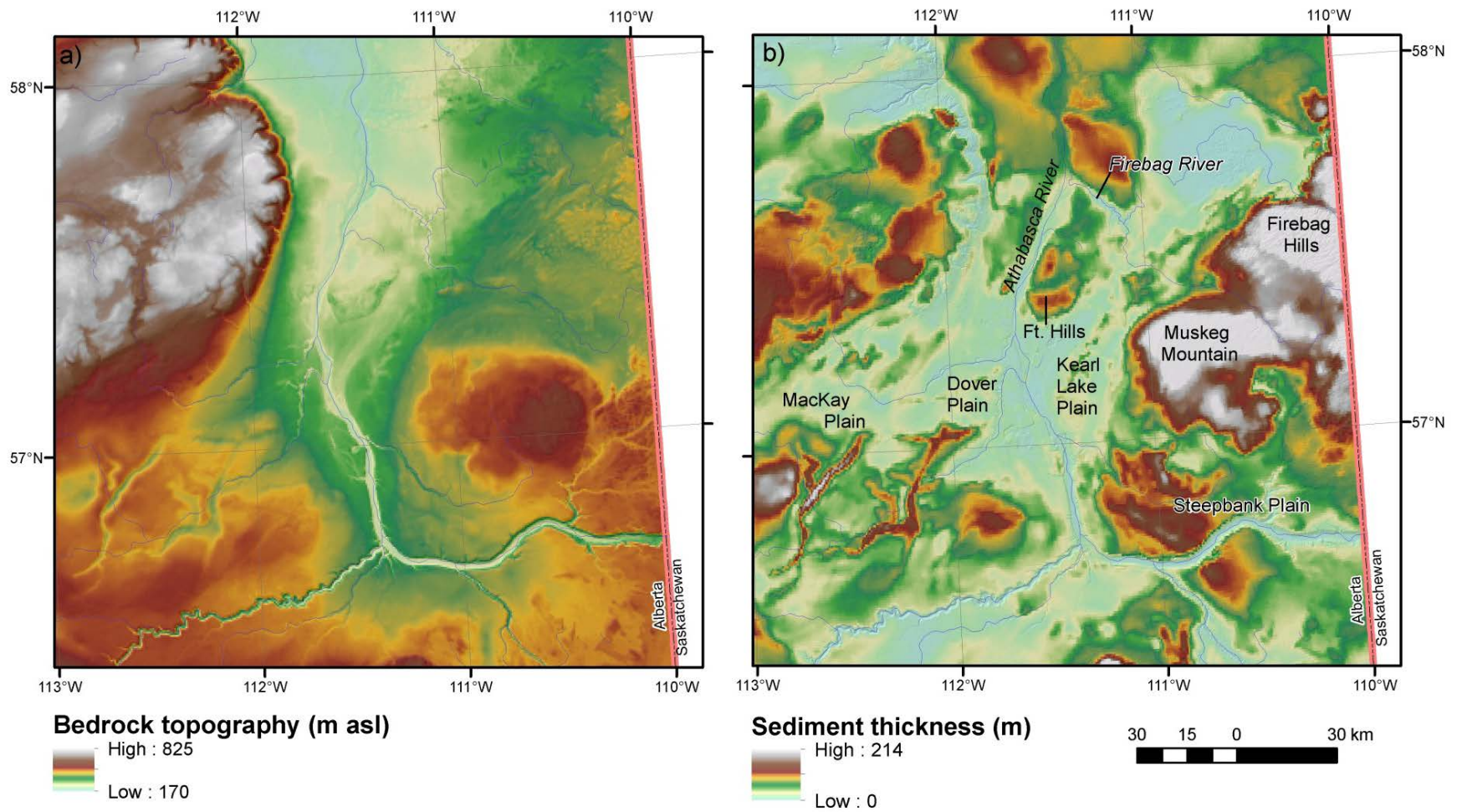


Figure 21. a) Bedrock topography and b) sediment thickness maps of the study area, northeastern Alberta. Rivers shown for geographic reference.

4.6 Till Composition, Differentiation, and Correlation

To understand the differences in geophysical responses of glaciogenic sequences and to further characterize the thick package of sediments resting on the bedrock topography, geochemical and grain size analyses were conducted on samples of glacial sediments from two cores (SUNCOR FIREBAG 10-31-94-5W4, CVE TLK A12 FIREBAG 12-12-95-3W4, Figure 6). Geochemical and grain size analyses have been successfully used to differentiate till units in core (e.g., Andriashek, 2003), which can then aid in correlating geophysical responses of similar sediments in neighbouring wells, thus allowing units to be mapped over a larger area. Cores were selected to be examined based on the length and quality of recovery. Two methods of geochemical analysis were used, ICP-MS on the silt–clay fraction and XRF on the whole sediment, the results are presented in Figures 22 and 23. The complete set of geochemical and grain size data are available in AER/AGS Digital Data 2020-0014 (Utting, 2020b).

Five elements were selected for comparison of the sediments. Calcium (Ca) and magnesium (Mg) were selected as proxies for limestone and dolostone, respectively. Potassium (K) and aluminum (Al) were selected as potential indicators of feldspars derived from metamorphic and igneous rocks in the Precambrian shield. Iron (Fe) was selected because it is commonly tested for in exploration geochemistry. Correlation coefficients (R-values) were calculated for some elements to compare the values derived from the XRF (whole sediment) analysis with results from the ICP-MS (silt–clay fraction) analysis (Table 4).

The results show there is a strong correlation (>0.5) for Al, Mg, and Fe for samples from both cores, Ca is only highly correlated in the SUNCOR FIREBAG 10-31-94-5W4 core, whereas K is weakly correlated in both cores. Because these analyses were done on different grain sizes (whole sediment versus silt–clay fraction), a poor correlation may indicate some elements are preferentially retained in certain grain sizes.

4.6.1 Representative Core: SUNCOR FIREBAG 10-31-94-5W4

The Suncor Firebag corehole (SUNCOR FIREBAG 10-31-94-5W4; Figure 6) is remarkable in that core recovery extends from the peat horizon at surface down into bedrock, providing an almost continuous 136 m thick record of Quaternary sediments in the Muskeg Mountain area. Based on geochemistry (from ICP-MS and XRF), grain size, and geophysical log signatures, five informal till units are evident in the core (Figure 22).

Unit 1 at the base of the core, has a light grey (Munsell colour code 5YR 7/1), fine-grained matrix (55% silt–clay), and high gamma-ray values, suggesting shale as a parent material. The upper part of this unit includes oxidized sand, with high As and Fe values, features that are indicative of pyrite, arsenopyrite, and amorphous iron-oxide concentrations in weathered horizons (Andriashek, 2003; Javad et al., 2014). The till also has moderately high levels of Ca but has no to moderate reaction to 10% HCl acid, suggesting much of the Ca may not be sourced from CaCO_3 .

Table 4. Correlation coefficients (R-values) for selected elements, comparing analysis from X-ray fluorescence (XRF; whole sediment) and inductively coupled plasma–mass spectrometry (ICP-MS; silt–clay fraction) geochemical analyses.

Element	SUNCOR FIREBAG 10-31-94-5W4 Core	CVE TLK A12 FIREBAG 12-12-95-3W4 Core
K	-0.29	-0.02
Al	0.60	0.78
Ca	0.86	0.24
Mg	0.51	0.55
Fe	0.78	0.76

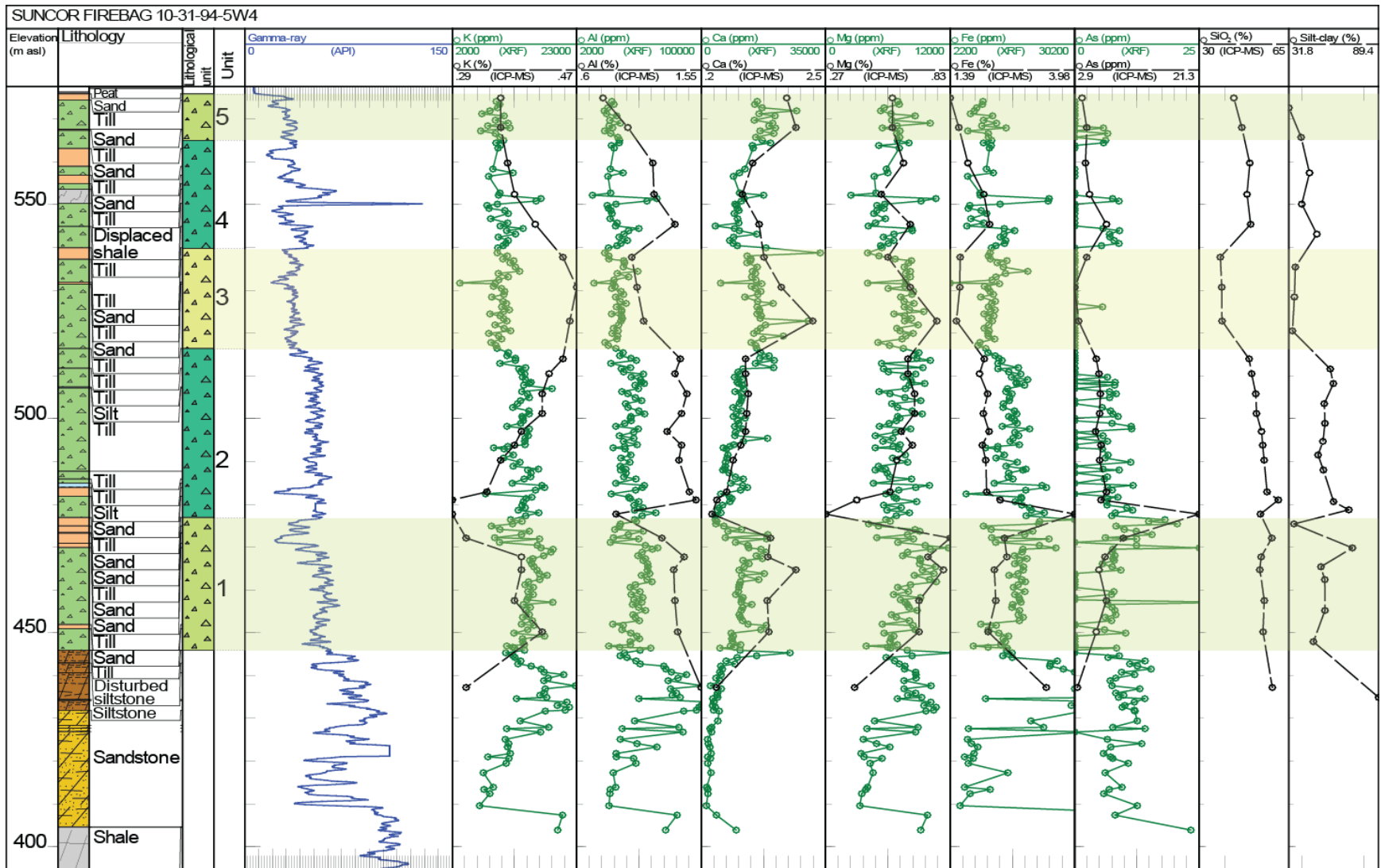


Figure 22. Logs for corehole SUNCOR FIREBAG 10-31-94-5W4, cored from surface. Five till units can be identified in this core, based on geochemistry, grain size, and geophysical logs. Abbreviations: ICP-MS, inductively coupled plasma-mass spectrometry; XRF, X-ray fluorescence.

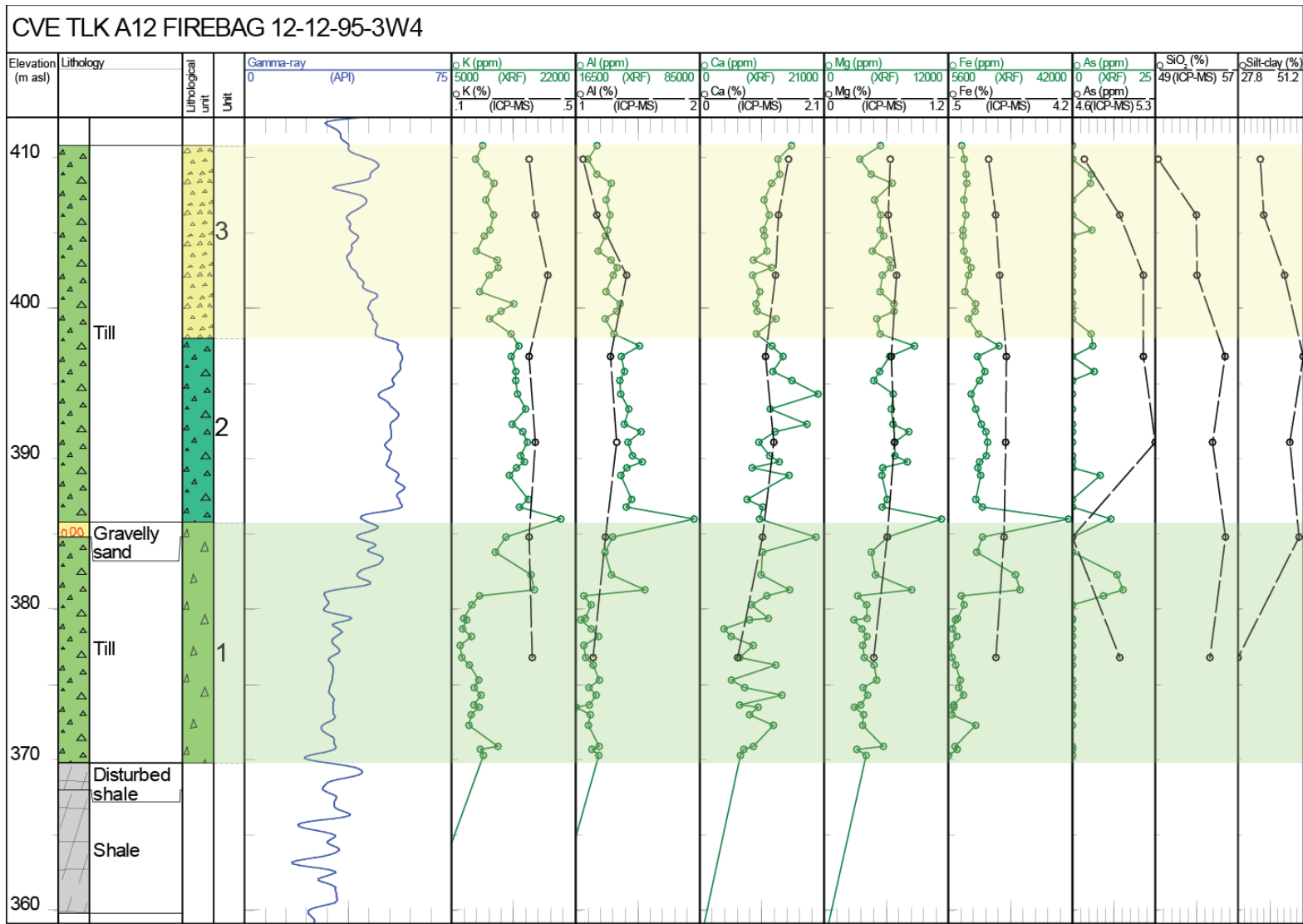


Figure 23. Logs for corehole CVE TLK A12 FIREBAG 12-12-95-3W4 with apparently homogeneous-looking till above bedrock, but with distinct differences in gamma-ray signal. Note coring did not start at surface (kelly bushing at 479.8 m asl), and the gamma-ray scale has been adjusted to 0–75 API units instead of the typical 0–150 API units. Abbreviations: ICP-MS, inductively coupled plasma–mass spectrometry; XRF, X-ray fluorescence.

Unit 2 is similar to unit 1 in concentrations of K, Al, Mg, Fe, and As, as well as the gamma-ray response, grain size (from analyses and core descriptions), and colour (light grey). Delineation of this unit is based on the intervening oxidized horizon suggesting there is a disconformable contact between the units. As well, unit 2 has low Ca values and only a weak reaction to HCl acid.

Unit 3 is differentiated from the underlying units 1 and 2 by a pronounced shift to a lower gamma-ray response, lower values of Al and Fe, higher Ca, and an increase in sand in the matrix (65%). Unit 3 also exhibits a difference in the values of K (Table 4) depending on the analysis method, with lower values in whole sediment analysis using XRF and higher values in the silt–clay fraction analysis using ICP-MS. This may indicate an enrichment of K in the finer fraction, potentially from mica or biotite derived from igneous and metamorphic rocks from the Precambrian shield (Figure 2). Despite these changes, its colour remains light grey, similar to that of units 1 and 2.

Unit 4 has a dark grey (Munsell colour code 5YR 4/1) and a more fine-grained matrix (40–50% silt–clay) than that of the underlying till of unit 3 (35% silt–clay). The fine-grained nature is reflected as an increase in gamma-ray values. The geochemistry values are similar to those of unit 2, except Fe and Mg are lower, and the grain size of the matrix is not as fine.

The uppermost till, unit 5, is light grey (Munsell colour code 5YR 7/1), has high Ca values, a sandy matrix (60% sand), and the lowest gamma-ray values of till in the core. The Fe and As values are low, similar to those for unit 3. Although it has high Ca values, it only reacted weakly to HCl acid.

4.6.2 Representative Core: CVE TLK A12 FIREBAG 12-12-95-3W4

Core CVE TLK A12 FIREBAG 12-12-95-3W4 (Figure 6) starts ~70 m from the surface (Figure 23), and includes about 40 m of till that, by visual inspection, appears similar in colour (light grey, Munsell colour code 5YR 7/1) and texture (pebbly sandy-silt diamict) throughout (Figure 24). However, three units can be delineated in this core based on geophysical logs, grain size analysis, and geochemical analysis (Figure 23). Gravelly sand marks the boundary between the lowest till (unit 1) and the overlying unit 2 till. From the whole rock XRF analysis, K values are lower in unit 1 than in unit 2 (though this is not reflected in the K values derived from the silt–clay fraction using ICP-MS). Based on gamma-ray response and percent sand values (68%), unit 1 is also the coarsest of the three till units.

In addition to higher K values, unit 2 has correspondingly higher Al, Ca, Mg, and gamma-ray values. Unit 2 also has a finer matrix, with the silt–clay fraction increasing to 50%. Compared with unit 2, the uppermost part of unit 3 has a lower gamma-ray response, and has a coarser grain size (57–65% sand), appearing similar to unit 1, except for having higher Ca values.

Visual examination of the CVE TLK A12 FIREBAG 12-12-95-3W4 core suggested one homogeneous till unit (Figure 24), however, the variability of the geophysical logs suggested there were other controls on the response besides grain size. The analytical results confirm that even though there is a small change in measured grain size (Figure 23), there are demonstrable differences in the concentration of Fe, K, Ca, Mg, and Al. These differences may indicate a change in the composition of the source bedrock, reflecting shifting ice-flow patterns. The variation in the gamma-ray signature in this core may be as much the result of differences in geochemistry as it is in grain size, and serves as a reminder that gamma-ray logs measure the count of natural gamma-ray emissions, rather than measure the grain size.

5 Quaternary Stratigraphic Domains

In the study area, six geographic areas were distinguished with the expectation that the Quaternary stratigraphic sequences in each of the areas might be similar (Figure 25). These Quaternary stratigraphic domains were delineated based on an understanding gleaned from representative cores (see Section 4.6), thousands of geophysical logs without core, exposures in the field, surface geomorphology, sediment thickness, and previous work. General geographic areas with similar Quaternary stratigraphic sequences serve to simplify the classification and discussion of regionally variable geological sediments.

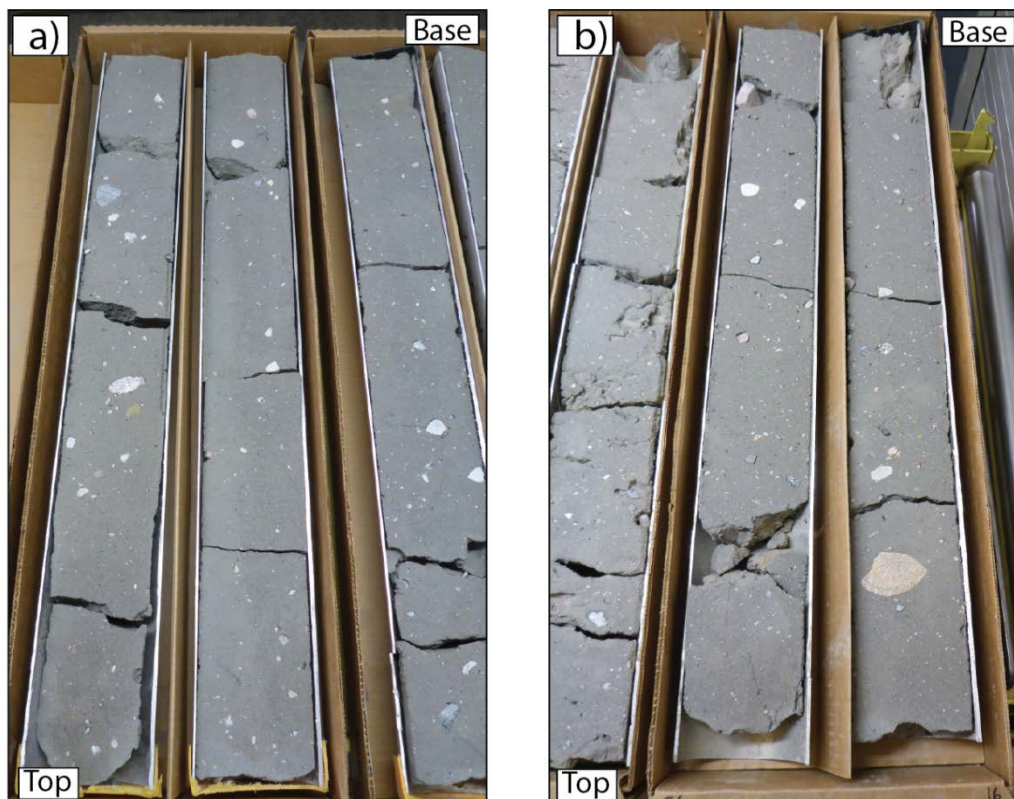


Figure 24. Similarity in appearance of unit 3 and unit 2 tills within CVE TLK A12 FIREBAG 12-12-95-3W4 core: a) unit 3 (75.4–80.27 m depth; 404.4–399.53 m asl); b) unit 2 (87.0–88.5 m; 392.8–391.3 m asl). Core boxes are 0.9 m long.

5.1 Muskeg Mountain Domain

Multiple till units, in an up to 200 m thick Quaternary succession, characterize the Muskeg Mountain domain. These till units were identified in core SUNCOR FIREBAG 10-31-94-5W4 and can also be recognized in geophysical logs from surrounding wells on Muskeg Mountain (Figure 26). It is apparent that units defined from the core can be traced on geophysical logs at least 5 km from the cored well. A lower sand unit rests on bedrock north of the cored well and extends laterally about 5 km to corehole SUNCOR FIREBAG 9-19-95-5W4.

Based on the descriptions of till stratigraphies in the literature (Tables 2 and 3), a correlation between those units and the Quaternary units described in the complete record of Quaternary sediments in core SUNCOR FIREBAG 10-31-94-5W4 is proposed here for the Muskeg Mountain domain.

The distribution of the Fort Hills till (MacPherson and Kathol, 1977; see Section 2.4), which is confined to the lowlands (outside of this domain) and western flank of Muskeg Mountain (Figure 1), precludes it from being present in this core. The corehole site does, however, correspond to an area mapped by Bayrock (1971) as covered by Gipsy till and by McPherson and Kathol (1977) as covered by the Firebag till (Figure 27). Based on the geomorphology and distribution of glacial landforms, it appears the Firebag till is the younger of these two tills. On the basis of its stratigraphic position (at surface) and high Ca values (interpreted to represent high carbonate content in this material), unit 5 is correlated with the Firebag till (Table 5). The sand unit recorded within unit 4 (Figure 26) may relate to the sandy Gipsy till. Because of the differences in the till units, it seems unlikely that the thickening of glacial sediments in this area is a result of thrusting of imbricate slabs (cf. Andriashek and Atkinson, 2007), but rather multiple tills from different ice-flow events.

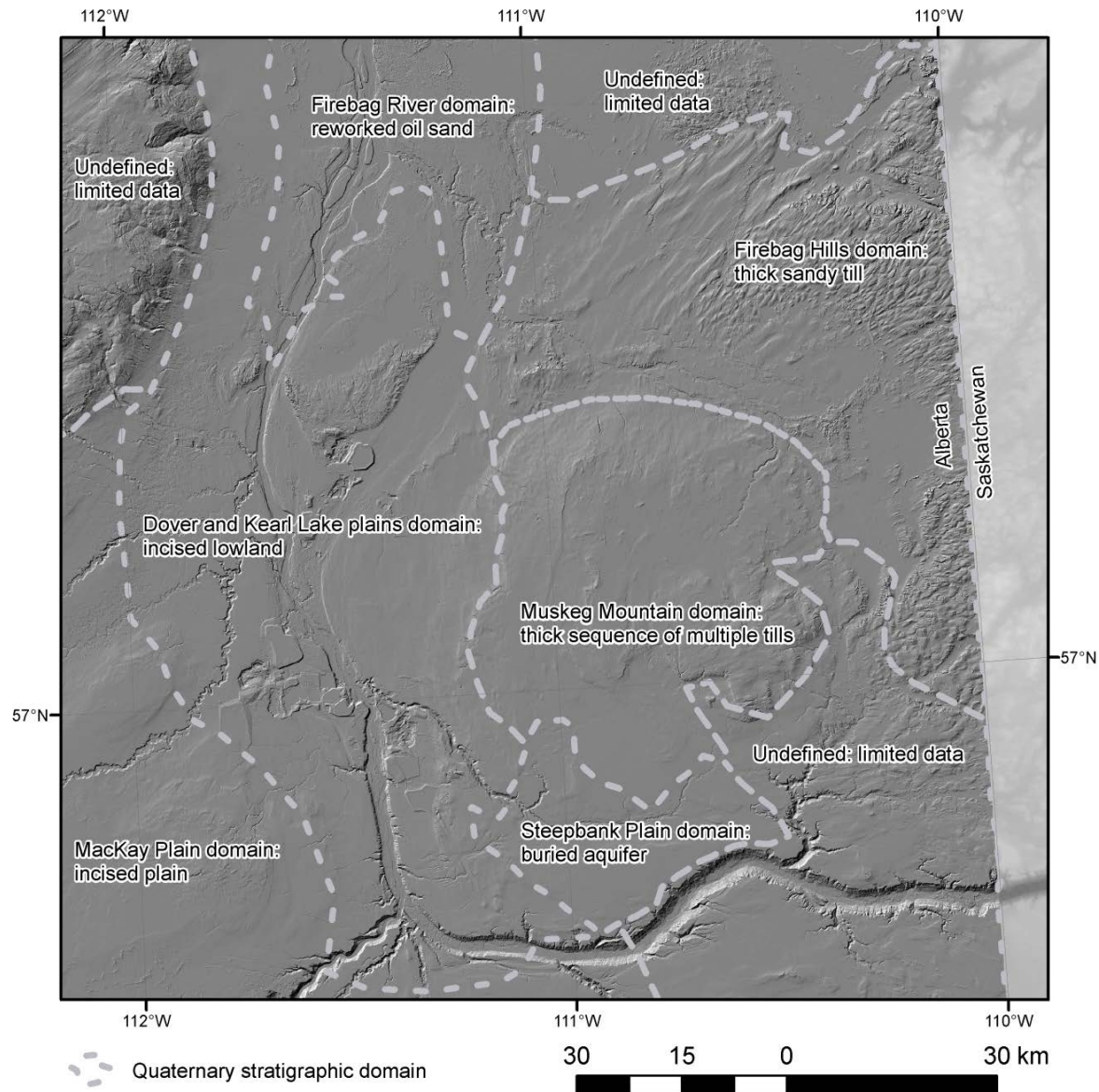


Figure 25. Map of Quaternary stratigraphic domains within the study area, northeastern Alberta. Background is a LiDAR (light detection and ranging) image with shaded relief.

Table 5. Possible correlations between till units in core SUNCOR FIREBAG 10-31-94-5W4 and previous stratigraphic nomenclature (Bayrock, 1971, 1974; McPherson and Kathol, 1977).

	Corresponding Unit	Rationale
Units 4, 5	Unit 5 equates to Firebag till; Gipsy till may correspond to sand bed near top of unit 4	High carbonate content, coarse matrix, displaced shale rafts
Unit 3	Kinosis till or unnamed till	High sand content
Unit 2	Horse River till	Fine grained
Unit 1	None	Related to advance phase (high carbonate content), or possible earlier glaciation. May be similar in nature to Marie Creek Formation, which is an earlier glacial unit separated by glaciofluvial material and is carbonate rich (Table 1).

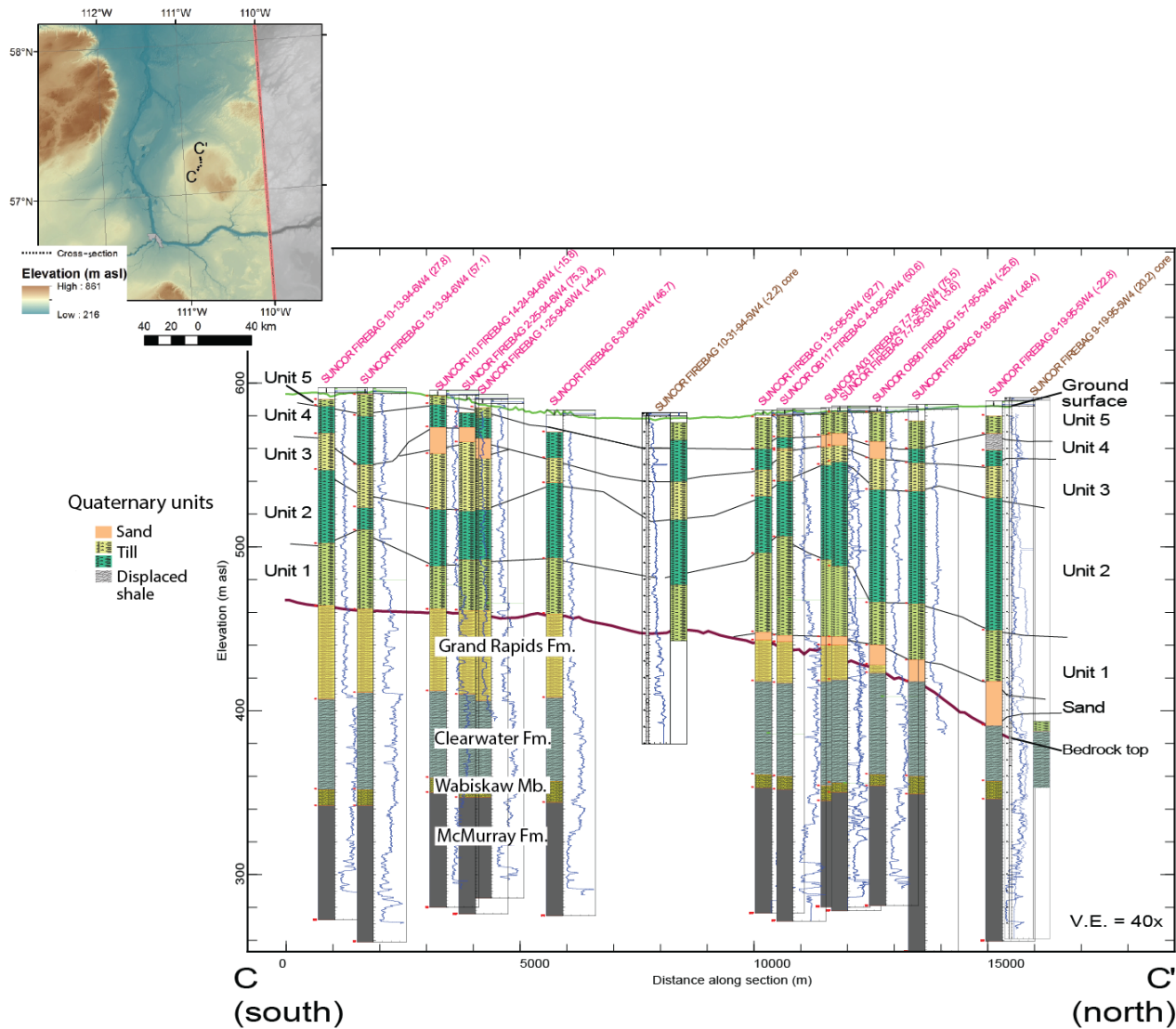


Figure 26. South-north cross-section centred at corehole SUNCOR FIREBAG 10-31-94-5W4 on Muskeg Mountain, northeastern Alberta. Units 1 to 5 identified in the core can be traced on geophysical well logs for kilometres to the north and south. Location of the cross-section is also shown on Figure 27. The number in parentheses following the core name is the distance (in metres) the well is offset from the cross-section line. Abbreviation: V.E., vertical exaggeration.

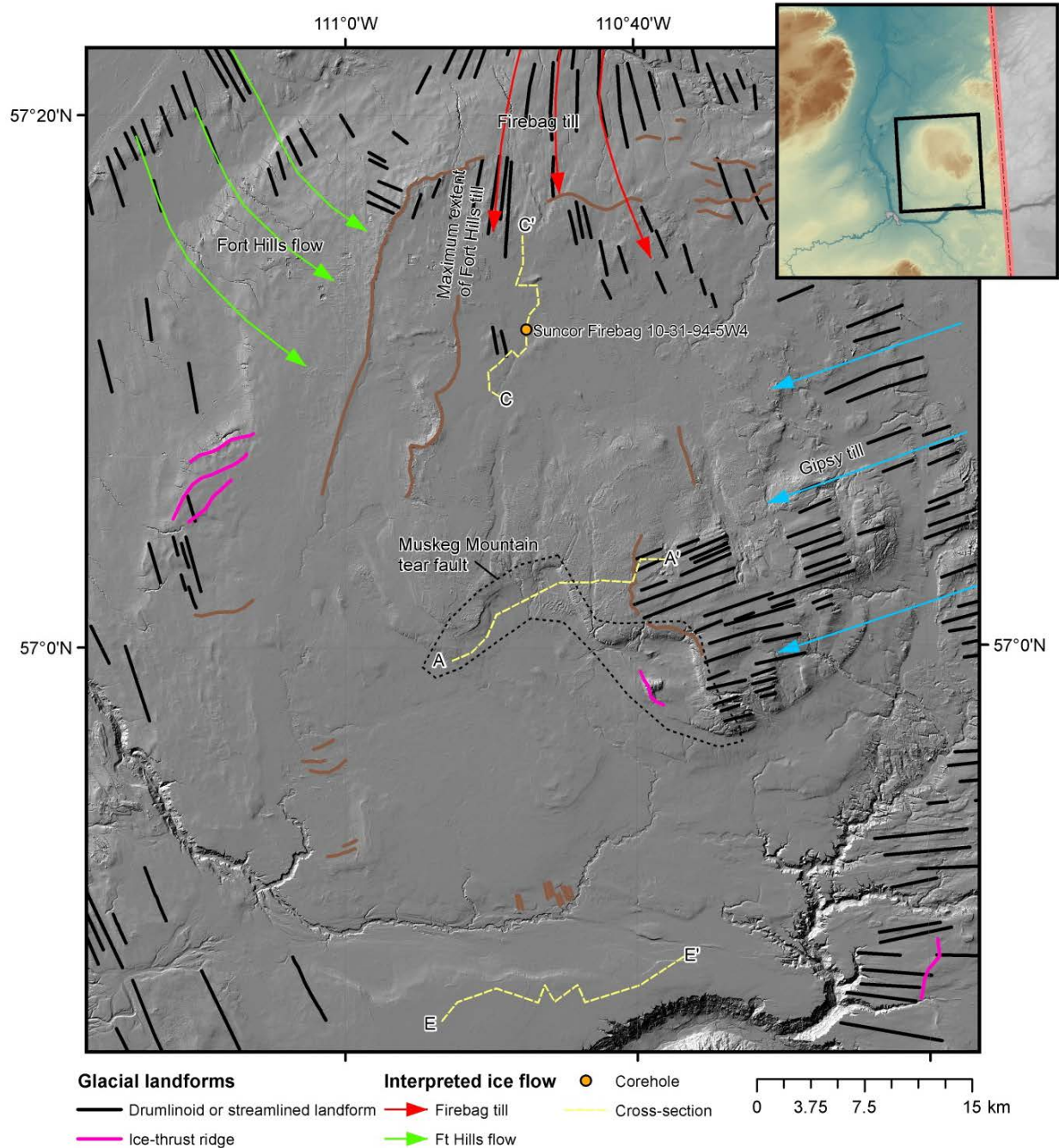


Figure 27. Location of SUNCOR FIREBAG 10-31-94-5W4 corehole in relation to glacial ice-flow patterns on Muskeg Mountain, northeastern Alberta. The Fort (Ft) Hills till relates to a glacial readvance ('Fort Hills flow'), which likely reached as far as the north-trending moraine on the western flank of Muskeg Mountain (McPherson and Kathol, 1977). The Gipsy till was mapped by Bayrock (1971, 1974) and the Firebag till by McPherson and Kathol (1977). Glacial ice-flow features are from Atkinson et al. (2014). Locations of cross-sections A–A', C–C', and E–E' are shown. Background is a LiDAR (light detection and ranging) image with shaded relief.

Unit 3 is tentatively correlated with the Kinosis till of Bayrock (1974), or the unnamed till of McPherson and Kathol (1977). Unit 3 has textural characteristics similar to these tills, although the Kinosis till was previously reported to be only at the surface.

Unit 2 is potentially correlative with the Horse River till, as both have similar textural characteristics. Although, as with unit 3, this till (unit 2) may not correlate with surface deposits and may relate to deposition by older ice-flow events. Nevertheless units 2 to 5 are likely deposited during the last glaciation, thus they are equivalent to the Grand Centre Formation in the 'Cold Lake stratigraphy' of Andriashek and Fenton (1989), which also has texturally distinct members (Table 1 and Figure 4). Unit 1 does not correlate with the previously identified tills in the area, and is separated from overlying tills by an oxidized horizon. It is therefore suggested that unit 1 relates to an earlier advance phase, or is from an earlier glaciation. A similar carbonate-rich till, the Marie Creek Formation, lies beneath glaciofluvial material in the Cold Lake area (Andriashek and Fenton, 1989) and this formation also has been correlated with an earlier glaciation (Table 1).

5.2 Firebag River Domain

The Firebag River domain flanks the Athabasca River in the northern end of the study area (Figure 25). It is characterized by the presence of reworked McMurray Formation oil sand resting on till. This is evident at a section on the Firebag River (Figure 28), which shows the typical sediment types in the Firebag River domain. The section reveals as much as 6 m of surficial cross-bedded glacial sand with beds of bitumen-rich sand. Beneath this sand unit is a 1–2 m thick bed of pink silty glaciolacustrine clay, which locally includes cobbles, pebbles, and thin beds of grey silty clay. This pink clay overlies 6 m of grey silty clay till. In a nearby section, Andriashek and Atkinson (2007, Figures 75–77) reported similar stratigraphy, but describe a 0.6 m thick gravel bed at the base of the upper sand unit.



Figure 28. Section of bitumen-rich glacial sand overlying pink stratified sediments above grey till along Firebag River, northeastern Alberta. Location shown on Figure 29.

The bituminous sand is interpreted to be reworked McMurray Formation, eroded south of the section, possibly in the channel next to the Fort Hills during the northward drainage of glacial Lake Agassiz (Woywitka et al., 2017; Figure 29). The pink sediments are interpreted to be of glaciolacustrine origin, likely relating to a deglacial lake dammed in the valley by retreating ice to the north. Based on its colour, texture, stratigraphic position, and geographic location, these glaciolacustrine sediments are presumed to be related to an ice dam created by the Fort Hills ice flow (Table 2; Figures 27 and 29). The lowermost unit in the Firebag River section is till that is similar in appearance, texture, and gamma-ray response to unit 2 in the Muskeg Mountain domain, and is tentatively correlated with the Horse River till.

A sedimentary sequence similar to the Firebag River section is also present in corehole Silverbirch 2-5-101-7W4, located about 10 km to the north of the section (Figure 29). A thin lower till with a relatively high gamma-ray response at the base of this core is overlain by pink sediments, which also have a high gamma-ray response. These sediments, in turn, are overlain by bituminous sand with a low gamma-ray response. From adjacent well logs, it appears that this stratigraphy can be traced across the region for at least 25 km west to east (Figure 30). In some wells the lower till is not present; nevertheless, the occurrence of the sand unit (low gamma-ray response) in several wells and sections suggests this deposit is present across a larger area (see inferred extent of reworked oil sand, Figure 29).

5.3 Steepbank Plain Domain

The stratigraphy in the Steepbank Plain domain south of Muskeg Mountain, interpreted from geophysical logs, generally consists of sand resting directly on the Grand Rapids Formation. This sand contains rafts of displaced shale and is overlain by sandy till (Figure 31). This sequence of material resting on bedrock is up to 100 m thick. The rafts of shale are likely composed of numerous discontinuous pieces, but generally occur at similar elevations (~440 m asl) over 15 km.

Andriashek and Atkinson (2007) reported an extensive buried aquifer within the western portion of the Steepbank Plain domain. Although not modelled, the limited data suggest this potential aquifer extends farther east over much of the Steepbank Plain domain. Based on its stratigraphic position, the basal sand is interpreted as the Empress Formation and may represent preglacial flow or fluvial reworking of sandstone from the Grand Rapids Formation. The shale rafts are likely a result of subglacial erosion and transport. This sequence is overlain by till, which may correlate with sediments deposited by the Fort Hills ice flow (Figure 27).

5.4 MacKay Plain Domain

In general, the MacKay Plain domain is covered with relatively thin surficial material (10–20 m), mostly till and glaciolacustrine sediments, which rests on bedrock. In places, the bedrock surface has been incised with up to 80 km long channels, which are buried. The till in this area was reported by Bayrock (1971) to be Horse River till (Table 3). However, from geophysical logs (Figure 19) it appears that the till texture is coarser than that described for the Horse River till, which has a much more clayey matrix. In addition, the position of this area down-ice from the Fort Hills ice flow (Figure 27) suggests that the till in the area may correlate with the Fort Hills till (McPherson and Kathol, 1977). Airborne EM surveys of the MacKay Plain area (Dawson et al., 2018) were used to delineate a number of buried bedrock channels (see Section 4.4; Figure 18). Two main channels recognized in the area, the herein named Alder channel and the Birch channel, contain thick valley-fill sand that is capped by till and glaciolacustrine sediments (Andriashek, 2001). Because of the apparent bedrock terraces flanking the most deeply incised portion of the Alder channel, it is suggested that some segments of the Alder channel may have been incised into a preglacial valley.

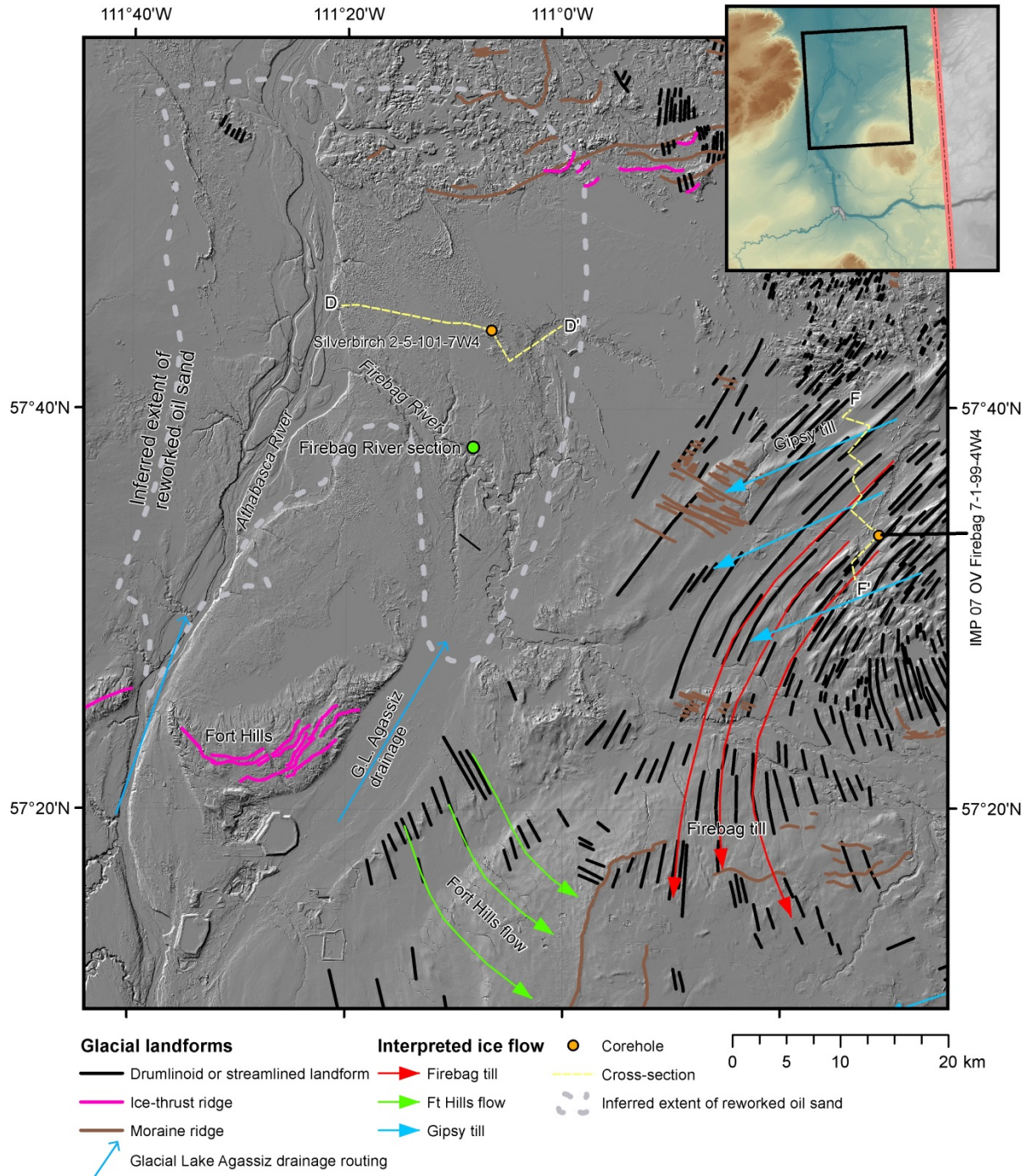


Figure 29. Location of Firebag River section and cross-sections D–D' and F–F' in relation to glacial ice-flow patterns, northeastern Alberta. The continuation of the Fort (Ft) Hills ice flow, the Firebag till, and the Gipsy till are shown on Figure 27. Glacial Lake (G.L.) Agassiz is thought to have drained northward along the present Athabasca River, as well as within a higher elevation channel to the east, along the eastern flank of the Fort Hills. Glacial ice-flow features are from Atkinson et al. (2014). Background is a LiDAR (light detection and ranging) image with shaded relief.

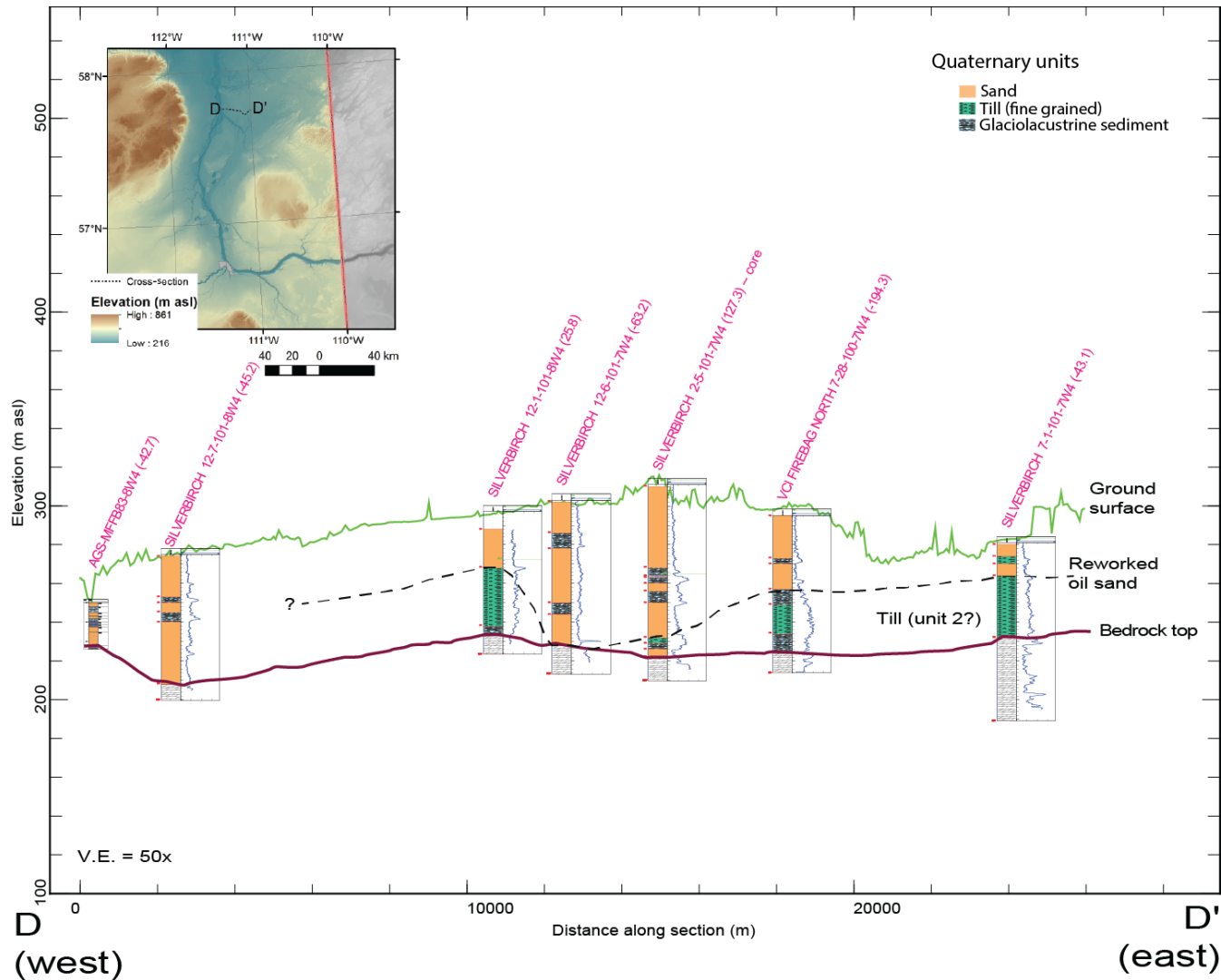


Figure 30. West-east cross-section north of the Firebag River on the Embarras Plain (Figure 1), northeastern Alberta. Location of the cross-section is also shown on Figure 29. Pink sediments with overlying reworked bituminous sand seen in the Firebag River section (Figure 28) may also be present in several holes (Silverbirch 12-1-101-8W4, Silverbirch 7-28-100-7W4, Silverbirch 7-1-101-7W4, Silverbirch 2-5-101-7W4). The number in parentheses following the core name is the distance (in metres) the well is offset from the cross-section line. Abbreviation: V.E., vertical exaggeration.

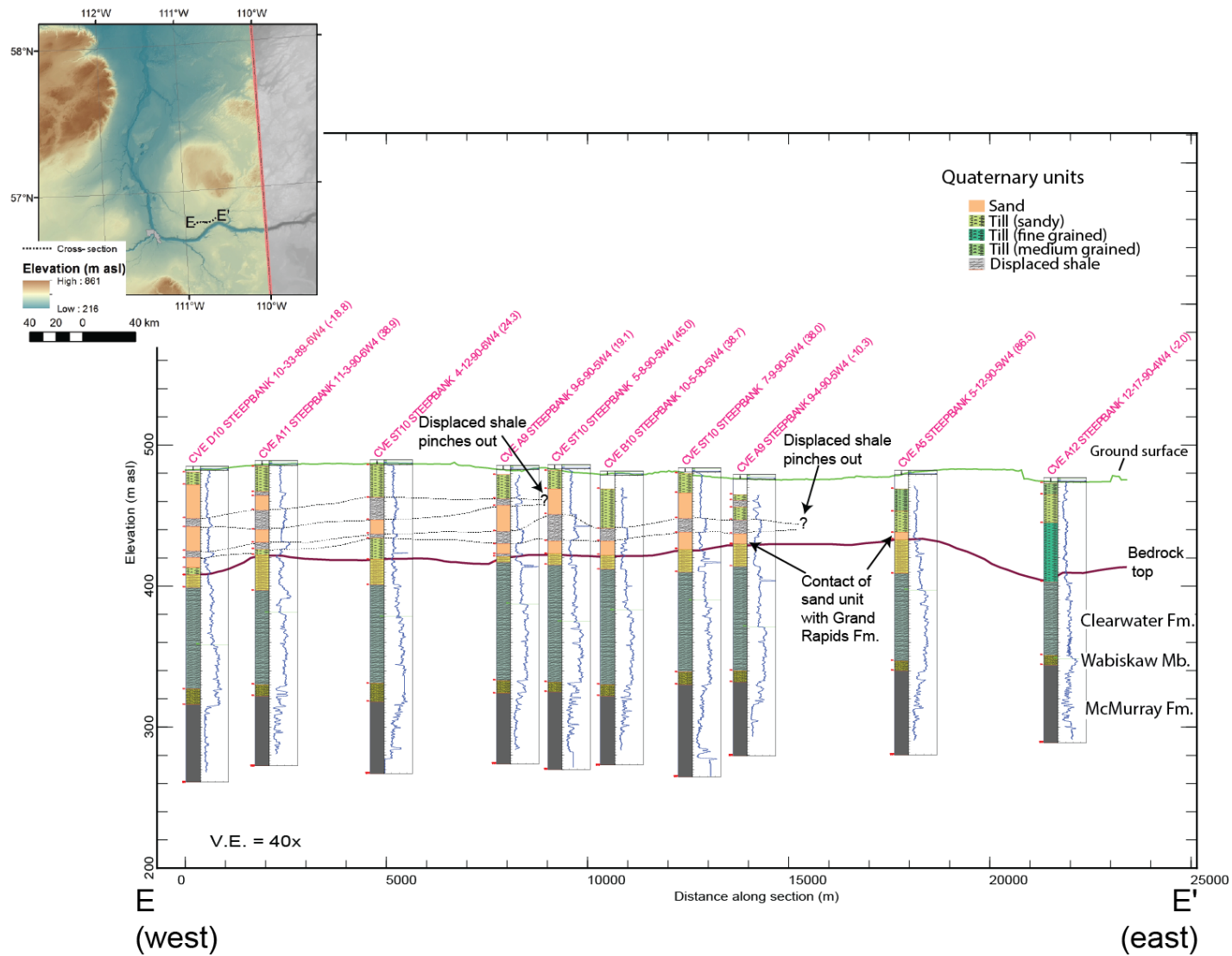


Figure 31. West-east cross-section in the Steepbank Plain domain highlighting the occurrence of sand resting on sandstone of the Grand Rapids Formation, northeastern Alberta. Note the two rafts of displaced shale embedded within the sand. Location of the cross-section is also shown on Figure 27. The number in parentheses following the core name is the distance (in metres) the well is offset from the cross-section line. Abbreviation: V.E., vertical exaggeration.

5.5 Firebag Hills Domain

Corehole IMP 07 OV FIREBAG 7-1-99-4W4 in the Firebag Hills domain reveals a stratigraphy consisting of a surface sandy till overlying fine-grained till (Figure 32), underlain by a repeating sequence of sand and fine-grained till resting on bedrock (Figure 33). This stratigraphic sequence can be recognized in geophysical logs from wells spanning a distance of more than 15 km (Figure 34), and is 50 to 180 m thick (Figure 21b).

The underlying fine-grained till in corehole IMP 07 OV FIREBAG 7-1-99-4W4 is similar in gamma-ray response and appearance to unit 2 till in corehole SUNCOR FIREBAG 10-31-94-5W4, as well as the till exposed in the Firebag River area, and is similarly interpreted as Horse River till. Based on its sandy texture, the upper till reported in corehole IMP 07 OV FIREBAG 7-1-99-4W4 is interpreted to be Gipsy till.



Figure 32. Example of sandy surface till in the Firebag Hills domain in core IMP 07 OV FIREBAG 7-1-99-4W4 (21.2–22.7 m depth, 399.8–398.3 m asl).

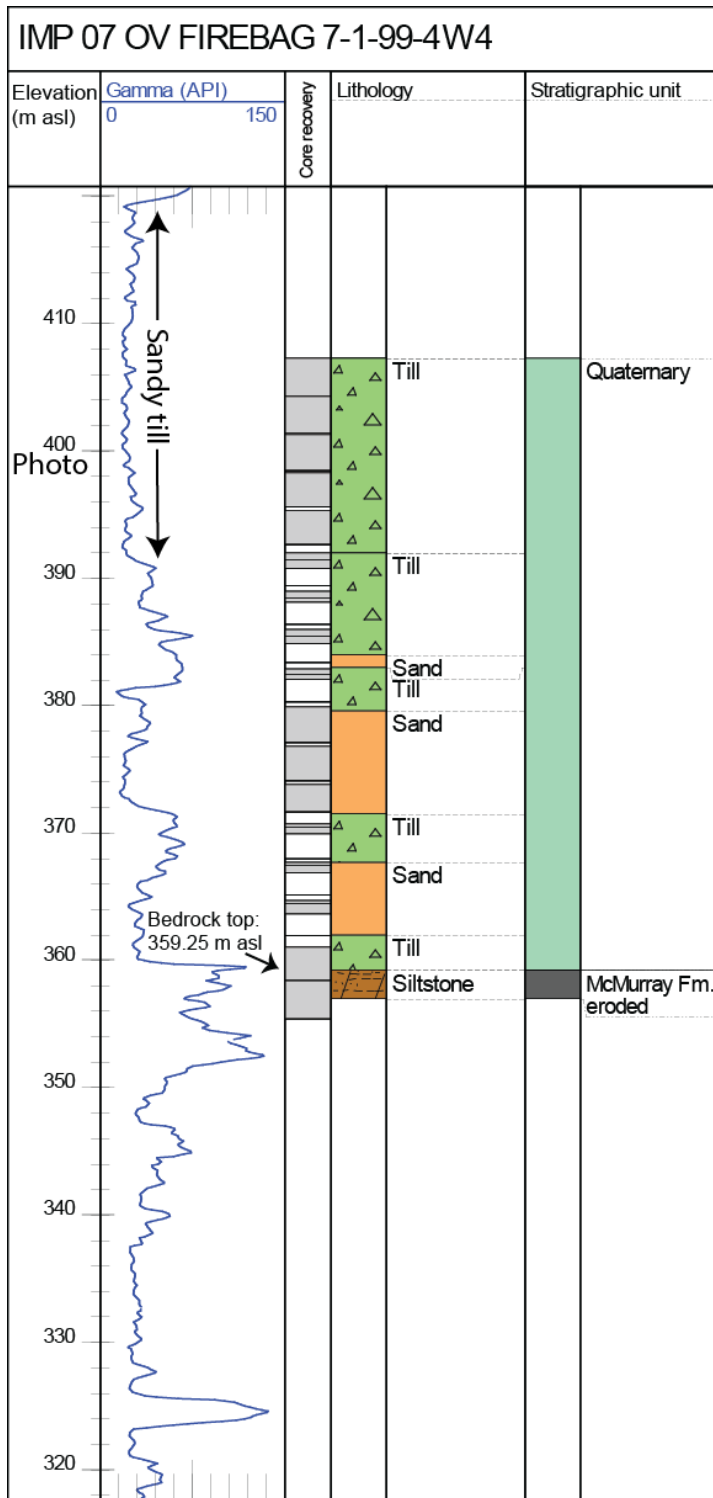


Figure 33. Logs for corehole IMP 07 OV FIREBAG 7-1-99-4W4 in the Firebag Hills domain illustrating near-surface sandy till interpreted to be Gipsy till (Bayrock, 1974), overlying interbedded silty clay till and sand. 'Photo' label on log indicates depth of core shown in Figure 32.

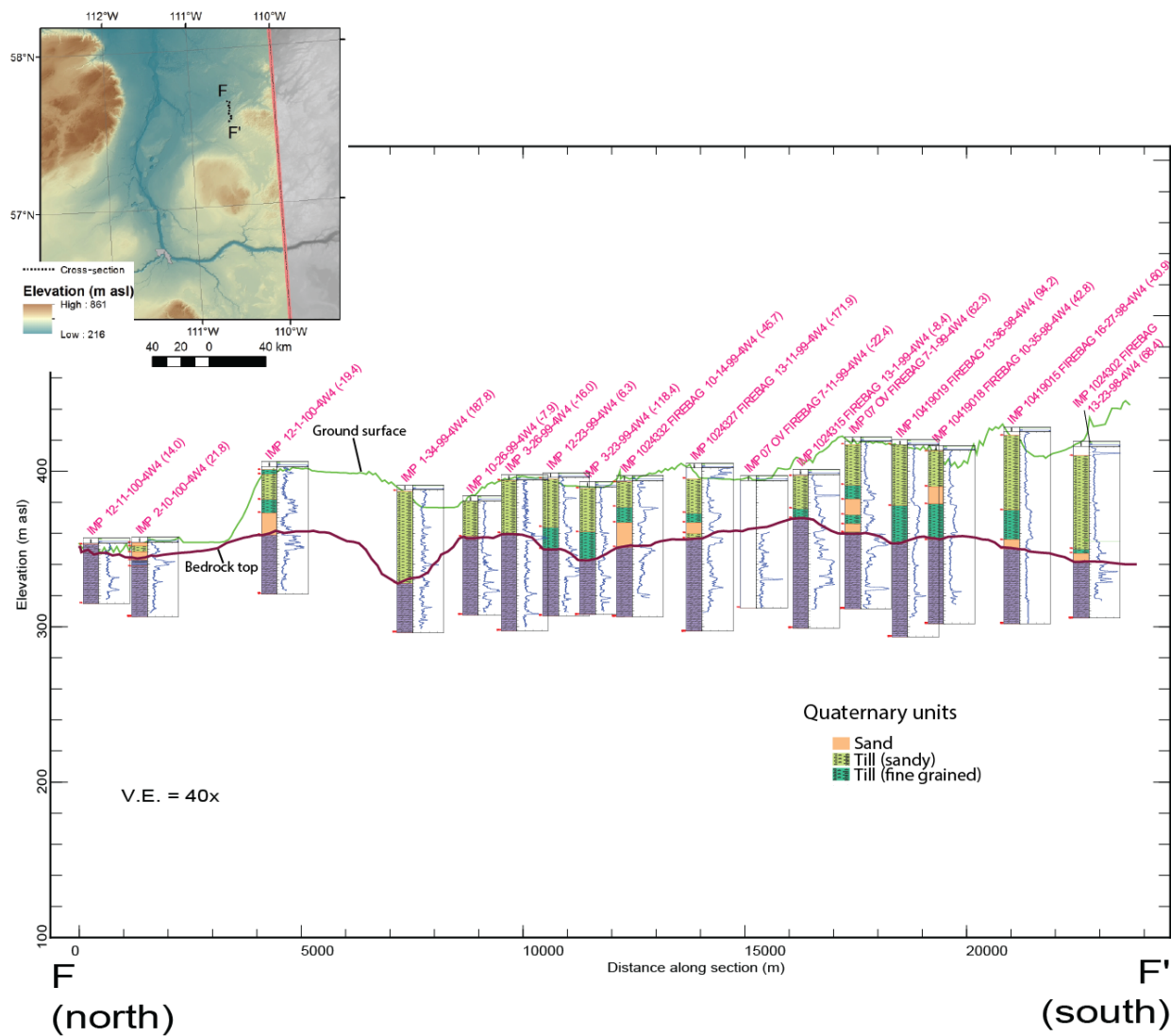


Figure 34. North-south cross-section on the Johnson Lake Plain and Firebag Hills (Figure 1), northeastern Alberta. Sandy till overlies a fine-grained till, with a basal sand in places. Location of the cross-section is also shown on Figure 29. The number in parentheses following the core name is the distance (in metres) the well is offset from the cross-section line. Abbreviation: V.E., vertical exaggeration.

5.6 Dover and Kearl Lake Plains Domain

The lowland in the middle of the study area that encompasses the Dover Plain on the west side of the Athabasca River and the Kearl Lake Plain on the east, is characterized by buried subglacial channels (Dover and Kearl Lake plains domain; Figures 3 and 25). A high density of geotechnical boreholes in the surface mineable oil sands area enabled Andriashek and Atkinson (2007) to map a network of subglacial channels, the Kearl channel complex, situated within the Kearl Lake Plain on the eastern flank of the Athabasca River (Atkinson et al., 2014; Andriashek, 2019). These channels were interpreted to originate as subglacial tunnel channels (Andriashek and Atkinson, 2007; Atkinson et al., 2014). They have varied fill, including sand, gravel, and diamict. The surface till likely corresponds to the Fort Hills till, based on the geographic location within the area of the Fort Hills ice flow, as well as geophysical responses similar to that of tills in the MacKay Plain that are also interpreted as Fort Hills till. Additionally, numerous rafts of displaced bedrock were identified within the Quaternary cover (Figures 15 and 16), similar to those identified in the Steepbank Plain domain.

6 Summary

The erosion of bedrock and the deposition of thick (>200 m) sequences of sediments in the region around Fort McMurray reflects a complex geological history, unraveled to some degree through the examination of 55 cores of bedrock and Neogene–Quaternary sediments in the Muskeg Mountain area. Core descriptions and lab analytical methods were used to identify the Cenozoic–bedrock contact on geophysical logs, and provide a basis for mapping the bedrock surface over the region. The methods for identifying the bedrock surface depended on the nature of the bedrock formation and Cenozoic lithology at the contact: where sandy Quaternary sediments overlay shale, the contact was relatively easy to identify on gamma-ray logs; where sandy Quaternary sediments overlay sandstone, the neutron porosity log was most effective for establishing the contact.

Cores revealed three types of contacts between Quaternary sediments and the underlying bedrock: sharp contacts with undisturbed bedrock; contacts with disturbed or glacially deformed bedrock; and contacts with water-laid sediments. Glaciotectonic deformation/displacement of the bedrock is typically limited to a thickness of 1 m from the contact, but can be as much as 6 m. Glacially displaced bedrock can also appear similar to in situ bedrock in log signatures, and can only be recognized from core or where units can be identified as out of stratigraphic sequence. Cores of Quaternary sediments from two holes were analyzed for geochemistry and grain size, and revealed five primarily till units. An attempt was made to relate these tills to ice-flow patterns, with the most recent two tills related to ice-flow landforms.

Six geographic domains with different Quaternary stratigraphic sequences were delineated in this study. Muskeg Mountain domain, in the central part of the study area, is typified by a thick sequence of multiple fine-grained tills capped by sandy till. To the north, the Firebag Hills domain is also composed of thick till sequences where sandy till overlies fine-grained till. In the area near the confluence of the Firebag and Athabasca rivers (Firebag River domain), glaciofluvially reworked McMurray Formation oil sand rests on pink clay-rich sediments thought to represent glaciolacustrine deposition in a proglacial lake impounded by the Fort Hills ice flow. The lower till in the Firebag Hills domain and Firebag River domain (north of the Firebag River) may correlate with the Horse River till. Although lacking core through the Quaternary succession, geophysical logs support the interpretation of an extensive buried sand deposit that is overlain by till containing rafts of bedrock in the Steepbank Plain domain, south of Muskeg Mountain. The bedrock surface in the MacKay Plain domain in the southwestern part of the study area has been incised by channels, which are inferred to have both a subaerial and subglacial origin. Here, channel-fill stratified sediments are overlain by a thin cover of till. Similarly, the lowland flanking both sides of the Athabasca River (Dover and Kearl Lake plains domain) is also incised with subglacial channels, and overlying sediments include channel-fill stratified sediments and rafts of bedrock. These six domains define areas where similar deposits might be expected to be found, which can be used as a basis for hydrogeological or other subsurface studies in the area.

In this study, it was possible to update the previous work by Andriashek and Atkinson (2007) because of the availability of additional data, including new wells drilled with geophysical logs run to surface, cores covering the bedrock contact and Quaternary succession, as well as airborne electromagnetic surveys that revealed the location of buried channels. As new datasets become available, further updates may be possible.

7 References

- Alberta Geological Survey (2019): 3D provincial geological framework model of Alberta, version 2 (methodology, model, dataset, multiple files); Alberta Energy Regulator / Alberta Geological Survey, AER/AGS Model 2018-02, URL <<https://ags.aer.ca/publication/3d-pgf-model-v2>> [December 2019].
- Alberta Geological Survey (2020a): Bedrock topography of Alberta, version 2; Alberta Energy Regulator / Alberta Geological Survey, AER/AGS Map 610, URL <<https://ags.aer.ca/data-maps-models/maps/map-610>> [October 2020].
- Alberta Geological Survey (2020b): Sediment thickness of Alberta, version 2; Alberta Energy Regulator / Alberta Geological Survey, AER/AGS Map 611, URL <<https://ags.aer.ca/data-maps-models/maps/map-611>> [October 2020].
- Andriashek, L.D. (2001): Quaternary stratigraphy of the buried Birch and Willow bedrock channels, NE Alberta; Alberta Energy and Utilities Board, EUB/AGS Earth Sciences Report 2000-15, 23 p., URL <https://ags.aer.ca/publications/ESR_2000_15.html> [November 2019].
- Andriashek, L.D. (2003): Quaternary geological setting of the Athabasca Oil Sands (in situ) area, northeast Alberta; Alberta Energy and Utilities Board, EUB/AGS Earth Sciences Report 2002-03, 295 p., URL <https://ags.aer.ca/publications/ESR_2002_03.html> [November 2019].
- Andriashek, L.D. comp. (2019): Thalwegs of bedrock valleys, Alberta (GIS data, line features); Alberta Energy Regulator / Alberta Geological Survey, AER/AGS Digital Data 2018-0001, URL <https://ags.aer.ca/publications/DIG_2018_0001.html> [November 2019].
- Andriashek, L.D. and Atkinson, N. (2007): Buried channels and glacial drift-aquifers in the Fort McMurray region, northeast Alberta; Alberta Energy and Utilities Board, EUB/AGS Earth Sciences Report 2007-01, 170 p., URL <https://ags.aer.ca/publications/ESR_2007_01.html> [March 2019].
- Andriashek, L.D. and Barendregt, R.W. (2017): Evidence for Early Pleistocene glaciation from borecore stratigraphy in north-central Alberta, Canada; Canadian Journal of Earth Sciences, v. 54, p. 445–460, [doi:10.1139/cjes-2016-0175](https://doi.org/10.1139/cjes-2016-0175)
- Andriashek, L.D. and Fenton, M.M. (1989): Quaternary stratigraphy and surficial geology of the Sand River area 73L; Alberta Research Council, AGS Bulletin 57, 136 p., URL <https://ags.aer.ca/publications/BUL_057.html> [November 2019].
- Andriashek, L.D., Fenton, M.M., de Freitas, T. and Mann, G. (1999): Glaciotectonics in the Cold Lake area and implications for steam-assisted heavy-oil recovery; Canadian Society of Petroleum Geologists and Petroleum Society Joint Convention, June 14–18, 1999, Calgary, Alberta, Abstract 99-25-O, 2 p.
- Atkinson, N., Andriashek, L.D. and Slattery, S.R. (2013): Morphological analysis and evolution of buried tunnel valleys in northeast Alberta, Canada; Quaternary Science Reviews, v. 65, p. 53–72.
- Atkinson, N., Pawley, S.M. and Utting, D.J. (2016): Flow-pattern evolution of the Laurentide and Cordilleran ice sheets across west-central Alberta, Canada: implications for ice sheet growth, retreat and dynamics during the last glacial cycle; Journal of Quaternary Science, v. 31, p. 753–768.
- Atkinson, N., Utting, D.J. and Pawley, S.M. (2014): Glacial landforms of Alberta; Alberta Energy Regulator, AER/AGS Map 604, scale 1:1 000 000, URL <https://ags.aer.ca/publications/MAP_604.html> [April 2019].
- Bayrock, L.A. (1971): Surficial geology Bitumount (NTS 74E); Research Council of Alberta, AGS Map 140, scale 1:250 000, URL <https://ags.aer.ca/document/MAP/Map_140.pdf> [April 2019].

- Bayrock, L.A. (1974): Surficial geology Waterways (NTS 74D); Alberta Research Council, AGS Map 148, scale 1:250 000, URL <https://ags.aer.ca/document/MAP/Map_148.pdf> [April 2019].
- Cant, D.J. and Abrahamson, B. (1997): Regional stratigraphy, sedimentology and petroleum geology of the Grand Rapids Formation, Mannville Group, northeastern Alberta; *Bulletin of Canadian Petroleum Geology*, v. 45, p. 141–154.
- Dawson, J., Perrin, R. and Henderson, J. (2018): A cost effective approach to regional and site-specific aquifer exploration using combined airborne and ground electromagnetics; *Canadian Society of Exploration Geologists, Recorder*, v. 43, p. 20–24.
- Fisher, T.G. and Smith, D.G. (1994): Glacial Lake Agassiz: its northwest maximum extent and outlet in Saskatchewan (Emerson phase); *Quaternary Science Reviews*, v. 13, p. 845–858.
- Hauck, T.E., Peterson, J.T., Hathway, B., Grobe, M. and MacCormack, K. (2017): New insights from regional-scale mapping and modelling of the Paleozoic succession in northeast Alberta: paleogeography, evaporite dissolution, and controls on Cretaceous depositional patterns on the sub-Cretaceous unconformity; *Bulletin of Canadian Petroleum Geology*, v. 65, p. 87–114.
- Haug, K.M., Greene, P. and Mei, S. (2014): Geological characterization of the Lower Clearwater Shale in the Athabasca Oil Sands area, Townships 87–99, Ranges 1–13, West of the Fourth Meridian; Alberta Energy Regulator, AER/AGS Open File Report 2014-04, 33 p., URL <https://ags.aer.ca/publications/OFR_2014_04.html> [October 2019].
- Hayes, B.J.R., Christopher, J.E., Rosenthal, L., Los, G., McKercher, B., Minken, D., Tremblay, Y.M. and Fennell, J. (1994): Cretaceous Mannville Group of the Western Canada Sedimentary Basin; *in Geological atlas of the Western Canada Sedimentary Basin*, G.D. Mossop and I. Shetsen (comp.), Canadian Society of Petroleum Geologists and Alberta Research Council, URL <<https://ags.aer.ca/publications/chapter-19-cretaceous-mannville-group.html>> [September 2019].
- Hein, F.J. and Cotterill, D.K. (2006): The Athabasca Oil Sands - a regional geological perspective, Fort McMurray area, Alberta, Canada; *Natural Resource Research*, v. 15, p. 85–102.
- Jackson, P.C. (1984): Paleogeography of the Lower Cretaceous Mannville Group of western Canada; *in Elmworth-case study of a deep basin gas field*, J.A. Masters (ed.), American Association of Petroleum Geologists, Memoir 38, p. 49–78.
- Javad, M.B., Kachanoski, G. and Siddique, T. (2014): Arsenic fractionation and mineralogical characterization of sediments in the Cold Lake area of Alberta, Canada; *Science of the Total Environment*, v. 500–501, p. 181–190.
- Kupsch, B.G. and Olson, R.A. (2006): Diamond drillhole locations (GIS data, point features); Alberta Energy and Utilities Board, EUB/AGS Digital Data 2005-0015, URL <https://ags.aer.ca/publications/DIG_2005_0015.html> [January 2020].
- Leckie, D.A. and Smith, D.G. (1992): Regional setting, evolution, and depositional cycles of the Western Canada foreland basin; *in Foreland basins and fold belts*, R.W. Macqueen and D.A. Leckie (ed.), American Association of Petroleum Geologists, Memoir 55, p. 9–46.
- Leckie, D.A., Bhattacharya, J.P., Bloch, J., Gilboy, C.F., Norris, B., Plint, G., Gilders, M., Holmstrom, G., Krause, F.F., Reinson, G.E., Safton, D., Sawicki, J. and Sawicki, O. (1994): Cretaceous Colorado/Alberta Group of the Western Canada Sedimentary Basin; *in Geological atlas of the Western Canada Sedimentary Basin*, G.D. Mossop and I. Shetsen (comp.), Canadian Society of Petroleum Geologists and Alberta Research Council, URL <<https://ags.aer.ca/publications/chapter-20-cretaceous-colorado-alberta-group.html>> [September 2019].

- McPherson, R.A. and Kathol, C.P. (1977): Surficial geology of potential mining areas in the Athabasca Oil Sands region; Alberta Research Council, AGS Open File Report 1977-04, 200 p., URL <https://ags.aer.ca/document/OFR/OFR_1977_04.pdf> [April 2019].
- Moran, S.R., Clayton, L., Hooke, R. LeB., Fenton, M.M. and Andriashek, L.D. (1980): Glacier-bed landforms of the Prairie region of North America; *Journal of Glaciology*, v. 25, no. 93, p. 457–476.
- Norris, S.L. (2019): Glacial flowsets in the lower Athabasca and Clearwater region, Alberta and Saskatchewan; Alberta Energy Regulator / Alberta Geological Survey, AER/AGS Map 595, scale 1:750 000.
- Ó Cofaigh, C., Evans, D.J.A. and Smith, I.R. (2010): Large-scale reorganization and sedimentation of terrestrial ice streams during late Wisconsinan Laurentide Ice Sheet deglaciation; *Geological Society of America Bulletin*, v. 122, p. 743–756.
- Pettapiece, W.W. (1986): Physiographic subdivisions of Alberta; Agriculture Canada, Research Branch, Land Resource Research Centre, scale 1:1 500 000.
- Phillips, E., Evans, D.J.A., Atkinson, N. and Kendall, A. (2017): Structural architecture and glacetectonic evolution of the Mud Buttes cupola hill complex, Southern Alberta, Canada; *Quaternary Science Reviews*, v. 164, p. 110–139.
- Prior, G.J., Hathway, B., Glombick, P.M., Pana, D.I., Banks, C.J., Hay, D.C., Schneider, C.L., Grobe, M., Elgr, R. and Weiss, J.A. (2013): Bedrock geology of Alberta; Alberta Energy Regulator, AER/AGS Map 600, scale 1:1 000 000, URL <https://ags.aer.ca/publications/MAP_600.html> [October 2019].
- Roed, M.A. (1975): Cordilleran and Laurentide multiple glaciation, west-central Alberta; *Canadian Journal of Earth Sciences*, v. 14, p. 1493–1515.
- Ross, M., Campbell, J.E., Parent, M. and Adams, R.S. (2009): Palaeo-ice streams and the subglacial landscape mosaic of the North American mid-continental prairies; *Boreas*, v. 38, p. 421–439.
- Teck Resources Limited (2016): Environmental assessment - Teck Resources Limited Frontier Oil Sands mine - environmental impact assessment (EIA) and application for approval; Alberta Environment and Parks, URL <<https://open.alberta.ca/publications/eia-teck-resources-limited-frontier-oil-sands-mine>> [January 2020].
- Utting, D.J. (2020a): Bedrock top elevation values from the Fort McMurray region of northeastern Alberta (tabular data, tab-delimited format); Alberta Energy Regulator / Alberta Geological Survey, AER/AGS Digital Data 2020-0021.
- Utting, D.J. (2020b): Geochemistry and grain size data of Quaternary sediments from two drillcores, Fort McMurray region, northeastern Alberta (tabular data, tab-delimited format); Alberta Energy Regulator / Alberta Geological Survey, AER/AGS Digital Data 2020-0014.
- Utting, D.J. and Atkinson, N. (2019): Proglacial lakes and the retreat pattern of the southwest Laurentide Ice Sheet across Alberta, Canada; *Quaternary Science Reviews*, v. 225, p. 1–25.
- Utting, D.J., Atkinson, N., Pawley, S. and Livingstone, S.J. (2016): Reconstructing the confluence zone between Laurentide and Cordilleran ice sheets along the Rocky Mountain Foothills, south-west Alberta; *Boreas*, v. 31, p. 769–787.
- Woywitka, R.J., Froese, D.G. and Wolfe, S.A. (2017): Raised landforms in the east-central oil sands region, origin, age, and archaeological implications; *in* Alberta's Lower Athabasca Basin: archaeology and palaeoenvironments, B.M. Ronaghan (ed.), Athabasca University, p. 69–82.

Appendix 1 – Core and Drill Cutting Descriptions

Core Descriptions

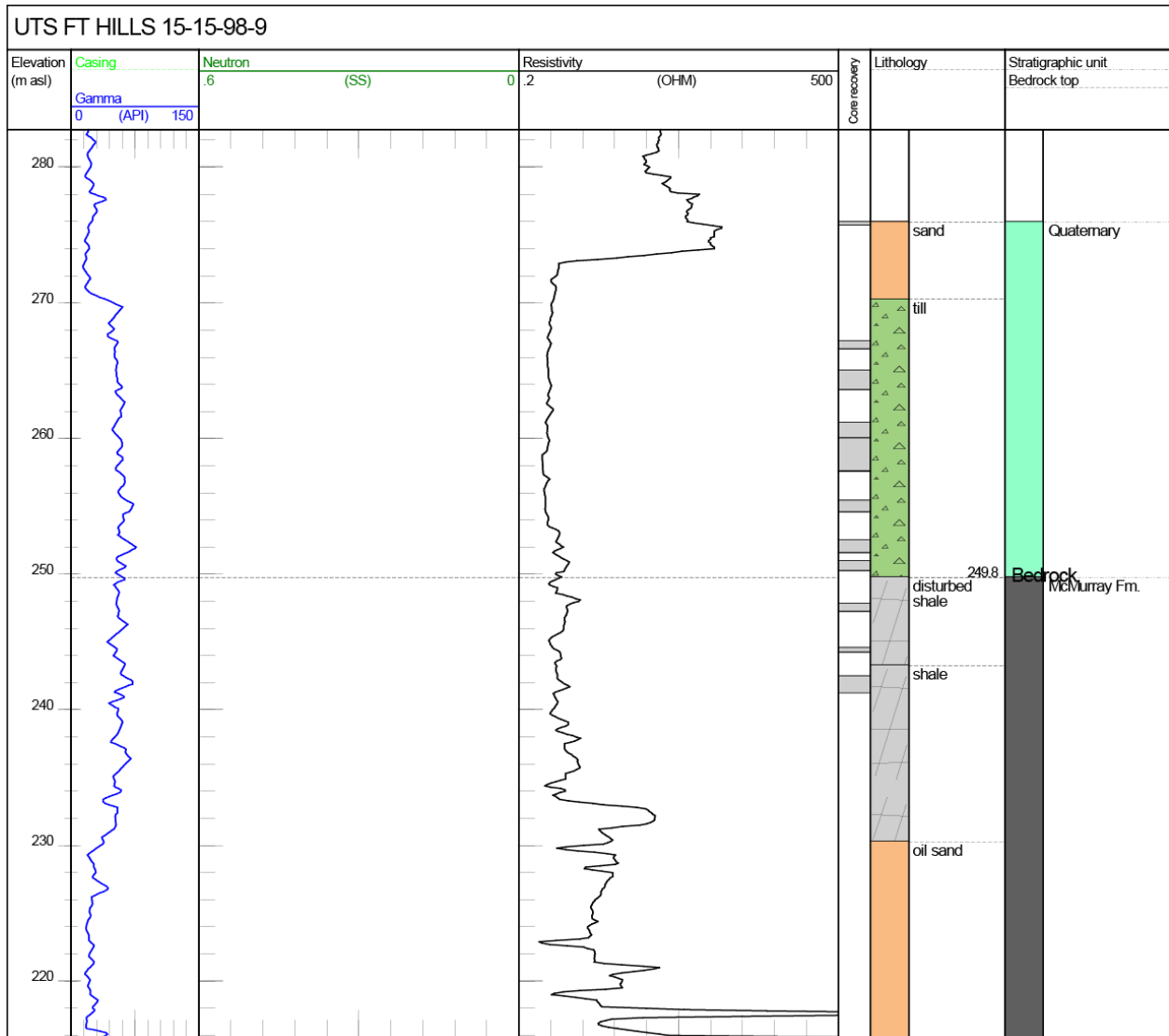


Figure 35. Logs for well UTS FT HILLS 15-15-98-9W4. Litholog determined from examination of core. Neutron data unavailable. Kelly bushing at 302.3 m asl and total depth at 205.3 m asl. Abbreviations: Gamma, gamma ray; Neutron, neutron porosity; OHM, ohm·m; SS, sandstone units.

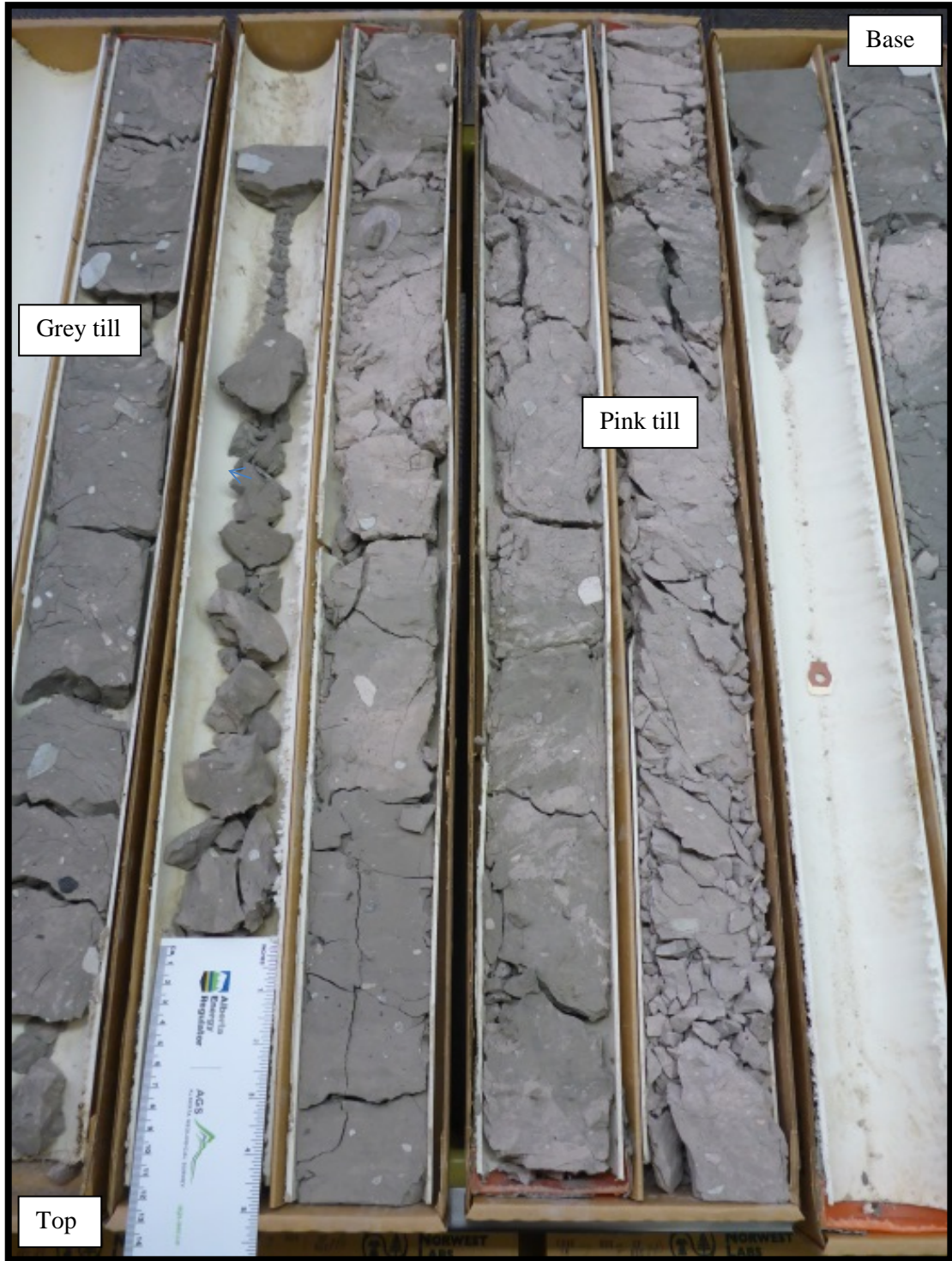


Figure 36. Photograph of core interval from well UTS FT HILLS 15-15-98-9W4 (42.25–46.85 m depth, 260.05–255.45 m asl). Pink till is calcareous and grey till is noncalcareous. Core boxes are 0.9 m long.



Figure 37. Photograph of core interval from well UTS FT HILLS 15-15-98-9W4 (57.0–63.3 m depth, 245.3–239.0 m asl) showing disturbed or contorted shale below the contact with overlying Quaternary sediments (not shown). Core boxes are 0.9 m long.

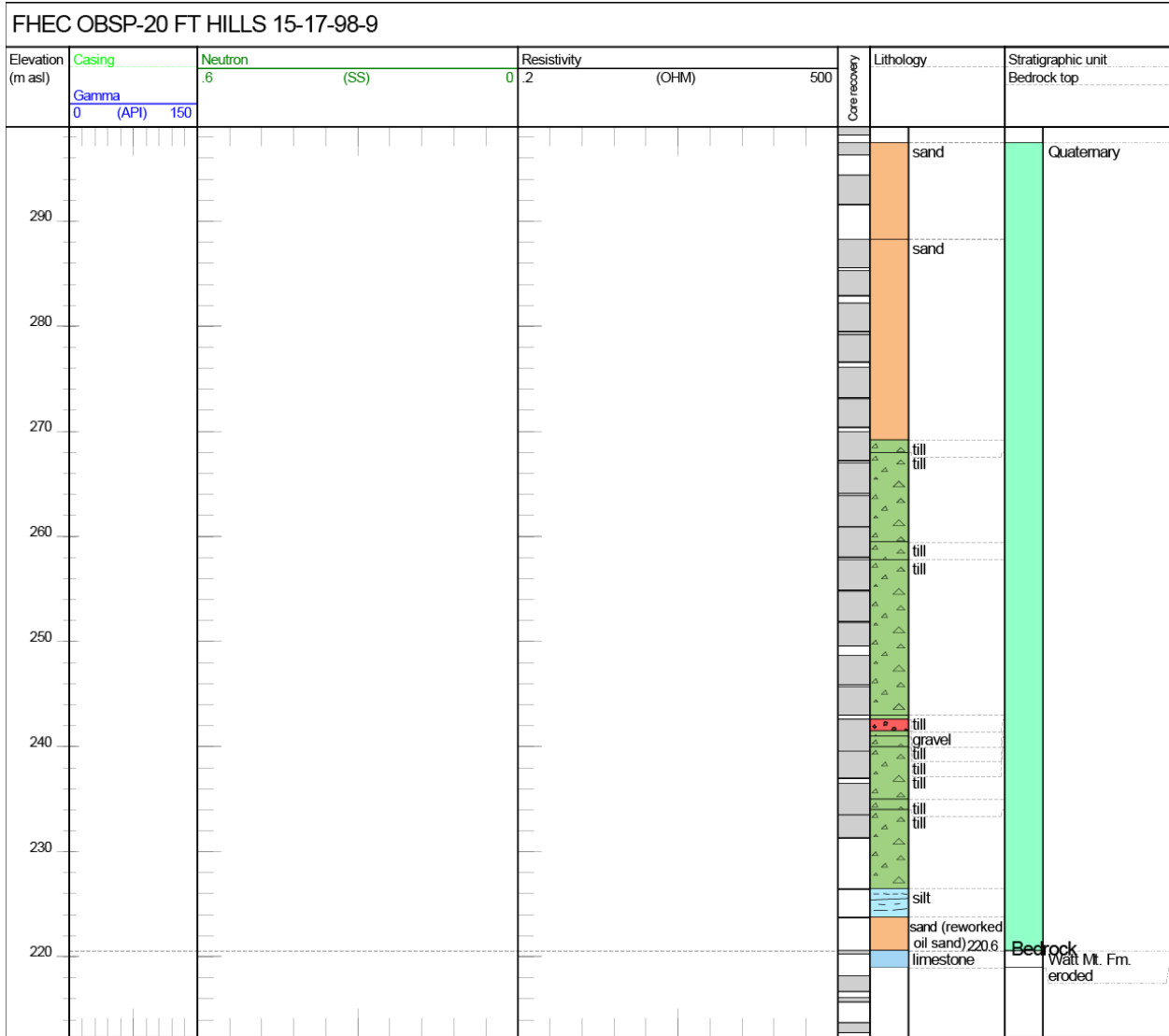


Figure 38. Litholog for well FHEC OBSP-20 FT HILLS 15-17-98-9W4. Litholog determined from examination of core. Geophysical data unavailable. Kelly bushing at 299.0 m asl and total depth at 206.7 m asl. Abbreviations: Gamma, gamma ray; Neutron, neutron porosity; OHM, ohm·m; SS, sandstone units.

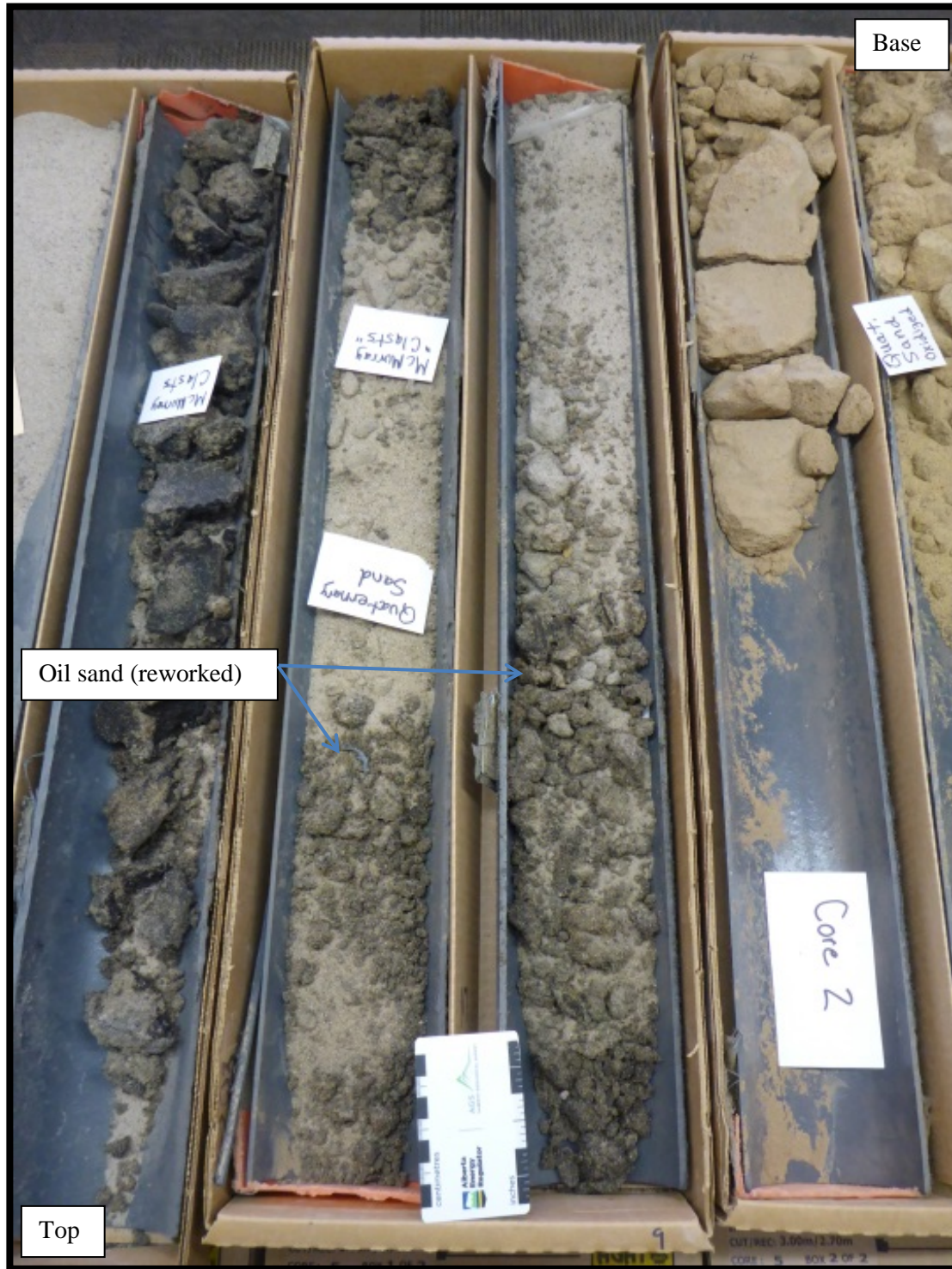


Figure 39. Photograph of core interval from well FHEC OBSP-20 FT HILLS 15-17-98-9W4 (10.70–12.70 m depth, 288.3–286.3 m asl) revealing reworked oil sand. Core boxes are 0.9 m long.

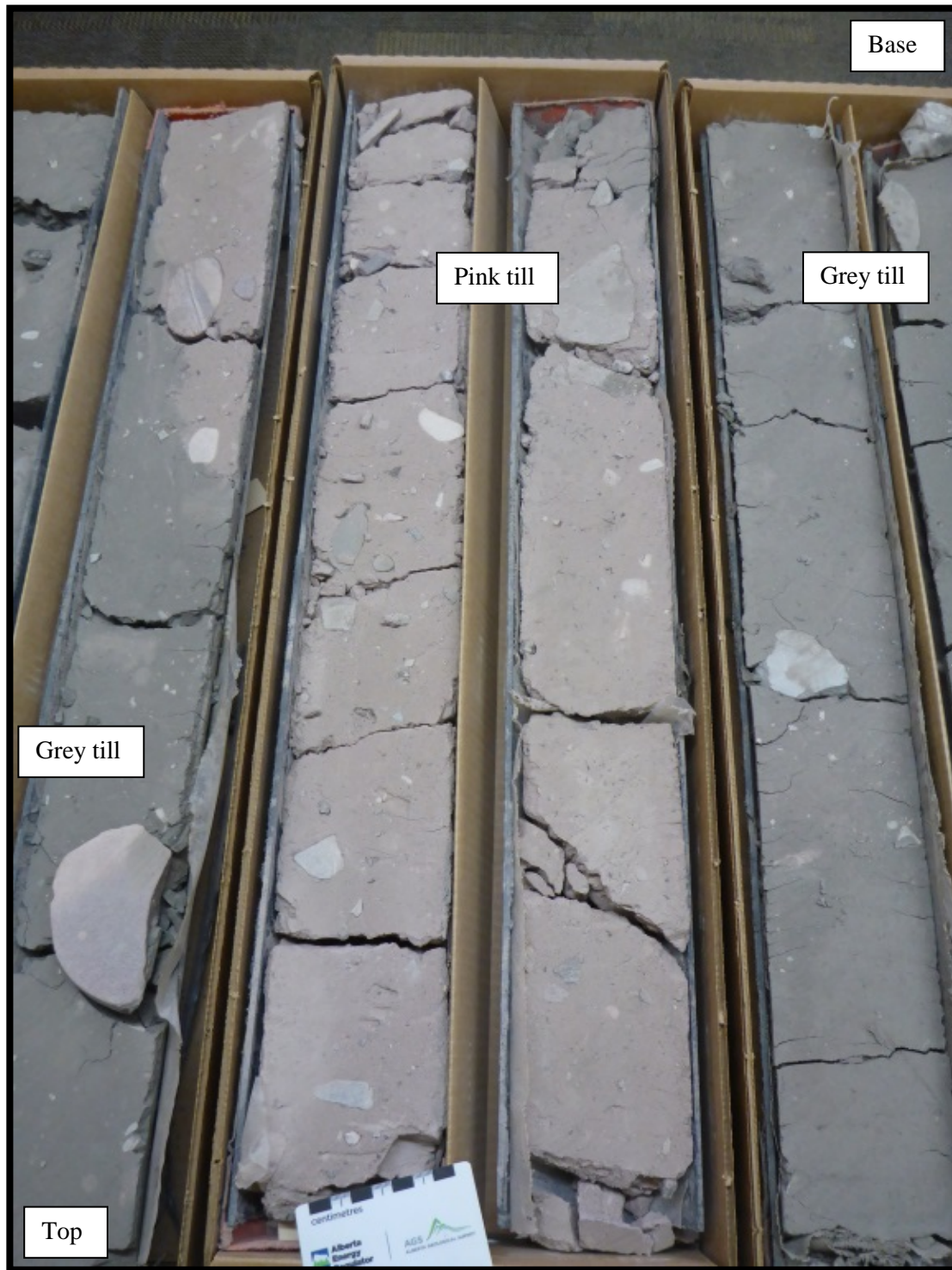


Figure 40. Photograph of core interval from well FHEC OBSP-20 FT HILLS 15-17-98-9W4 (38.1–40.1 m depth, 260.9–258.9 m asl) showing pink till. Core boxes are 0.9 m long.

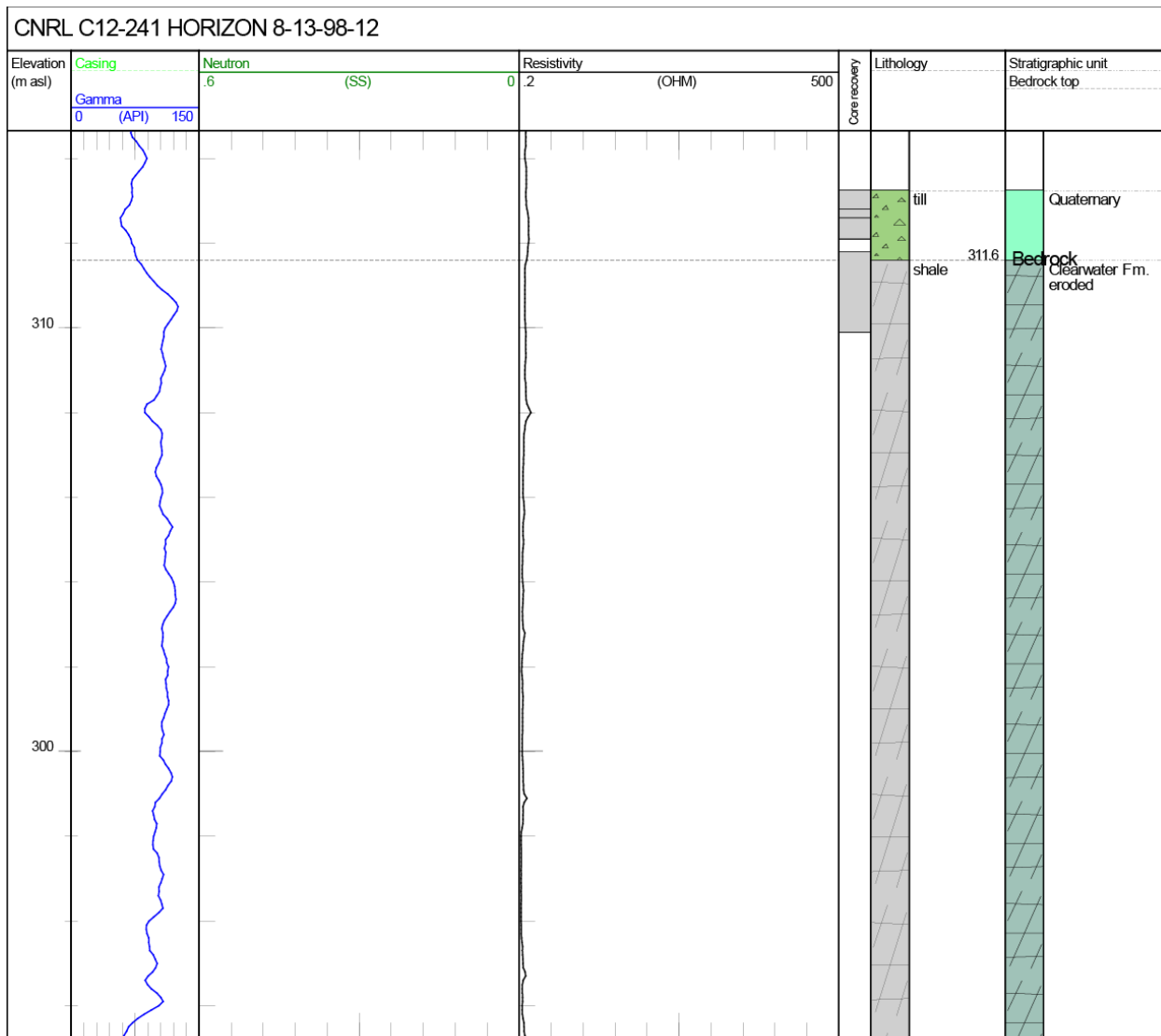


Figure 41. Logs for well CNRL C12-241 HORIZON 8-13-98-12W4. Litholog determined from examination of core. Neutron data unavailable. Kelly bushing at 343.6 m asl and total depth at 212.5 m asl. Abbreviations: Gamma, gamma ray; Neutron, neutron porosity; OHM, ohm·m; SS, sandstone units.



Figure 42. Photograph of core interval from well CNRL C12-241 HORIZON 8-13-98-12W4 (31.60–32.50 m depth, 312.0–311.1 m asl) showing bedrock contact.

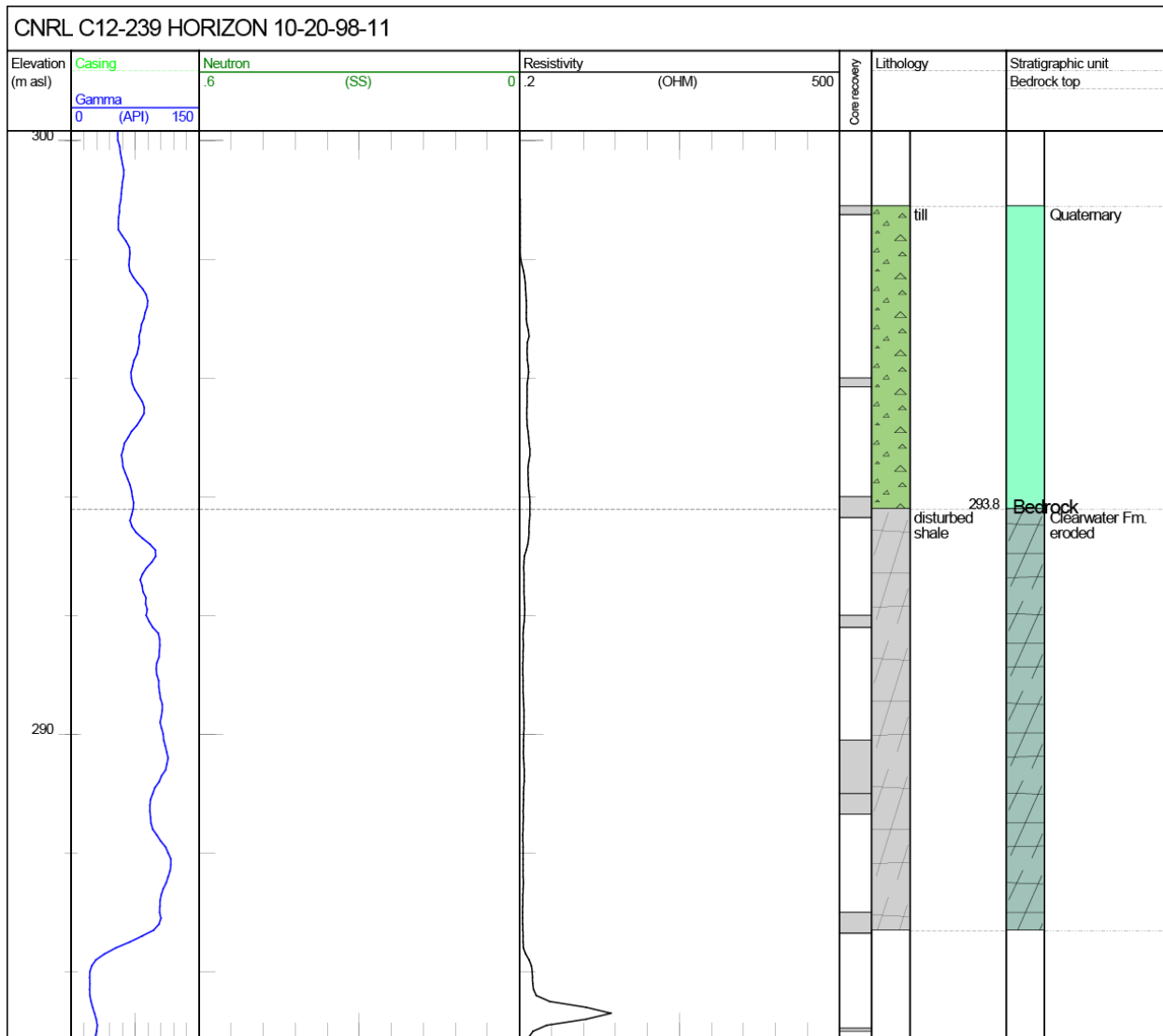


Figure 43. Logs for well CNRL C12-239 HORIZON 10-20-98-11W4. Lithology determined from examination of core. Neutron data unavailable. Kelly bushing at 323.7 m asl and total depth at 215.0 m asl. Abbreviations: Gamma, gamma ray; Neutron, neutron porosity; OHM, ohm·m; SS, sandstone units.



Figure 44. Photograph of core interval from well CNRL C12-239 HORIZON 10-20-98-11W4 (33.80–36.7 m depth, 289.9–287.0 m asl) showing disturbed Clearwater Formation shale (note, poor core recovery). Core boxes are 0.9 m long.

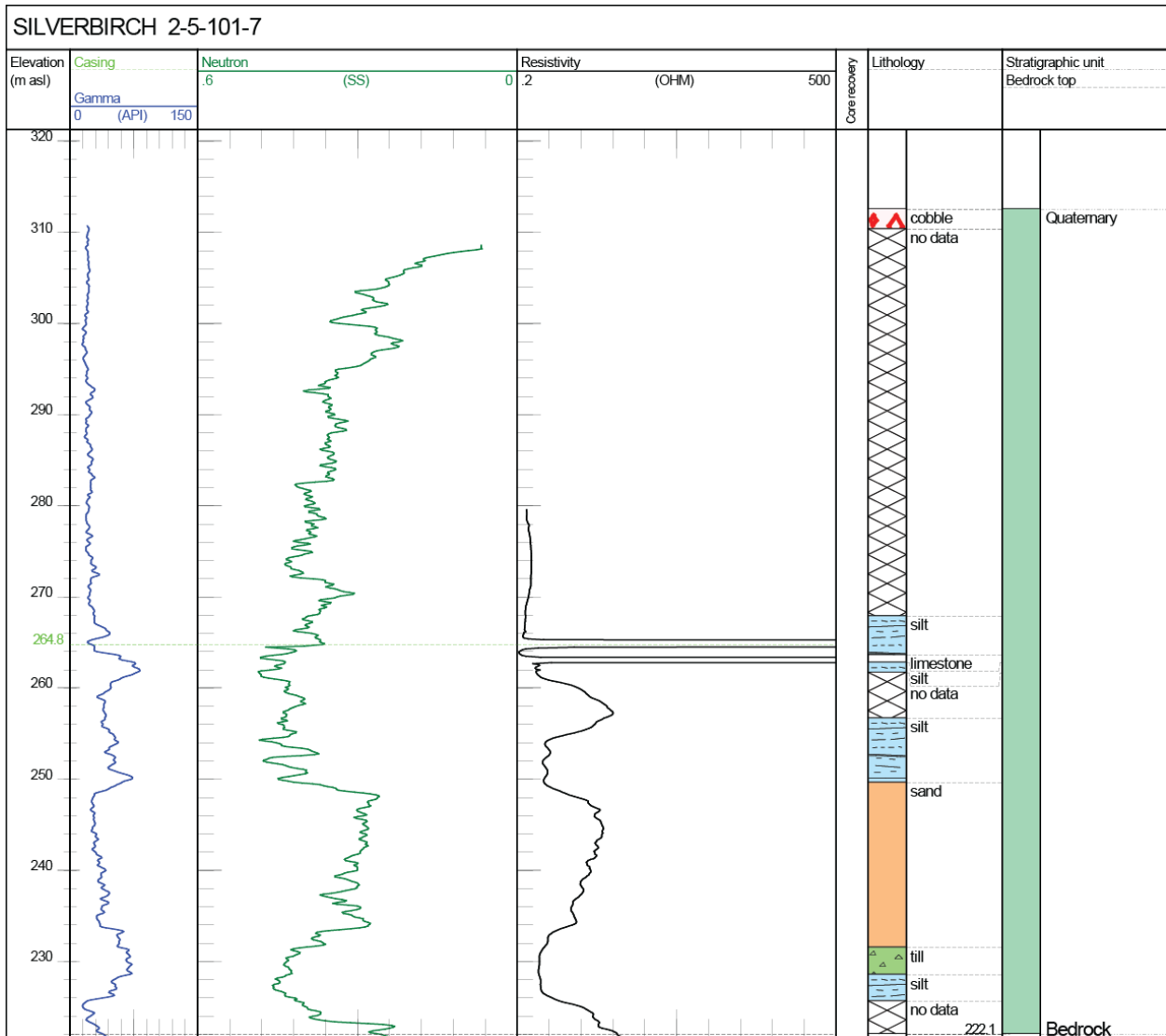


Figure 45. Logs for well SILVERBIRCH 2-5-101-7W4. Litholog determined from examination of core. Core recovery unavailable. Kelly bushing at 312.6 m asl and total depth at 210.6 m asl. Abbreviations: Gamma, gamma ray; Neutron, neutron porosity; OHM, ohm·m; SS, sandstone units.

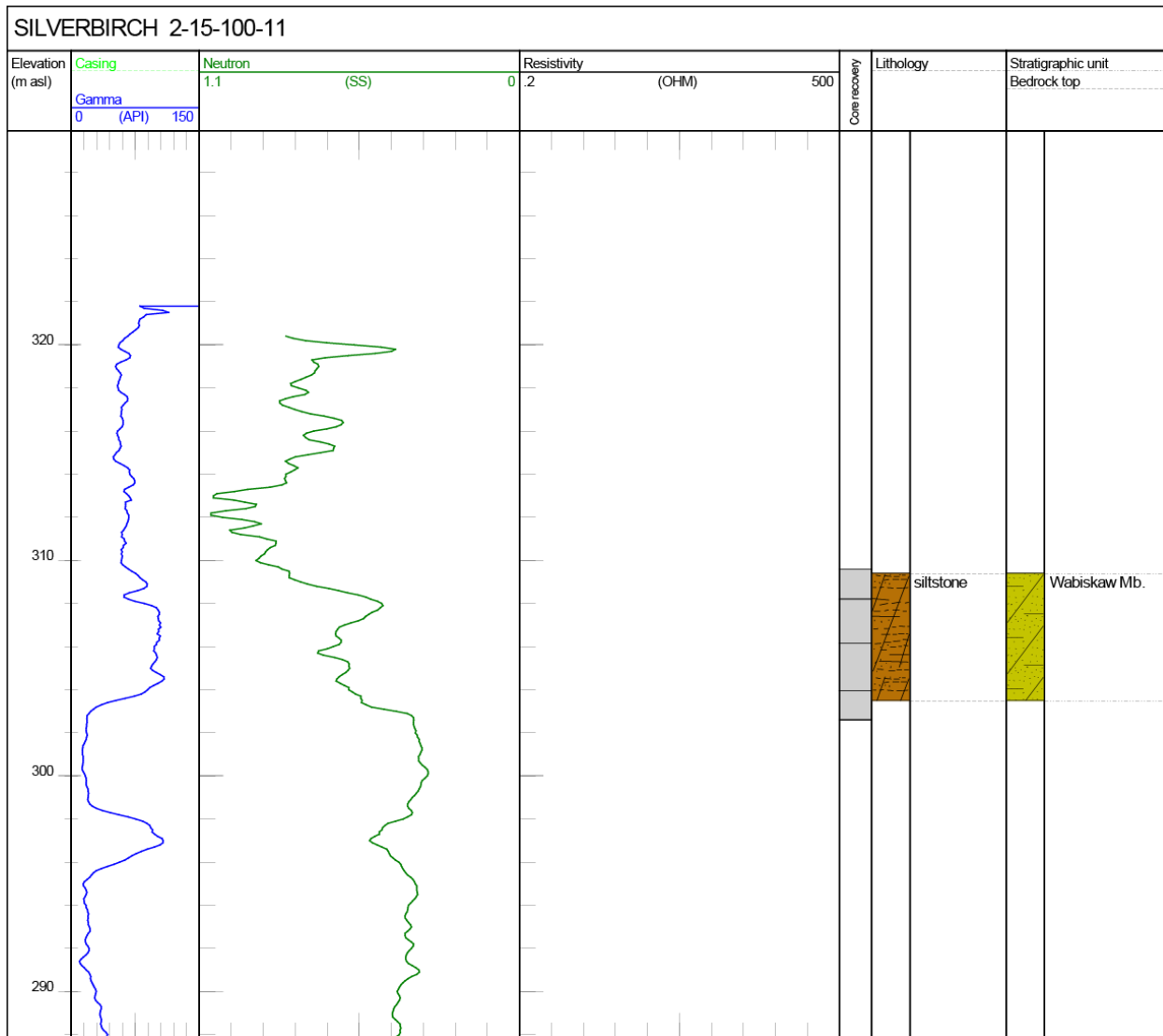


Figure 46. Logs for well SILVERBIRCH 2-15-100-11W4. Litholog determined from examination of core. Resistivity data unavailable. No Quaternary sediments in core. Kelly bushing at 322.6 m asl and total depth at 202.6 m asl. Abbreviations: Gamma, gamma ray; Neutron, neutron porosity; OHM, ohm•m; SS, sandstone units.

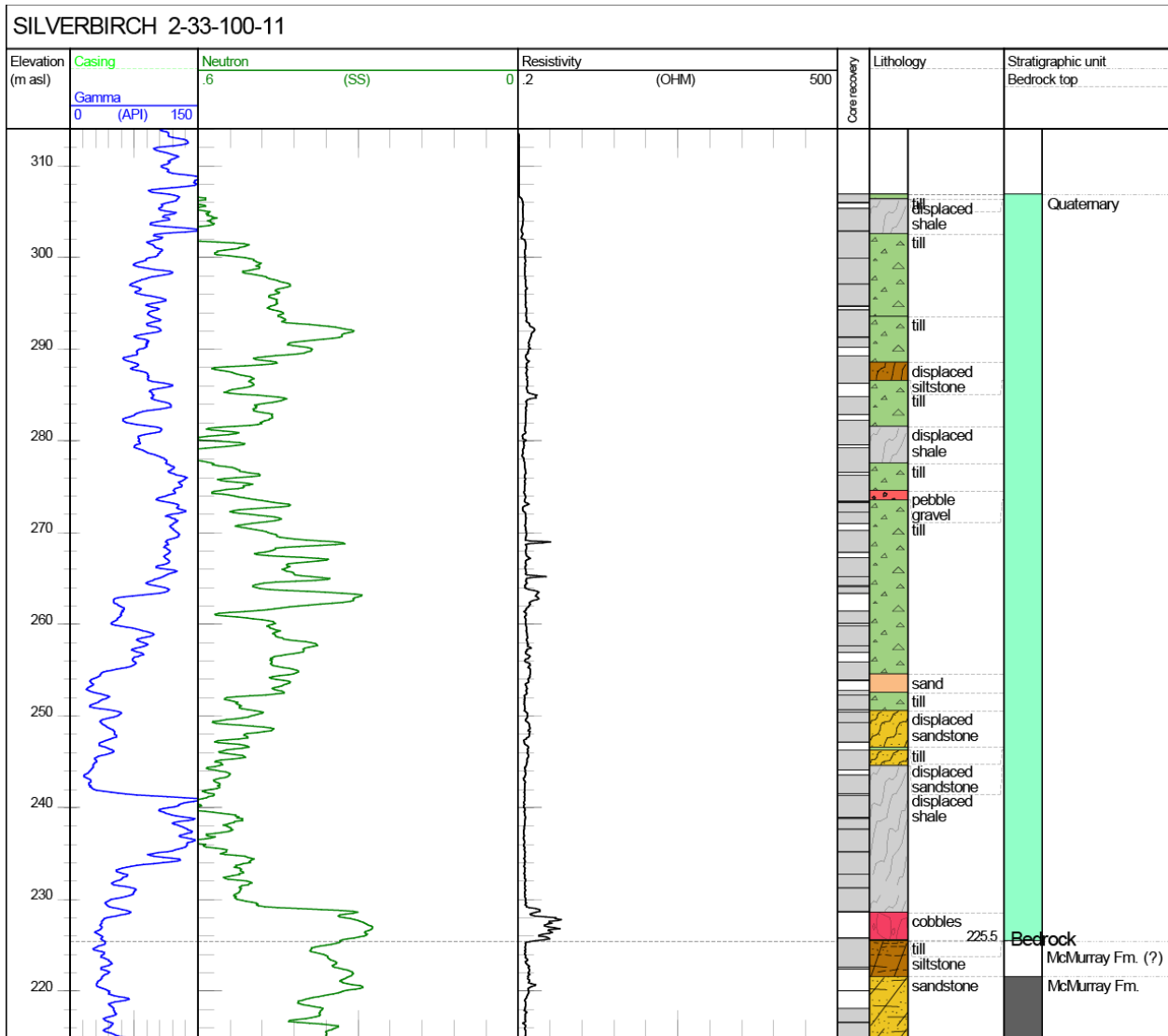


Figure 47. Logs for well SILVERBIRCH 2-33-100-11W4. Litholog determined from examination of core. Kelly bushing at 348.6 m asl and total depth at 168.3 m asl. Abbreviations: Gamma, gamma ray; Neutron, neutron porosity; OHM, ohm•m; SS, sandstone units.



Figure 48. Photograph of core interval from well SILVERBIRCH 2-33-100-11W4 (43.25–45.75 m depth, 305.35–302.85 m asl) showing displaced shale. Core boxes are 0.9 m long.

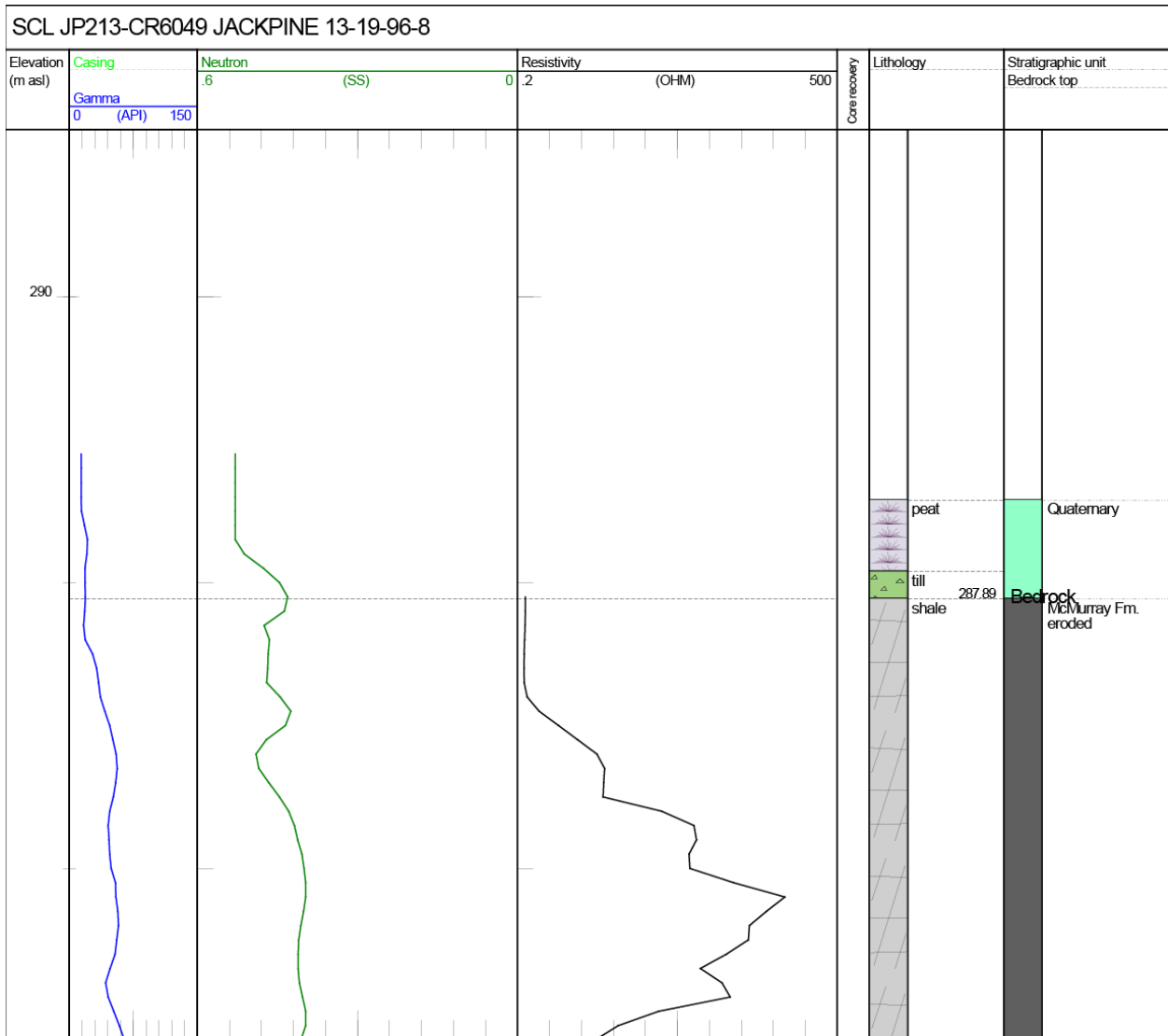


Figure 49. Logs for well SCL JP213-CR6049 JACKPINE 13-19-96-8W4. Litholog determined from examination of core. Core recovery unavailable. Kelly bushing at 289.9 m asl and total depth at 189.9 m asl. Abbreviations: Gamma, gamma ray; Neutron, neutron porosity; OHM, ohm·m; SS, sandstone units.

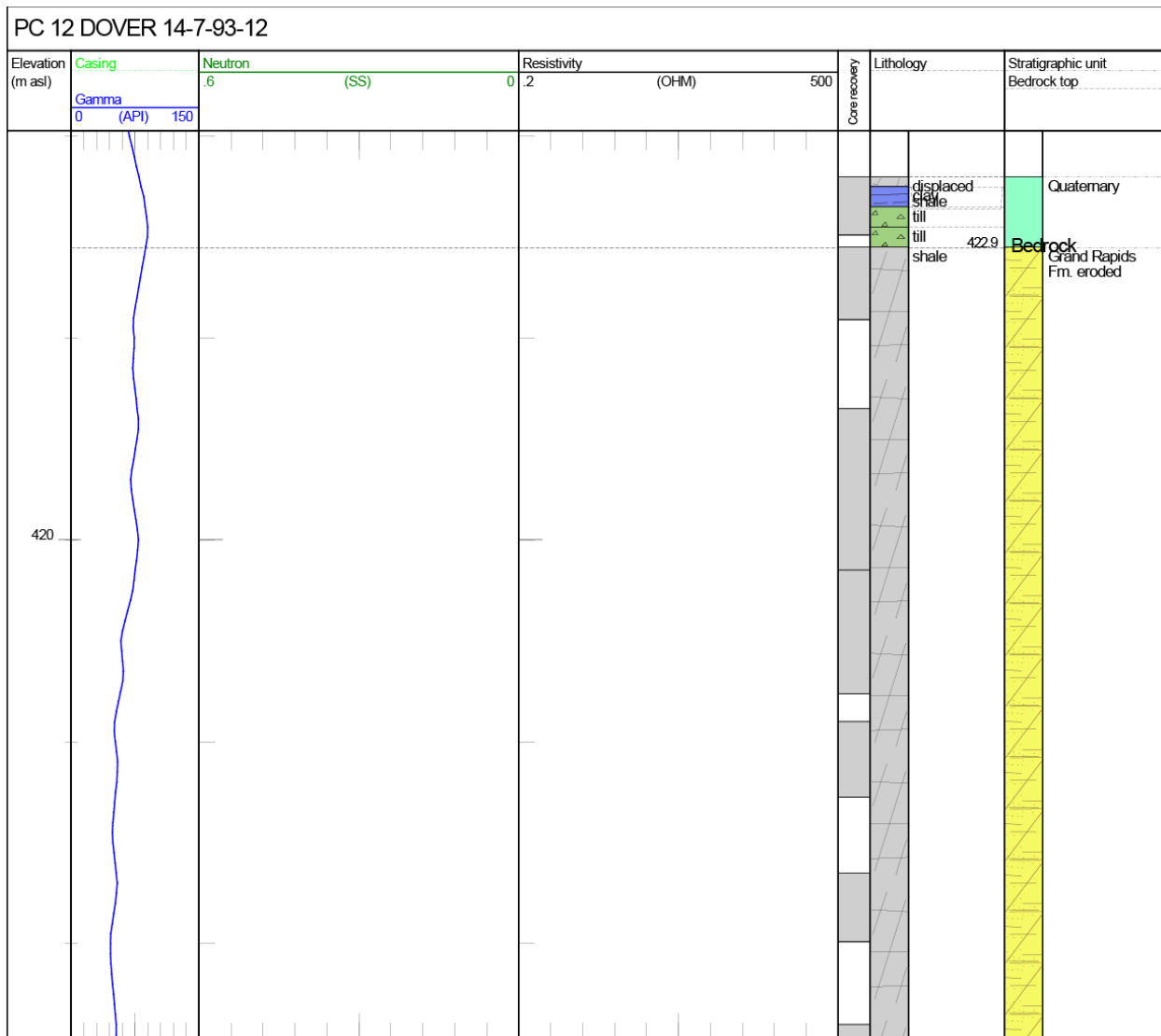


Figure 50. Logs for well PC 12 DOVER 14-7-93-12W4. Litholog determined from examination of core. Neutron and resistivity data unavailable. Kelly bushing at 433.3 m asl and total depth at 252.9 m asl. Abbreviations: Gamma, gamma ray; Neutron, neutron porosity; OHM, ohm•m; SS, sandstone units.



Figure 51. Photograph of core interval from well PC 12 DOVER 14-7-93-12W4 (9.7–11 m depth, 423.6–422.3 m asl) showing till (light grey) overlying shale. Core boxes are 0.9 m long.

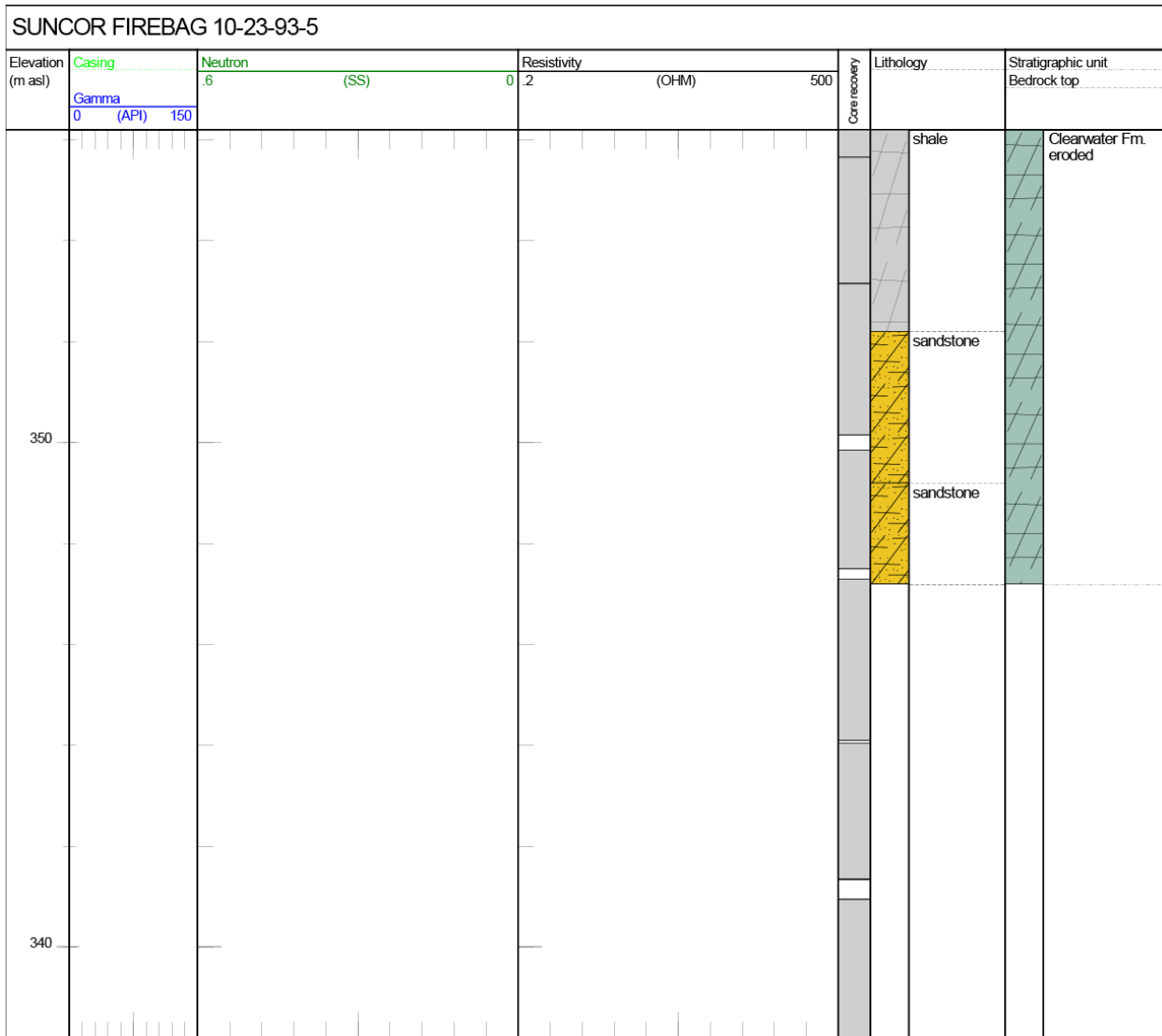


Figure 52. Log for well SUNCOR FIREBAG 10-23-93-5W4. Lithology determined from examination of core. Geophysical data unavailable. No Quaternary sediments in core. Kelly bushing at 639.2 m asl and total depth at 293.7 m asl. Abbreviations: Gamma, gamma ray; Neutron, neutron porosity; OHM, ohm•m; SS, sandstone units.

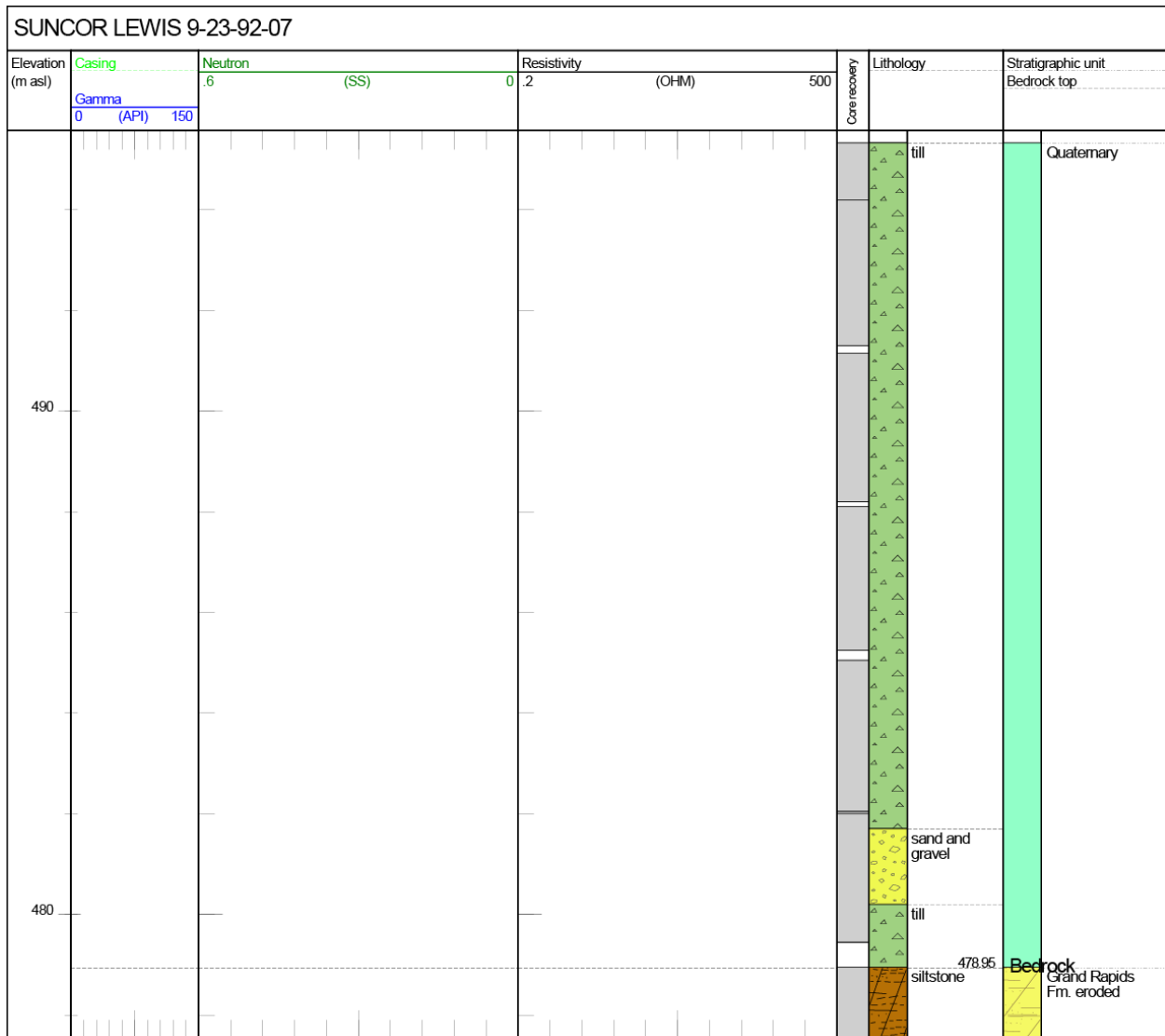


Figure 53. Log for well SUNCOR LEWIS 9-23-92-07W4. Litholog determined from examination of core. Geophysical data unavailable. Kelly bushing at 498.7 m asl and total depth at 234.7 m asl. Abbreviations: Gamma, gamma ray; Neutron, neutron porosity; OHM, ohm•m; SS, sandstone units.

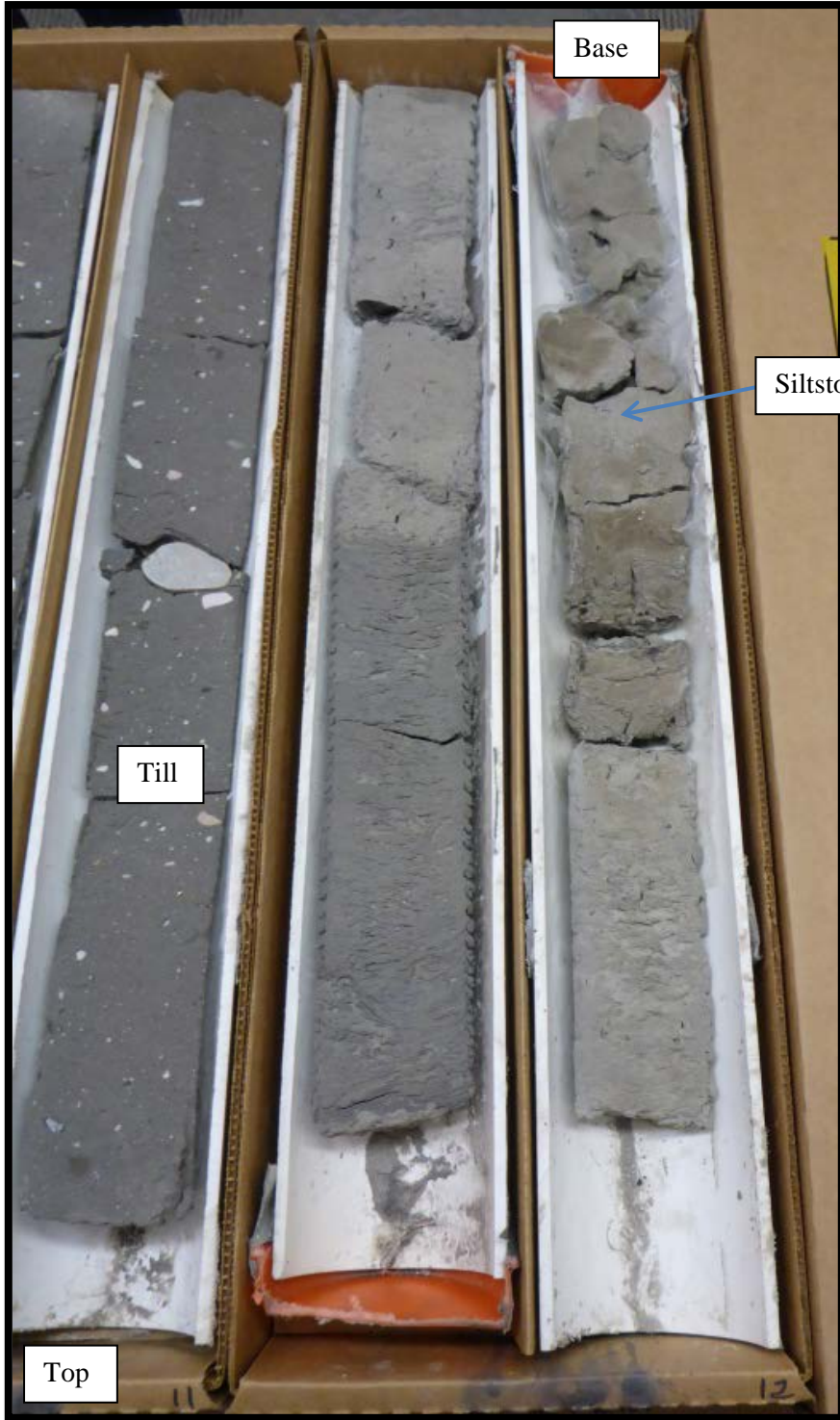


Figure 54. Photograph of core interval from well SUNCOR LEWIS 9-23-92-07W4 (18.55–21 m depth, 480.15–477.7 m asl) showing till (darker grey) with sharp contact with siltstone (light grey). Core boxes are 0.9 m long.

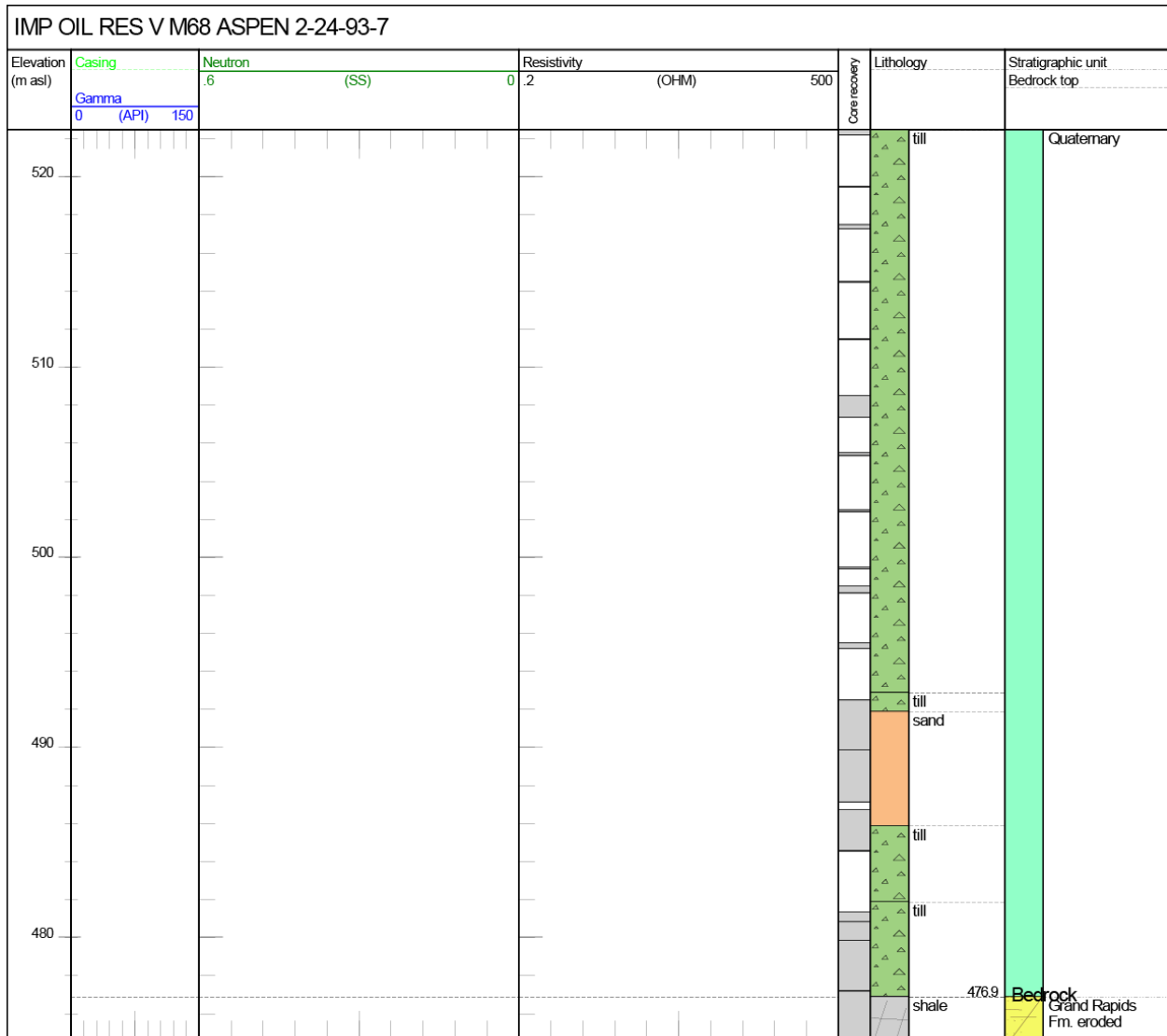


Figure 55. Log for well IMP OIL RES V M68 ASPEN 2-24-93-7W4. Litholog determined from examination of core. Geophysical data unavailable. Kelly bushing at 529.9 m asl and total depth at 242.9 m asl. Abbreviations: Gamma, gamma ray; Neutron, neutron porosity; OHM, ohm•m; SS, sandstone units.

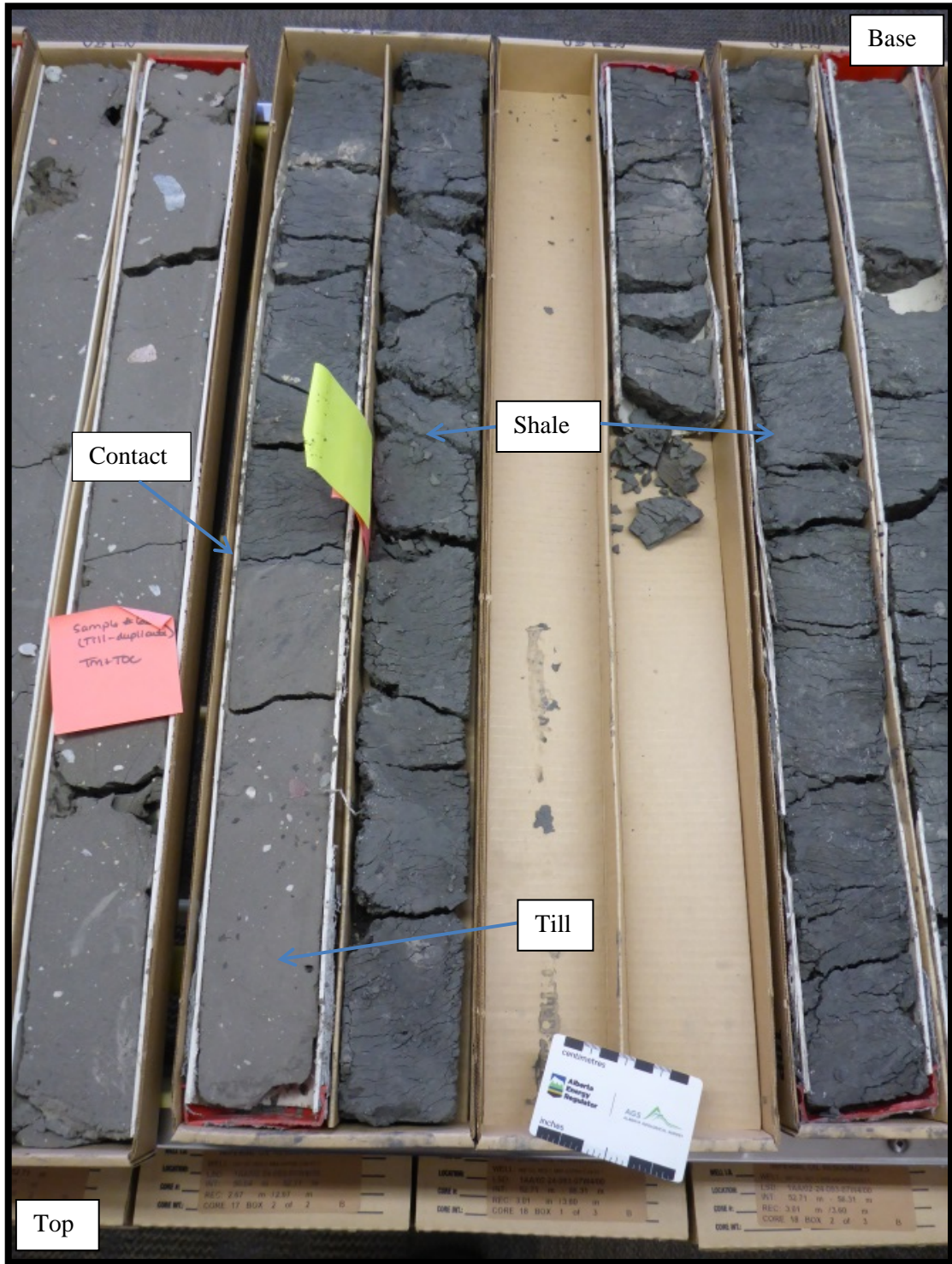


Figure 56. Photograph of core interval from well IMP OIL RES V M68 ASPEN 2-24-93-7W4 (52.7–56.3 m depth, 477.2–473.6 m asl) showing till in sharp contact with shale. Core boxes are 0.9 m long.

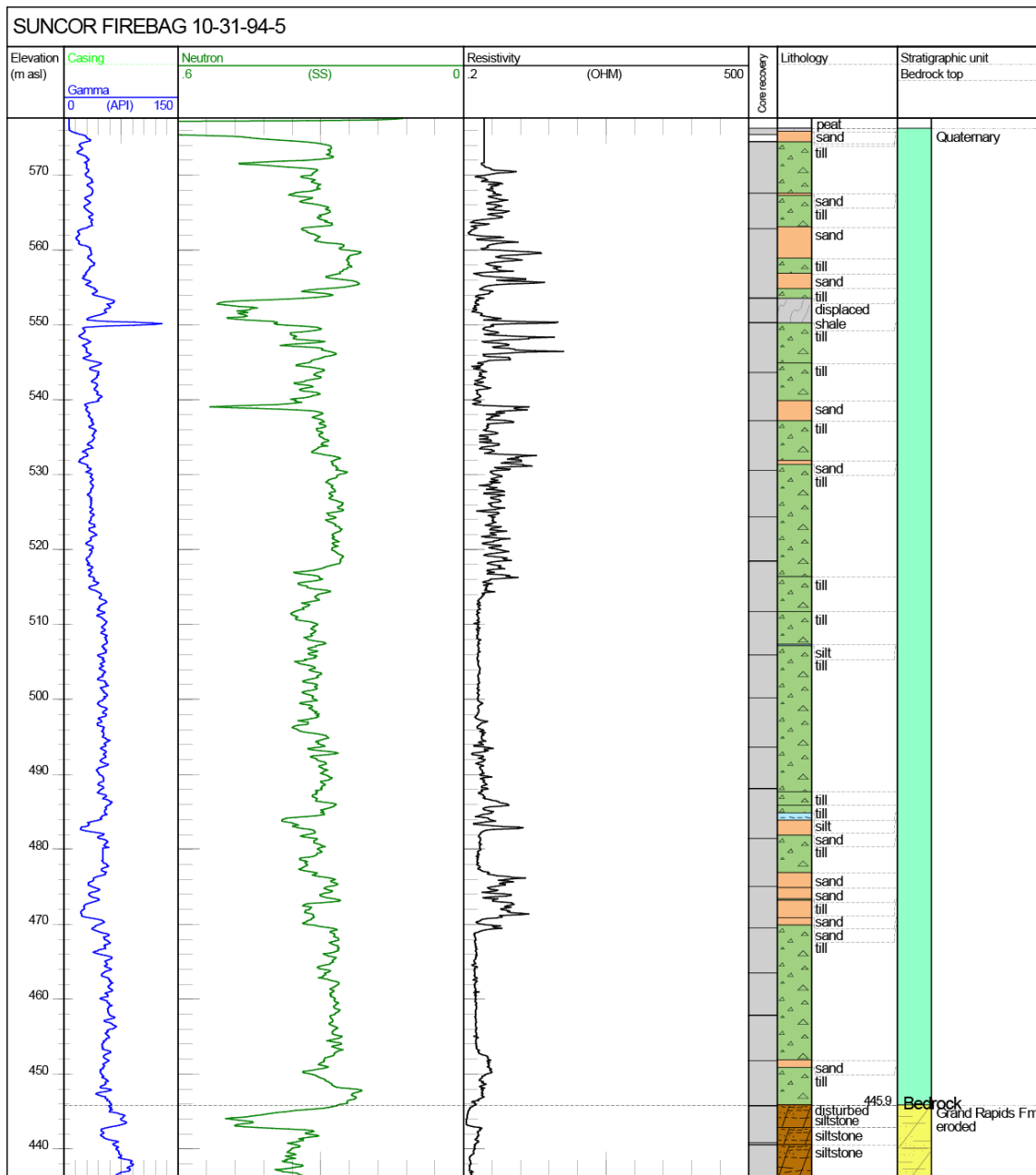


Figure 57. Logs for well SUNCOR FIREBAG 10-31-94-5W4. Litholog determined from examination of core. Kelly bushing at 579.9 m asl and total depth at 379.9 m asl. Abbreviations: Gamma, gamma ray; Neutron, neutron porosity; OHM, ohm*m; SS, sandstone units.



Figure 58. Photograph of core interval from well SUNCOR FIREBAG 10-31-94-5W4 (6.5–9.5 m depth, 573.4–570.4 m asl) showing till (unit 5). Core boxes are 0.9 m long.

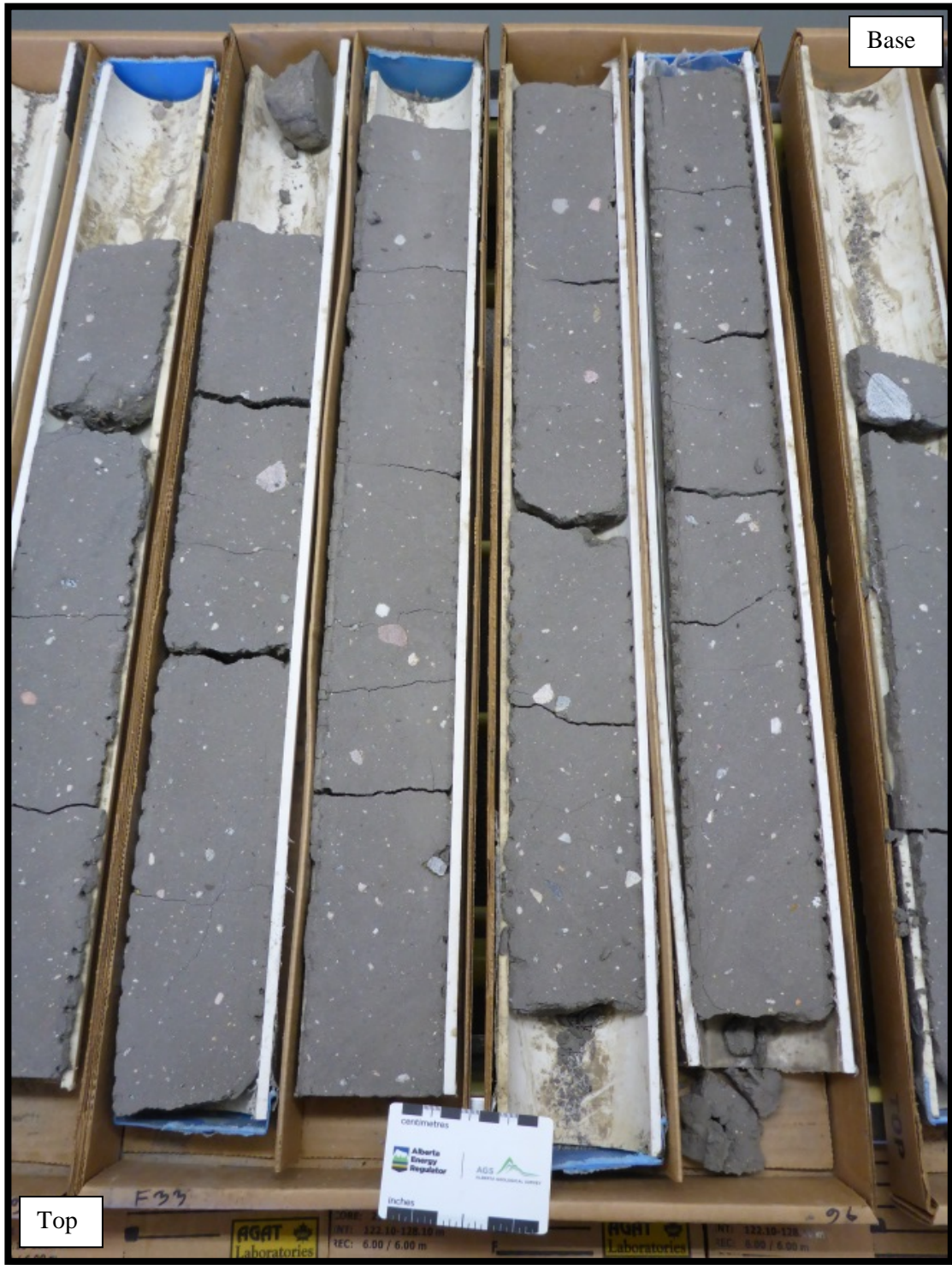


Figure 59. Photograph of core interval from well SUNCOR FIREBAG 10-31-94-5W4 (125–127.5 m depth, 454.9–452.4 m asl) showing till (unit 1). Core boxes are 0.9 m long.

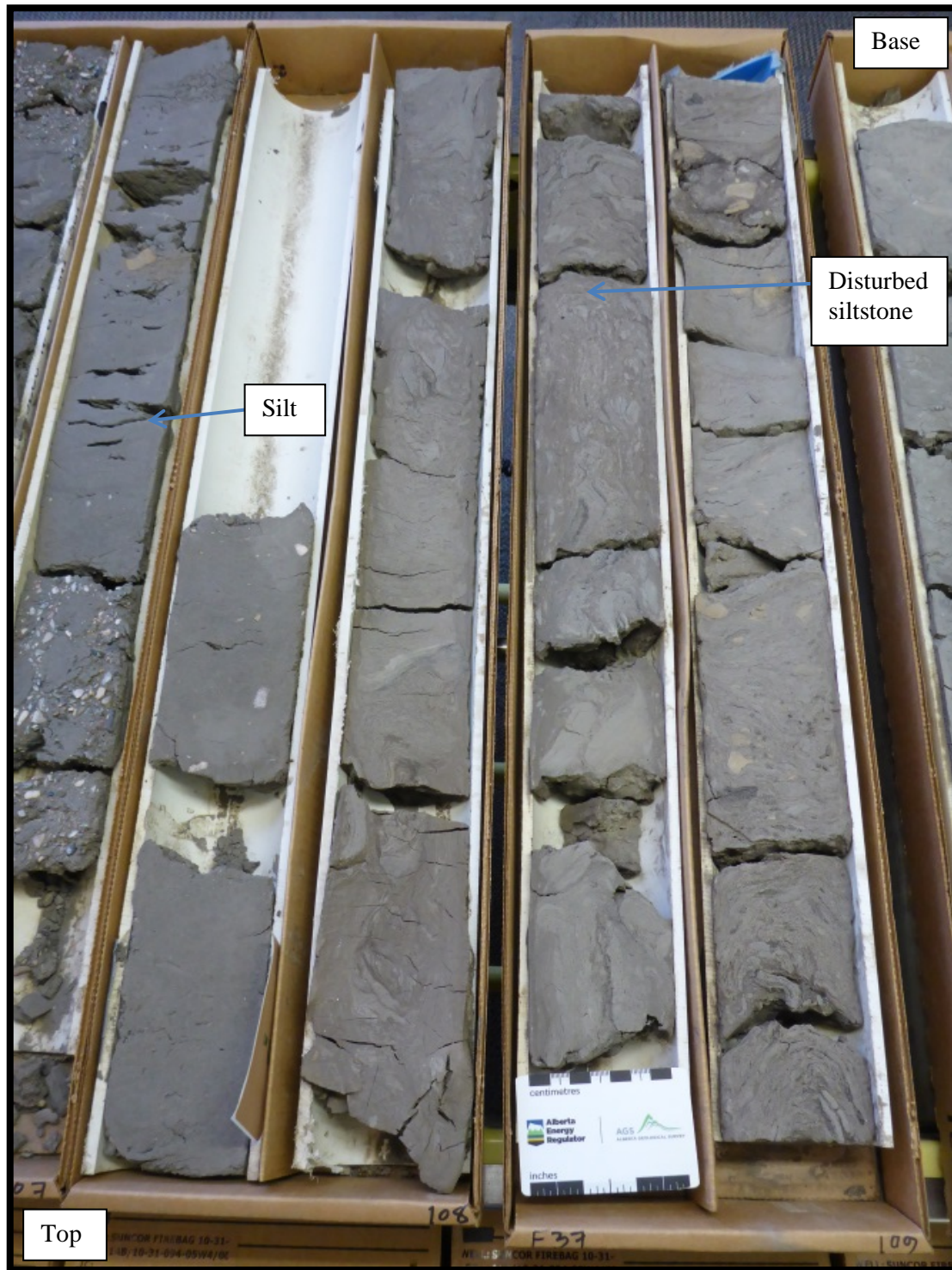


Figure 60. Photograph of core interval from well SUNCOR FIREBAG 10-31-94-5W4 (135–139 m depth, 444.9–440.9 m asl) showing silt, with a few pebble layers, overlying disturbed siltstone (lighter grey). Core boxes are 0.9 m long.

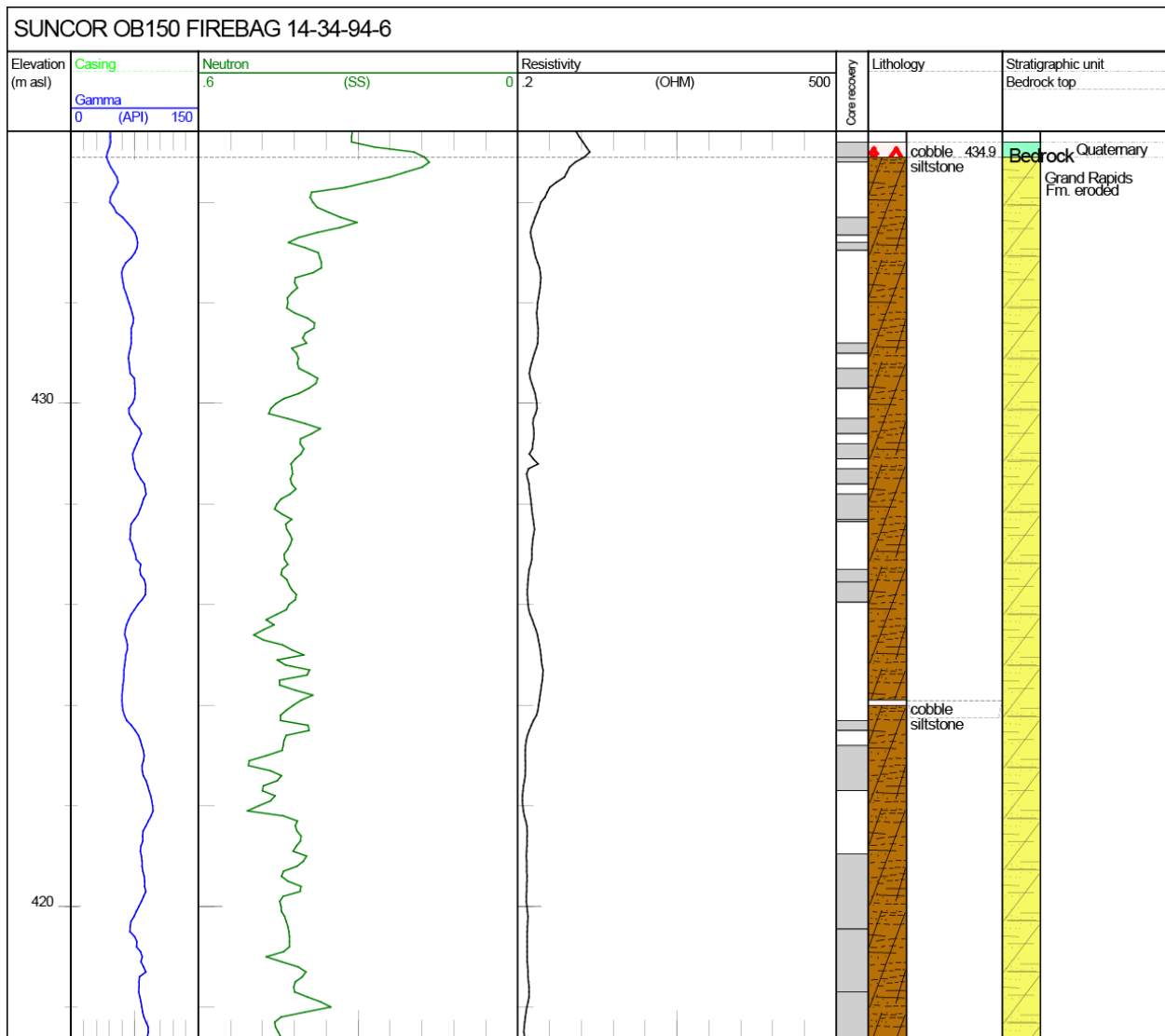


Figure 61. Logs for well SUNCOR OB150 FIREBAG 14-34-94-6W4. Litholog determined from examination of core. Kelly bushing at 604.1 m asl and total depth at 241.2 m asl. Abbreviations: Gamma, gamma ray; Neutron, neutron porosity; OHM, ohm·m; SS, sandstone units.

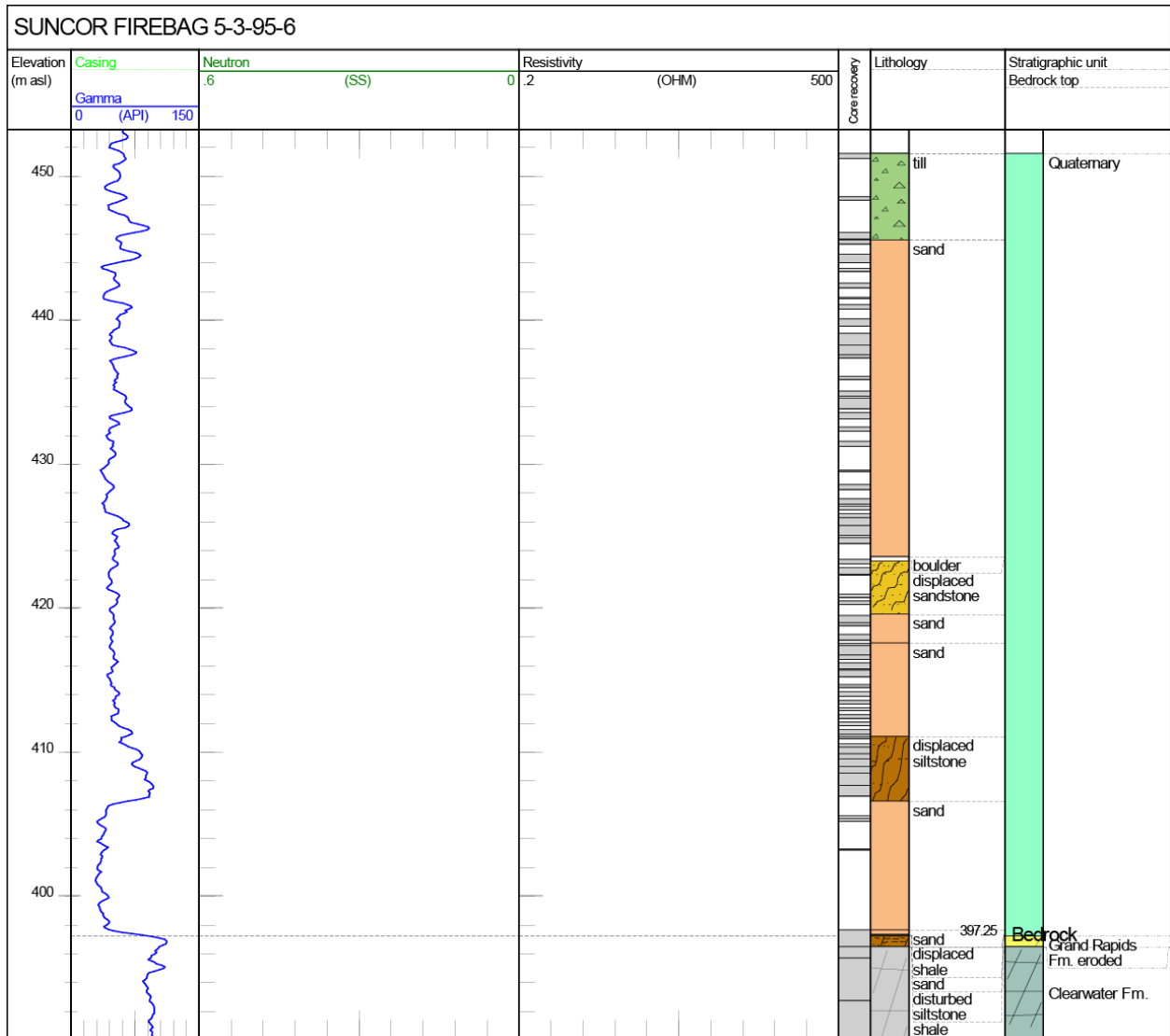


Figure 62. Logs for well SUNCOR FIREBAG 5-3-95-6W4. Litholog determined from examination of core. Neutron and resistivity data unavailable. Kelly bushing at 603.6 m asl and total depth at 260.1 m asl. Abbreviations: Gamma, gamma ray; Neutron, neutron porosity; OHM, ohm·m; SS, sandstone units.



Figure 63. Photograph of core interval from well SUNCOR FIREBAG 5-3-95-6W4 (194–195 m depth, 409.6–408.6 m asl) showing displaced siltstone. Core boxes are 0.9 m long.

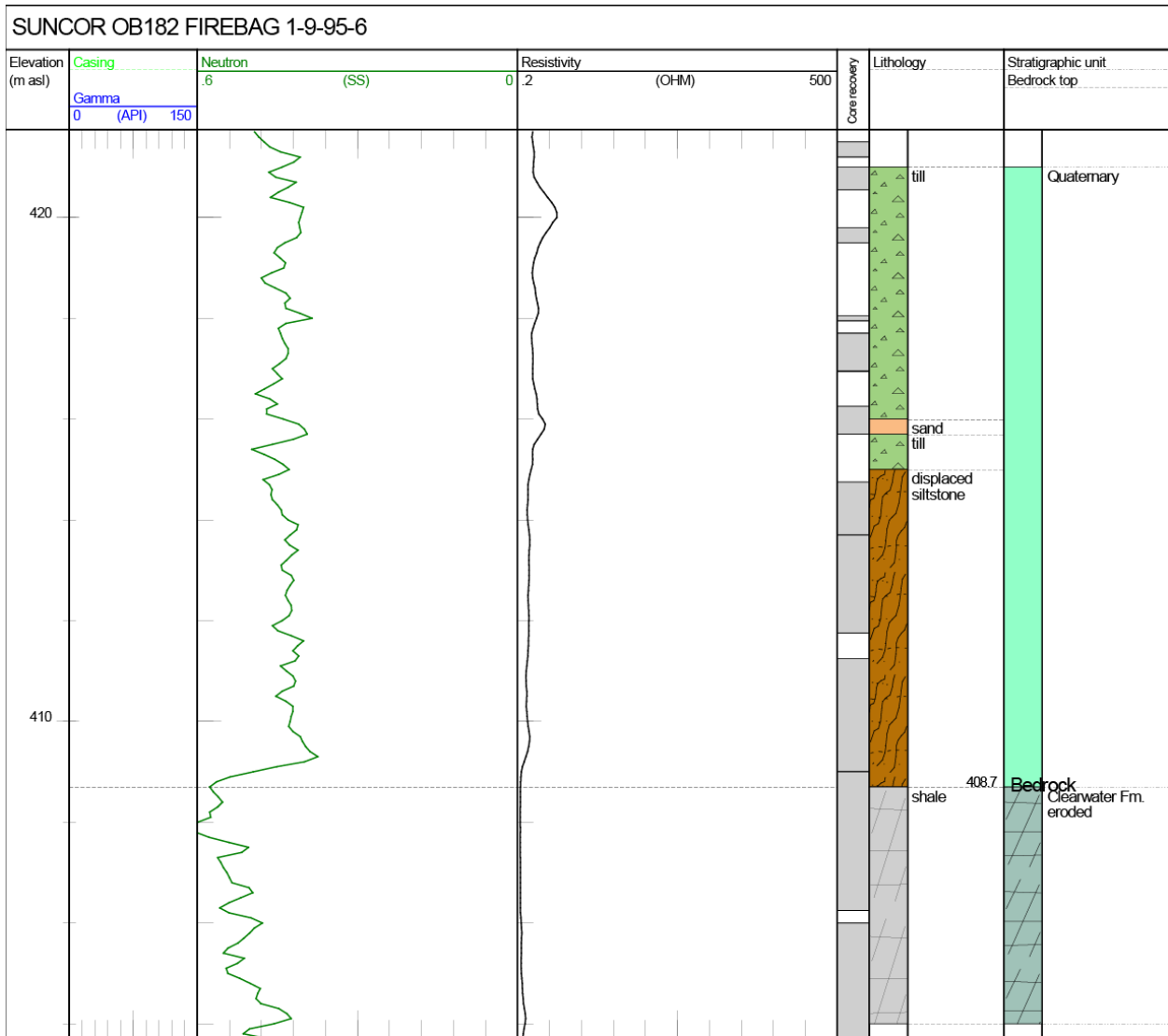


Figure 64. Logs for well SUNCOR OB182 FIREBAG 1-9-95-6W4. Litholog determined from examination of core. Gamma-ray data unavailable. Kelly bushing at 589.0 m asl and total depth at 340.0 m asl. Abbreviations: Gamma, gamma ray; Neutron, neutron porosity; OHM, ohm·m; SS, sandstone units.



Figure 65. Photograph of core interval from well SUNCOR OB182 FIREBAG 1-9-95-6W4 (175.30–177.75 m depth, 413.70–411.25 m asl) showing displaced siltstone. Core boxes are 0.9 m long.

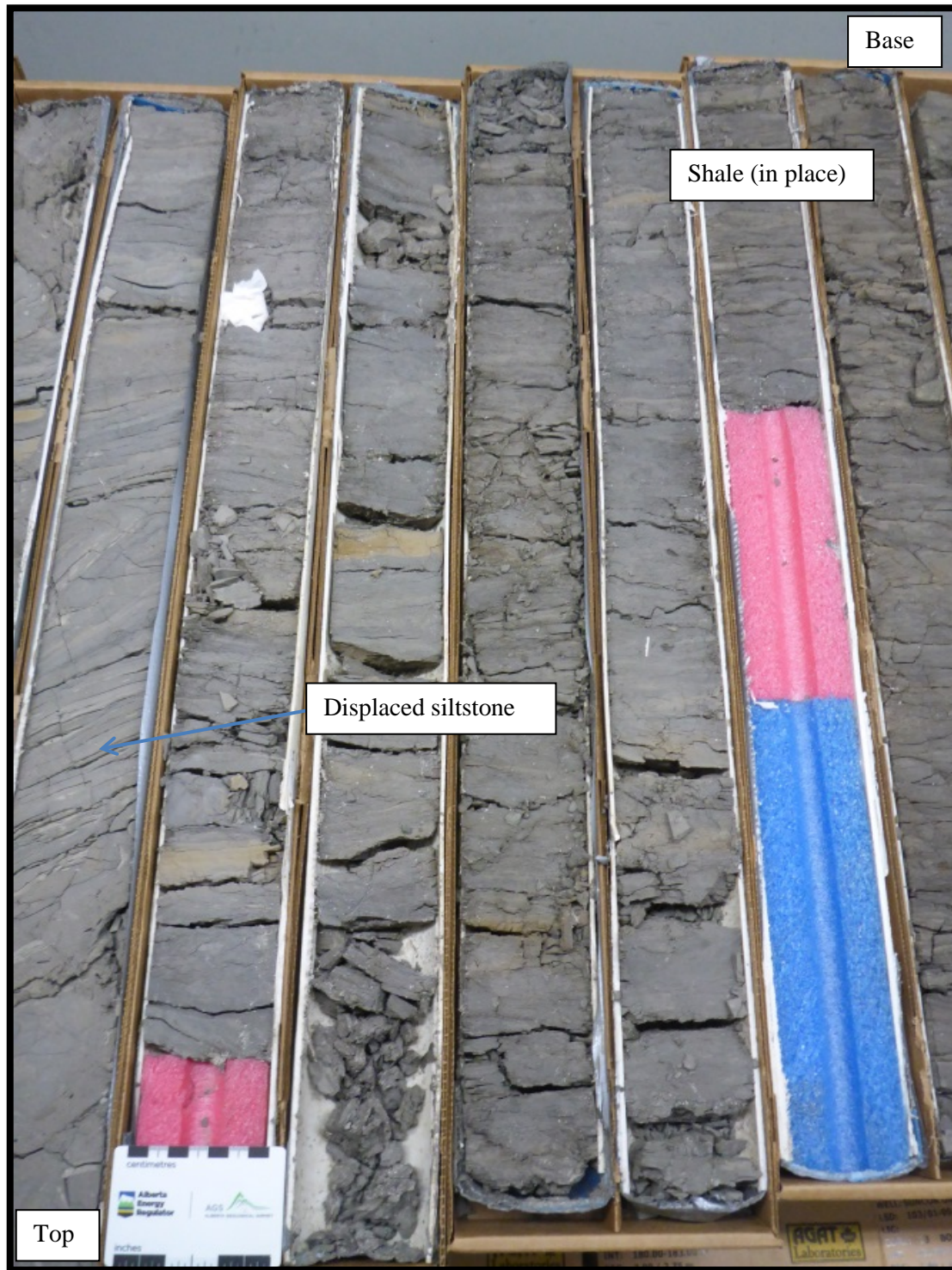


Figure 66. Photograph of core interval from well SUNCOR OB182 FIREBAG 1-9-95-6W4 (180–183 m depth, 409.0–406.0 m asl) showing displaced siltstone (with angled bedding) overlying in place shale. Core boxes are 0.9 m long.

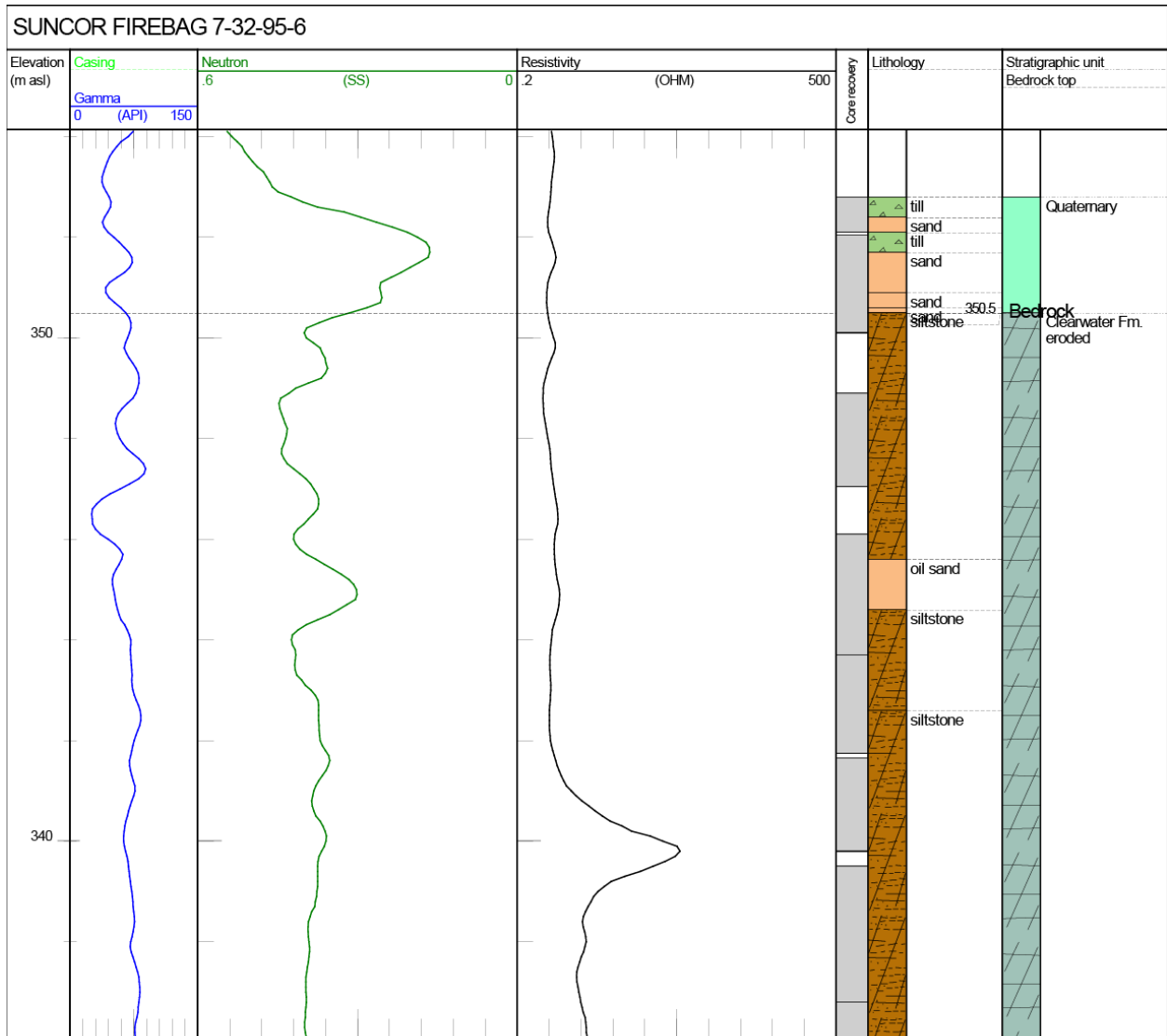


Figure 67. Logs for well SUNCOR FIREBAG 7-32-95-6W4. Litholog determined from examination of core. Kelly bushing at 565.6 m asl and total depth at 280.8 m asl. Abbreviations: Gamma, gamma ray; Neutron, neutron porosity; OHM, ohm•m; SS, sandstone units.



Figure 69. Photograph of core interval from well HUSKY SUNRISE 7-2-96-6W4 (199.0–202.25 m depth, 355.6–352.35 m asl) showing till. Core boxes are 0.9 m long.

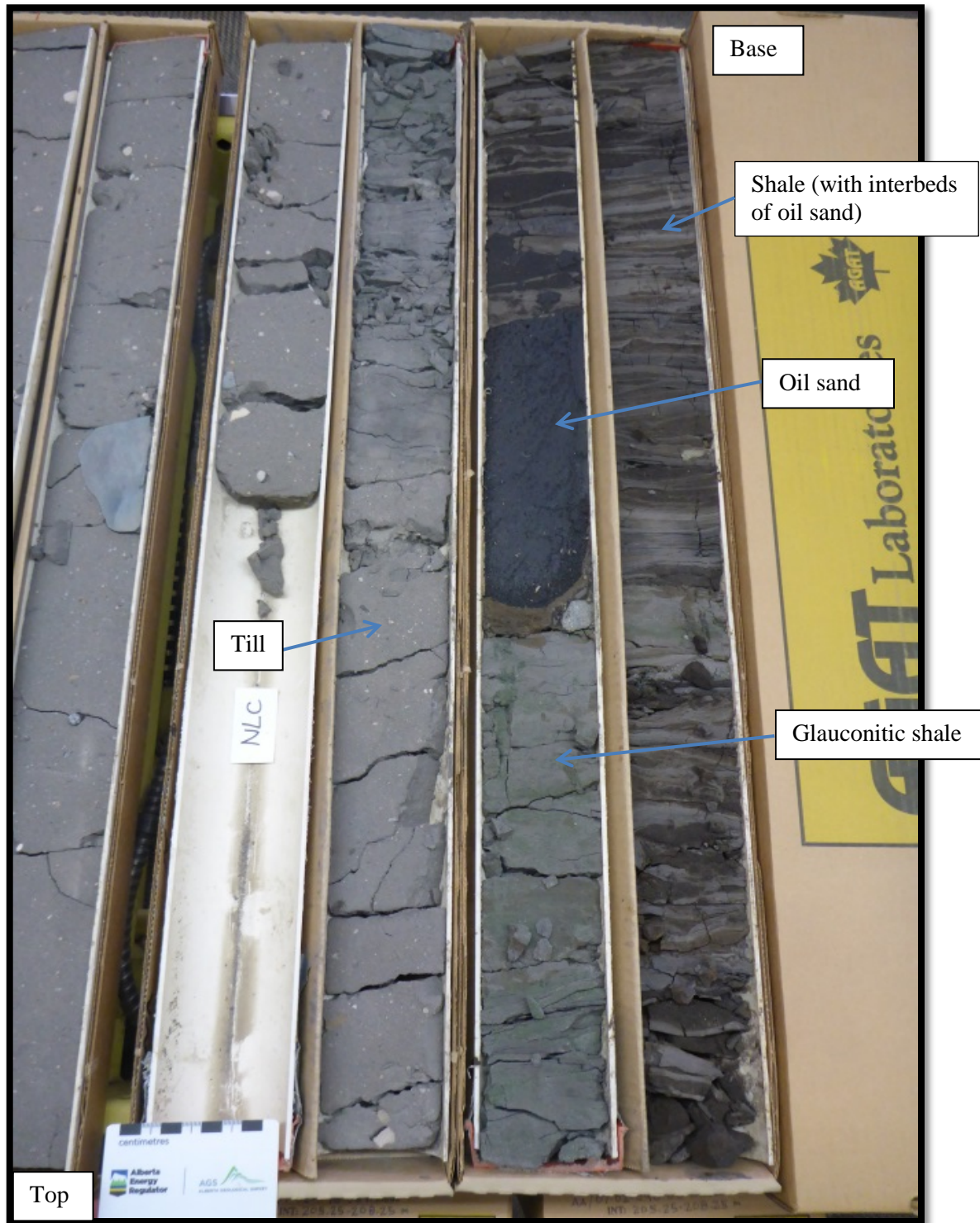


Figure 70. Photograph of core interval from well HUSKY SUNRISE 7-2-96-6W4 (205.25–208.25 m depth, 349.35–346.35 m asl) showing till overlying glauconitic shale (Wabiskaw Member of Clearwater Formation), oil sand, and shale (with interbeds of oil sand). Core boxes are 0.9 m long.

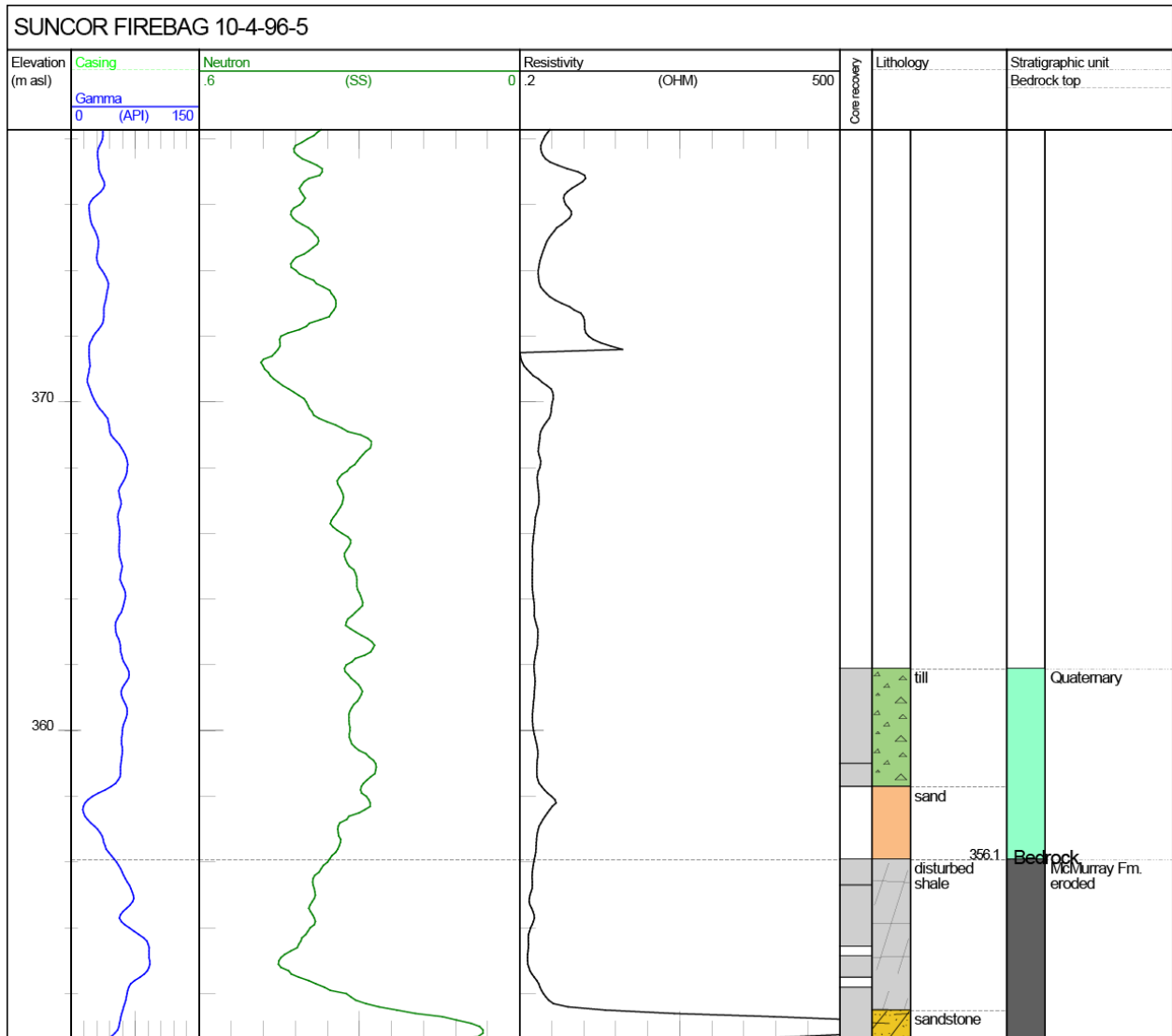


Figure 71. Logs for well SUNCOR FIREBAG 10-4-96-5W4. Litholog determined from examination of core. Kelly bushing at 531.5 m asl and total depth at 284.9 m asl. Abbreviations: Gamma, gamma ray; Neutron, neutron porosity; OHM, ohm•m; SS, sandstone units.



Figure 72. Photograph of core interval from well SUNCOR FIREBAG 10-4-96-5W4 (169.60–172.50 m depth, 361.9–359.0 m asl) showing till. Core boxes are 0.9 m long.

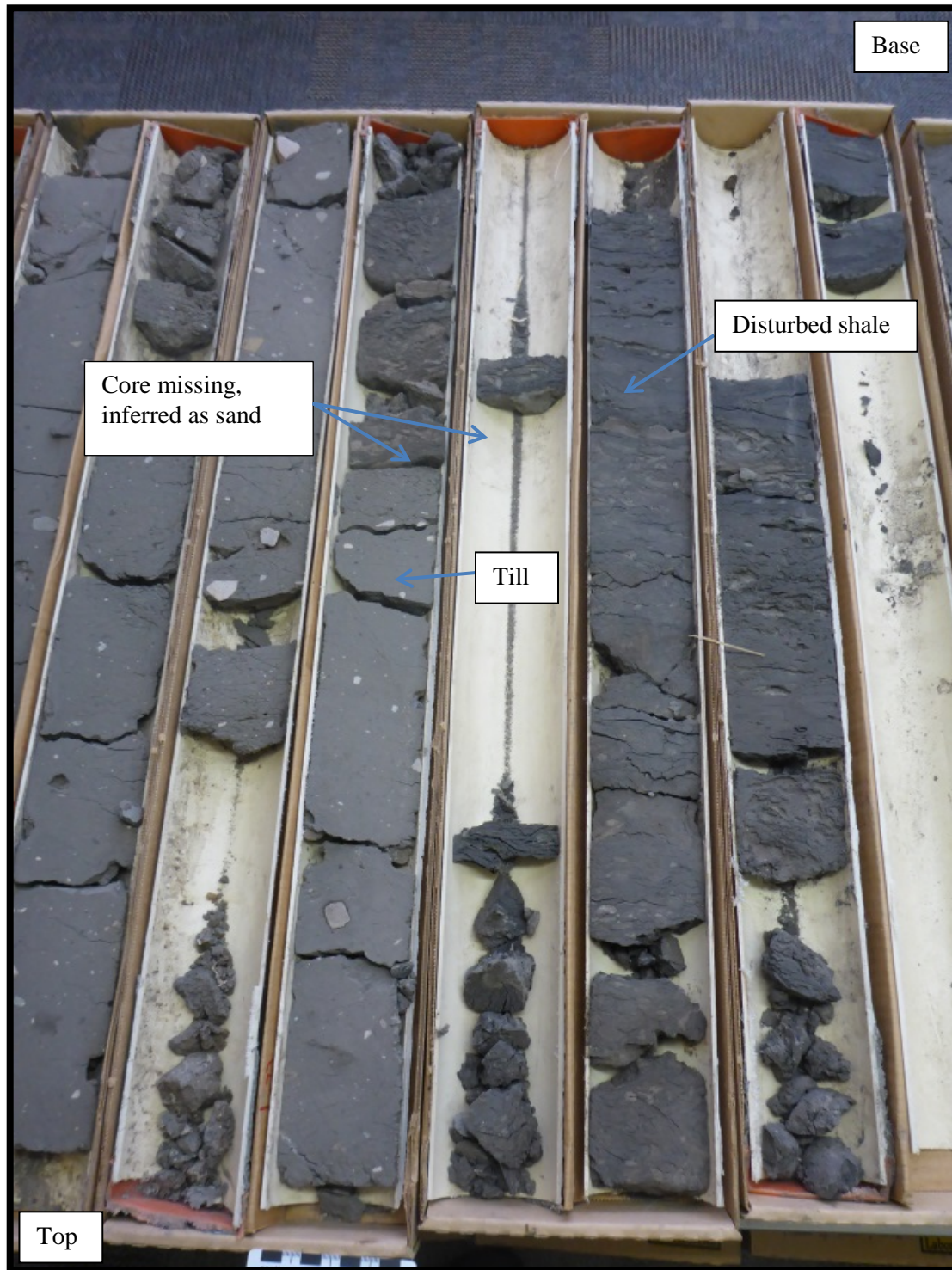


Figure 73. Photograph of core interval from well SUNCOR FIREBAG 10-4-96-5W4 (172.5–176.2 m depth, 359.0–355.3 m asl) showing till overlying disturbed shale. The nonrecovered interval between the till and disturbed shale is interpreted to be sand. Core boxes are 0.9 m long.

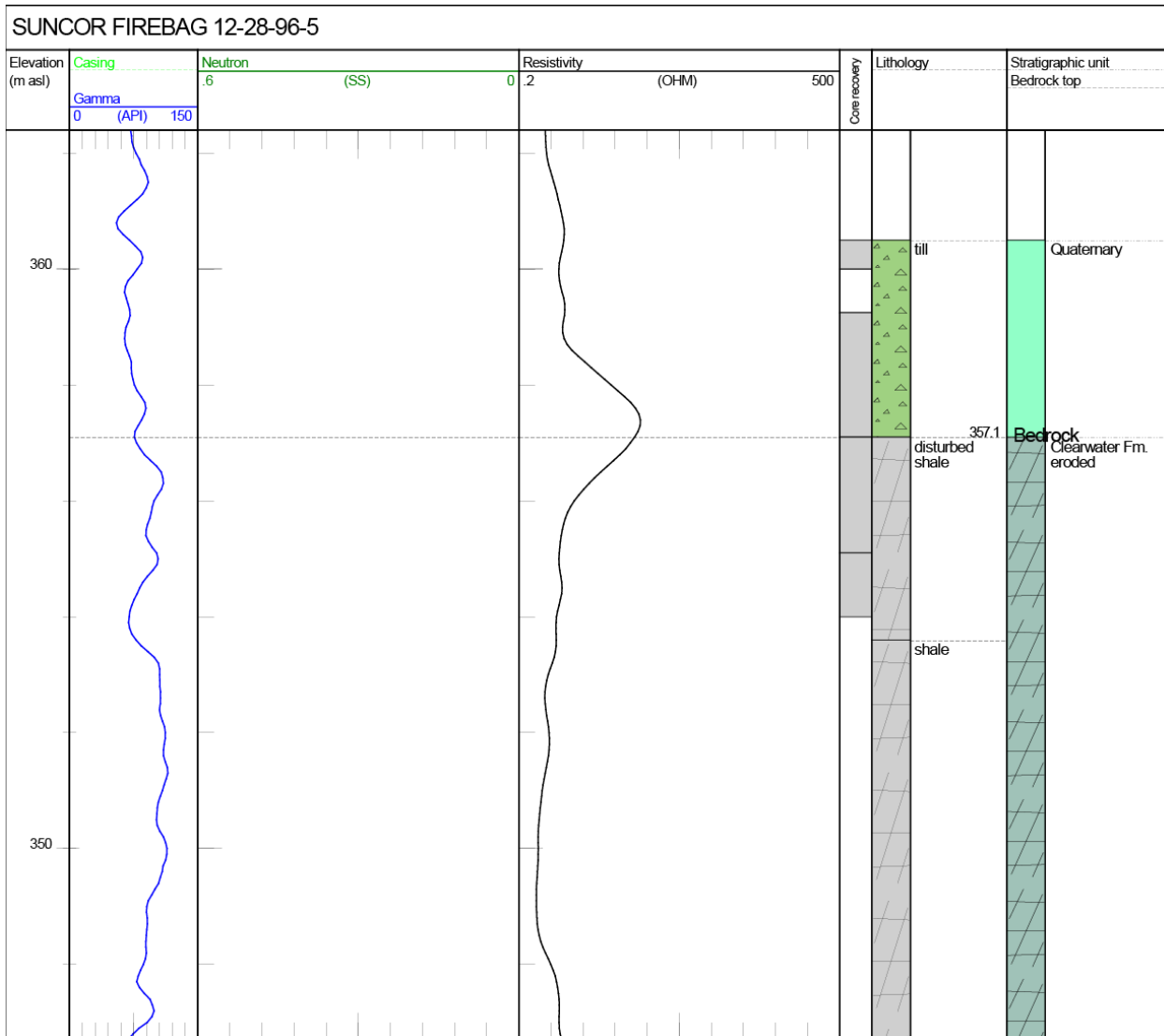


Figure 74. Logs for well SUNCOR FIREBAG 12-28-96-5W4. Litholog determined from examination of core. Neutron data unavailable. Kelly bushing at 448.1 m asl and total depth at 301.6 m asl. Abbreviations: Gamma, gamma ray; Neutron, neutron porosity; OHM, ohm·m; SS, sandstone units.

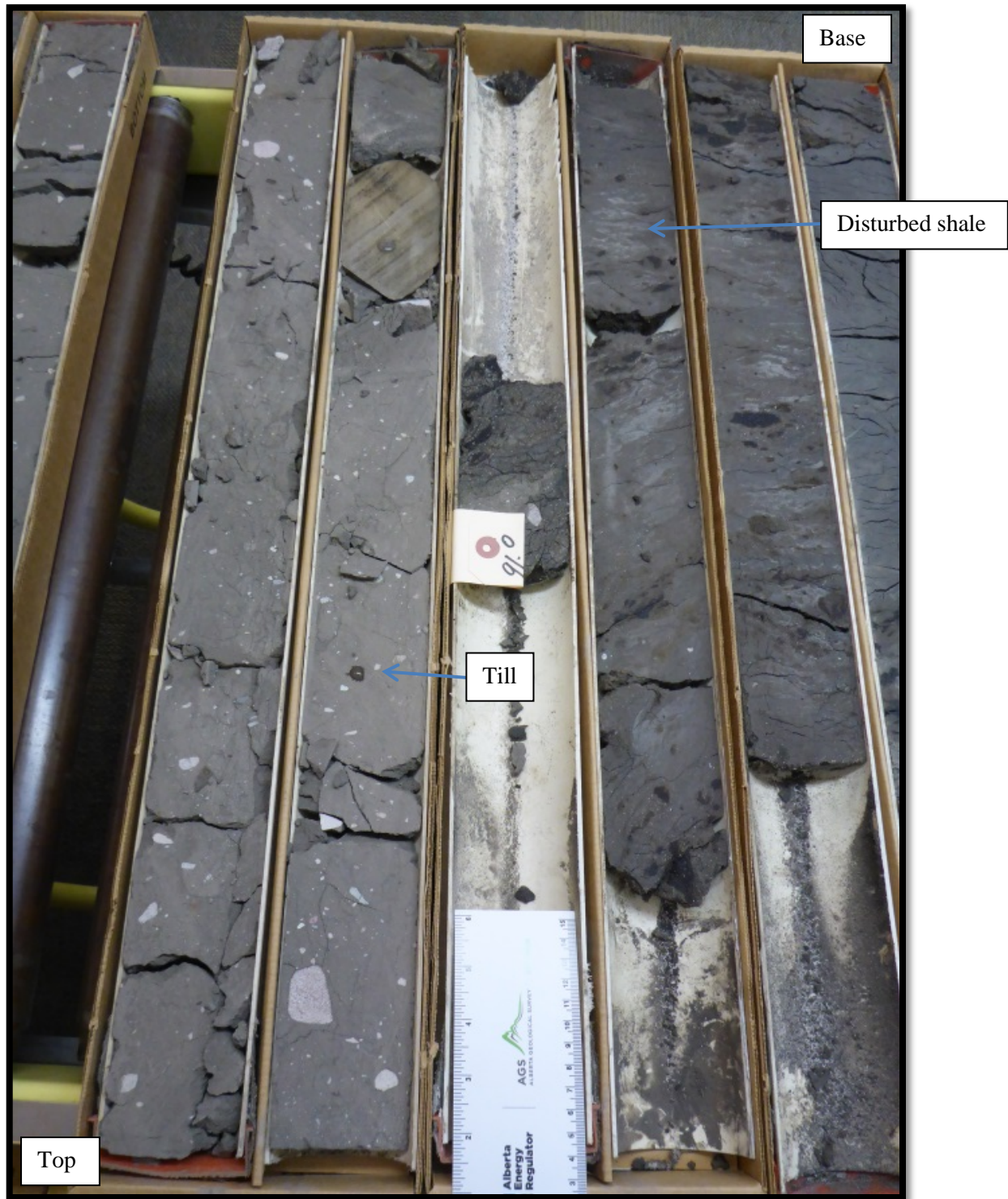


Figure 75. Photograph of core interval from well SUNCOR FIREBAG 12-28-96-5W4 (89–92 m depth, 359.1–356.1 m asl) showing till overlying disturbed shale. Core boxes are 0.9 m long.



Figure 76. Photograph of core interval from well SUNCOR FIREBAG 12-28-96-5W4 (92–95.1 m depth, 356.1–353.0 m asl) showing disturbed shale (dark grey) over lighter grey undisturbed shale. Core boxes are 0.9 m long.

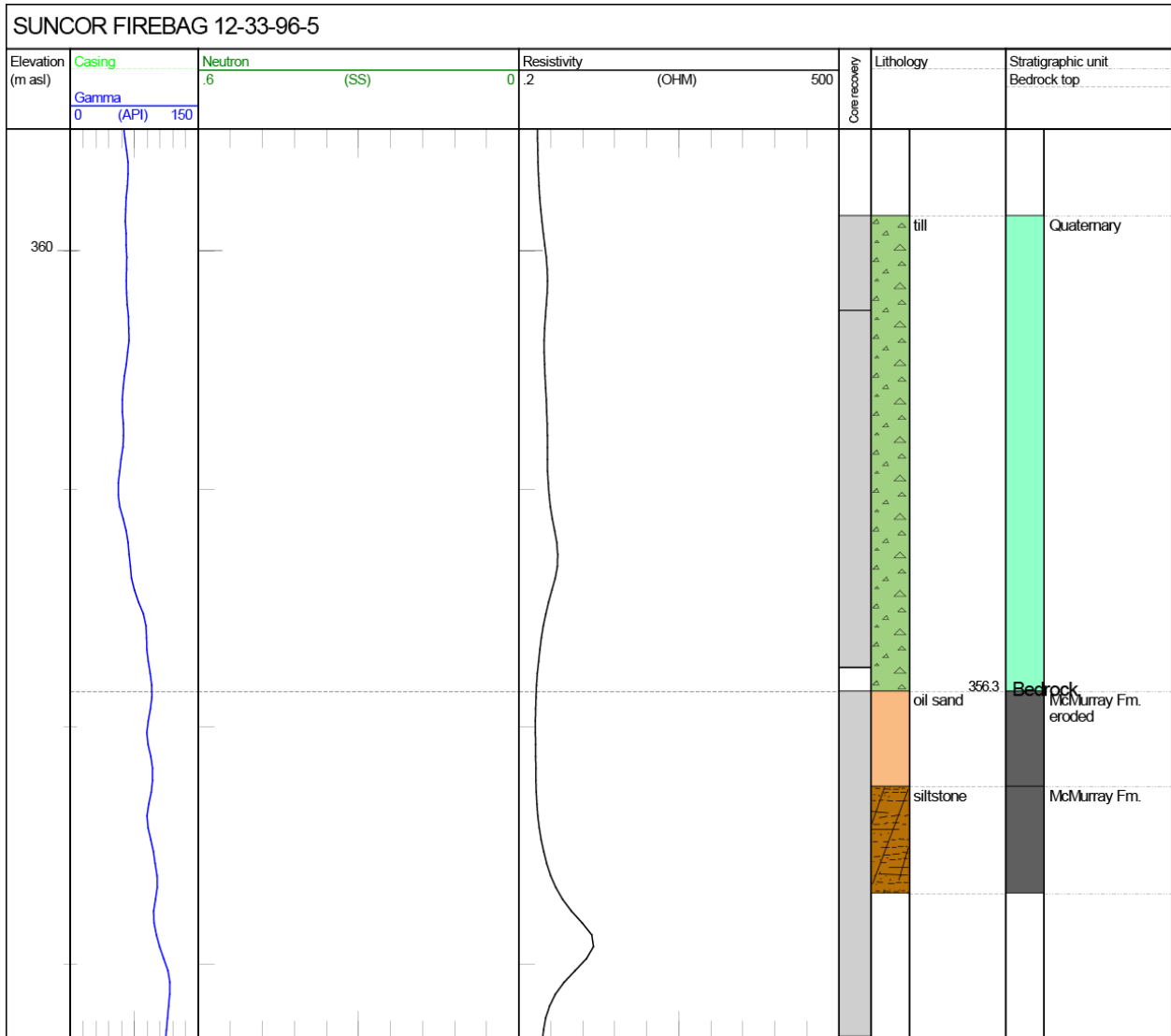


Figure 77. Logs for well SUNCOR FIREBAG 12-33-96-5W4. Litholog determined from examination of core. Neutron data unavailable. Kelly bushing at 417.5 m asl and total depth at 301.6 m asl. Abbreviations: Gamma, gamma ray; Neutron, neutron porosity; OHM, ohm•m; SS, sandstone units.

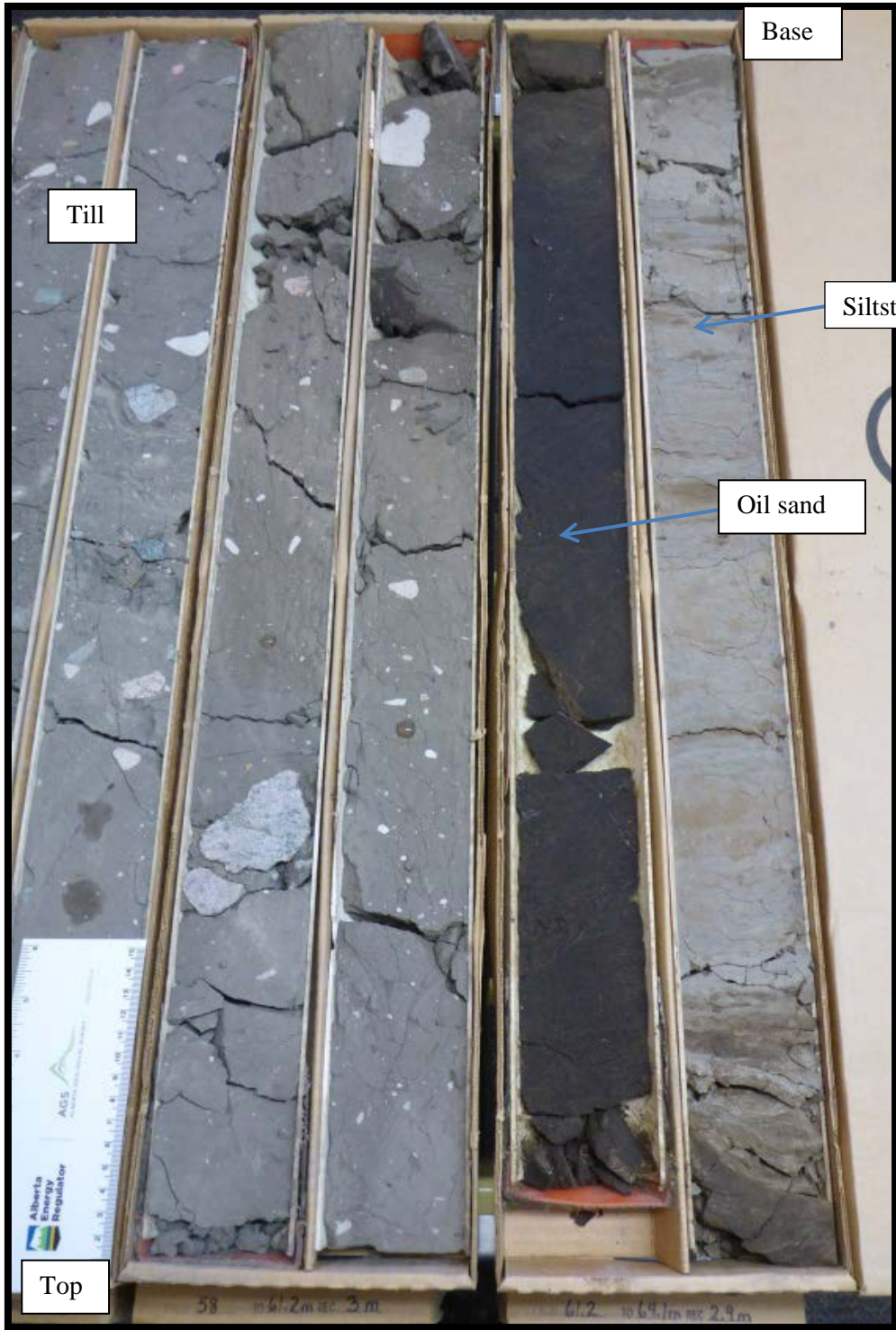


Figure 78. Photograph of core interval from well SUNCOR FIREBAG 12-33-96-5W4 (59.0–62.5 m depth, 358.5–355.0 m asl) showing till over oil sand and siltstone. Core boxes are 0.9 m long.

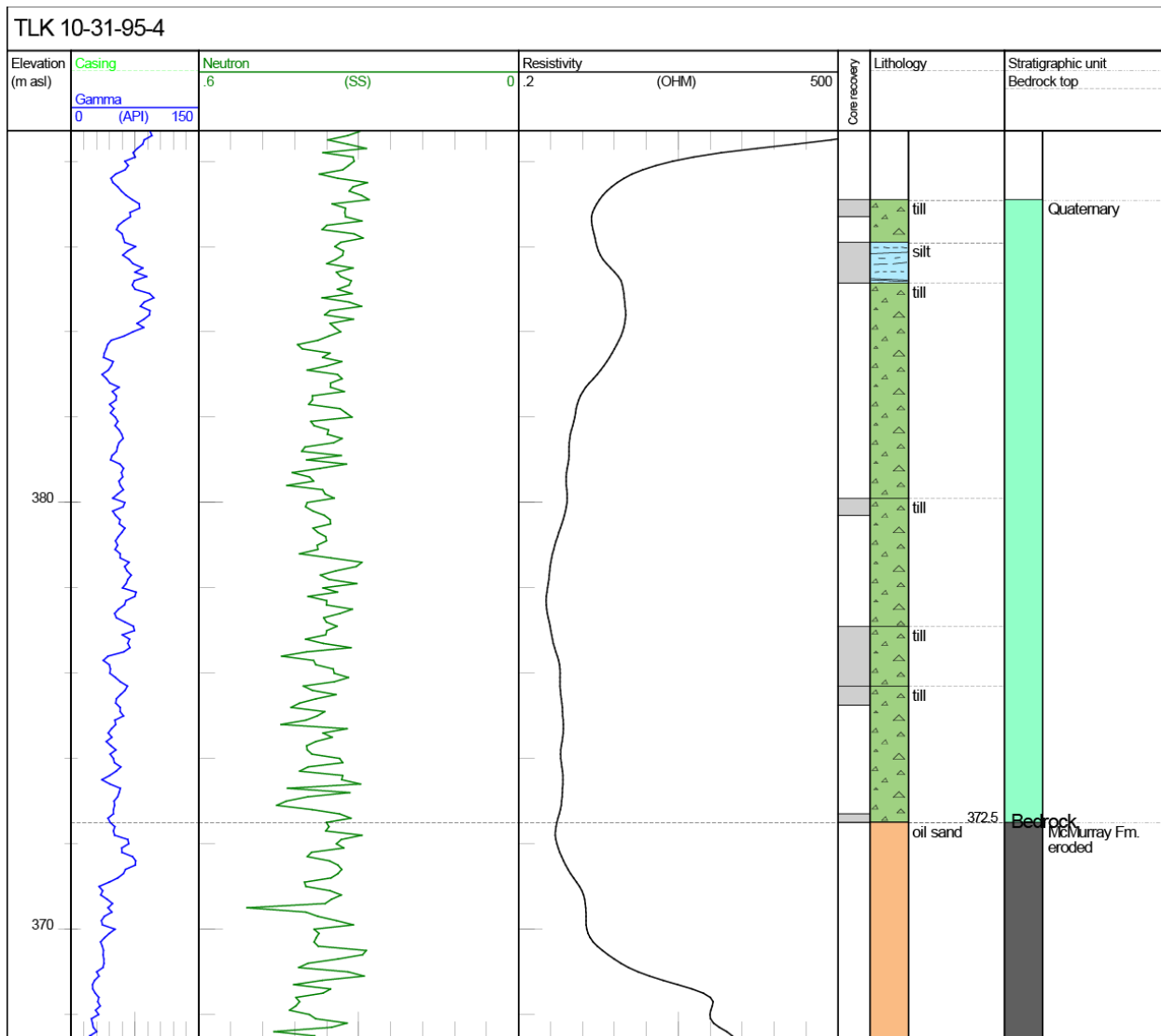


Figure 79. Logs for well TLK 10-31-95-4W4. Litholog determined from examination of core. Kelly bushing at 551.1 m asl and total depth at 311.1 m asl. Abbreviations: Gamma, gamma ray; Neutron, neutron porosity; OHM, ohm•m; SS, sandstone units.

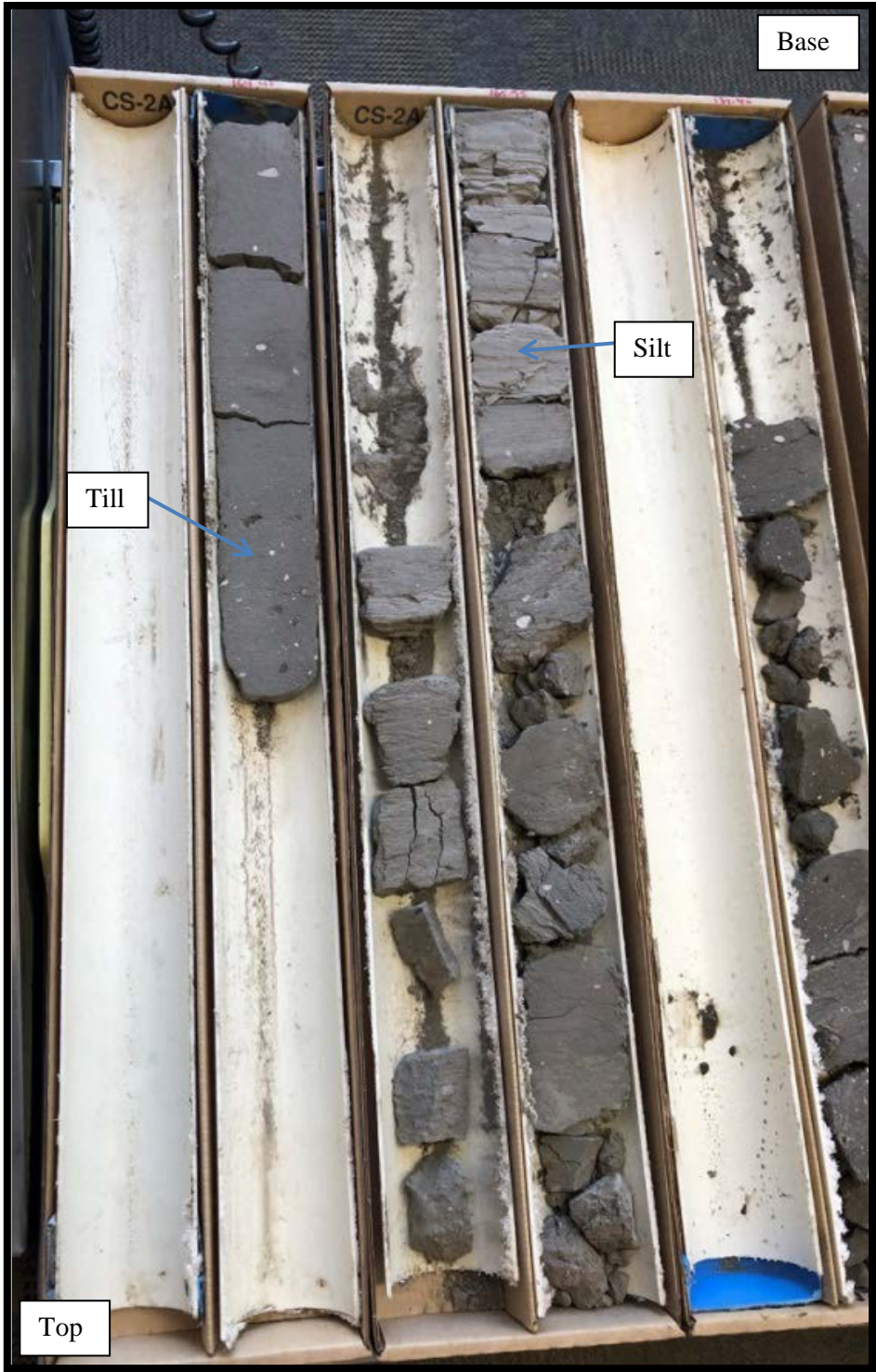


Figure 80. Photograph of core interval from well TLK 10-31-95-4W4 (164.0–165.95 m depth, 387.1–385.15 m asl) showing till with interbed of silt (lighter grey). Core boxes are 0.9 m long.

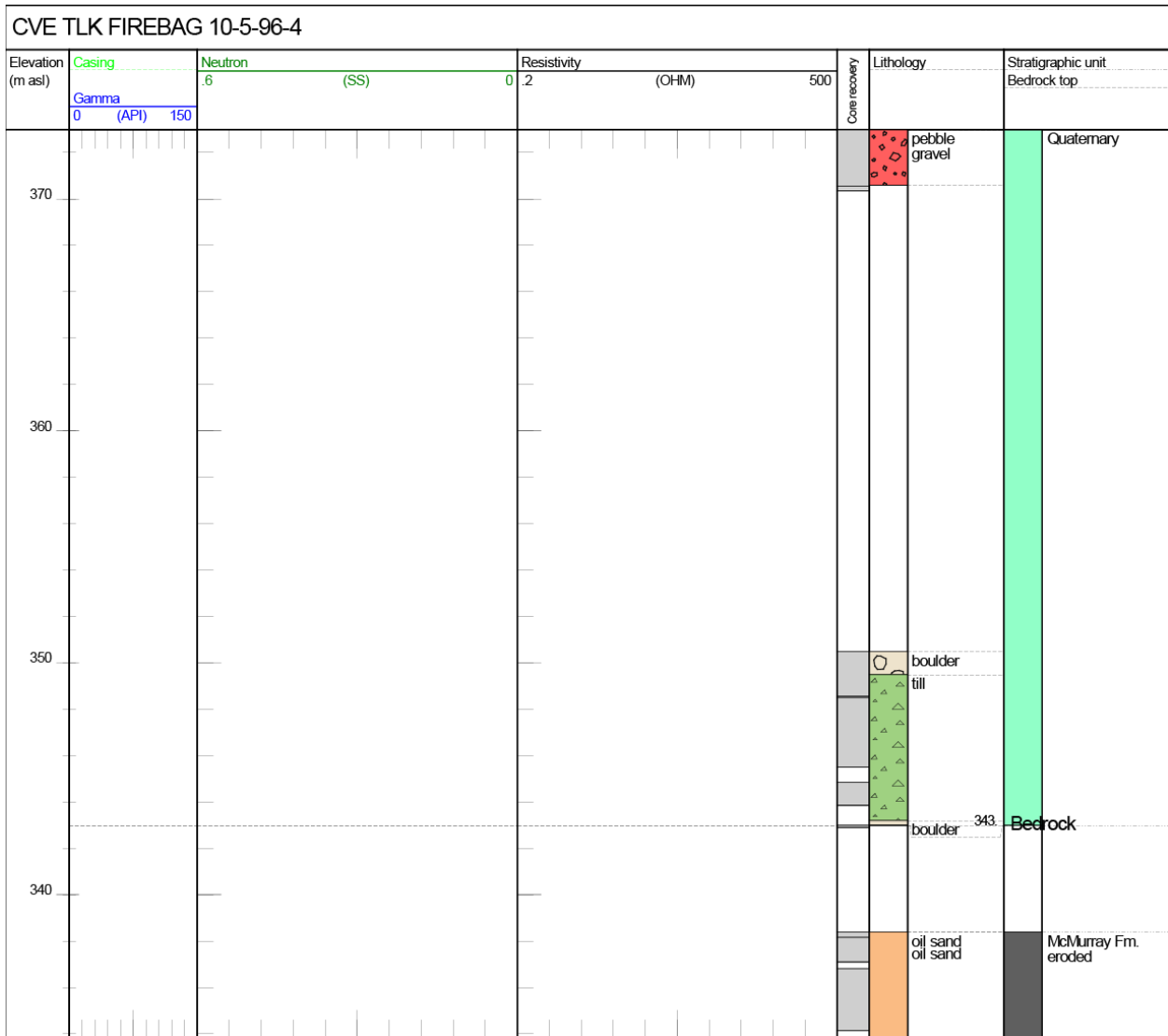


Figure 81. Log for well CVE TLK FIREBAG 10-5-96-4W4. Litholog determined from examination of core. Geophysical data unavailable. Kelly bushing at 521.0 m asl and total depth at 211.0 m asl. Abbreviations: Gamma, gamma ray; Neutron, neutron porosity; OHM, ohm•m; SS, sandstone units.

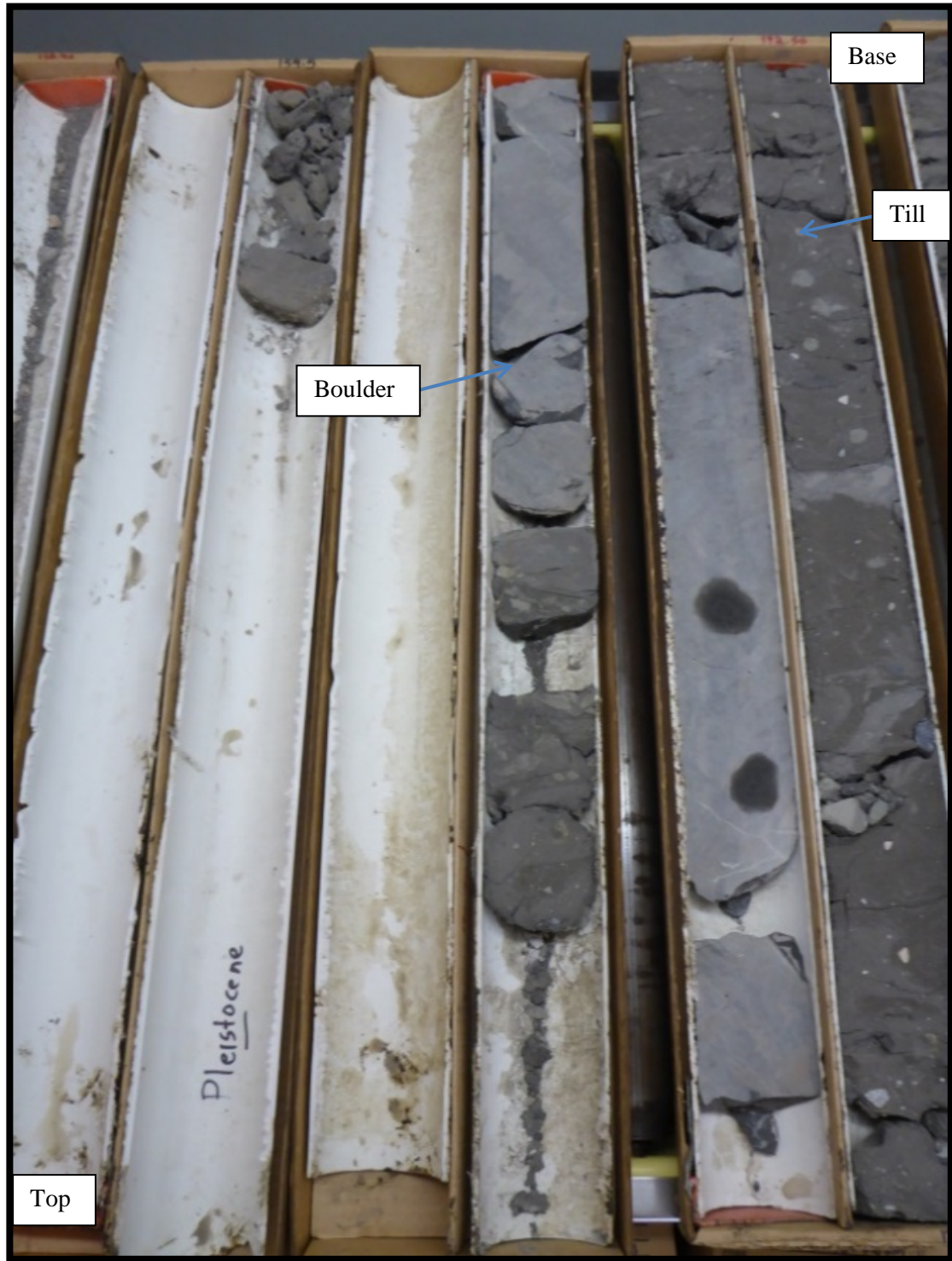


Figure 82. Photograph of core interval from well CVE TLK FIREBAG 10-5-96-4W4 (154.5–172.5 m depth, 366.5–348.5 m asl) showing boulder in till. Core boxes are 0.9 m long.

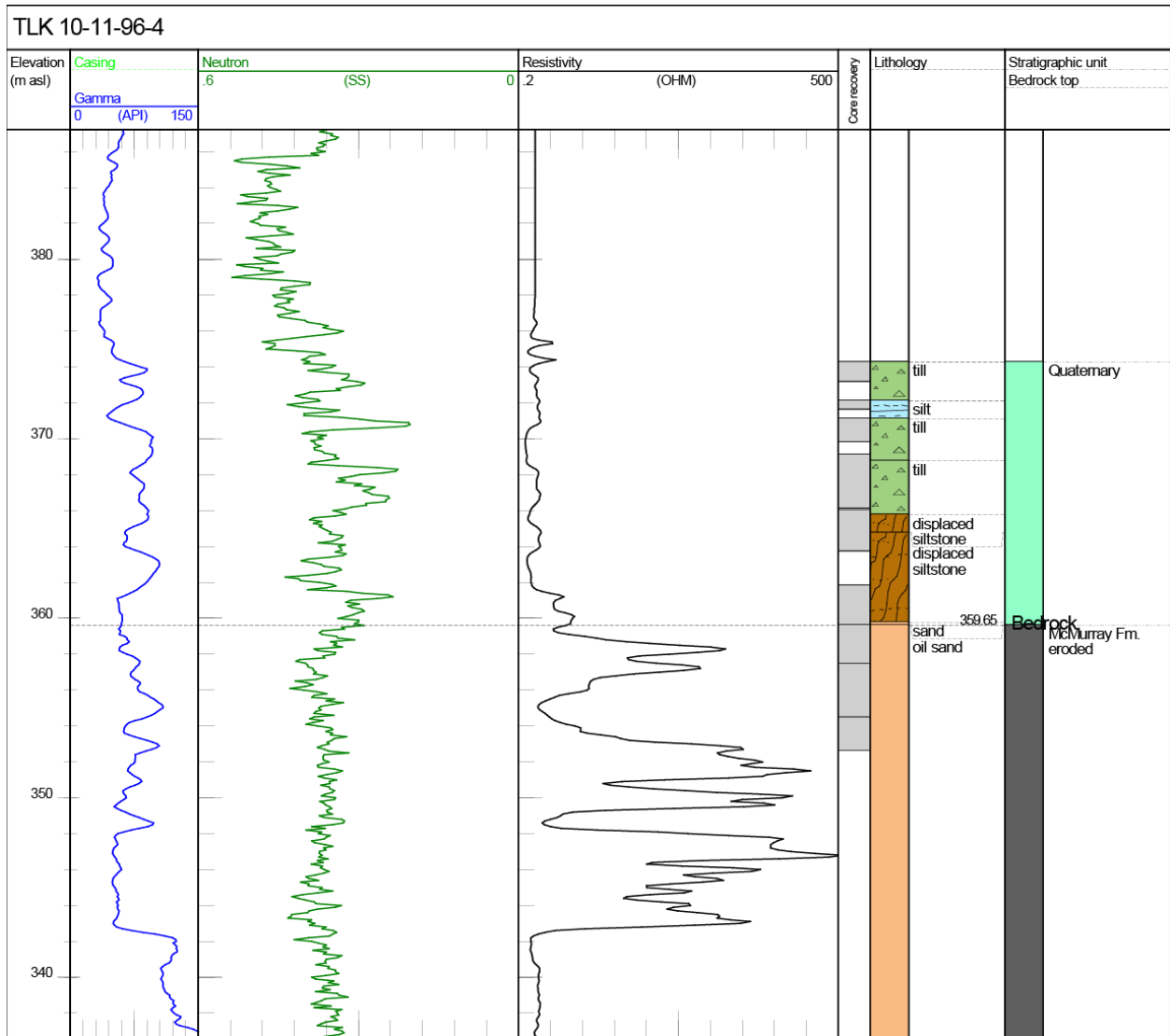


Figure 83. Logs for well TLK 10-11-96-4W4. Litholog determined from examination of core. Kelly bushing at 491.8 m asl and total depth at 277.8 m asl. Abbreviations: Gamma, gamma ray; Neutron, neutron porosity; OHM, ohm•m; SS, sandstone units.

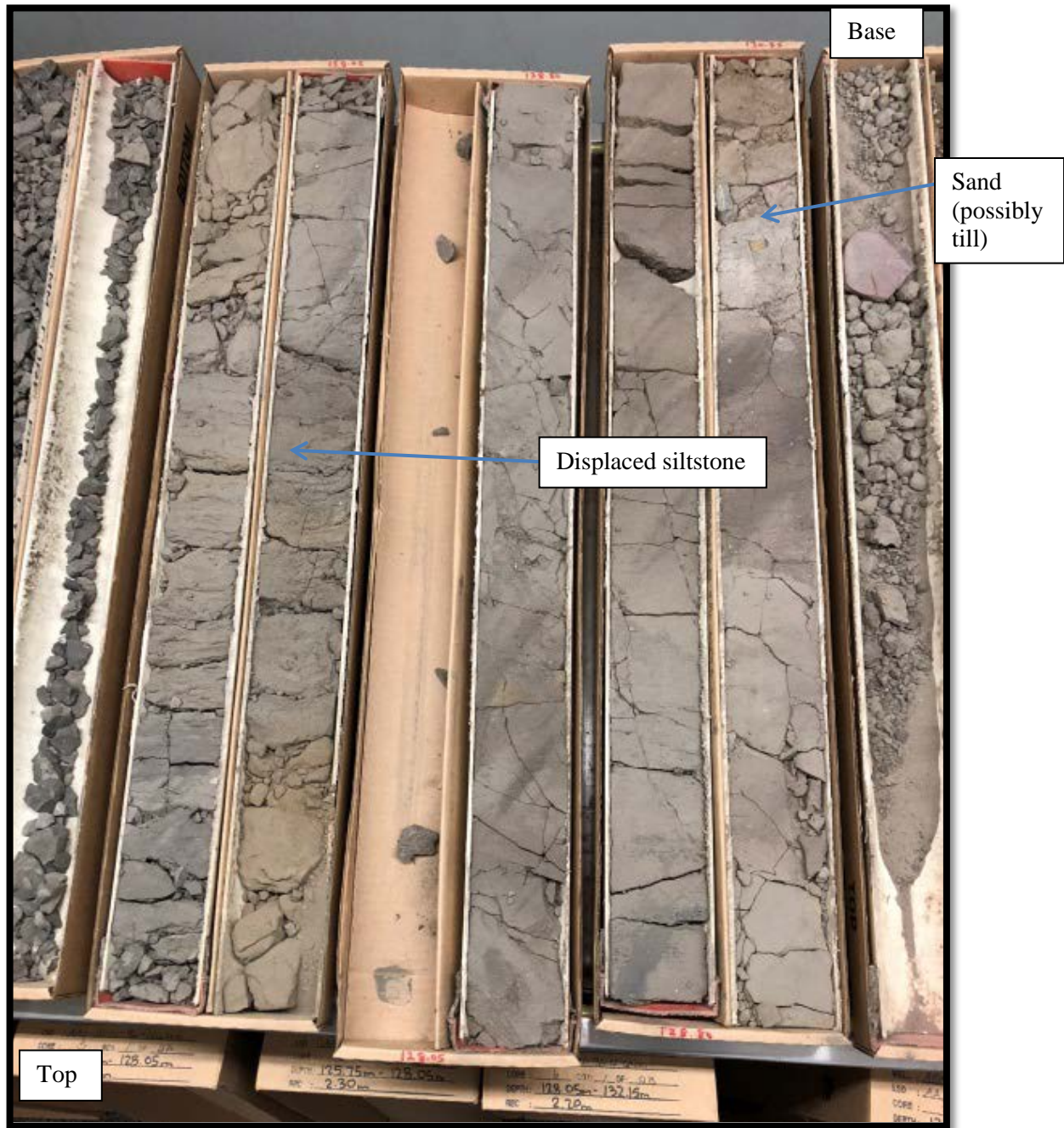


Figure 84. Photograph of core interval from well TLK 10-11-96-4W4 (125.75–132.15 m depth, 366.05–359.65 m asl) showing displaced siltstone, note pebbly sand, possibly till, at base. Core boxes are 0.9 m long.

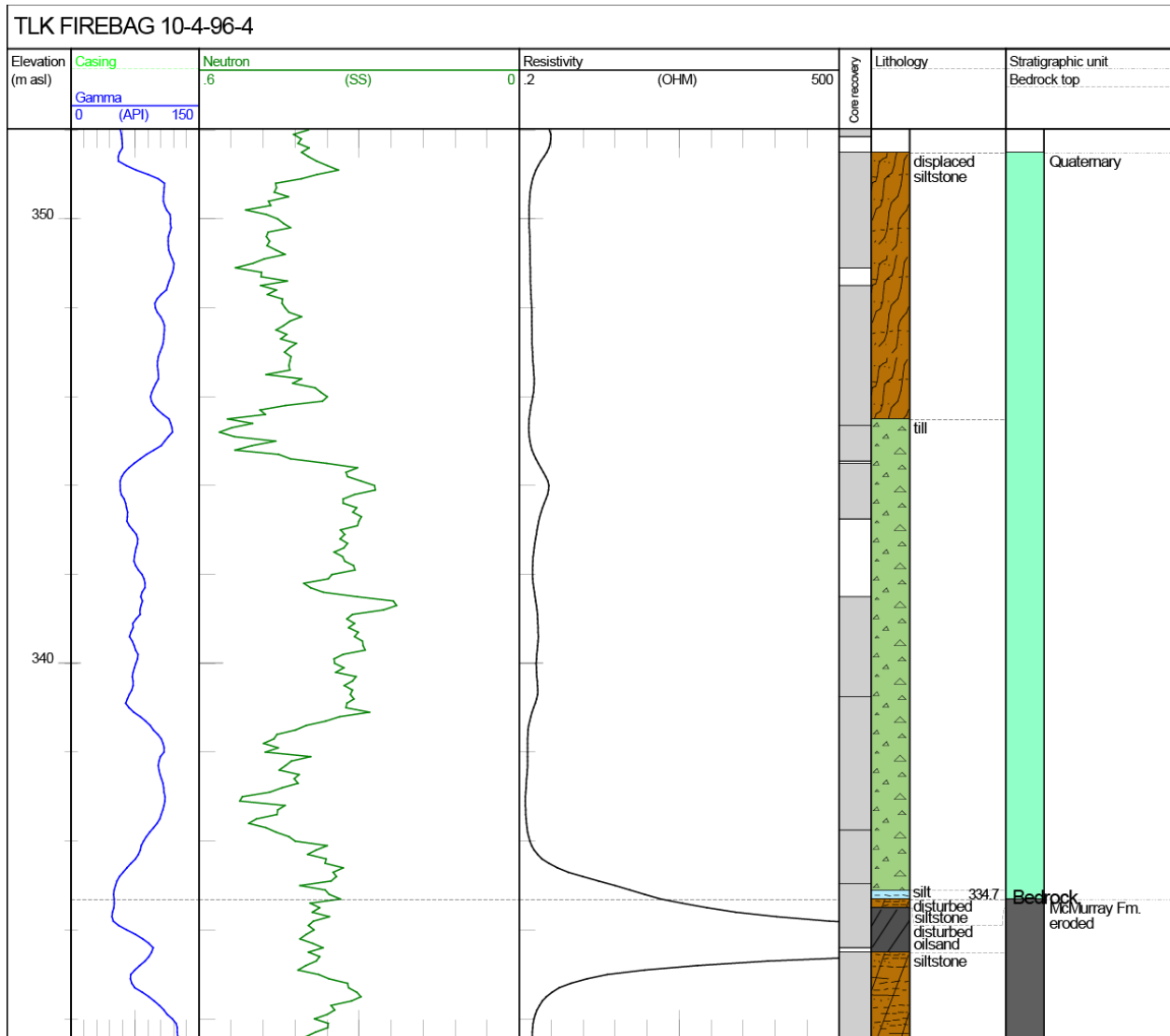


Figure 85. Logs for well TLK FIREBAG 10-4-96-4W4. Litholog determined from examination of core. Kelly bushing at 523.5 m asl and total depth at 312.4 m asl. Abbreviations: Gamma, gamma ray; Neutron, neutron porosity; OHM, ohm•m; SS, sandstone units.

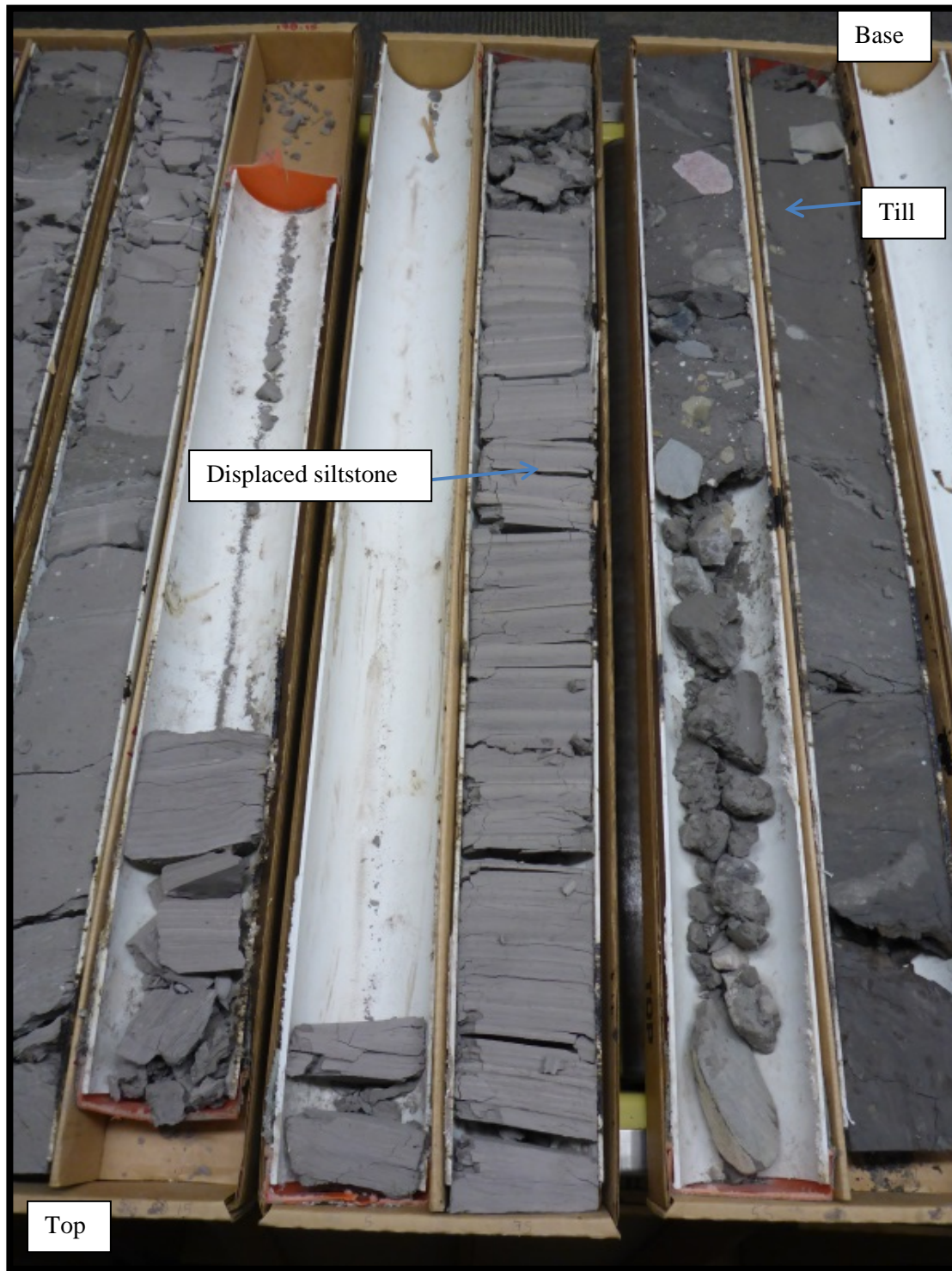


Figure 86. Photograph of core interval from well TLK FIREBAG 10-4-96-4W4 (176.5–182.0 m depth, 347.0–341.5 m asl) showing displaced siltstone overlying dark grey till. Core boxes are 0.9 m long.

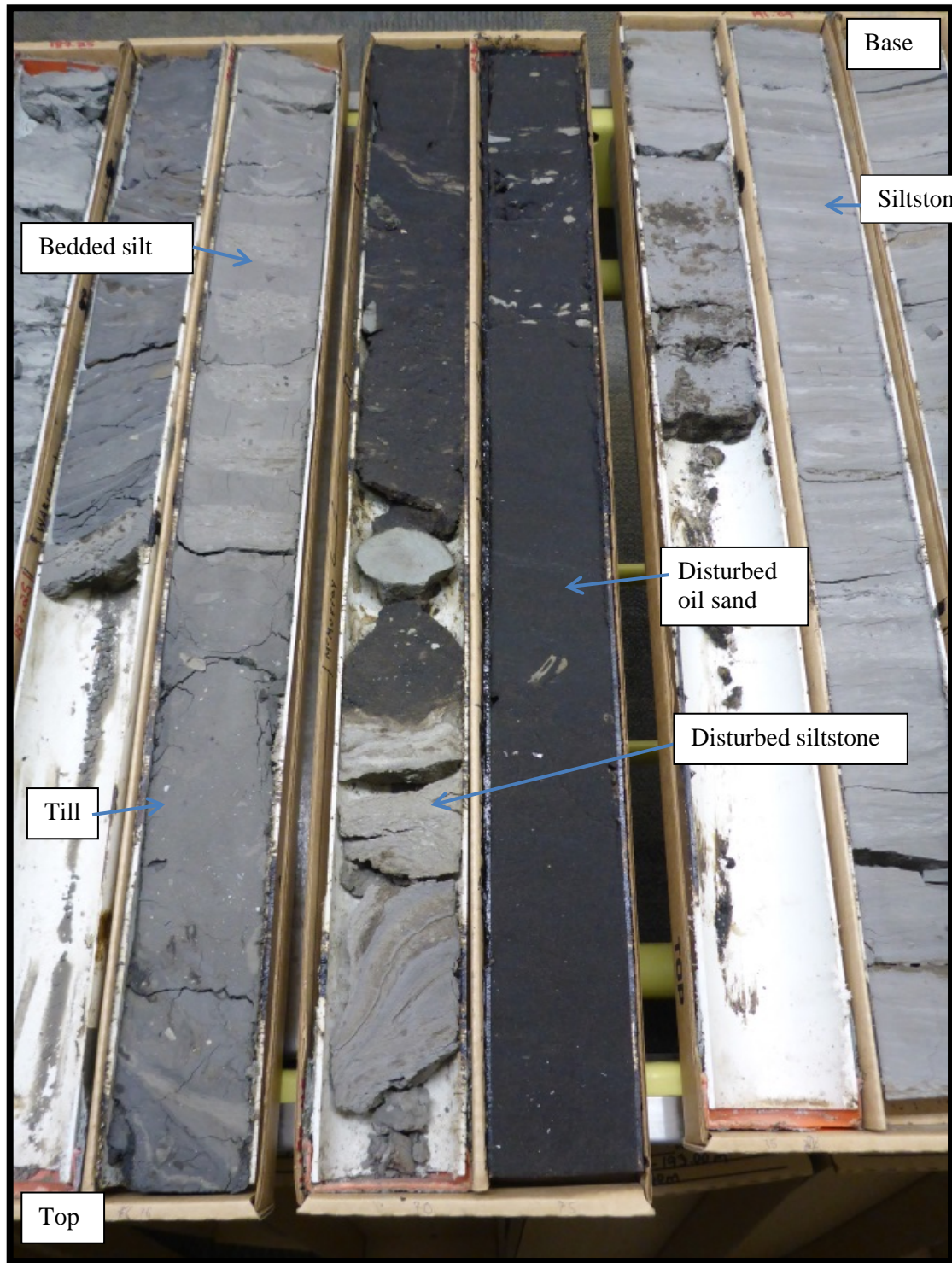


Figure 87. Photograph of core interval from well TLK FIREBAG 10-4-96-4W4 (187.25–191.0 m depth, 336.25–332.5 m asl) showing till (dark grey) overlying bedded silt, overlying disturbed siltstone, overlying disturbed oil sand. Core boxes are 0.9 m long.

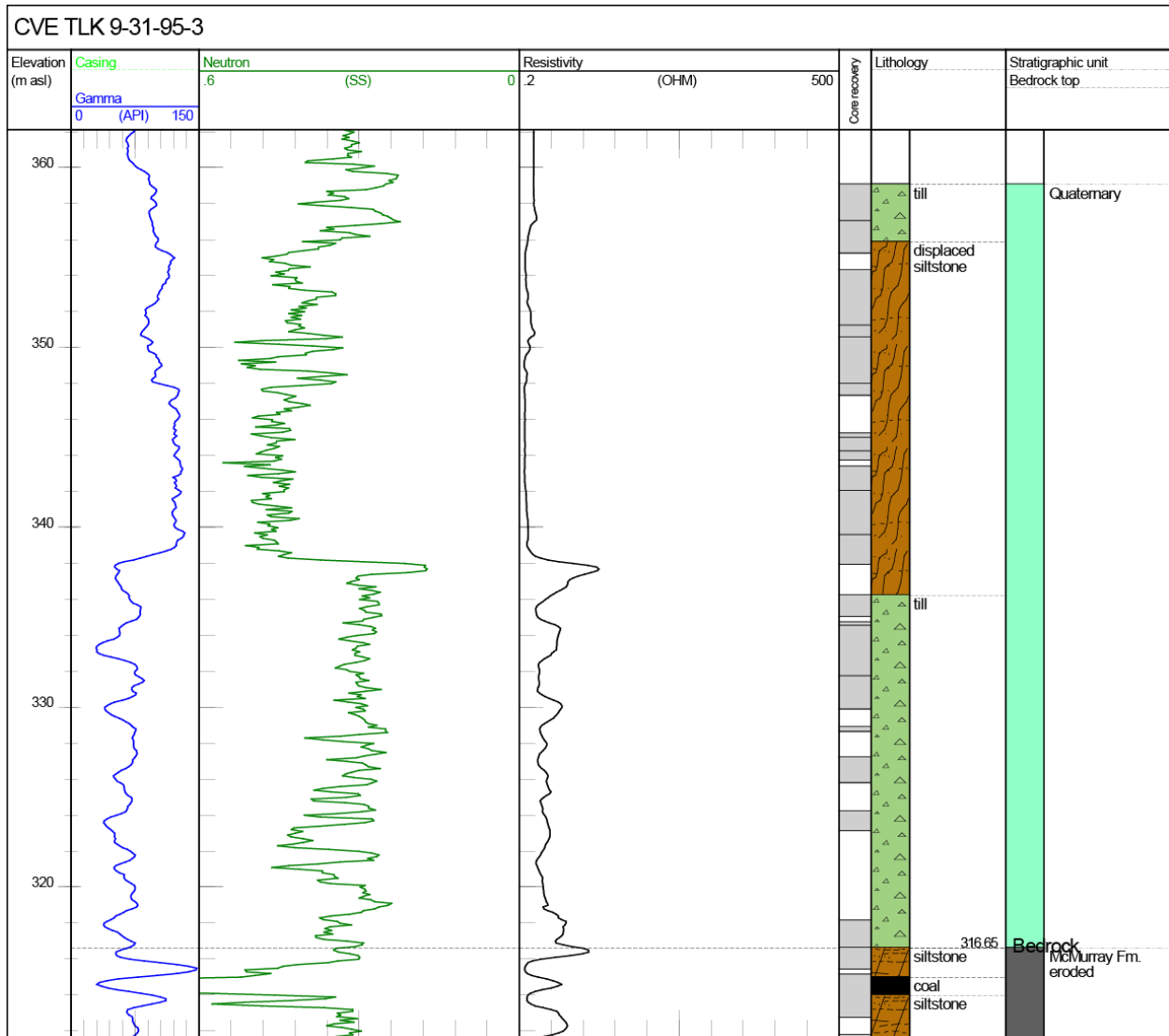


Figure 88. Logs for well CVE TLK 9-31-95-3W4. Litholog determined from examination of core. Kelly bushing at 505.9 m asl and total depth at 285.9 m asl. Abbreviations: Gamma, gamma ray; Neutron, neutron porosity; OHM, ohm•m; SS, sandstone units.

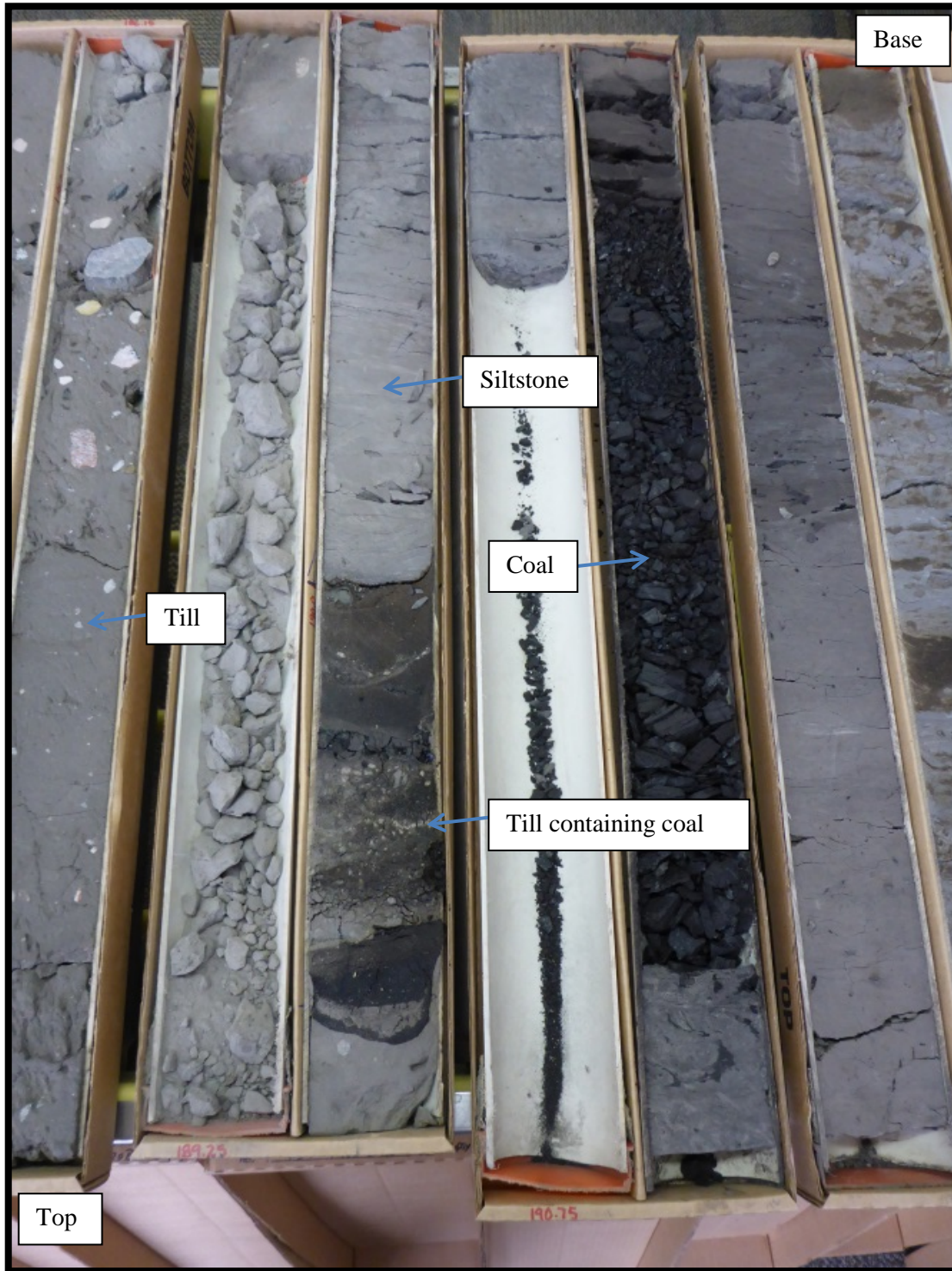


Figure 90. Photograph of core interval from well CVE TLK 9-31-95-3W4 (188–193 m depth, 317.9–312.9 m asl) showing till, including a darker bed containing coal, over siltstone (then coal). Core boxes are 0.9 m long.

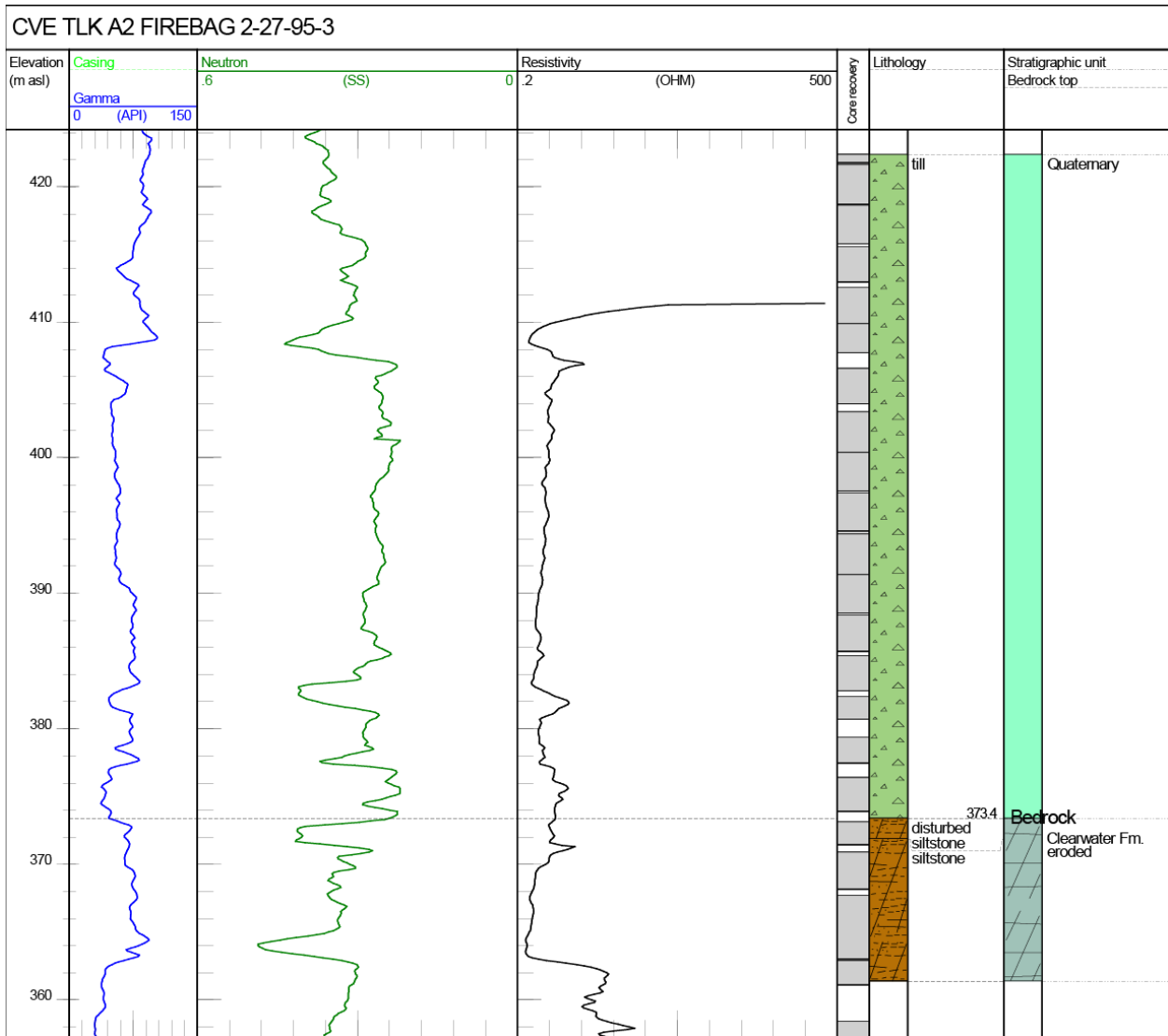


Figure 92. Logs for well CVE TLK A2 FIREBAG 2-27-95-3W4. Litholog determined from examination of core. Kelly bushing at 491.4 m asl and total depth at 293.9 m asl. Abbreviations: Gamma, gamma ray; Neutron, neutron porosity; OHM, ohm•m; SS, sandstone units.

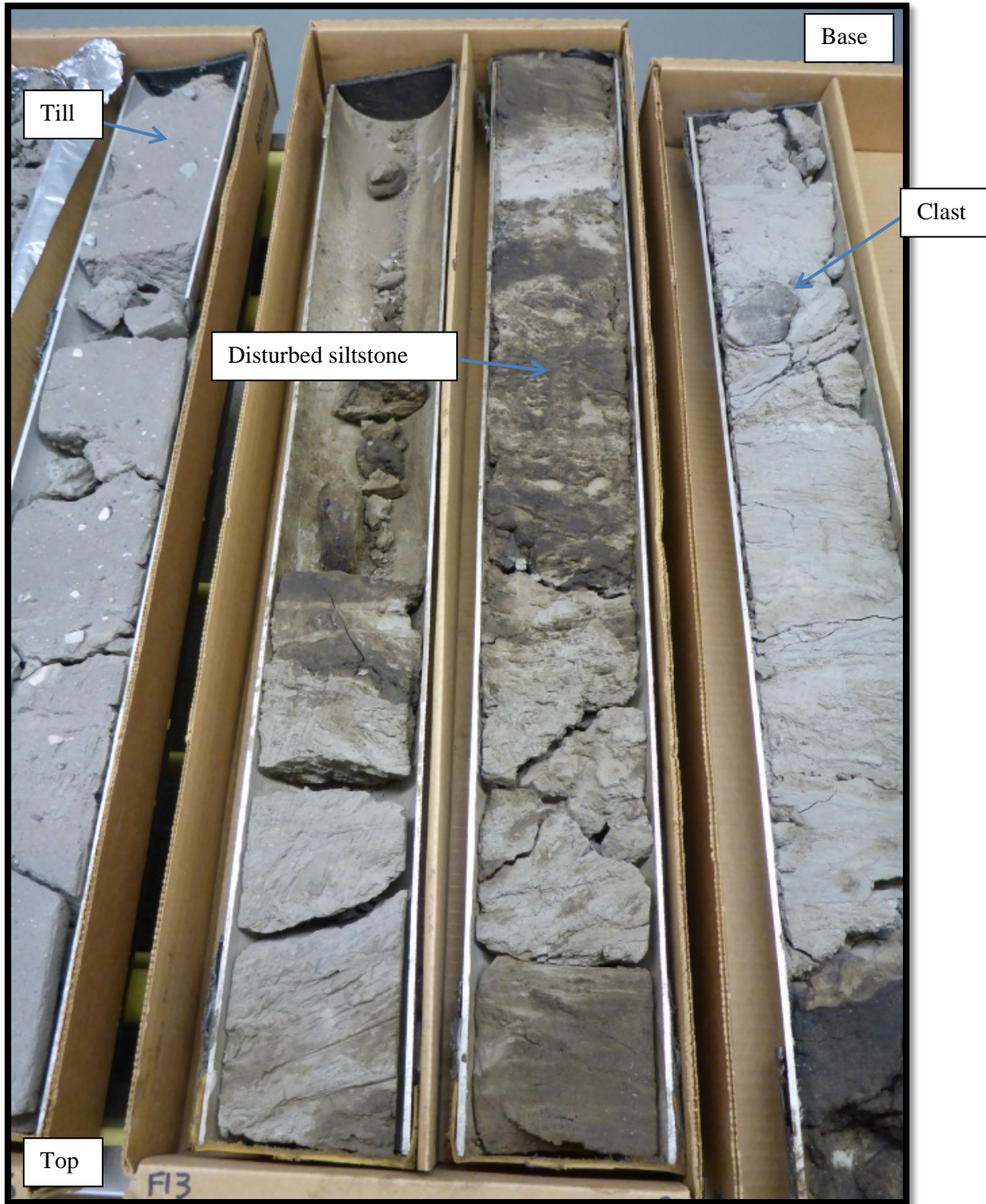


Figure 93. Photograph of core interval from well CVE TLK A2 FIREBAG 2-27-95-3W4 (117–120 m depth, 374.4–370.4 m asl) showing till overlying oil-stained disturbed Clearwater Formation siltstone, note clast towards the base of the disturbed rock. Core boxes are 0.9 m long.

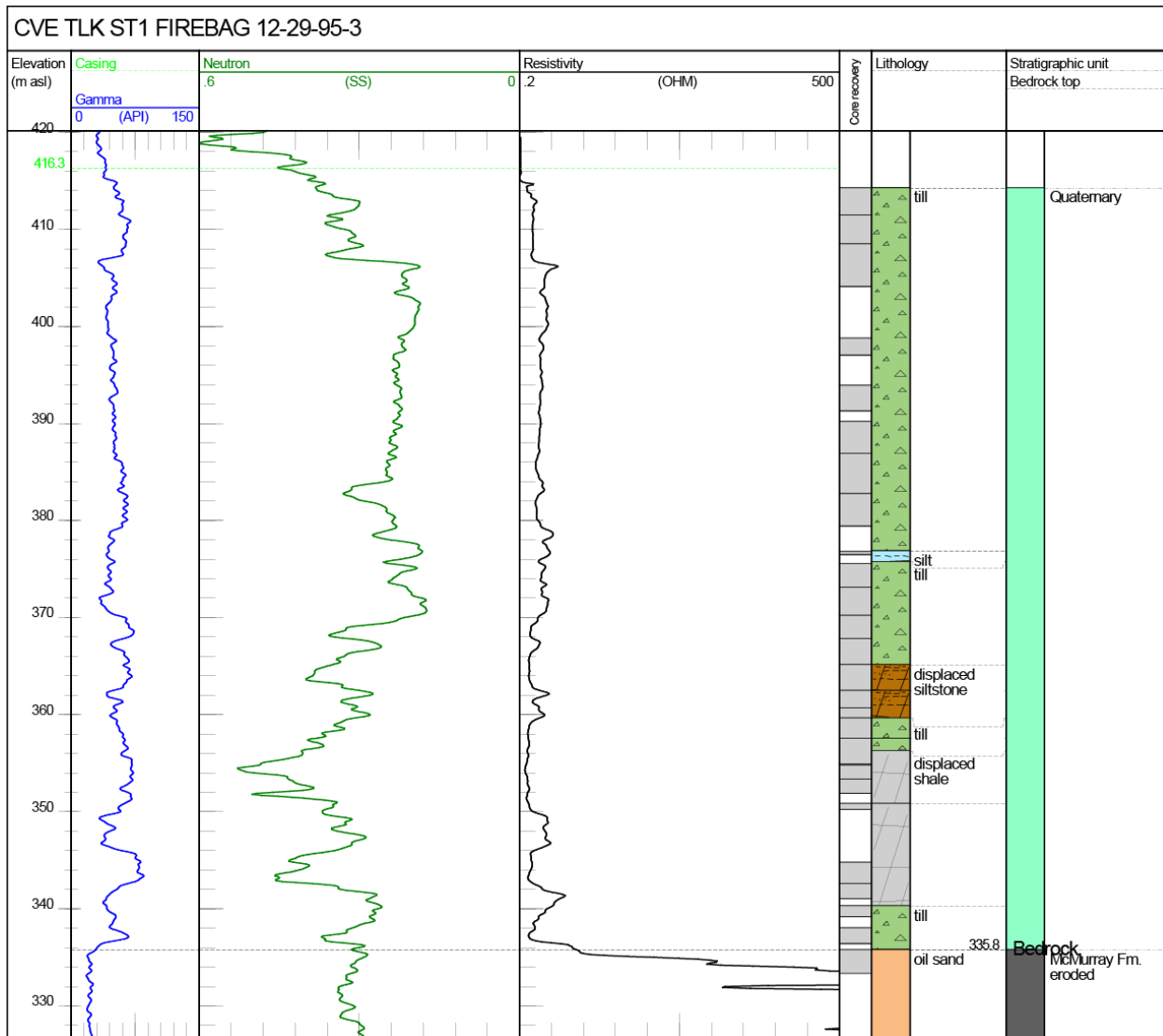


Figure 94. Logs for well CVE TLK ST1 FIREBAG 12-29-95-3W4. Litholog determined from examination of core. Kelly bushing at 513.3 m asl and total depth at 272.3 m asl. Abbreviations: Gamma, gamma ray; Neutron, neutron porosity; OHM, ohm•m; SS, sandstone units.

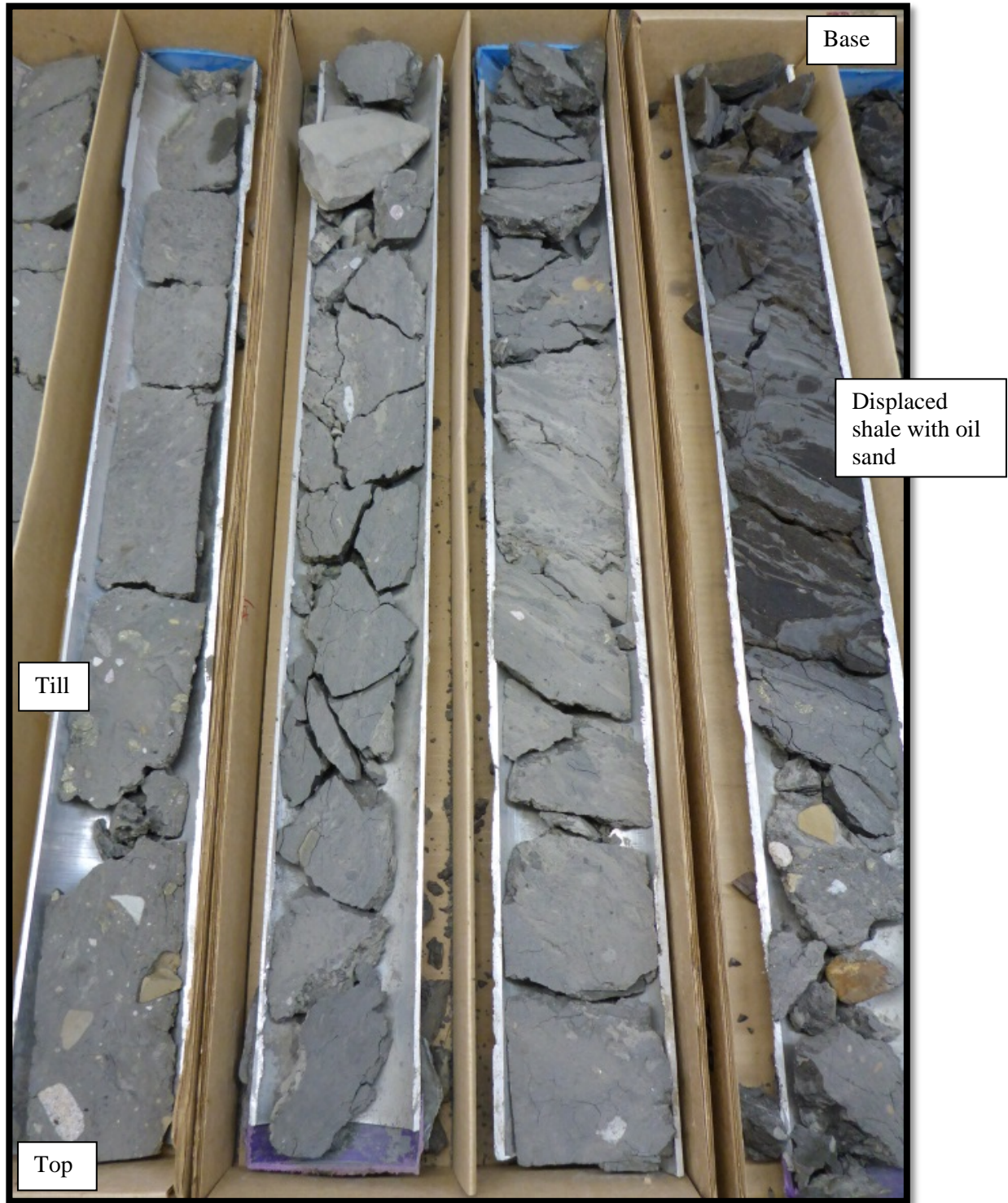


Figure 95. Photograph of core interval from well CVE TLK ST1 FIREBAG 12-29-95-3W4 (154–157 m depth, 359.3–356.3 m asl) showing till overlying displaced shale with oil sand. Core boxes are 0.9 m long.

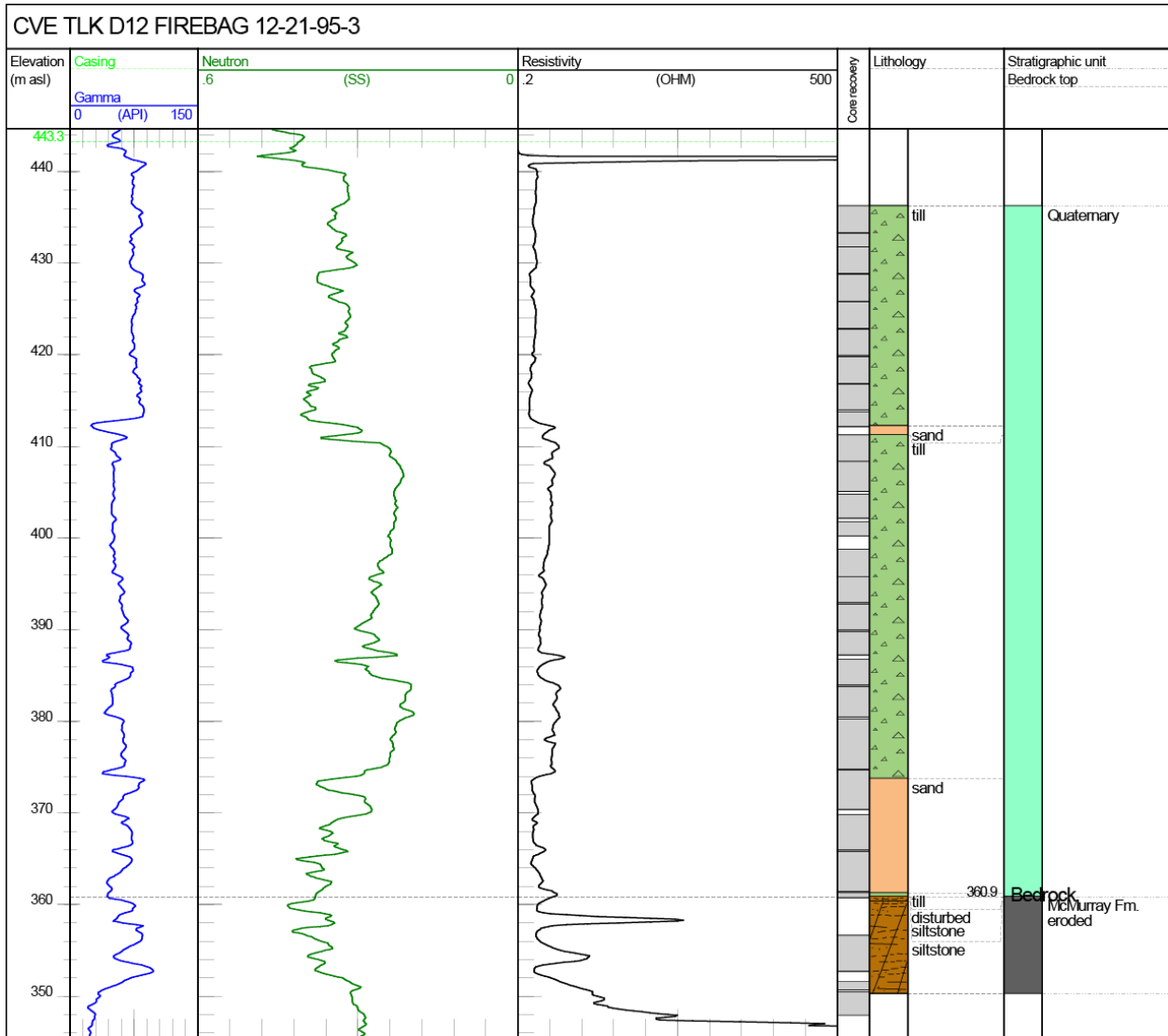


Figure 96. Logs for well CVE TLK D12 FIREBAG 12-21-95-3W4. Litholog determined from examination of core. Kelly bushing at 516.3 m asl and total depth at 277.8 m asl. Abbreviations: Gamma, gamma ray; Neutron, neutron porosity; OHM, ohm•m; SS, sandstone units.

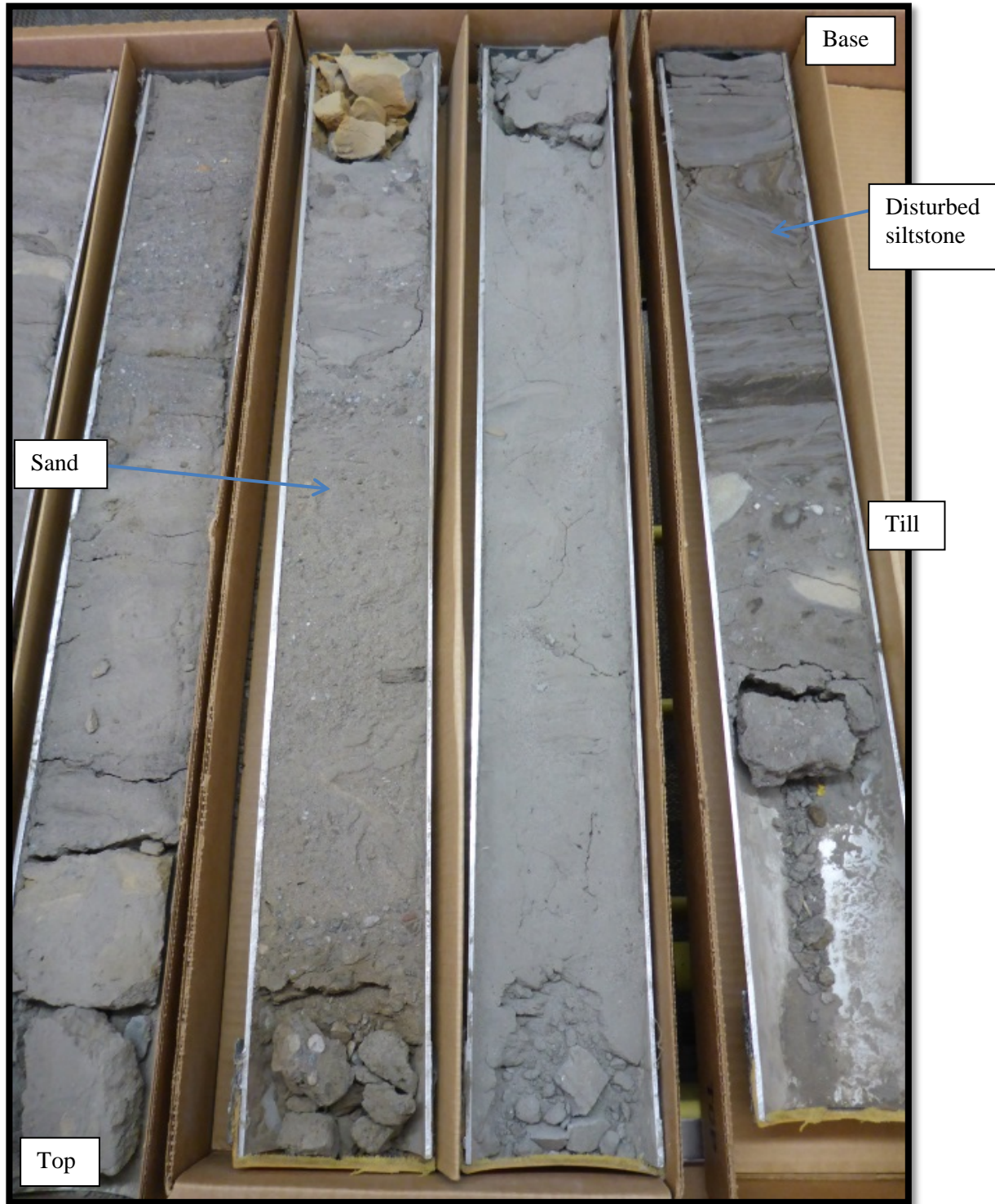


Figure 97. Photograph of core interval from well CVE TLK D12 FIREBAG 12-21-95-3W4 (152.0–156.0 m depth, 364.3–360.3 m asl) showing sand overlying till overlying the upper portion of disturbed bedrock. Core boxes are 0.9 m long.

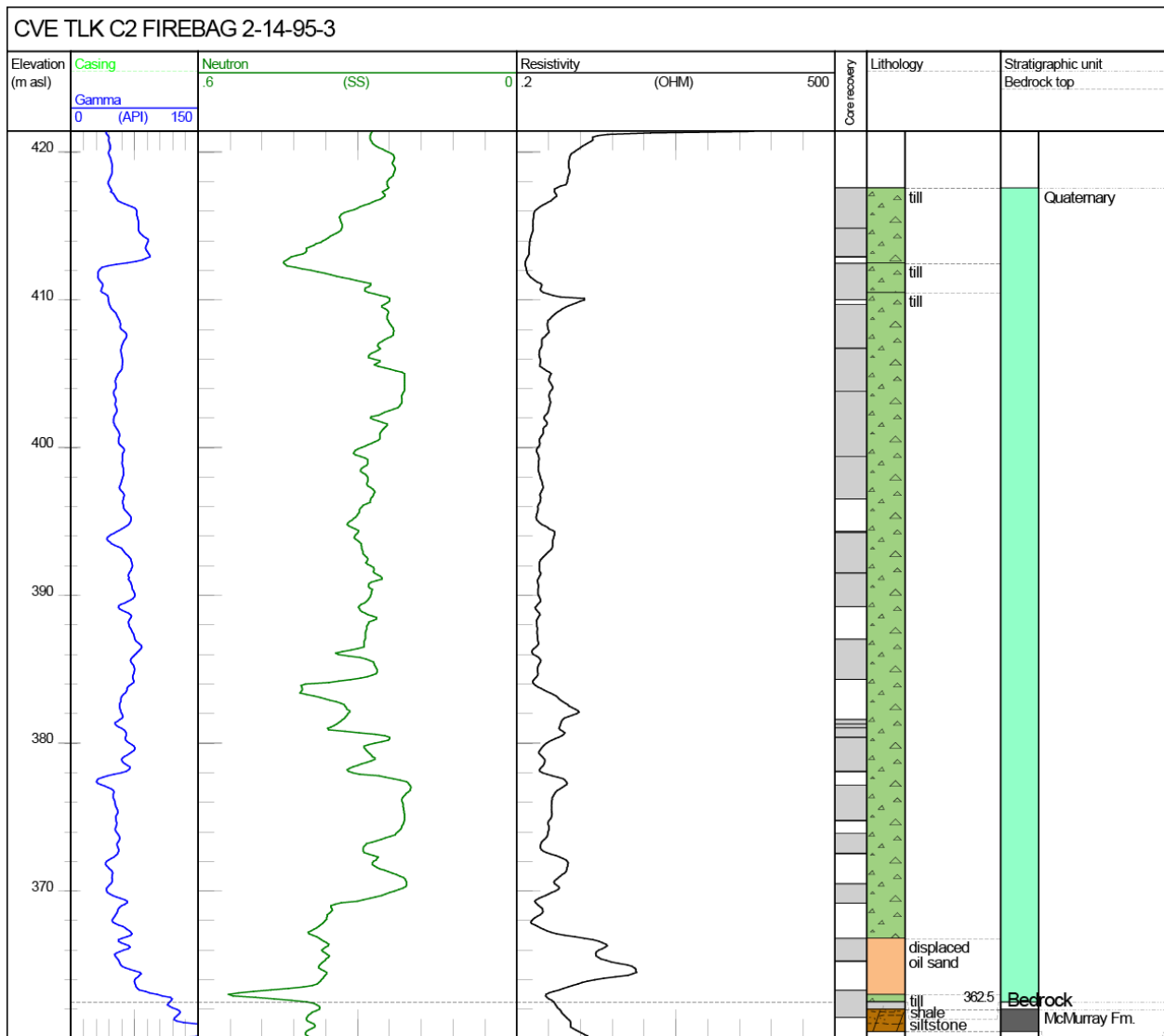


Figure 98. Logs for well CVE TLK C2 FIREBAG 2-14-95-3W4. Litholog determined from examination of core. Kelly bushing at 496.5 m asl and total depth at 297.5 m asl. Abbreviations: Gamma, gamma ray; Neutron, neutron porosity; OHM, ohm*m; SS, sandstone units.

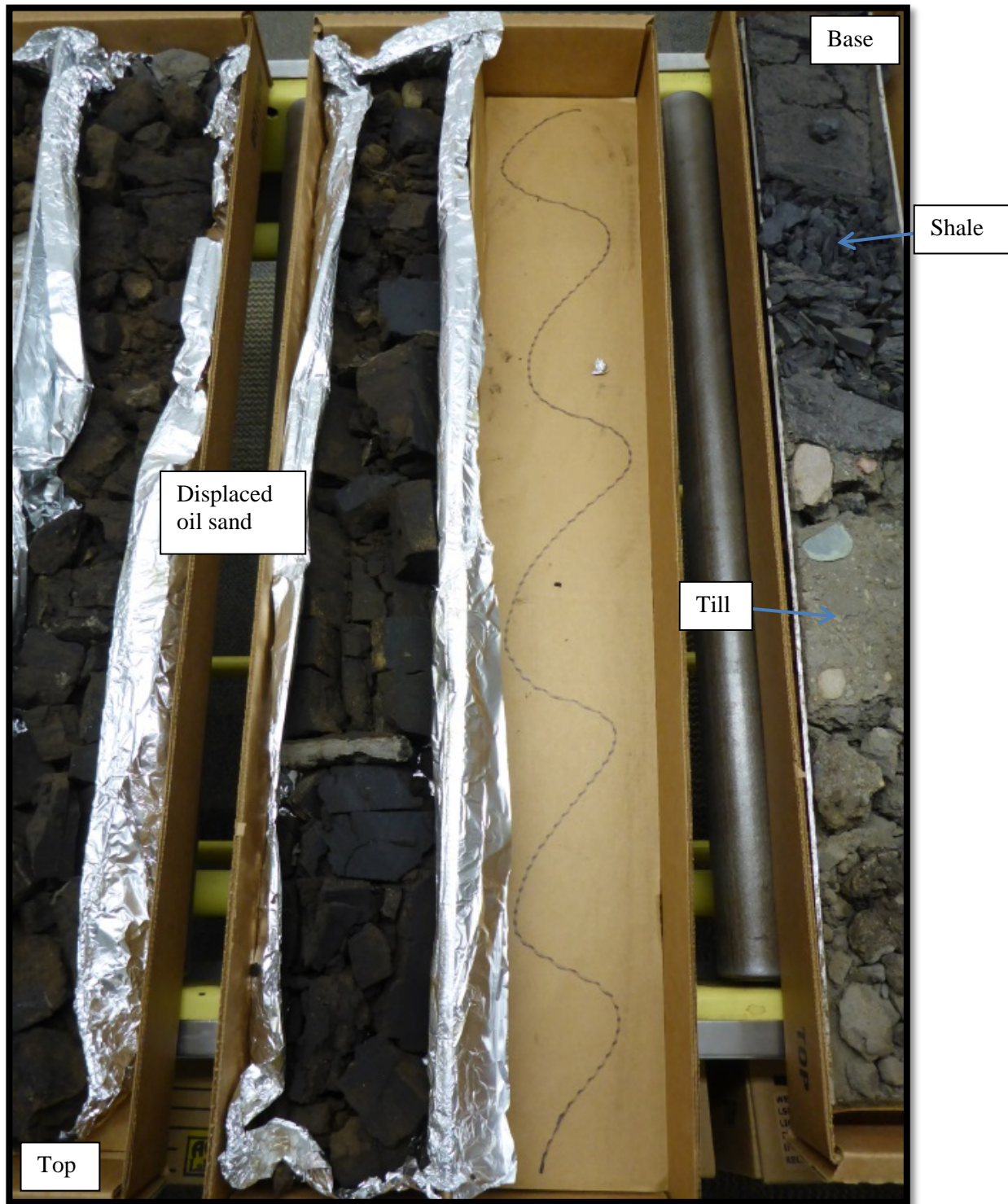


Figure 99. Photograph of core interval from well CVE TLK C2 FIREBAG 2-14-95-3W4 (132.0–134.5 m depth, 364.5–362.0 m asl) showing displaced oil sand, above till overlying shale. Core boxes are 0.9 m long.



Figure 101. Photograph of core interval from well CVE TLK A12 FIREBAG 12-10-95-3W4 (149–153 m depth, 364.8–360.8 m asl) showing disturbed siltstone. Core boxes are 0.9 m long.

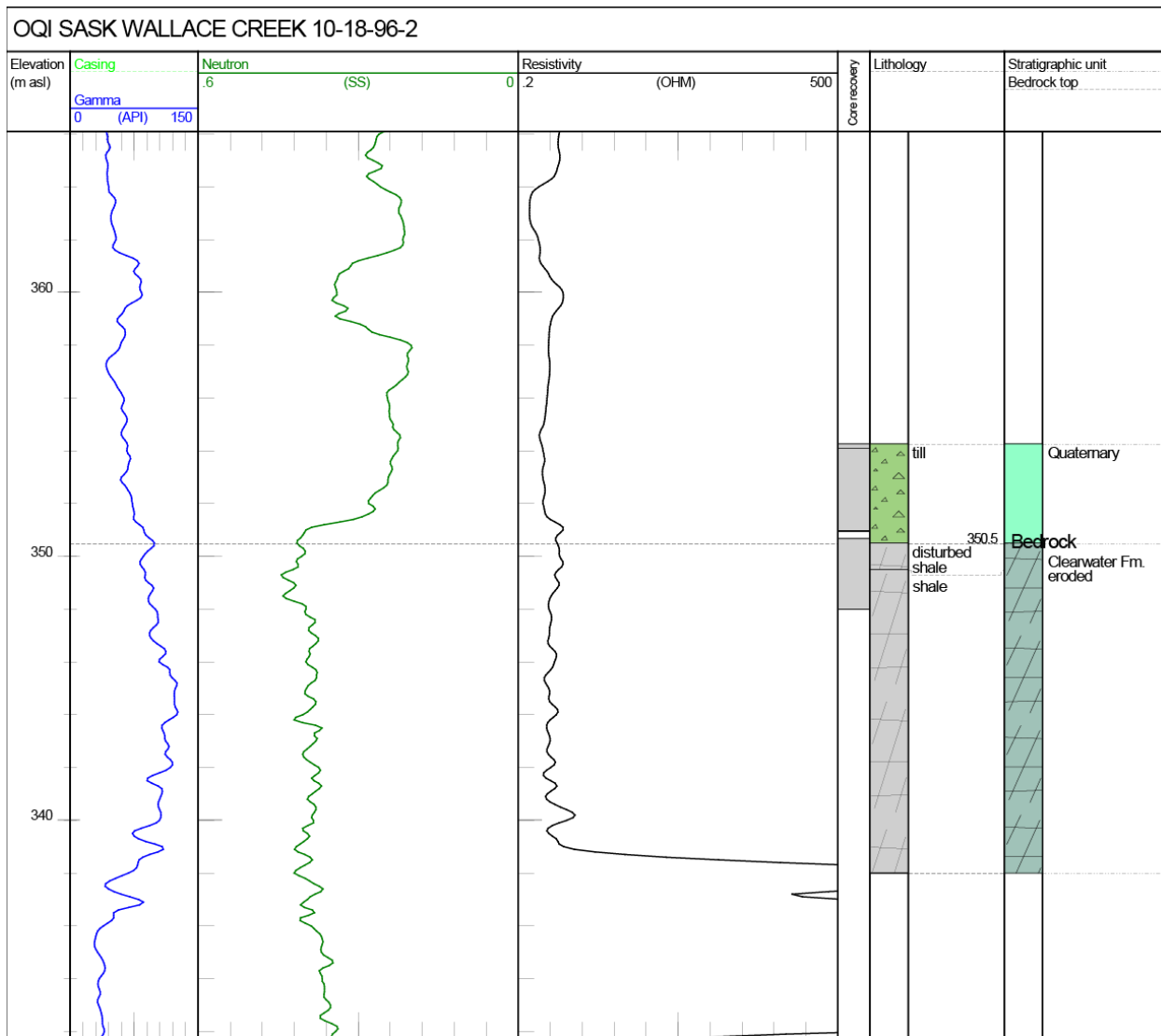


Figure 102. Logs for well OQI SASK WALLACE CREEK 10-18-96-2W4. Litholog determined from examination of core. Kelly bushing at 508.0 m asl and total depth at 295.0 m asl. Abbreviations: Gamma, gamma ray; Neutron, neutron porosity; OHM, ohm·m; SS, sandstone units.

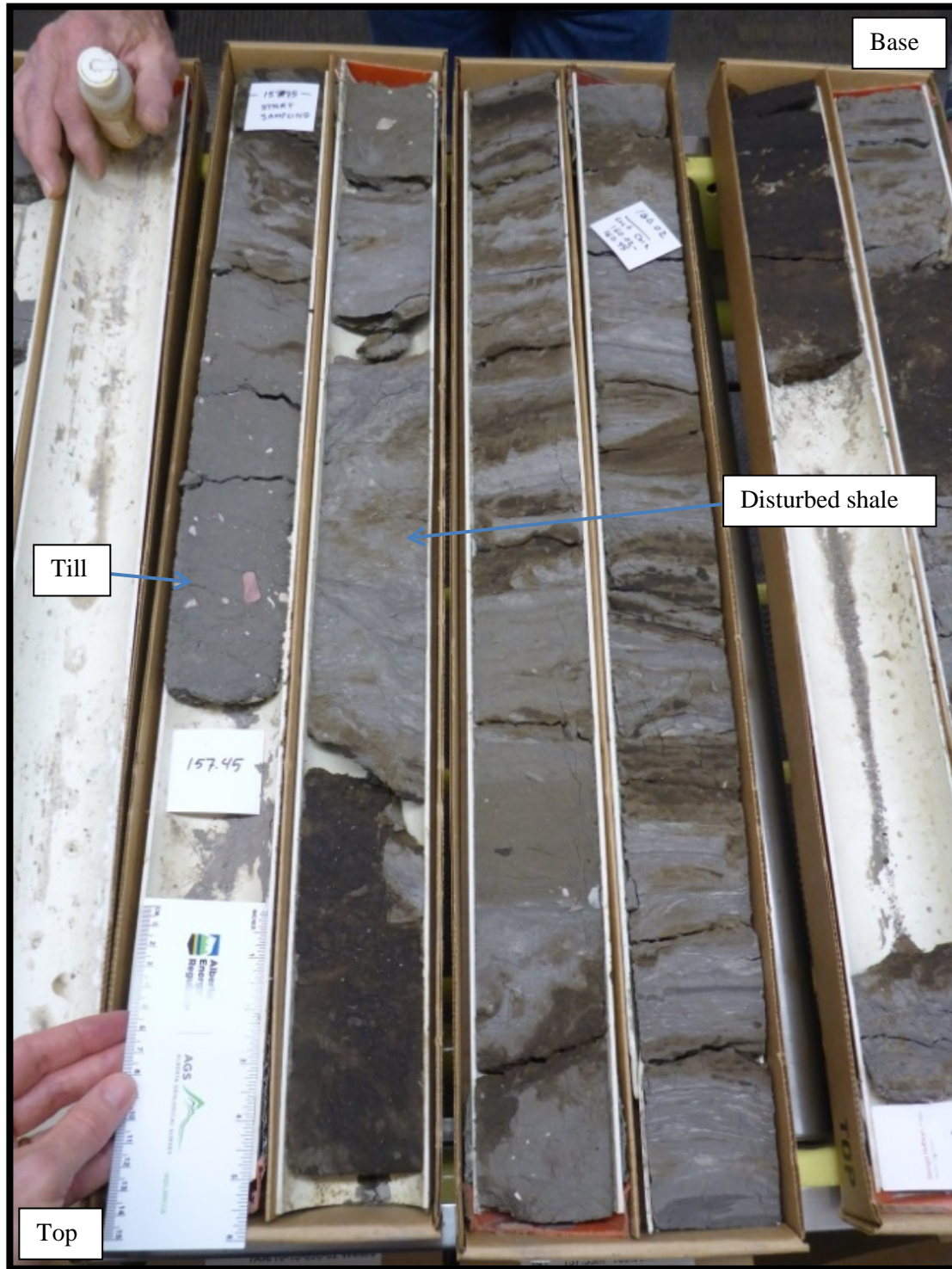


Figure 103. Photograph of core interval from well OQI SASK WALLACE CREEK 10-18-96-2W4 (157.0–160.5 m depth, 351.0–347.5 m asl) showing till overlying disturbed eroded shale of the Clearwater Formation. Core boxes are 0.9 m long.

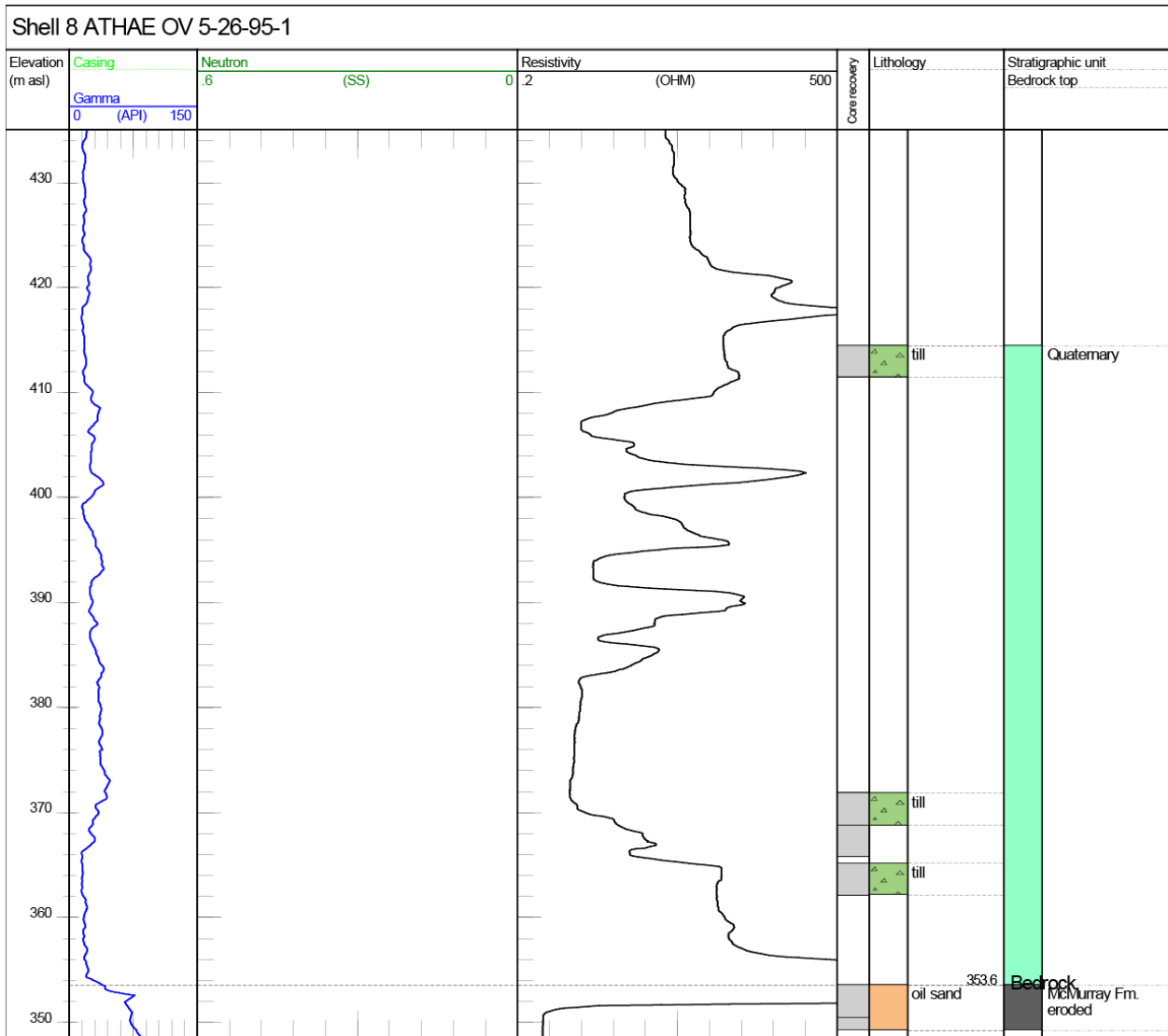


Figure 104. Logs for well Shell 8 ATHAE OV 5-26-95-1W4. Litholog determined from examination of core. Neutron data unavailable. Kelly bushing at 487.7 m asl and total depth at 328.0 m asl. Abbreviations: Gamma, gamma ray; Neutron, neutron porosity; OHM, ohm•m; SS, sandstone units.



Figure 105. Photograph of core interval from well Shell 8 ATHAE OV 5-26-95-1W4 (115.82–121.92 m depth, 371.9–365.8 m asl) showing matrix-dominated till. Core boxes are 0.9 m long.

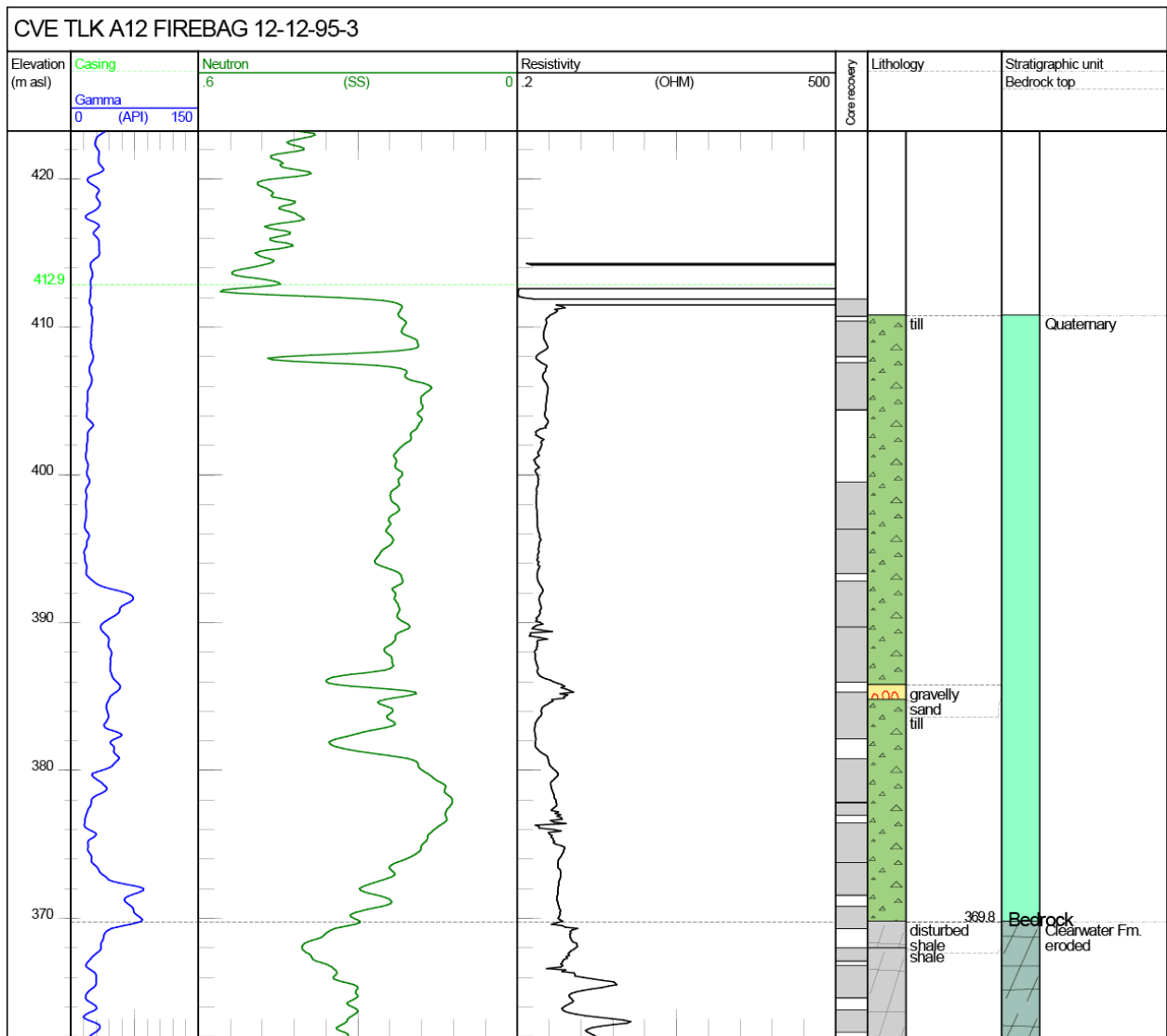


Figure 106. Logs for well CVE TLK A12 FIREBAG 12-12-95-3W4. Litholog determined from examination of core. Kelly bushing at 479.8 m asl and total depth at 291.3 m asl. Abbreviations: Gamma, gamma ray; Neutron, neutron porosity; OHM, ohm*m; SS, sandstone units.

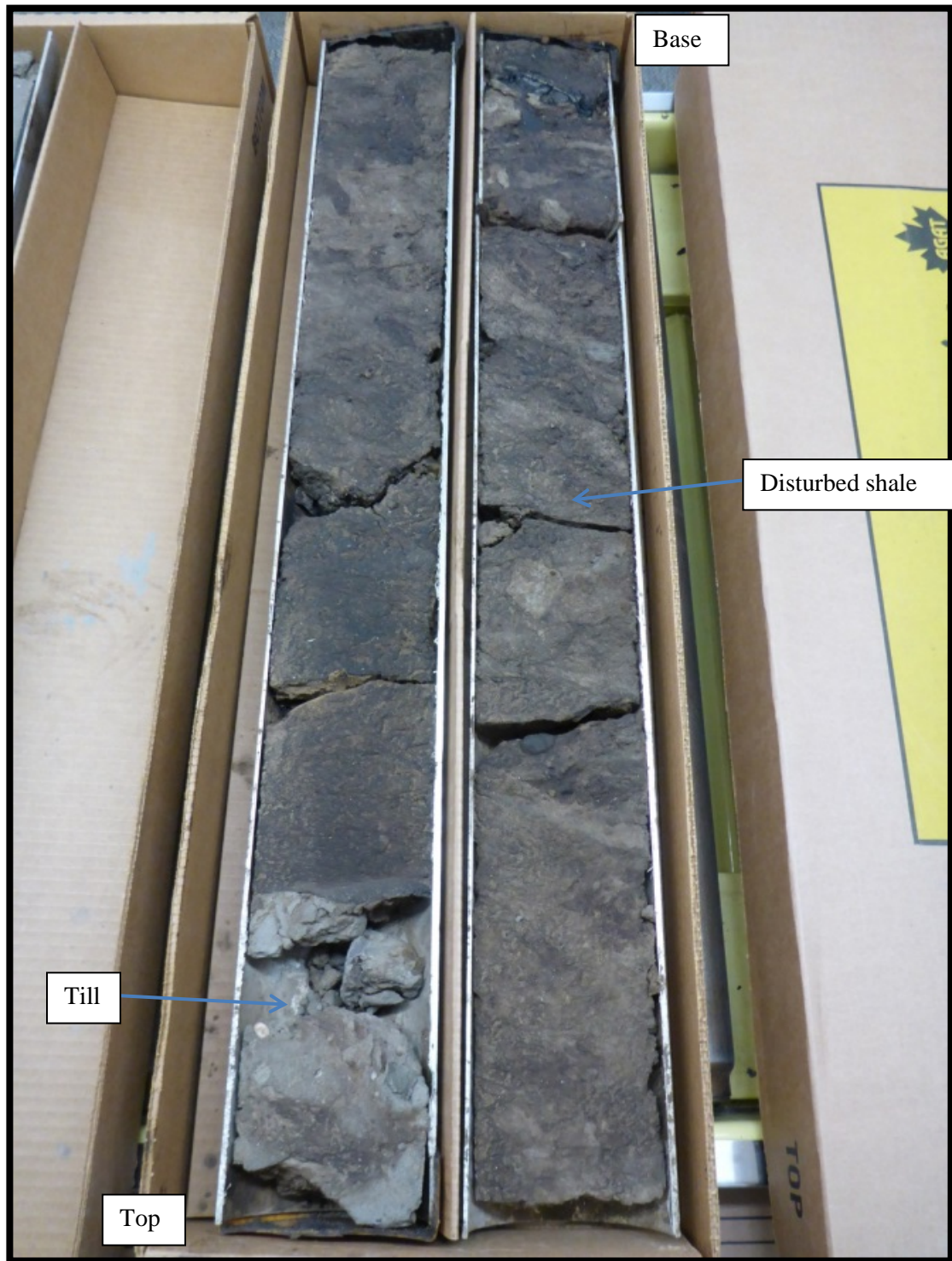


Figure 107. Photograph of core interval from well CVE TLK A12 FIREBAG 12-12-95-3W4 (109.0–111.8 m depth, 370.8–368 m asl) showing till overlying disturbed shale (possibly also bioturbated), possibly glacially modified in the upper 1 m. Core boxes are 0.9 m long.

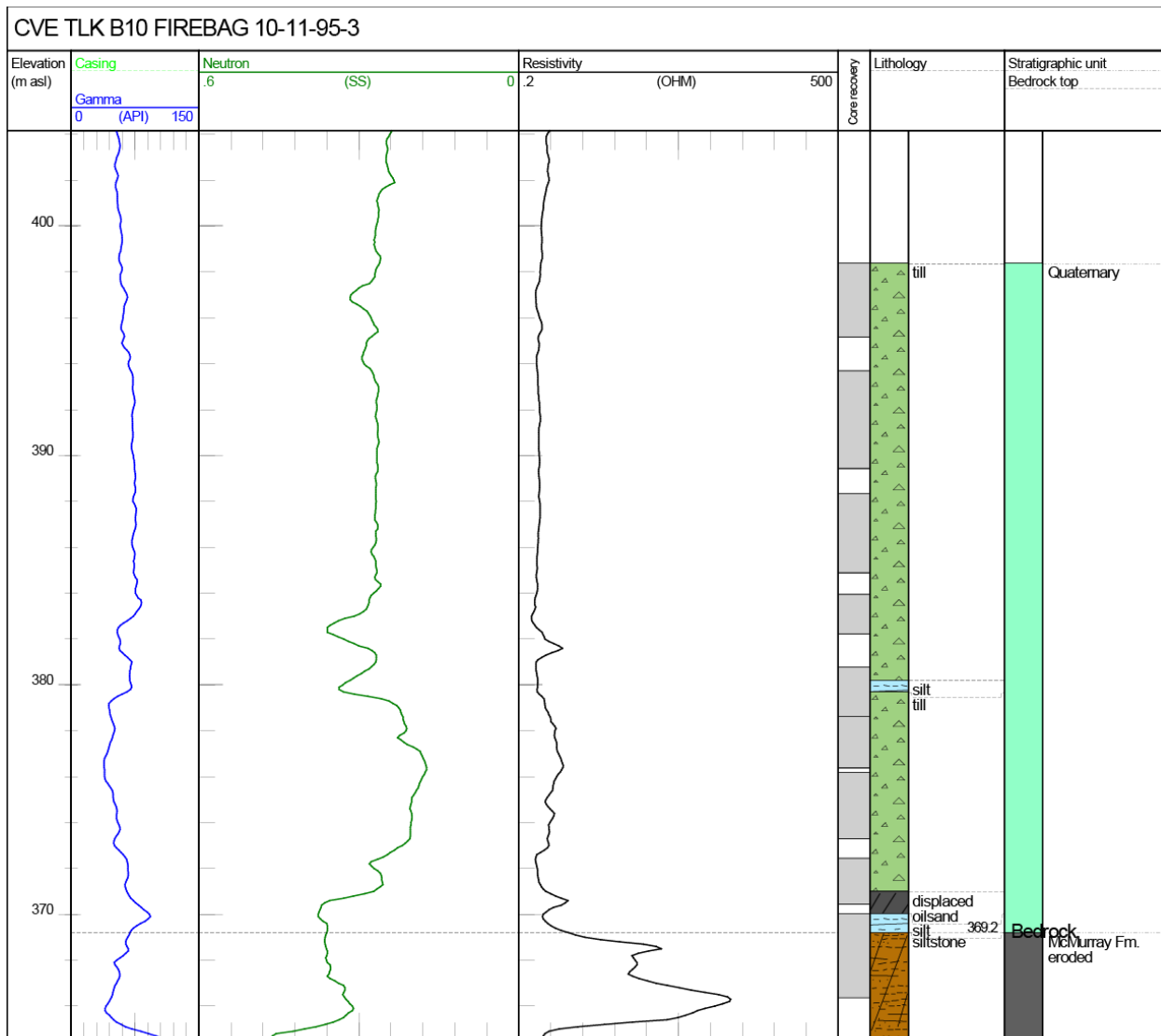


Figure 108. Logs for well CVE TLK B10 FIREBAG 10-11-95-3W4. Litholog determined from examination of core. Kelly bushing at 496.2 m asl and total depth at 294.2 m asl. Abbreviations: Gamma, gamma ray; Neutron, neutron porosity; OHM, ohm*m; SS, sandstone units.

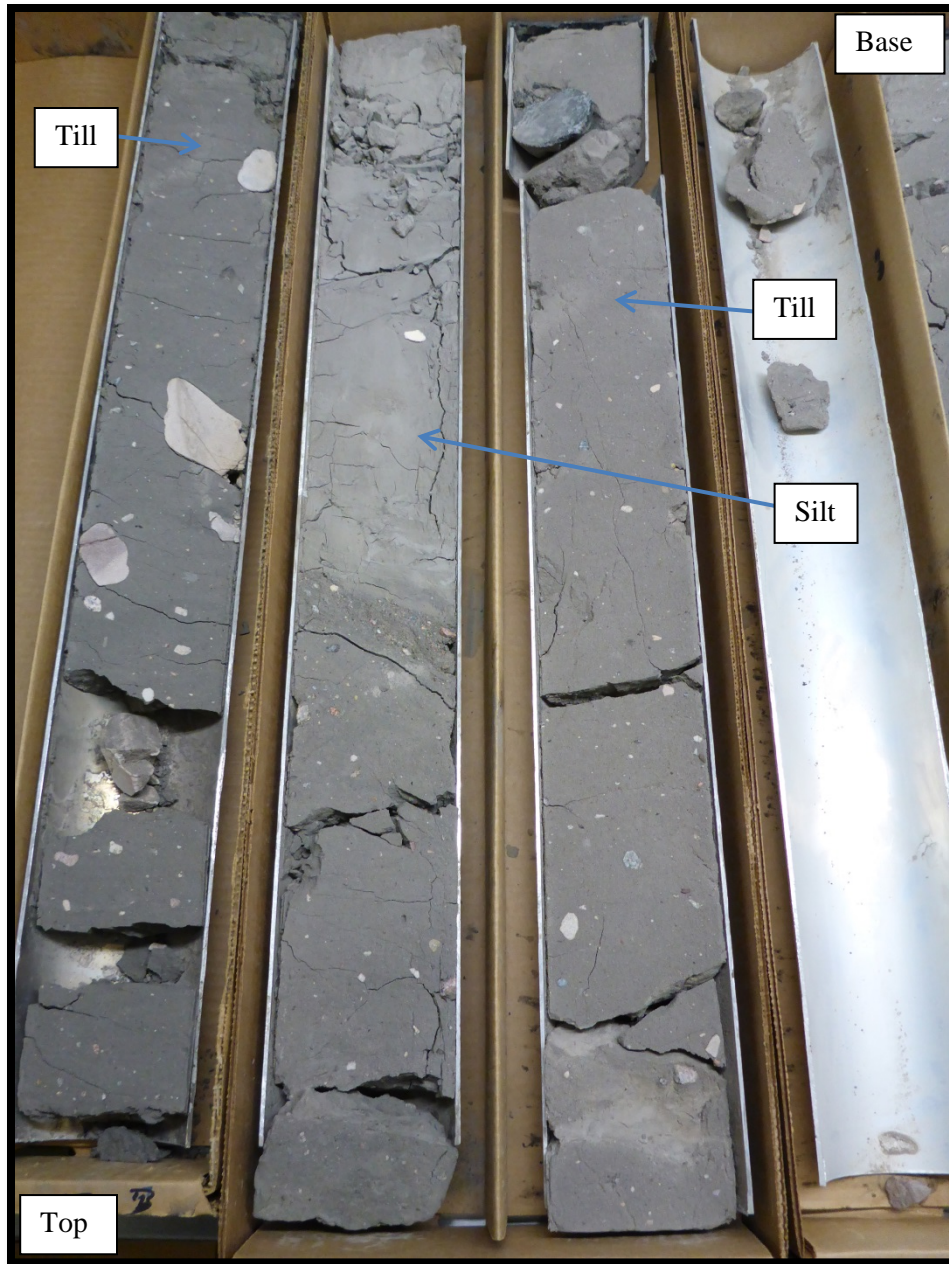


Figure 109. Photograph of core interval from well CVE TLK B10 FIREBAG 10-11-95-3W4 (115–117.5 m depth, 381.2–378.7 m asl) showing silt bed between till layers, note colour difference above and below silt. Each till layer corresponds to a different gamma-ray and neutron porosity signature. Core boxes are 0.9 m long.

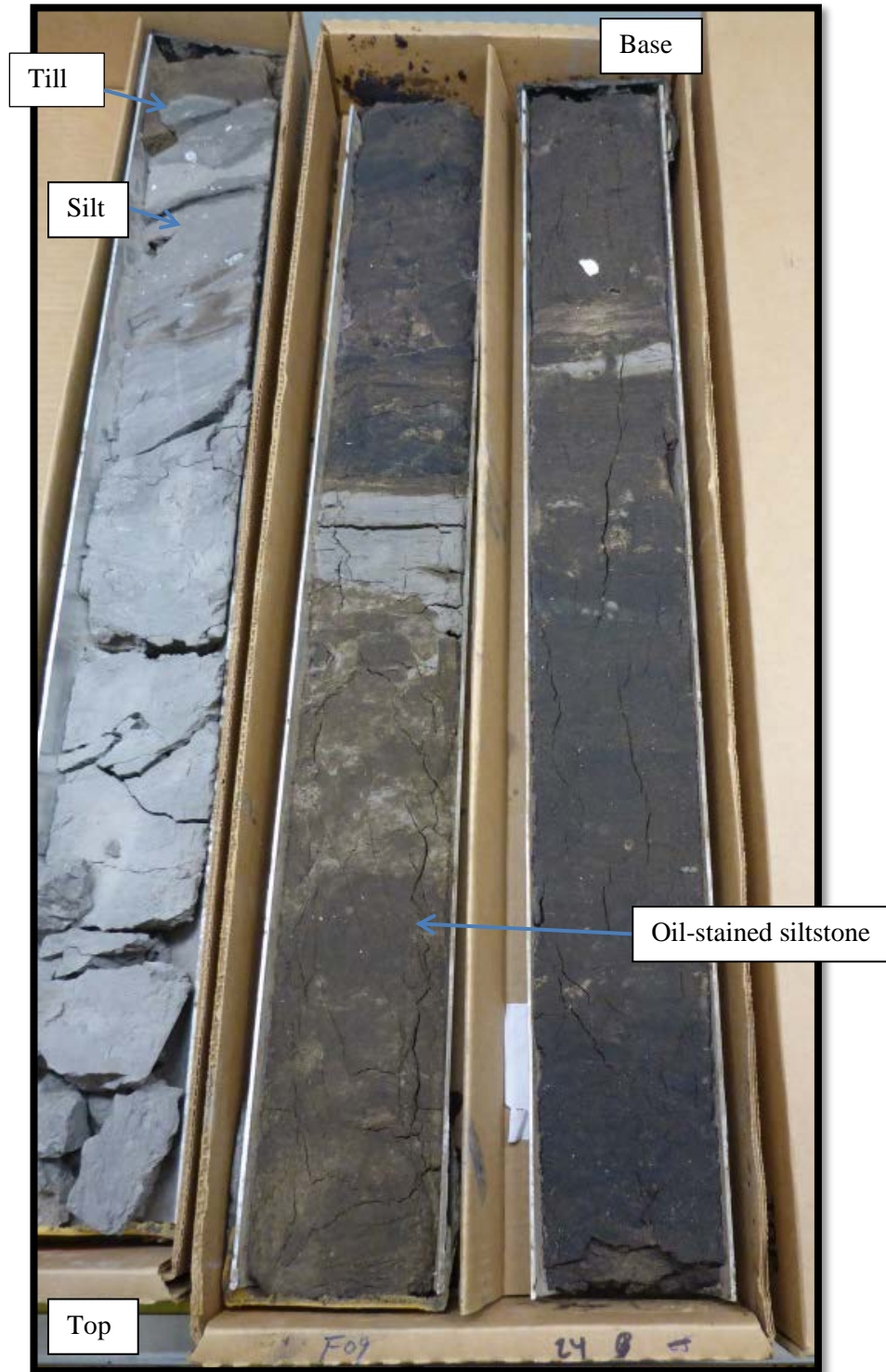


Figure 110. Photograph of core interval from well CVE TLK B10 FIREBAG 10-11-95-3W4 (126–128.5 m depth, 370.2–367.7 m asl) showing silt (light grey), overlying 10 cm of till (not shown on litholog), overlying 0.4 m of disturbed oil-stained siltstone. Core boxes are 0.9 m long.

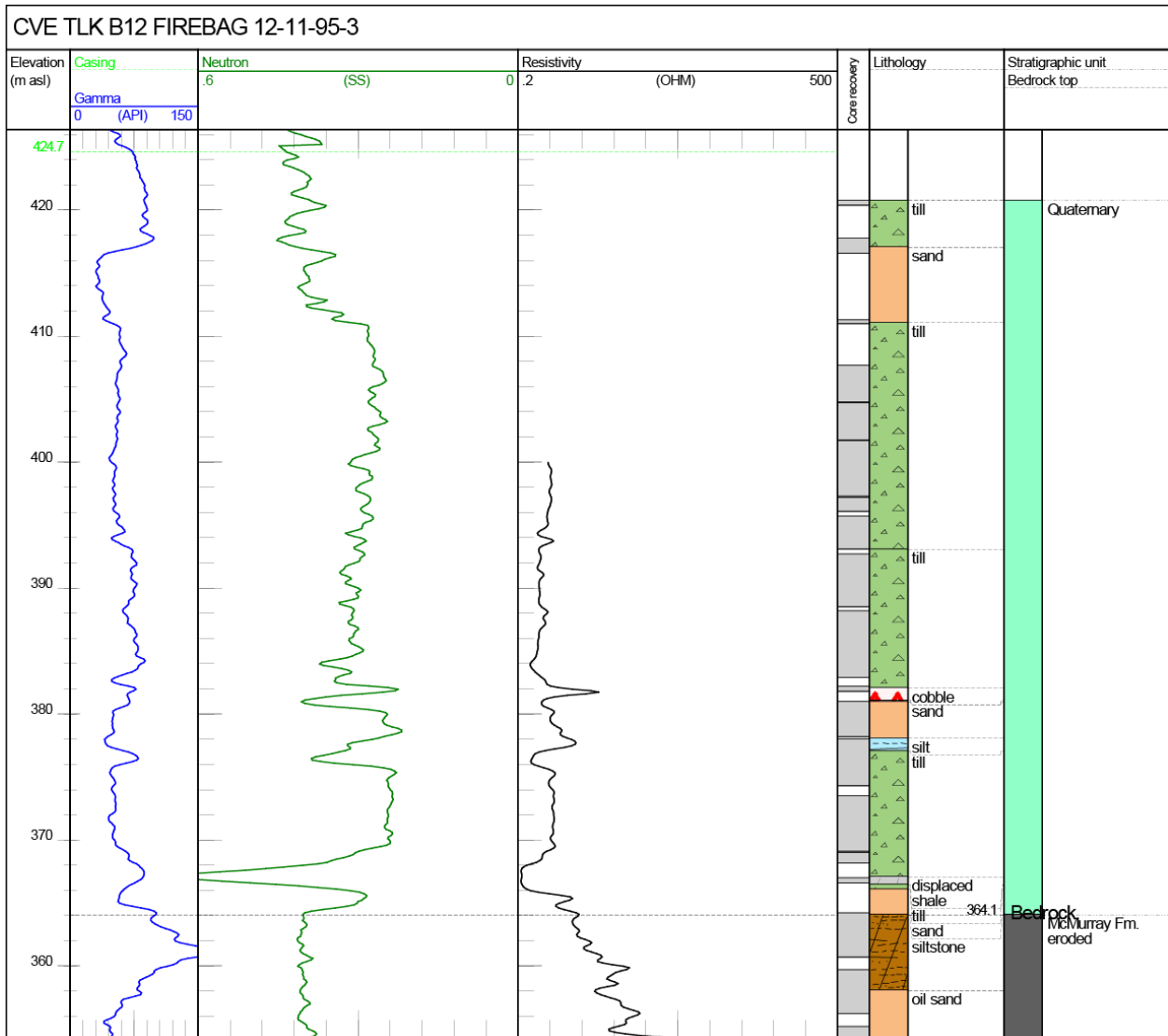


Figure 111. Logs for well CVE TLK B12 FIREBAG 12-11-95-3W4. Litholog determined from examination of core. Kelly bushing at 495.1 m asl and total depth at 301.4 m asl. Abbreviations: Gamma, gamma ray; Neutron, neutron porosity; OHM, ohm*m; SS, sandstone units.

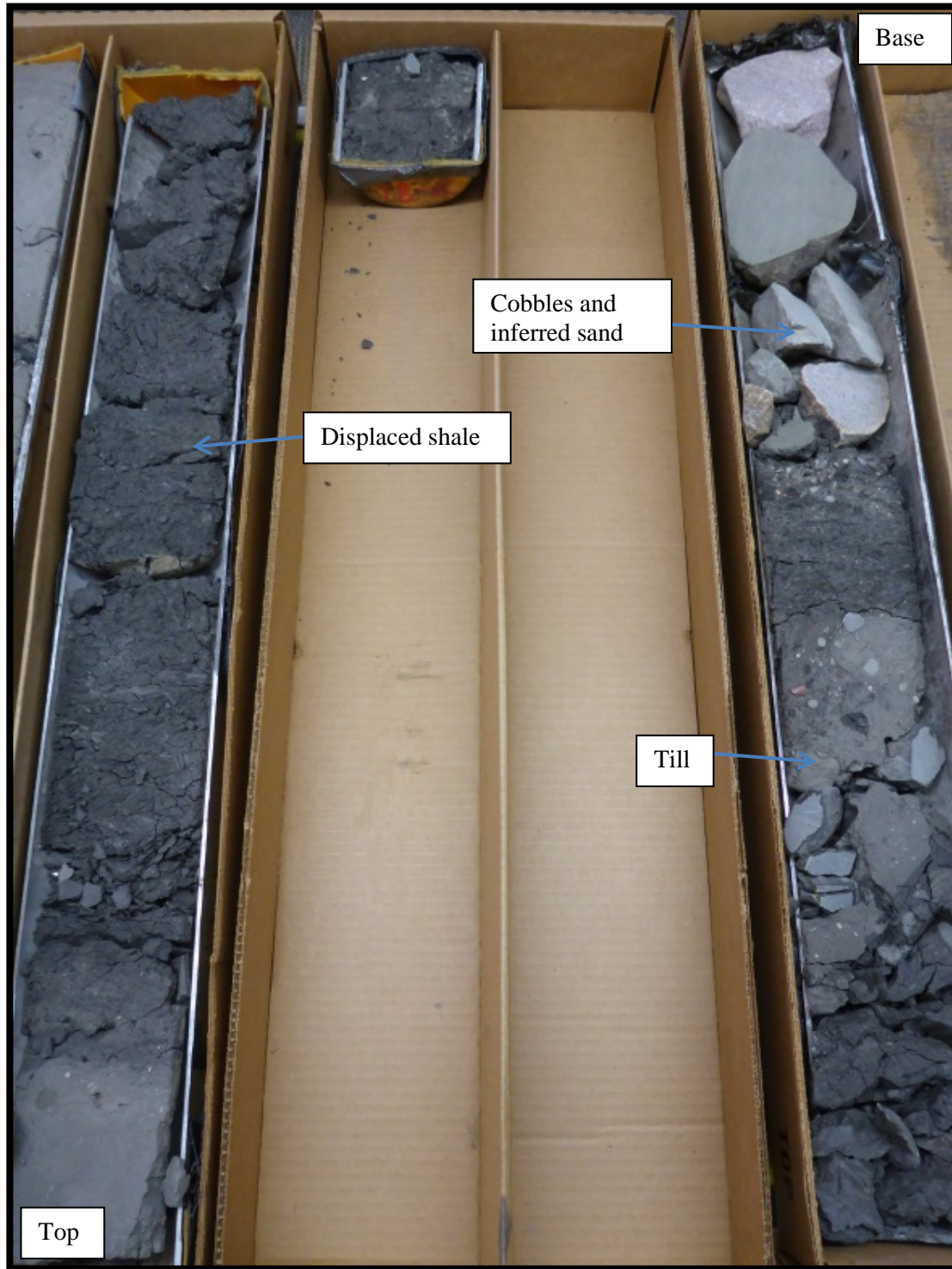


Figure 112. Photograph of core interval from well CVE TLK B12 FIREBAG 12-11-95-3W4 (125–129 m depth, 370.1–366.1 m asl) showing displaced shale above till and sand (which were inferred from the logs and the presence of two cobbles in the core box). Also note that gamma-ray values shift near top of core (from till to sand, which was also inferred from the logs, back to till). Core boxes are 0.9 m long.

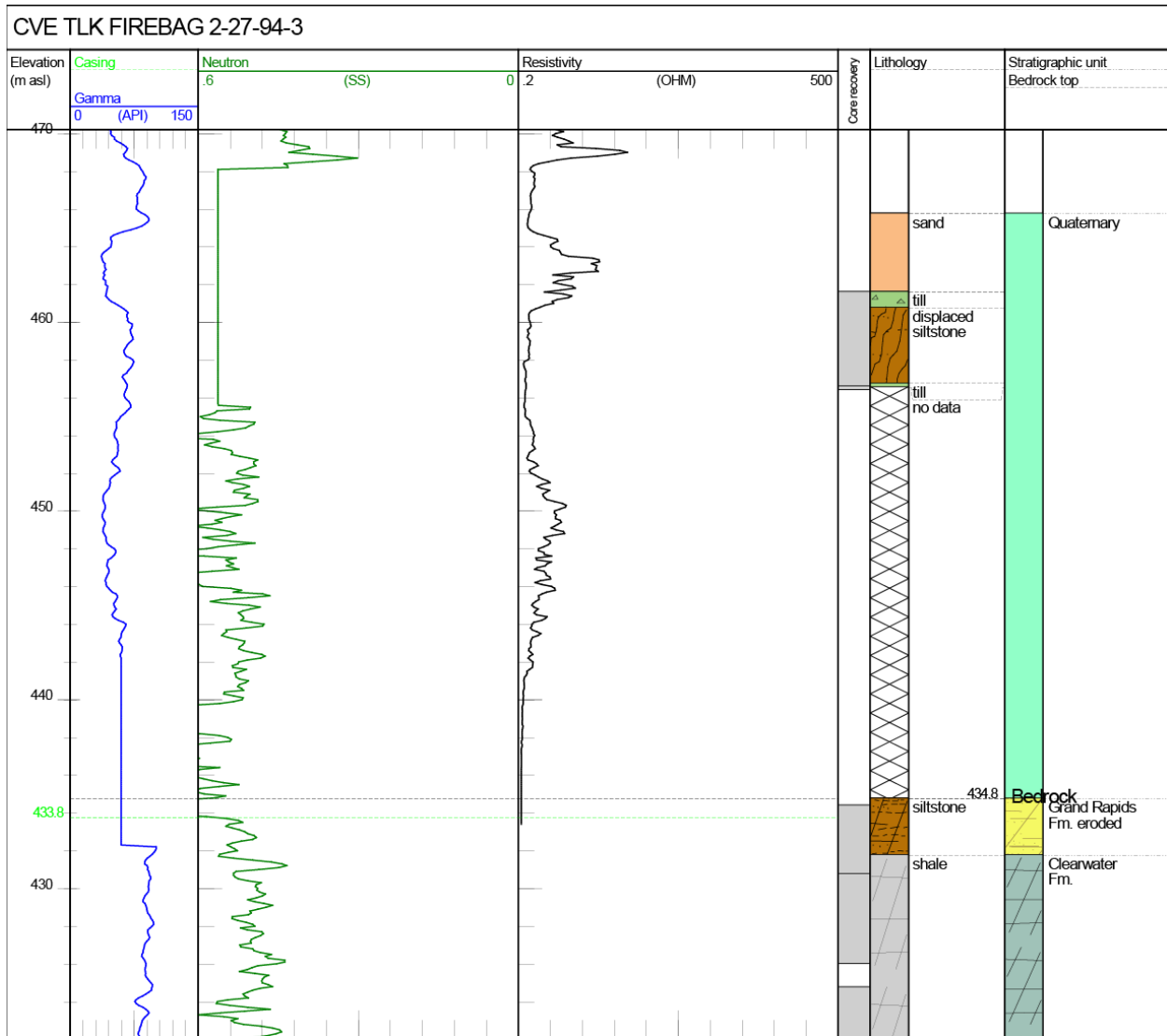


Figure 113. Logs for well CVE TLK FIREBAG 2-27-94-3W4. Litholog determined from examination of core. Bedrock top uncertain due to poor recovery and error in neutron porosity responses over the sequence. Kelly bushing at 515.8 m asl and total depth at 281.8 m asl. Abbreviations: Gamma, gamma ray; Neutron, neutron porosity; OHM, ohm•m; SS, sandstone units.

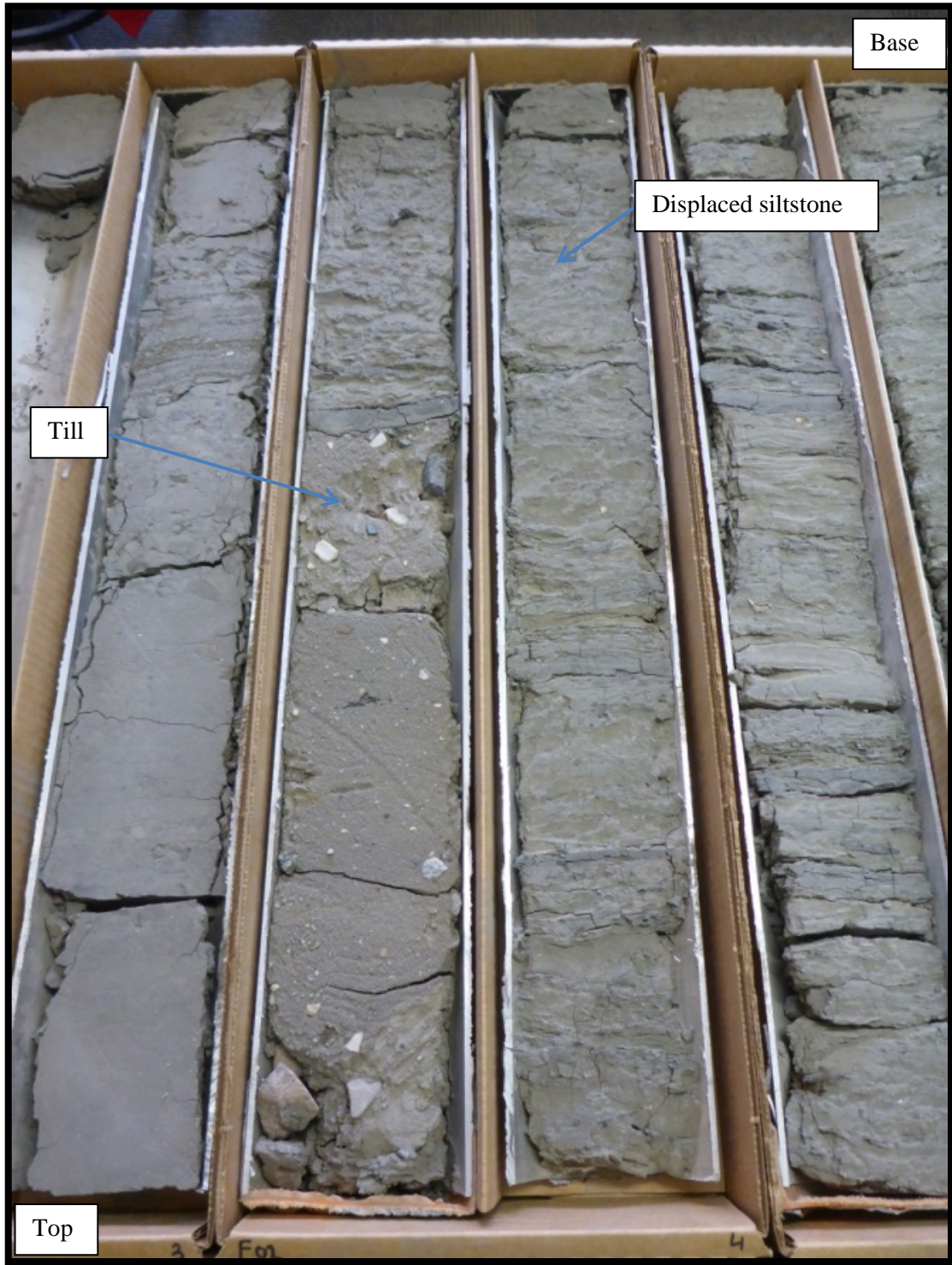


Figure 114. Photograph of core interval from well CVE TLK FIREBAG 2-27-94-3W4 (55–57 m depth, 462.0–460.0 m asl) showing till overlying displaced siltstone. Core boxes are 0.9 m long.

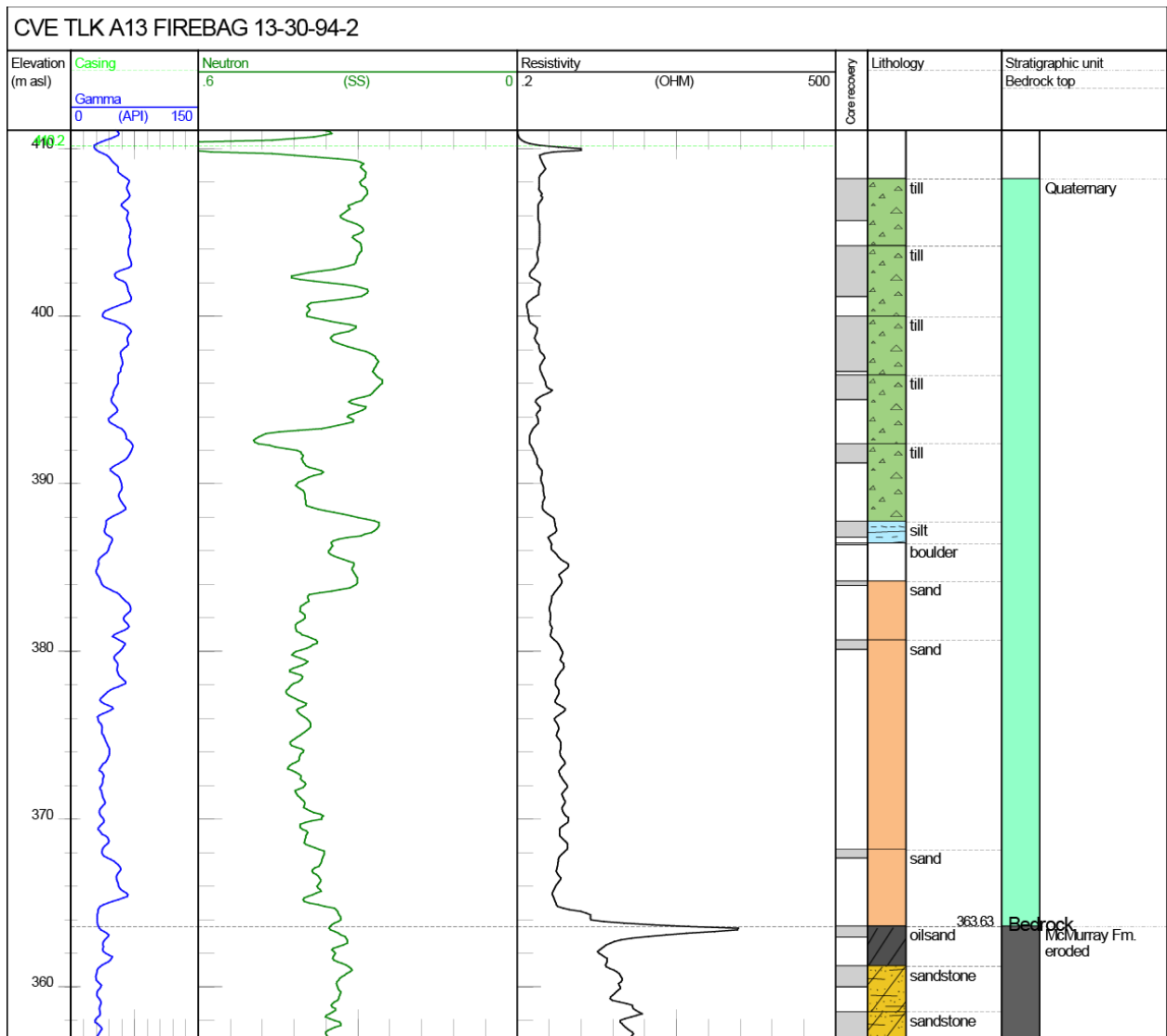


Figure 115. Logs for well CVE TLK A13 FIREBAG 13-30-94-2W4. Litholog determined from examination of core. Kelly bushing at 476.2 m asl and total depth at 298.2 m asl. Abbreviations: Gamma, gamma ray; Neutron, neutron porosity; OHM, ohm*m; SS, sandstone units.

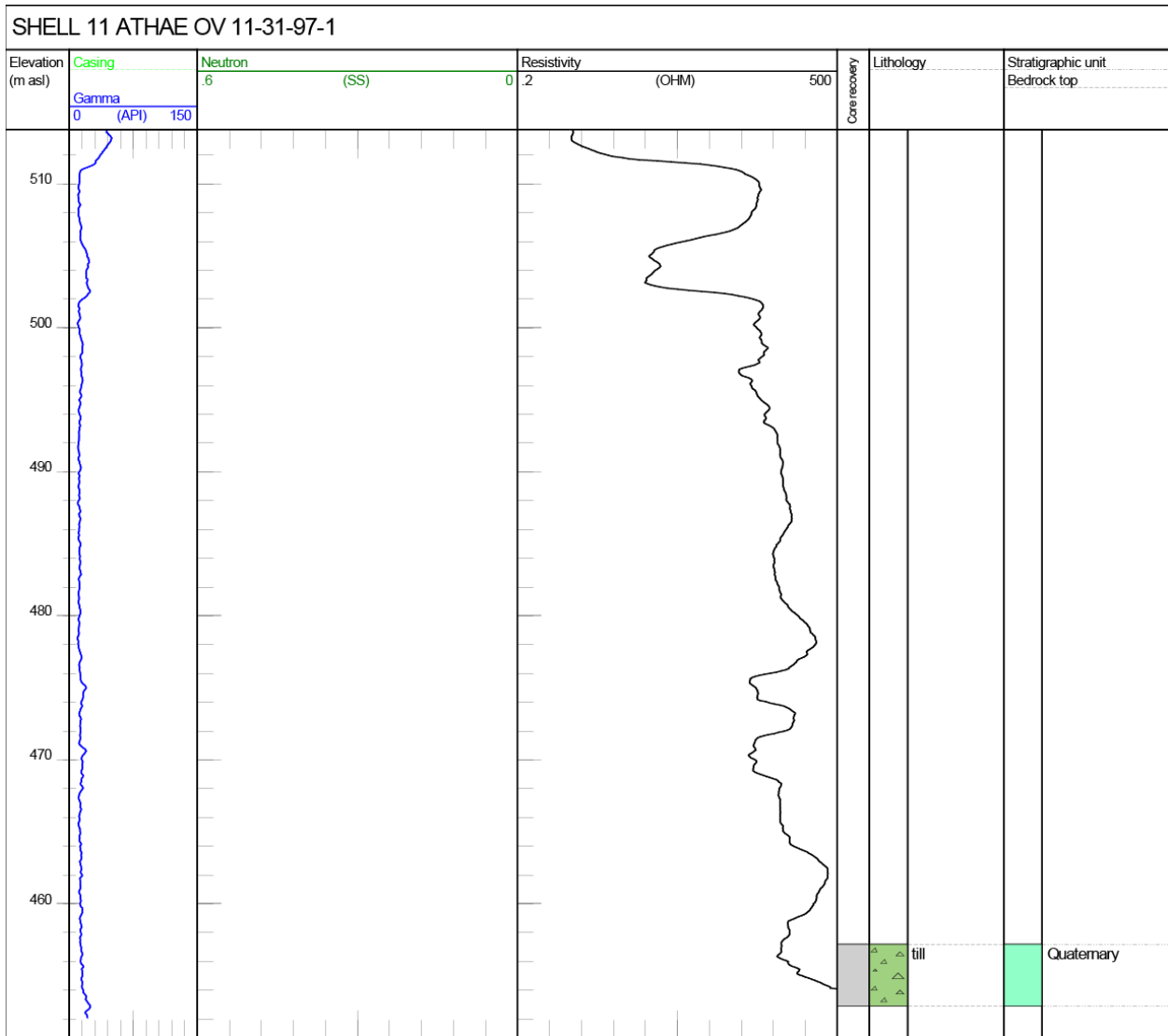


Figure 116. Logs for well SHELL 11 ATHAE OV 11-31-97-1W4. Litholog determined from examination of core. Neutron data unavailable. Kelly bushing at 533.4 m asl and total depth at 451.7 m asl. Abbreviations: Gamma, gamma ray; Neutron, neutron porosity; OHM, ohm·m; SS, sandstone units.

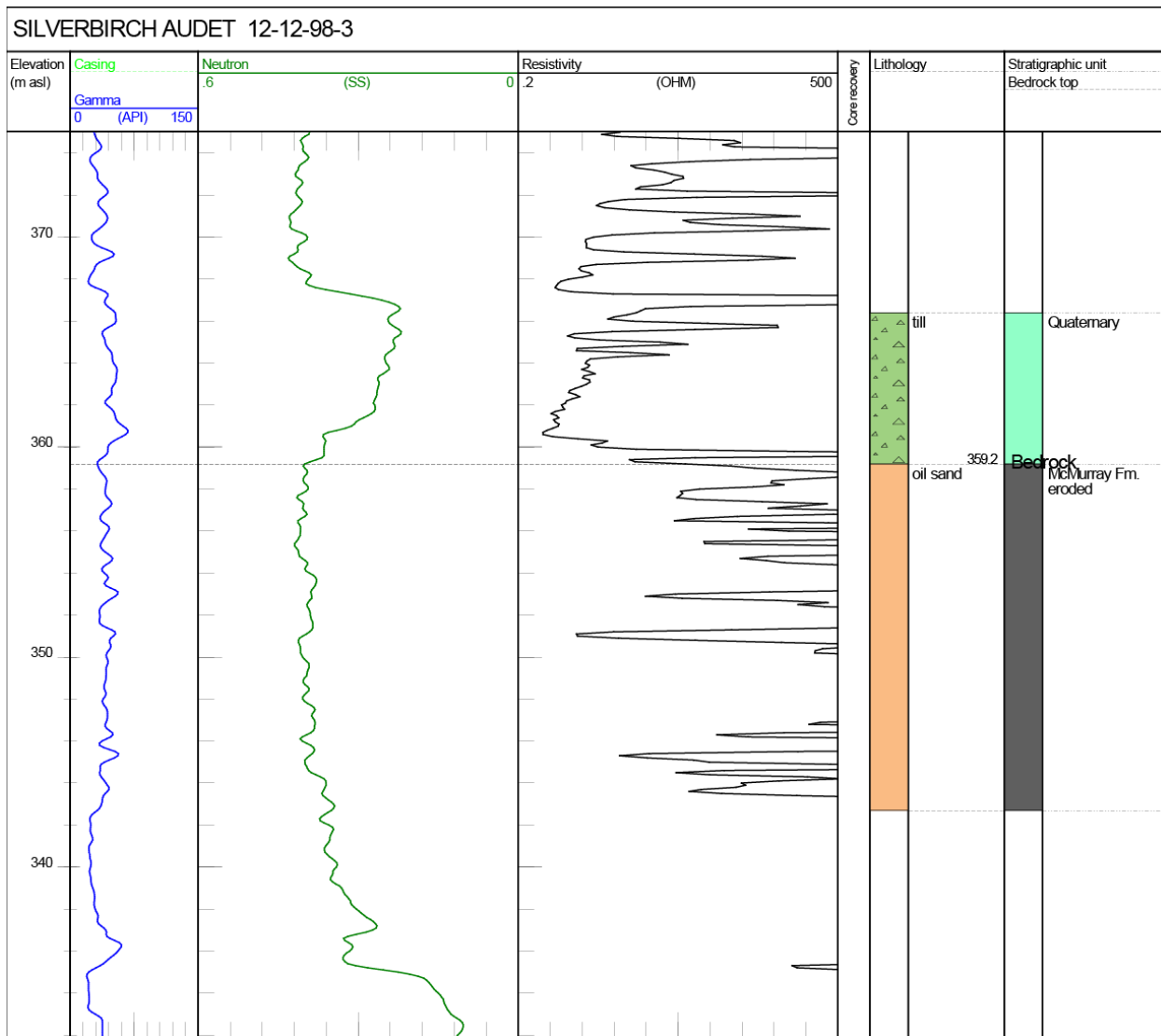


Figure 117. Logs for well SILVERBIRCH AUDET 12-12-98-3W4. Lithology determined from examination of core. No core recovery information. Kelly bushing at 517.7 m asl and total depth at 321.4 m asl. Abbreviations: Gamma, gamma ray; Neutron, neutron porosity; OHM, ohm·m; SS, sandstone units.

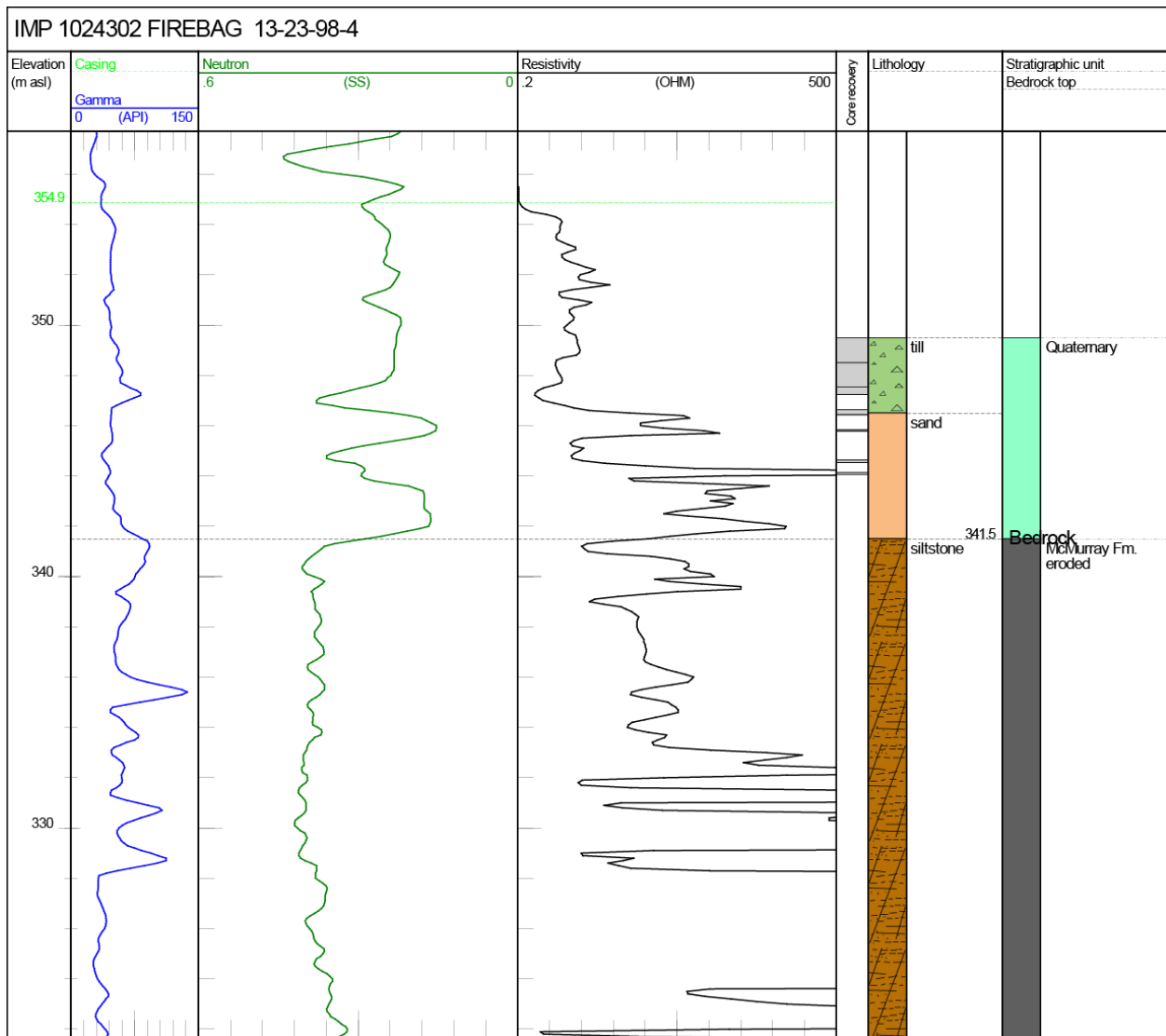


Figure 118. Logs for well IMP 1024302 FIREBAG 13-23-98-4W4. Litholog determined from examination of core. Kelly bushing at 416.5 m asl and total depth at 305.2 m asl. Abbreviations: Gamma, gamma ray; Neutron, neutron porosity; OHM, ohm·m; SS, sandstone units.

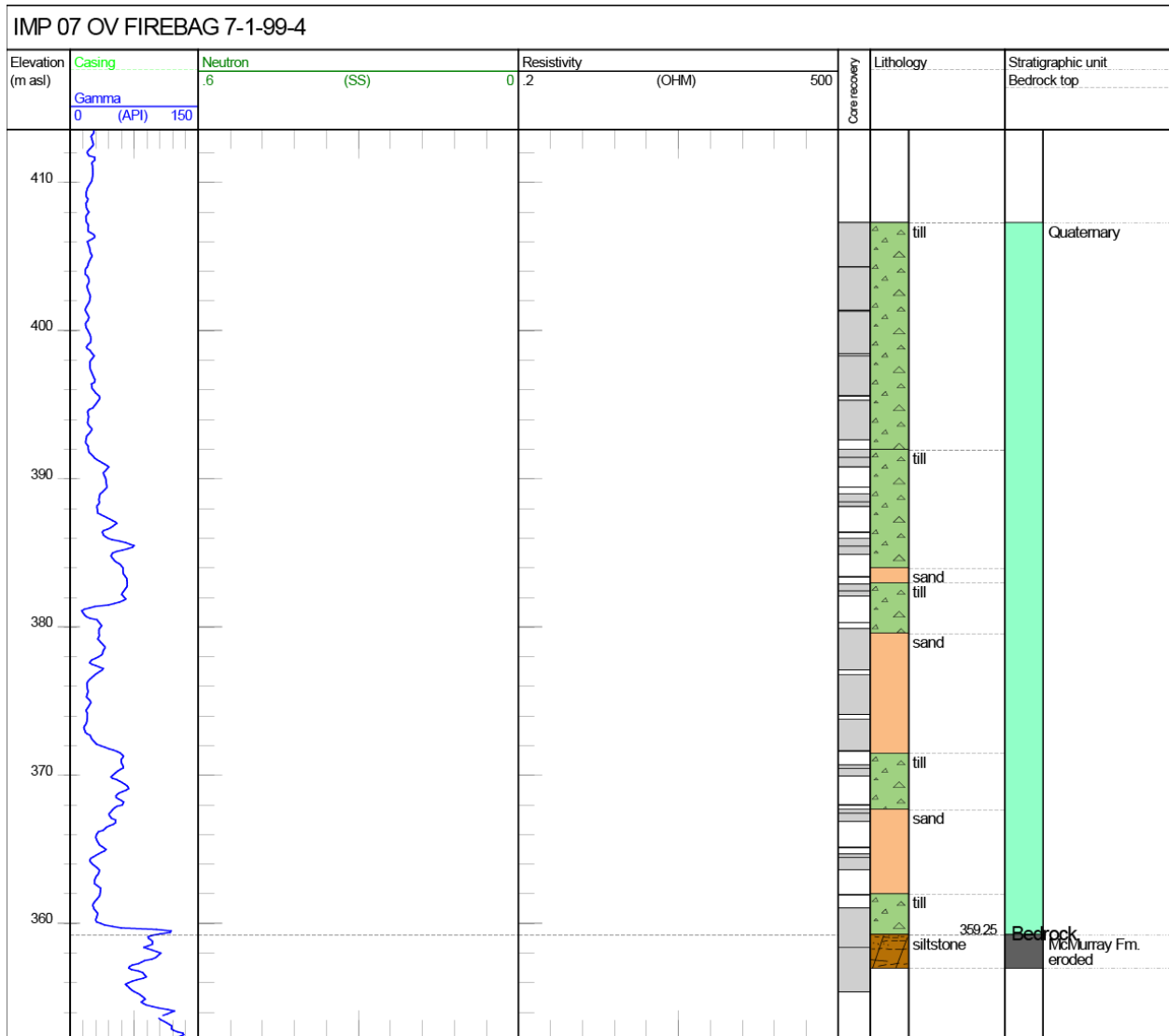


Figure 119. Logs for well IMP 07 OV FIREBAG 7-1-99-4W4. Litholog determined from examination of core. Neutron and resistivity data unavailable. Kelly bushing at 421.0 m asl and total depth at 307.4 m asl. Abbreviations: Gamma, gamma ray; Neutron, neutron porosity; OHM, ohm·m; SS, sandstone units.



Figure 120. Photograph of core interval from well IMP 07 OV FIREBAG 7-1-99-4W4 (61.5–62.0 m depth, 359.5–359.0 m asl) showing bedrock contact with till. Core boxes are 0.9 m long.

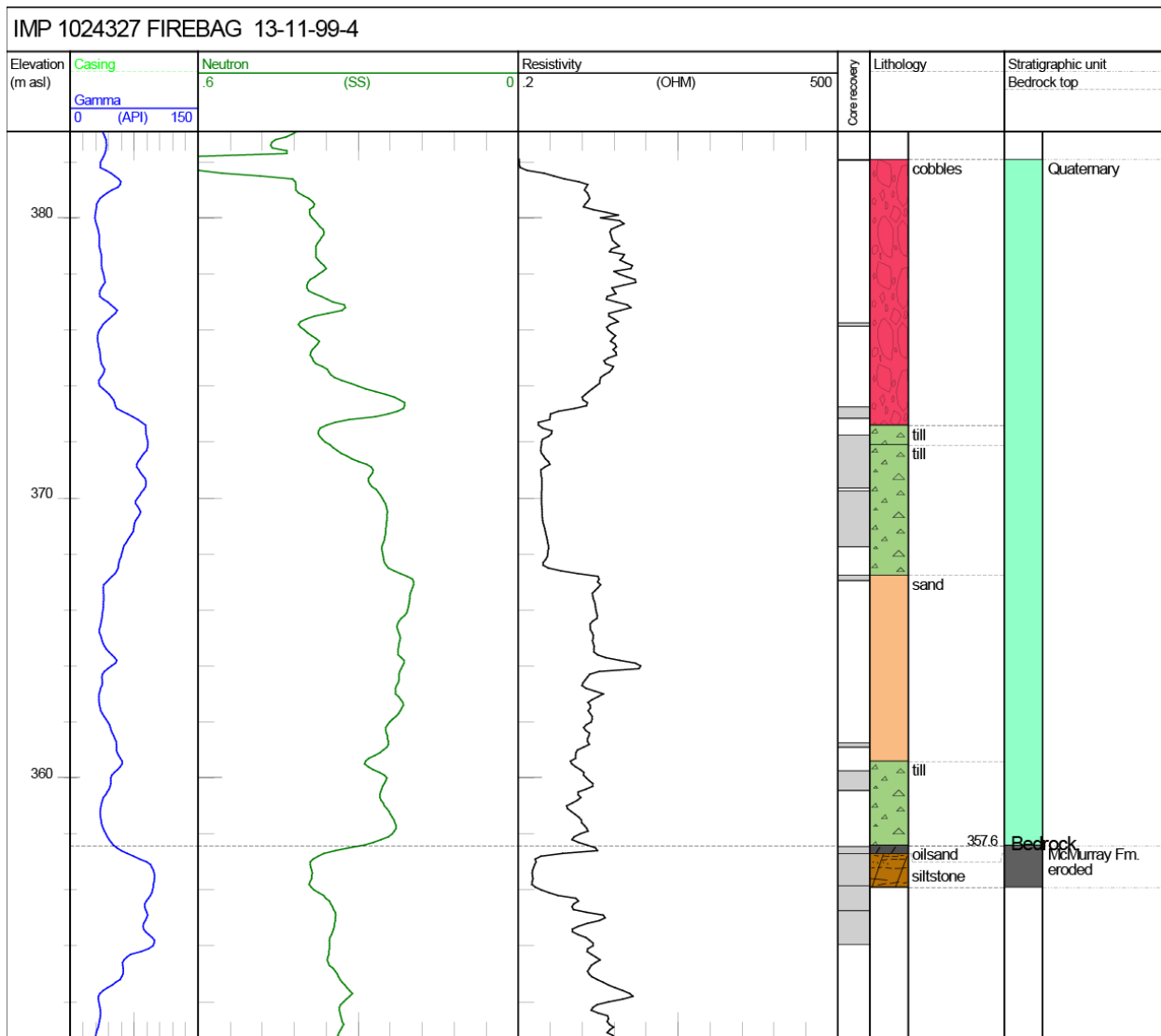


Figure 121. Logs for well IMP 1024327 FIREBAG 13-11-99-4W4. Litholog determined from examination of core. Kelly bushing at 403.1 m asl and total depth at 296.2 m asl. Abbreviations: Gamma, gamma ray; Neutron, neutron porosity; OHM, ohm·m; SS, sandstone units.

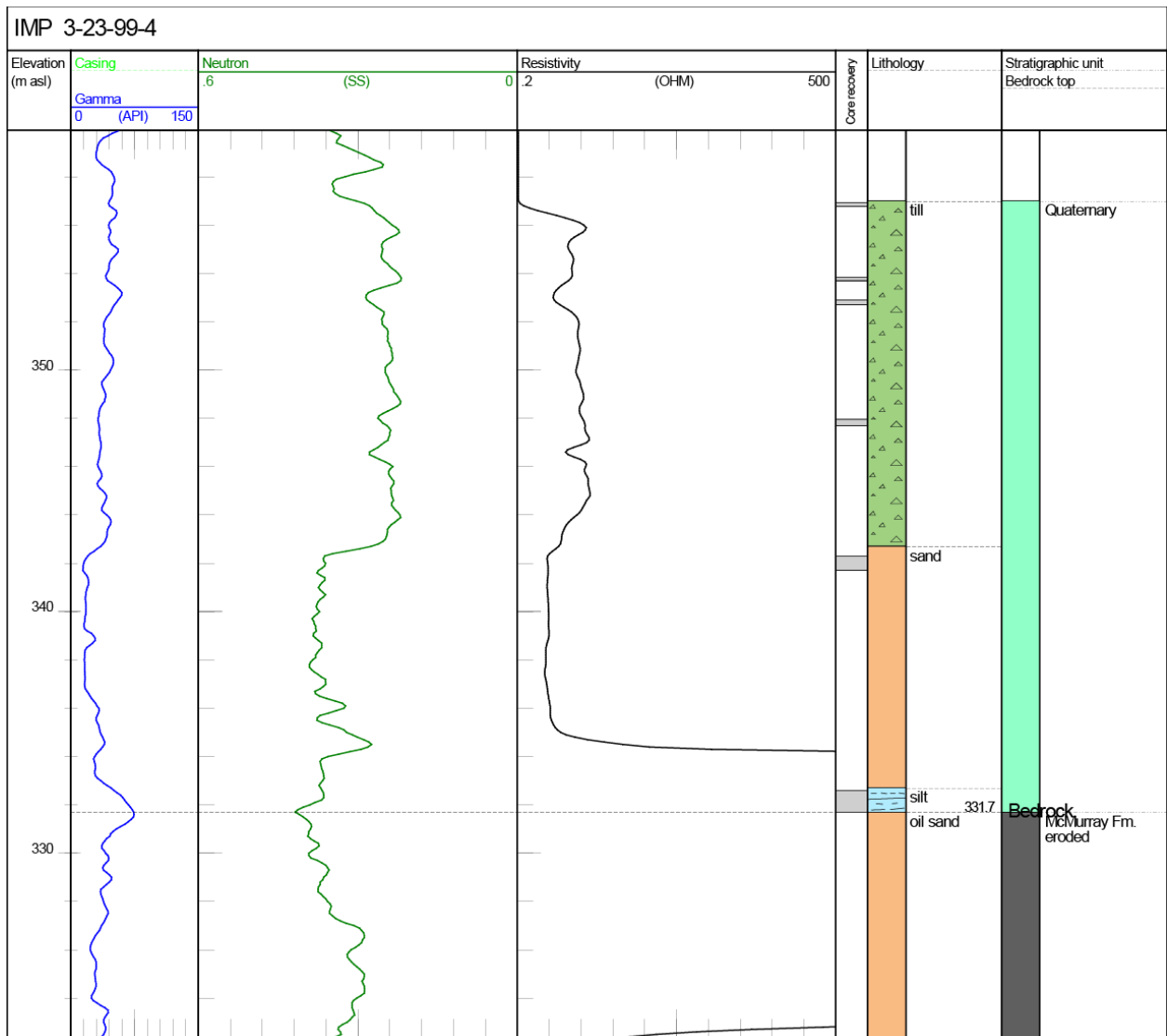


Figure 122. Logs for well IMP 3-23-99-4W4. Litholog determined from examination of core. Poor core recovery; it is possible that the bedrock top is at 342 m asl. Kelly bushing at 391.7 m asl and total depth at 307.7 m asl. Abbreviations: Gamma, gamma ray; Neutron, neutron porosity; OHM, ohm·m; SS, sandstone units.

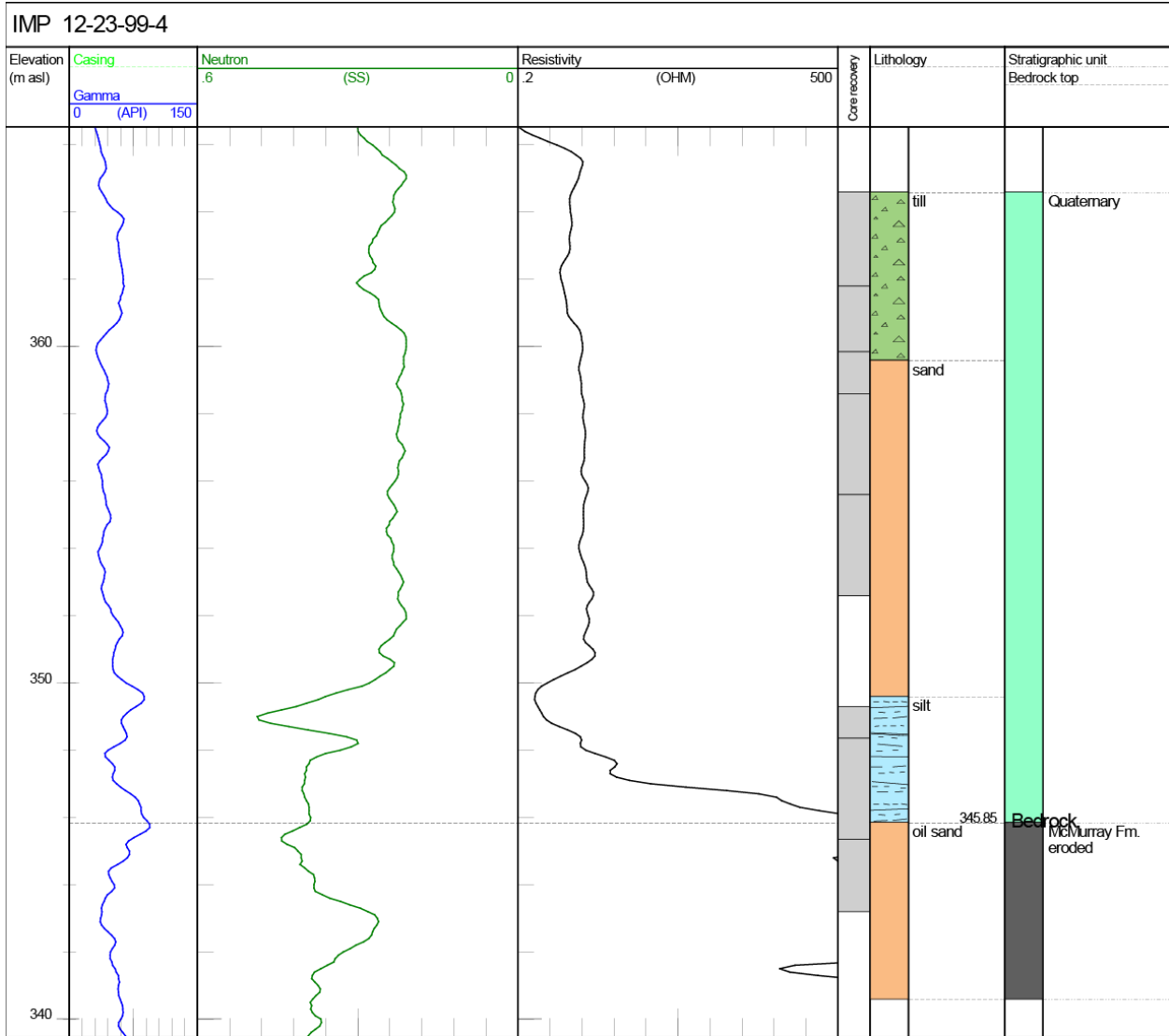


Figure 123. Logs for well IMP 12-23-99-4W4. Litholog determined from examination of core. Kelly bushing at 397.6 m asl and total depth at 306.6 m asl. Abbreviations: Gamma, gamma ray; Neutron, neutron porosity; OHM, ohm•m; SS, sandstone units.

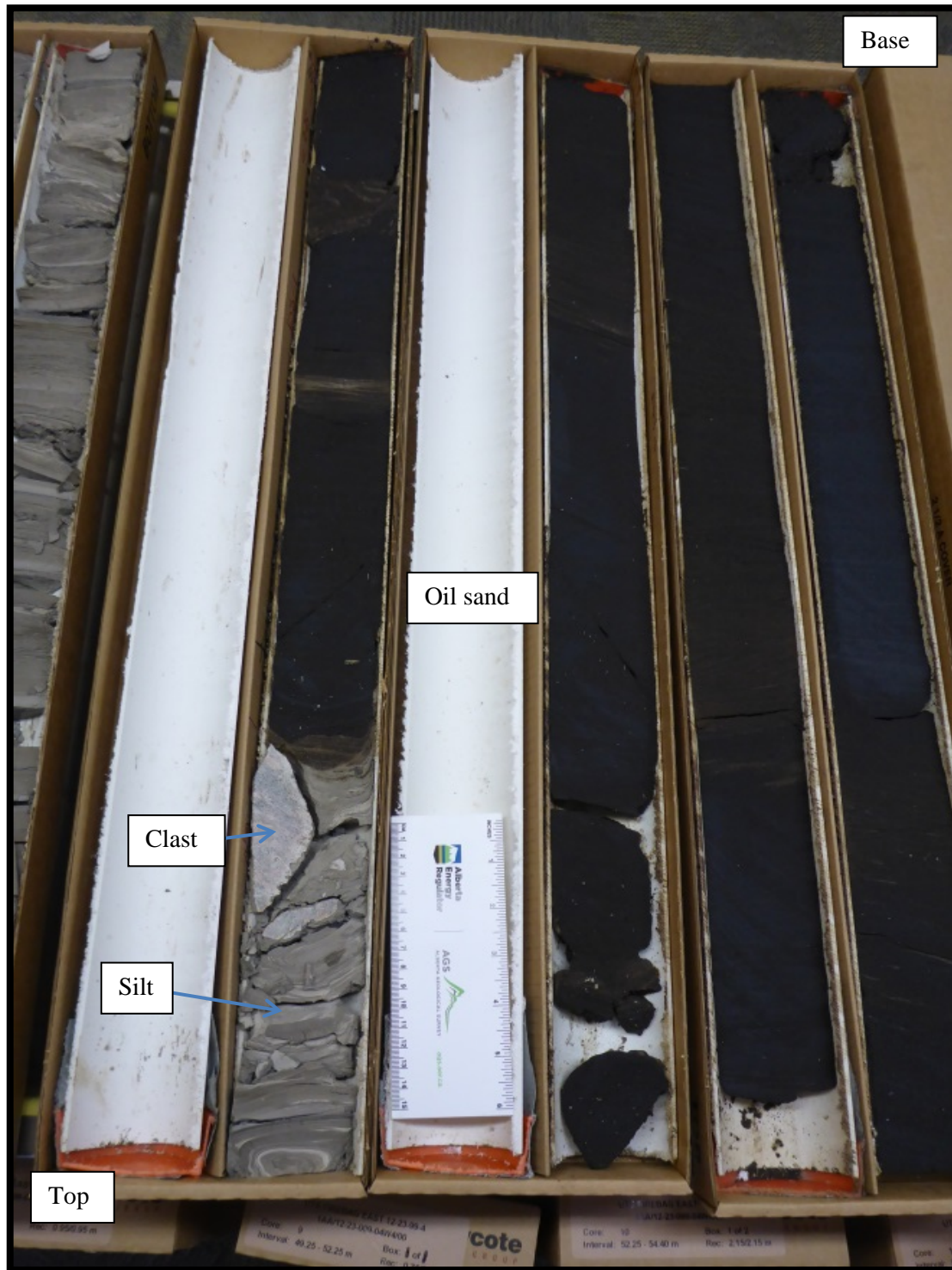


Figure 124. Photograph of core interval from well IMP 12-23-99-4W4 (52.0–55.0 m depth, 345.6–342.6 m asl) showing silt overlying oil sand. The silt looks similar to siltstone, however, there are two granitic clasts near the bedrock contact, which looks like it is in place. Core boxes are 0.9 m long.

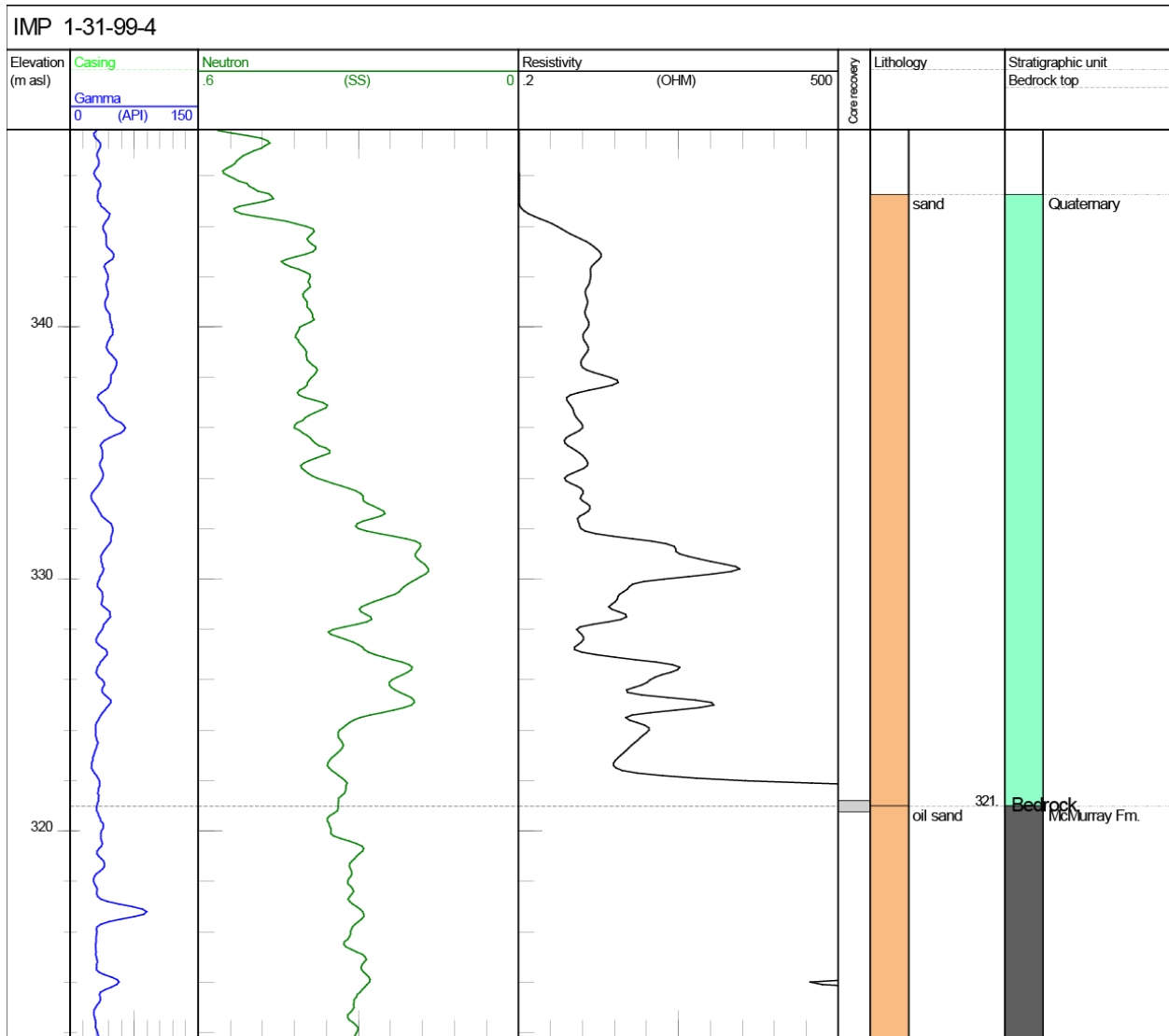


Figure 125. Logs for well IMP 1-31-99-4W4. Litholog determined from examination of core. Poor core recovery; bedrock top primarily based on log interpretation. Kelly bushing at 358.0 m asl and total depth at 295.0 m asl. Abbreviations: Gamma, gamma ray; Neutron, neutron porosity; OHM, ohm•m; SS, sandstone units.

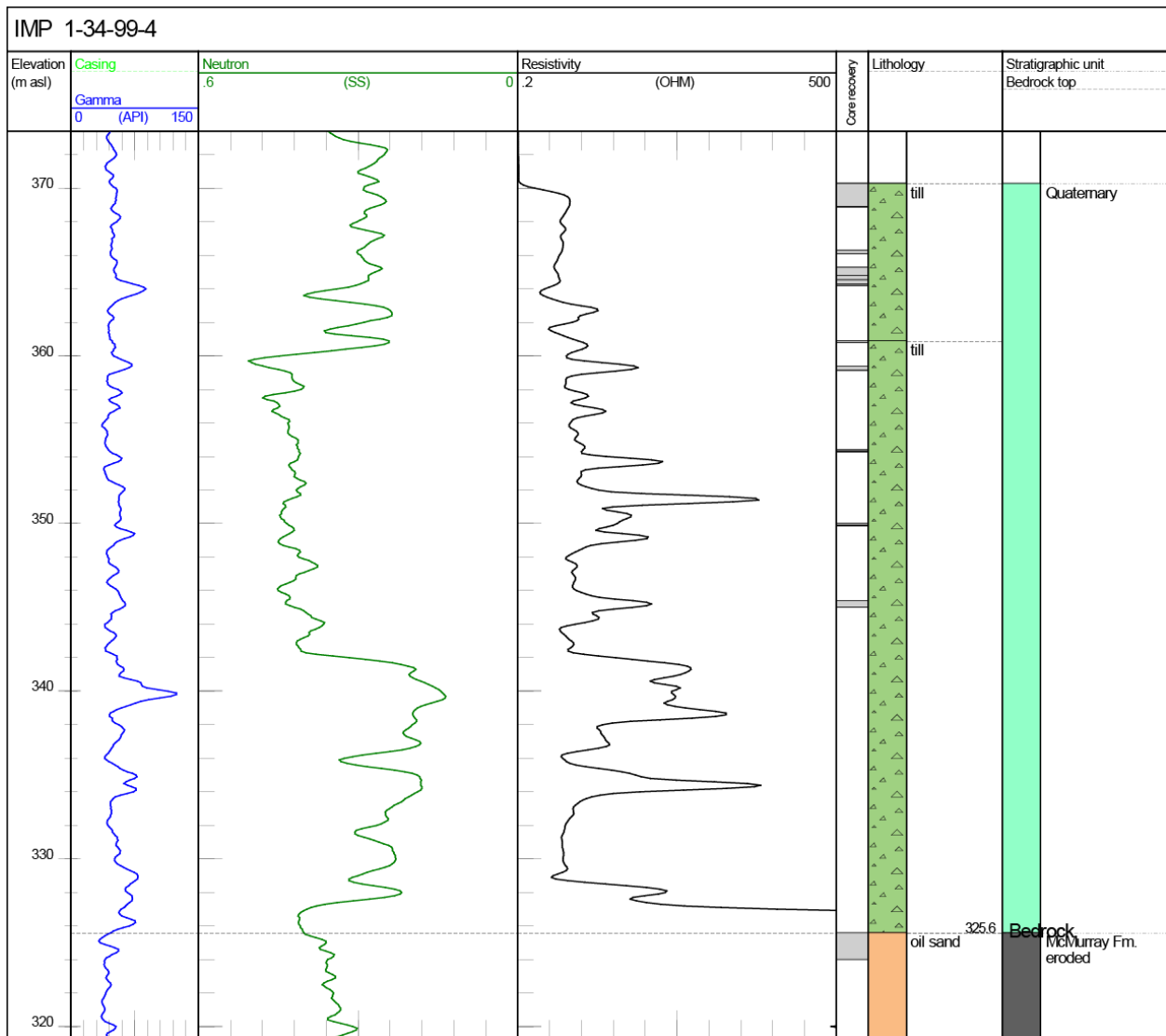


Figure 126. Logs for well IMP 1-34-99-4W4. Litholog determined from examination of core. Bedrock top may be higher than indicated (e.g., 360 m asl), difficult to determine due to poor core recovery. Kelly bushing at 389.6 m asl and total depth at 296.0 m asl. Abbreviations: Gamma, gamma ray; Neutron, neutron porosity; OHM, ohm·m; SS, sandstone units.

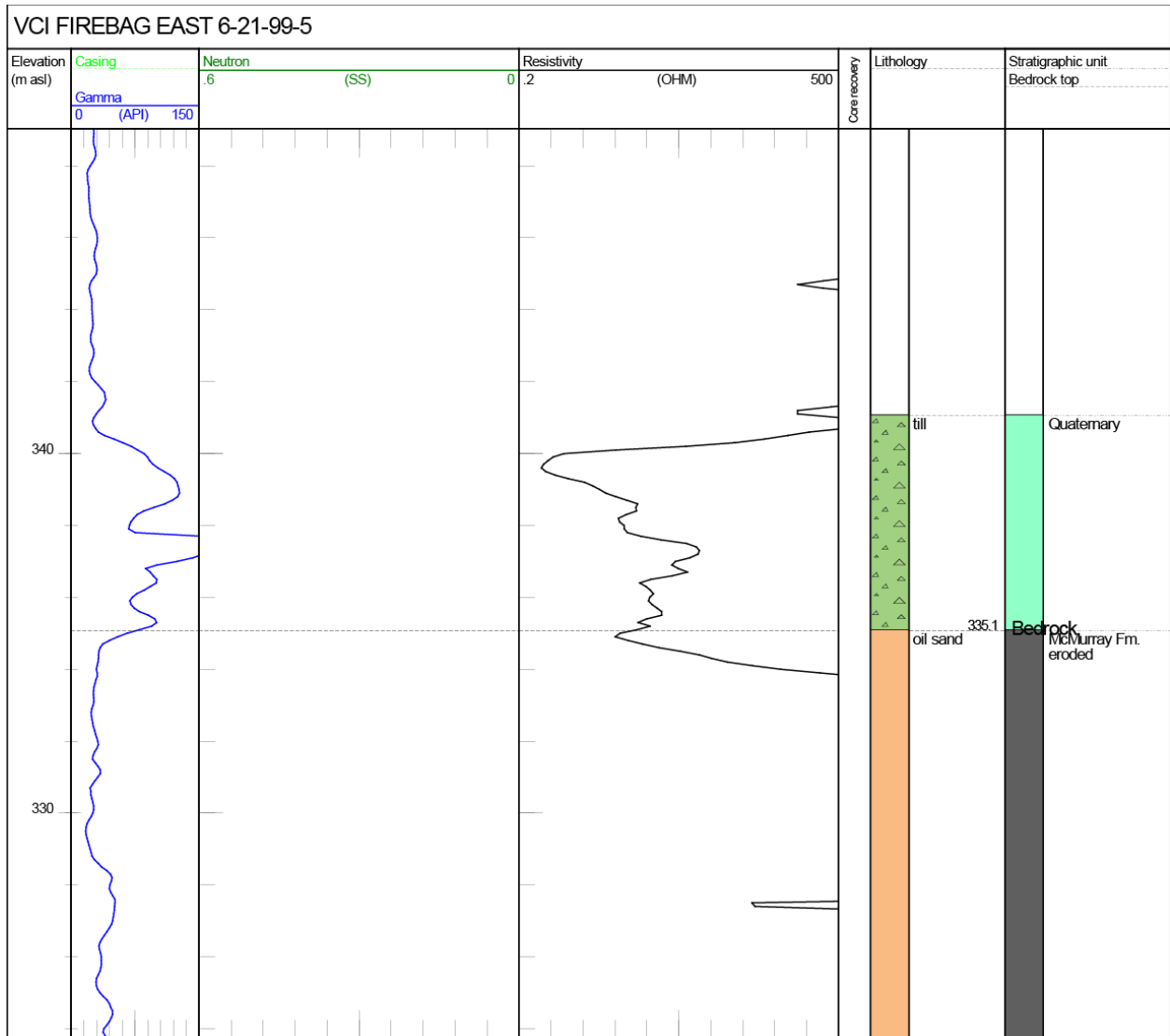


Figure 127. Logs for well VCI FIREBAG EAST 6-21-99-5W4. Litholog determined from examination of core. Neutron data and core recovery unavailable. Kelly bushing at 352.6 m asl and total depth at 245.6 m asl. Abbreviations: Gamma, gamma ray; Neutron, neutron porosity; OHM, ohm*m; SS, sandstone units.

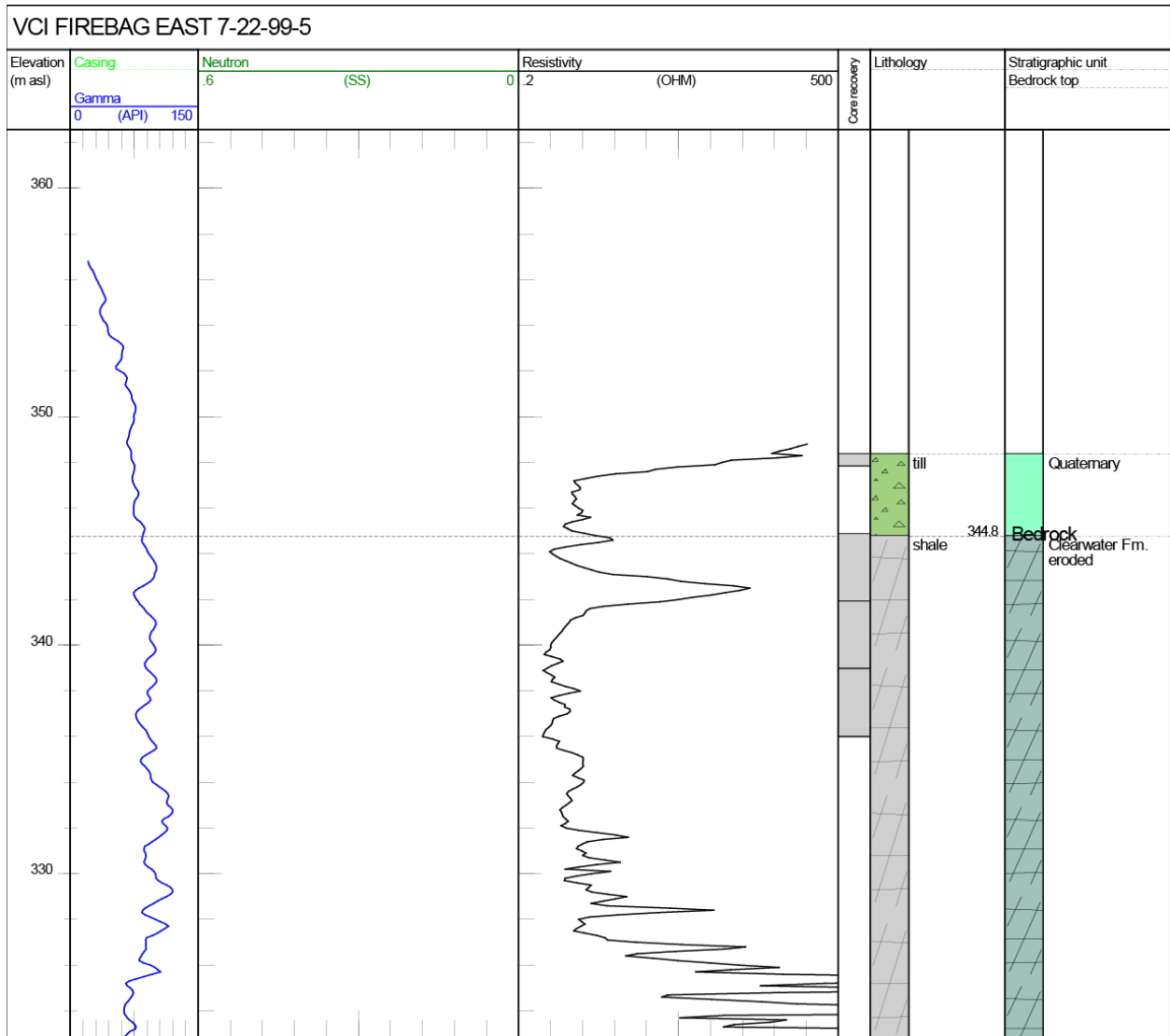


Figure 128. Logs for well VCI FIREBAG EAST 7-22-99-5W4. Litholog determined from examination of core. Neutron data unavailable. Kelly bushing at 357.8 m asl and total depth at 237.8 m asl. Abbreviations: Gamma, gamma ray; Neutron, neutron porosity; OHM, ohm•m; SS, sandstone units.

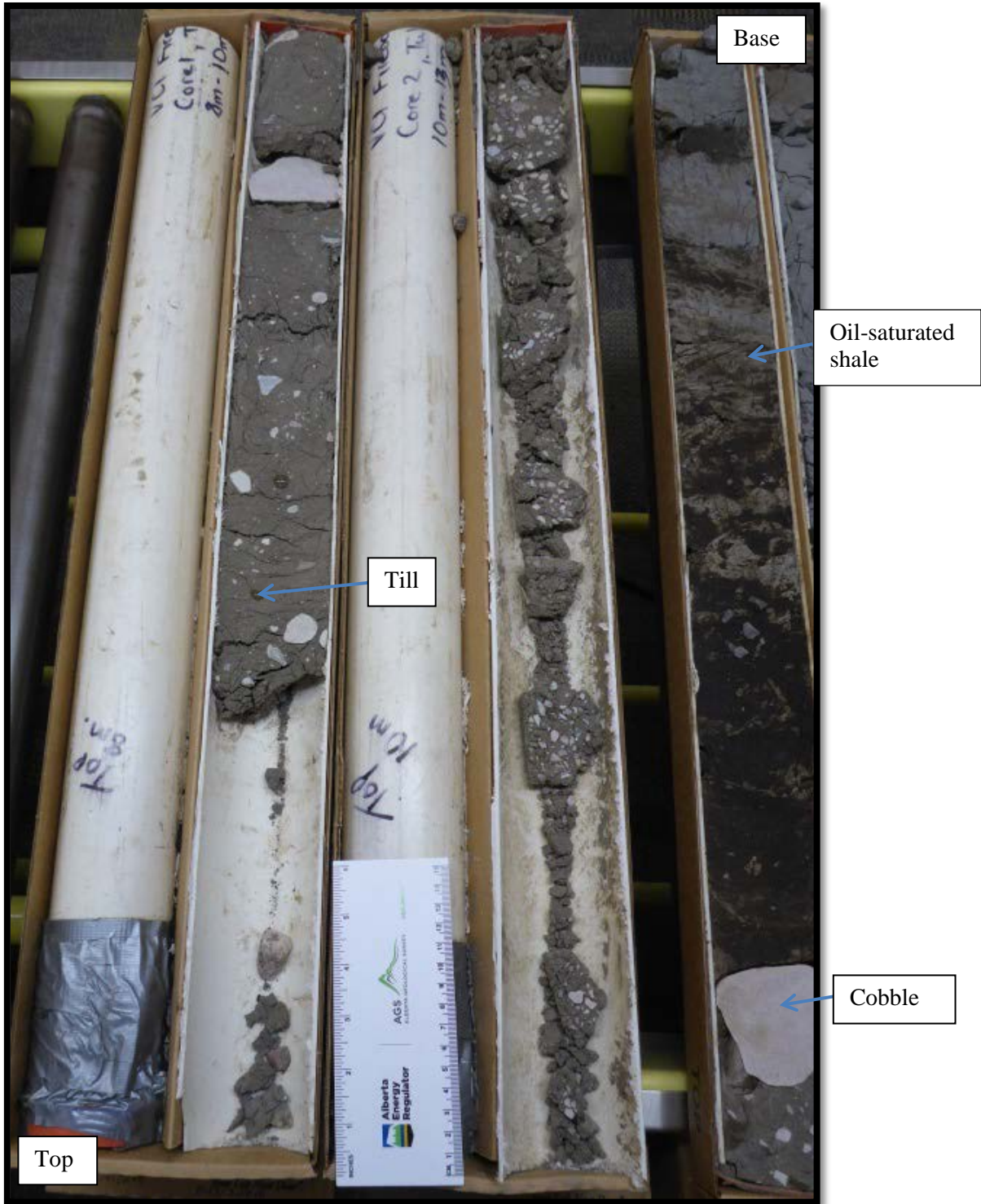


Figure 129. Photograph of core interval from well VCI FIREBAG EAST 7-22-99-5W4 (9.42–14 m depth, 348.38–343.8 m asl) showing till overlying bedrock (with cobble at contact). Core boxes are 0.9 m long.

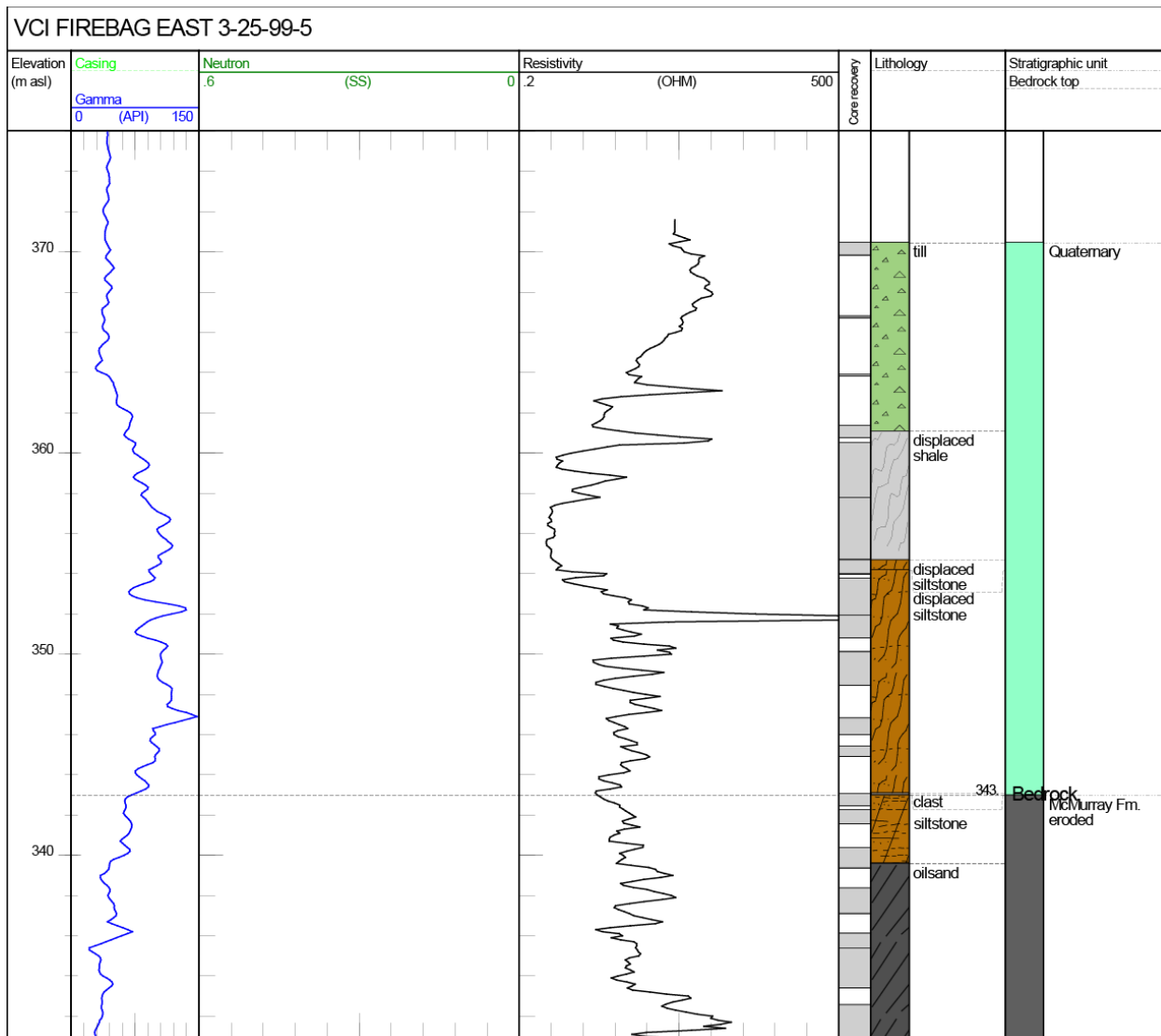


Figure 130. Logs for well VCI FIREBAG EAST 3-25-99-5W4. Litholog determined from examination of core. Neutron data unavailable. Kelly bushing at 379.6 m asl and total depth at 288.6 m asl. Abbreviations: Gamma, gamma ray; Neutron, neutron porosity; OHM, ohm•m; SS, sandstone units.



Figure 131. Photograph of core interval from well VCI FIREBAG EAST 3-25-99-5W4 (36.5–36.8 m depth, 343.1–342.8 m asl) showing clast above bedrock. If this clast is out of place, the bedrock top would be above the material reported as displaced, putting it at 361 m asl.

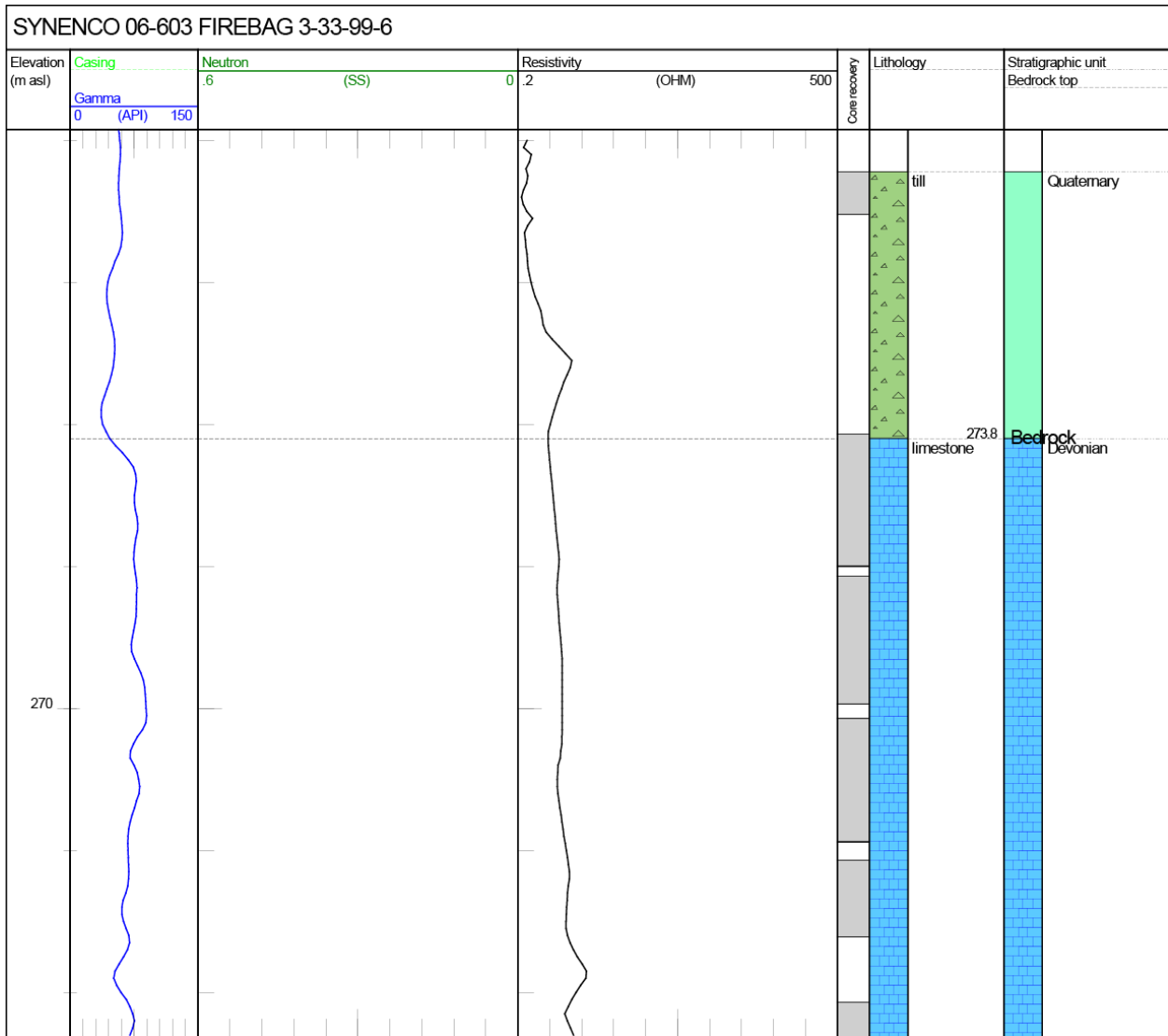


Figure 132. Logs for well SYNENCO 06-603 FIREBAG 3-33-99-6W4. Litholog determined from examination of core. Neutron data unavailable. Kelly bushing at 299.0 m asl and total depth at 253.9 m asl. Abbreviations: Gamma, gamma ray; Neutron, neutron porosity; OHM, ohm*m; SS, sandstone units.



Figure 133. Photograph of core interval from well SYNENCO 06-603 FIREBAG 3-33-99-6W4 (21.44–25.14 m depth, 277.56–273.86 m asl) showing pink till. Core boxes are 0.9 m long.

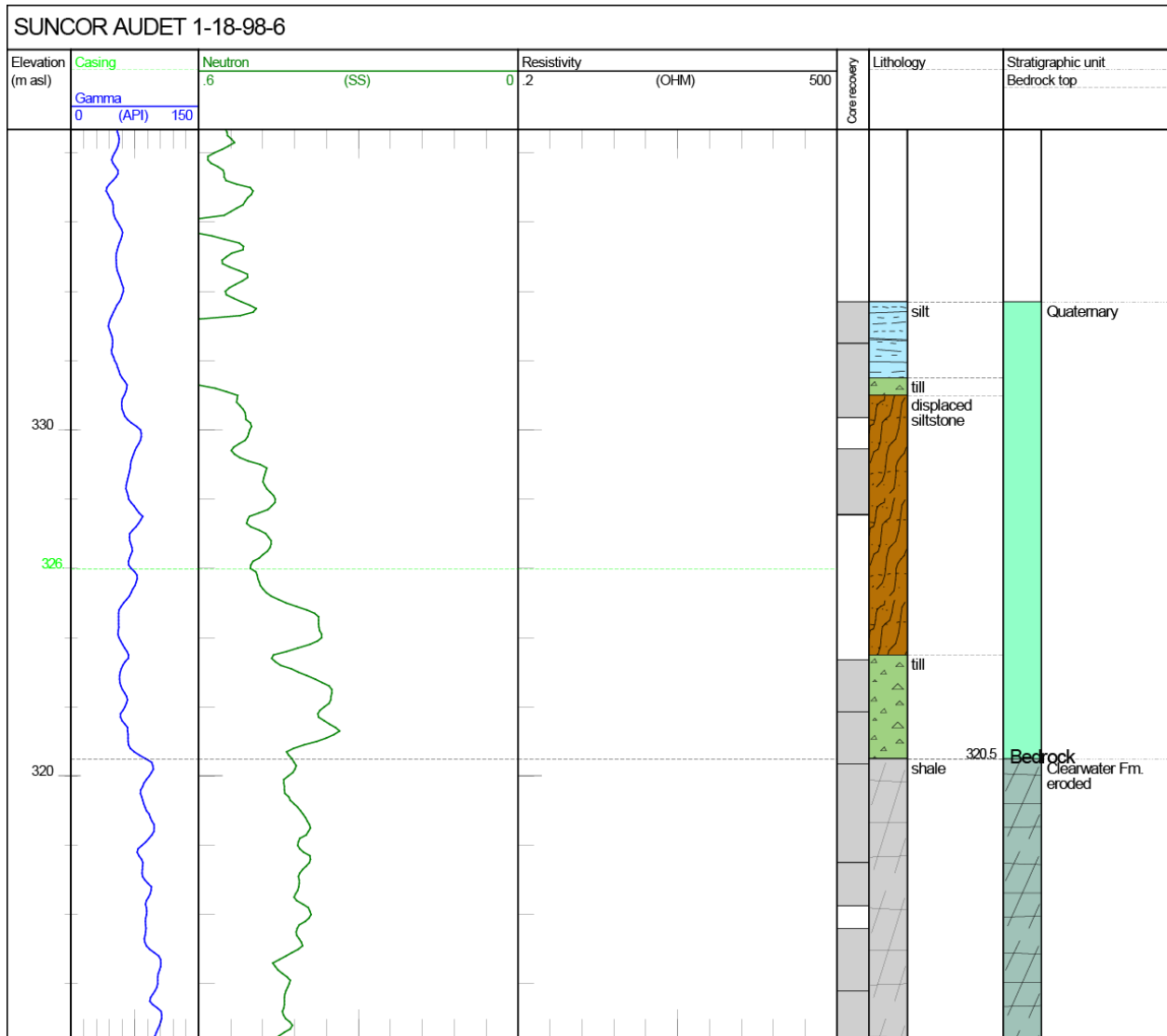


Figure 134. Logs for well SUNCOR AUDET 1-18-98-6W4. Litholog determined from examination of core. Resistivity data unavailable. Kelly bushing at 353.5 m asl and total depth at 277.2 m asl. Abbreviations: Gamma, gamma ray; Neutron, neutron porosity; OHM, ohm•m; SS, sandstone units.

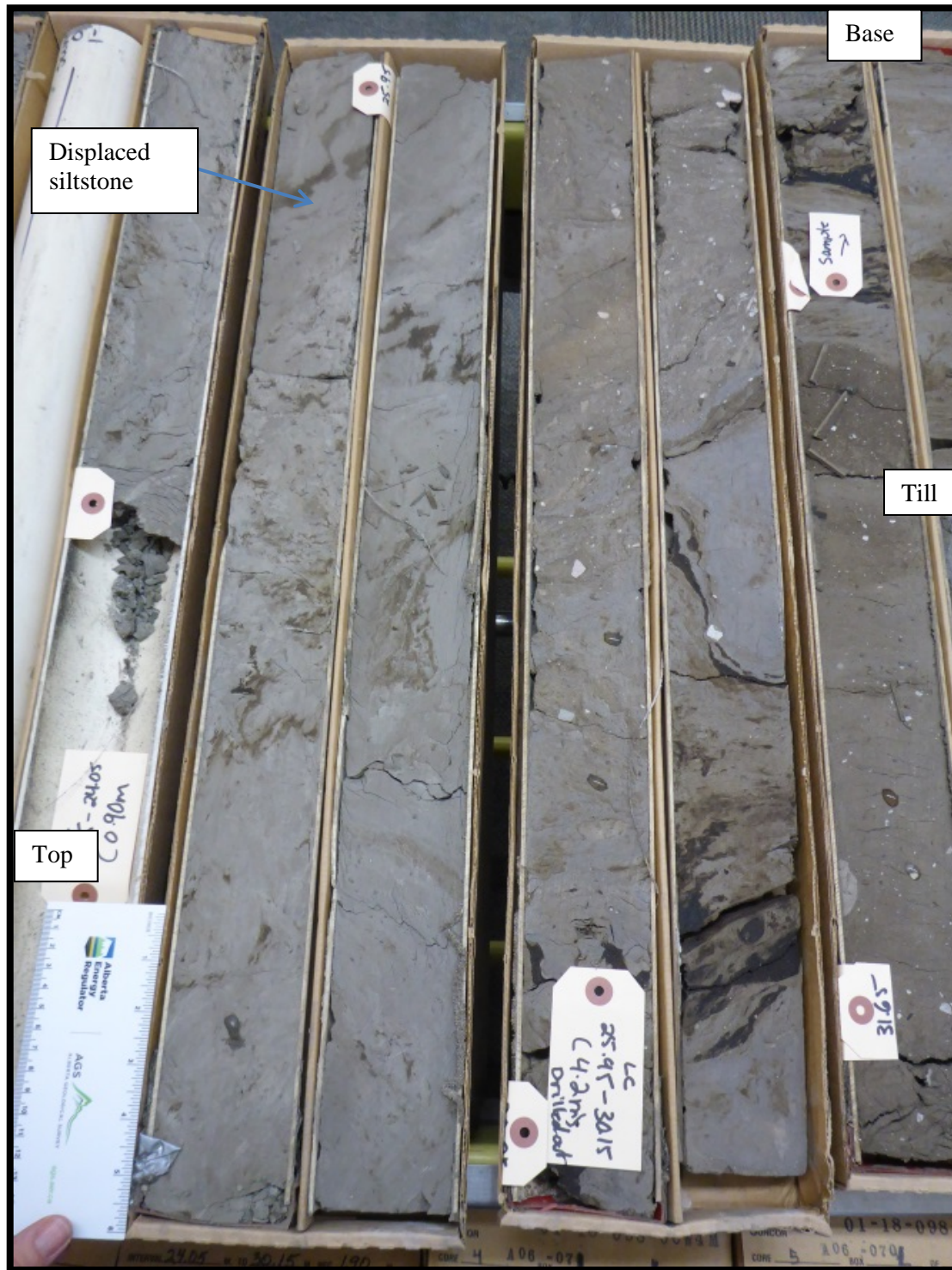


Figure 135. Photograph of core interval from well SUNCOR AUDET 1-18-98-6W4 (28–32 m depth, 325.5–321.5 m asl) showing displaced siltstone with underlying till. Core boxes are 0.9 m long.

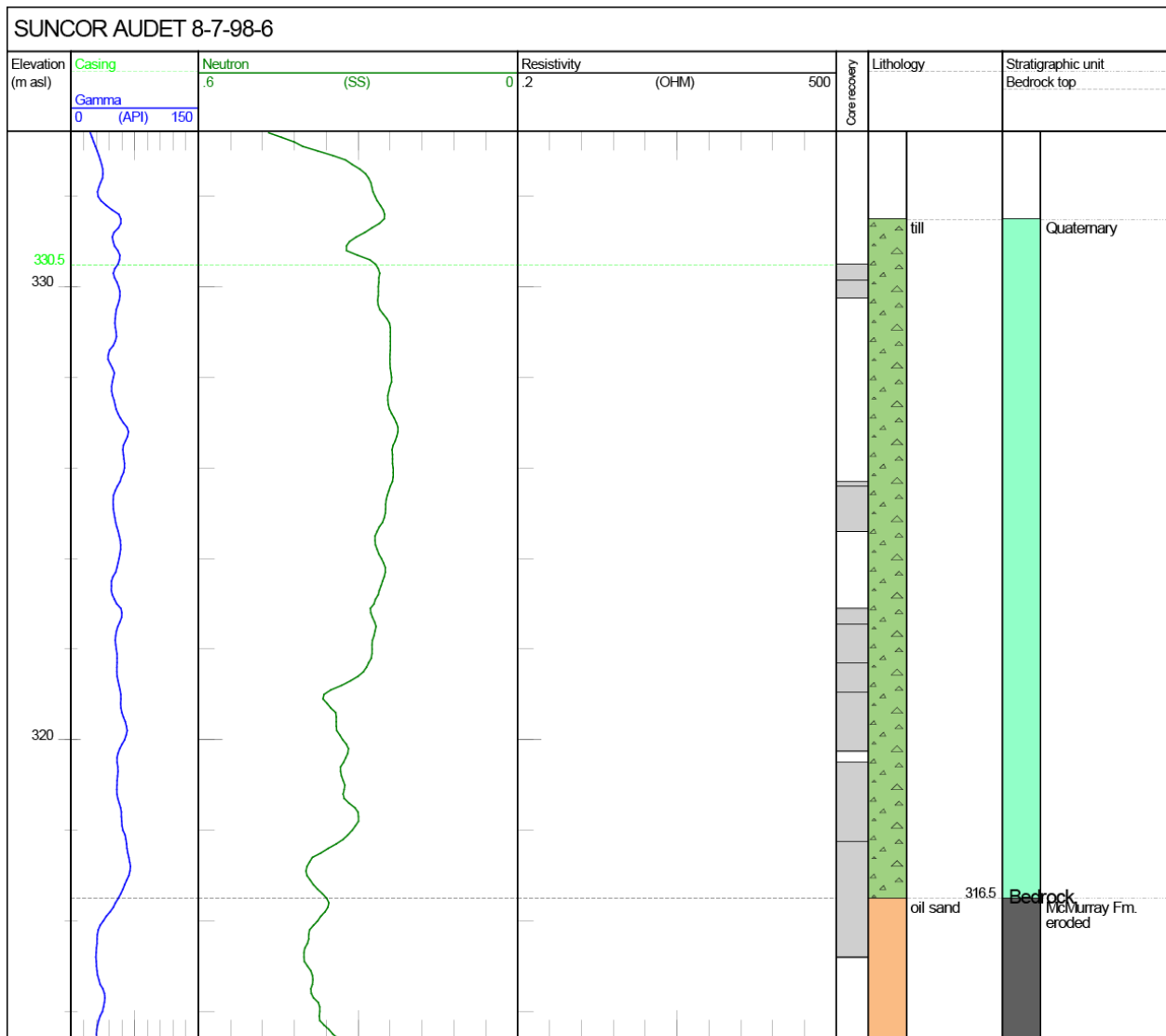


Figure 136. Logs for well SUNCOR AUDET 8-7-98-6W4. Litholog determined from examination of core. Resistivity data unavailable. Kelly bushing at 348.5 m asl and total depth at 299.7 m asl. Abbreviations: Gamma, gamma ray; Neutron, neutron porosity; OHM, ohm•m; SS, sandstone units.

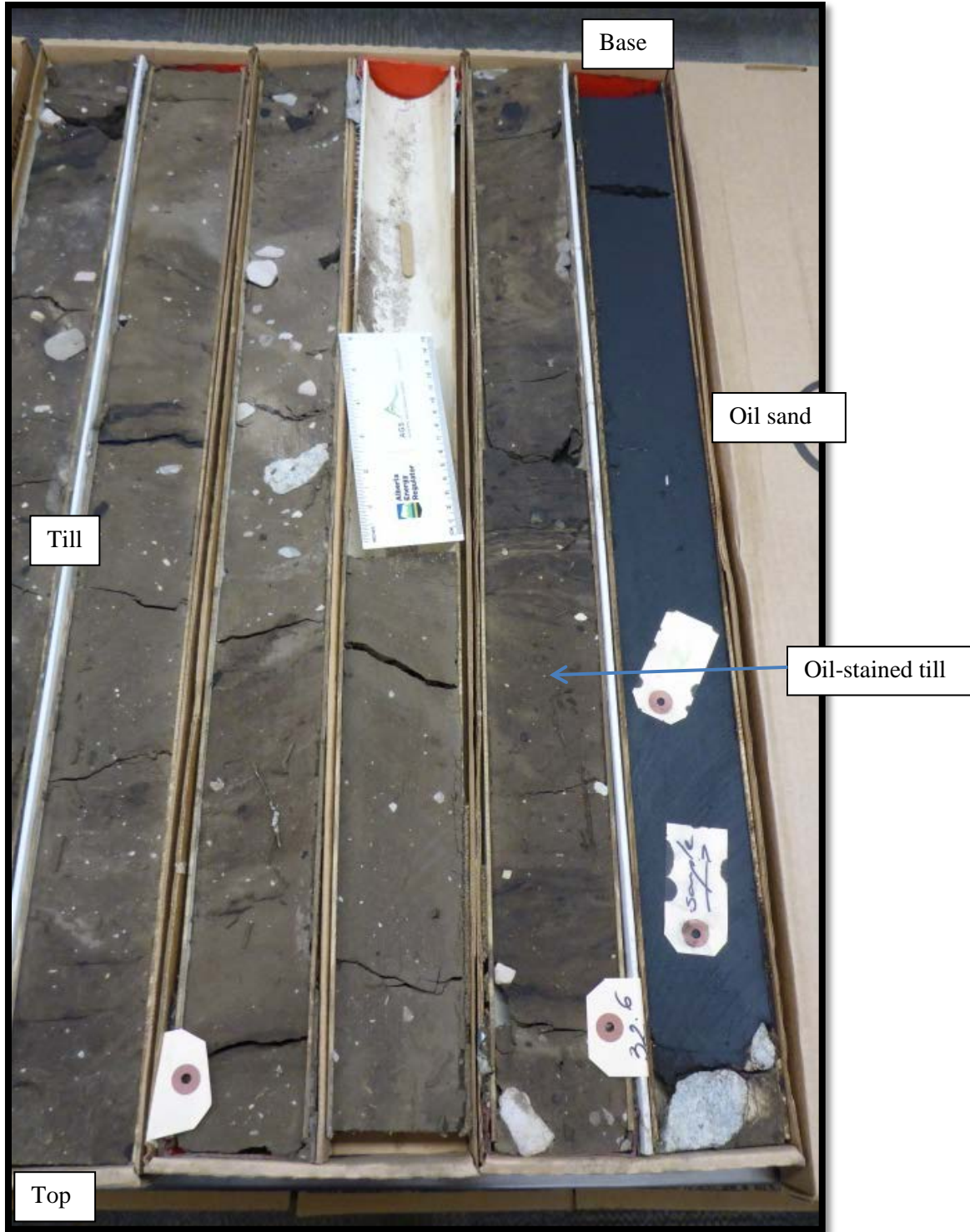


Figure 137. Photograph of core interval from well SUNCOR AUDET 8-7-98-6W4 (29–33 m depth, 319.5–315.5 m asl) showing oil sand bedrock underlying oil-stained till. Core boxes are 0.9 m long.

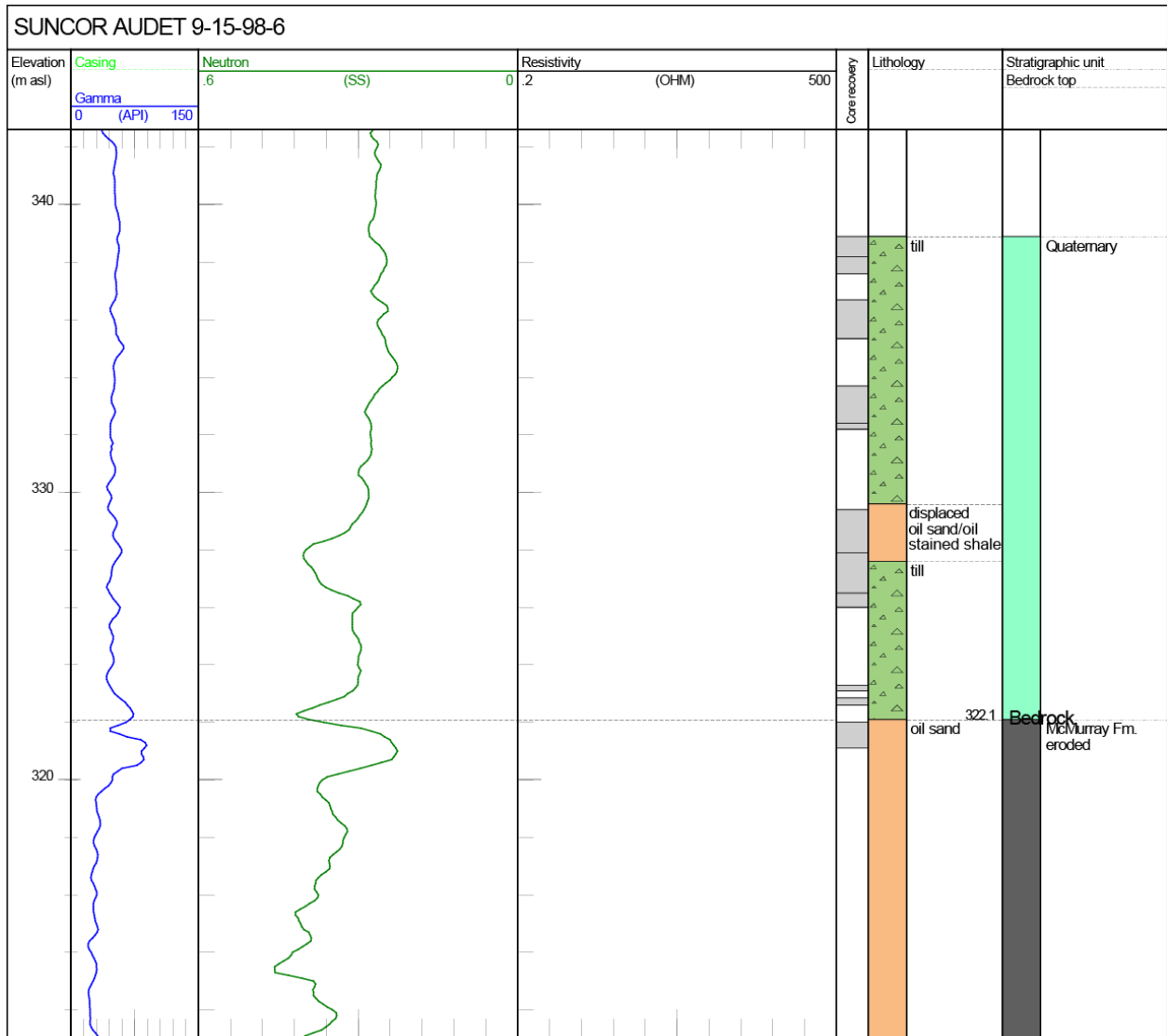


Figure 138. Logs for well SUNCOR AUDET 9-15-98-6W4. Litholog determined from examination of core. Resistivity data unavailable. Kelly bushing at 359.6 m asl and total depth at 279.1 m asl. Abbreviations: Gamma, gamma ray; Neutron, neutron porosity; OHM, ohm•m; SS, sandstone units.

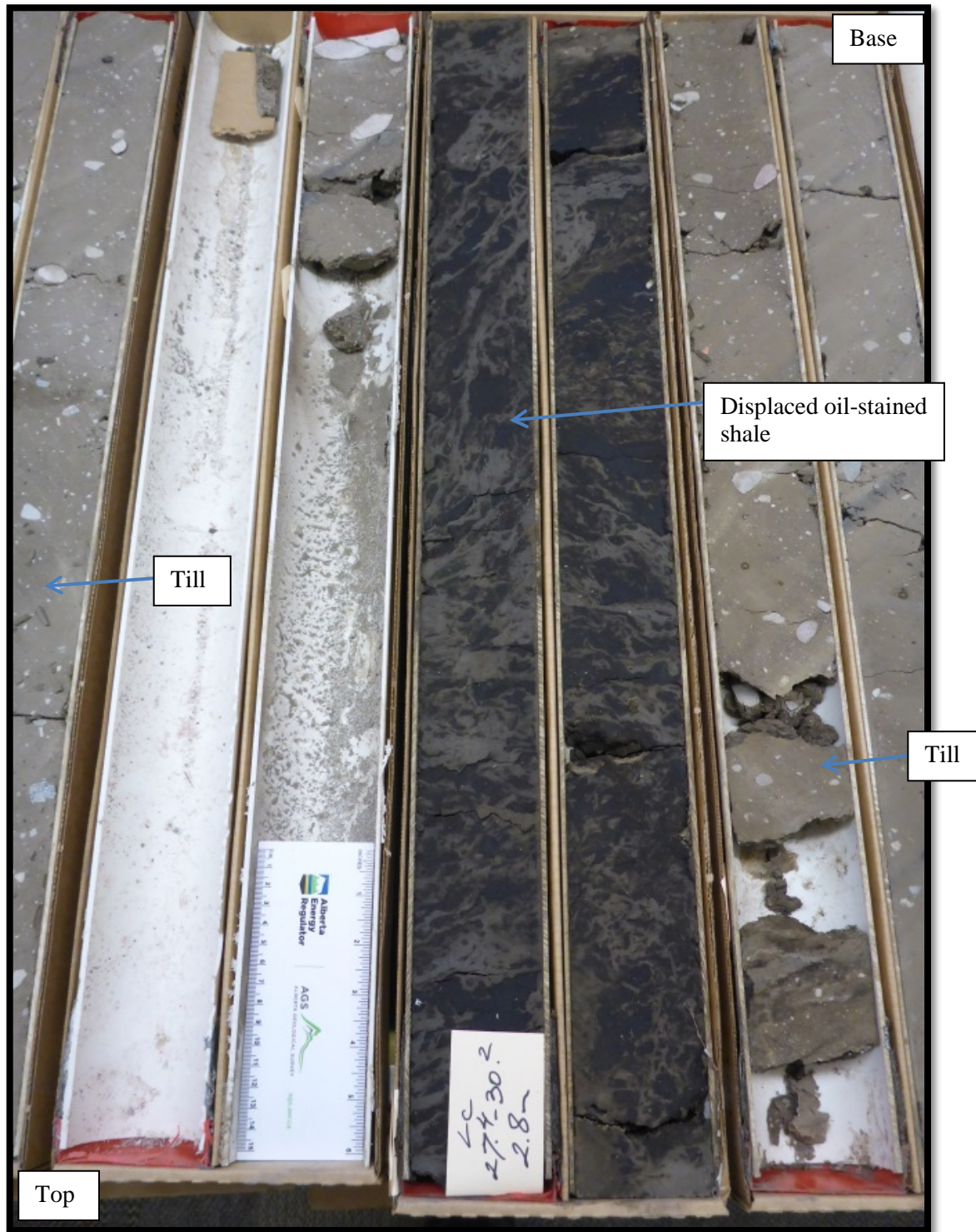


Figure 139. Photograph of core interval from well SUNCOR AUDET 9-15-98-6W4 (26–33 m depth, 333.6–326.6 m asl) of displaced oil-stained shale between till. Core boxes are 0.9 m long.

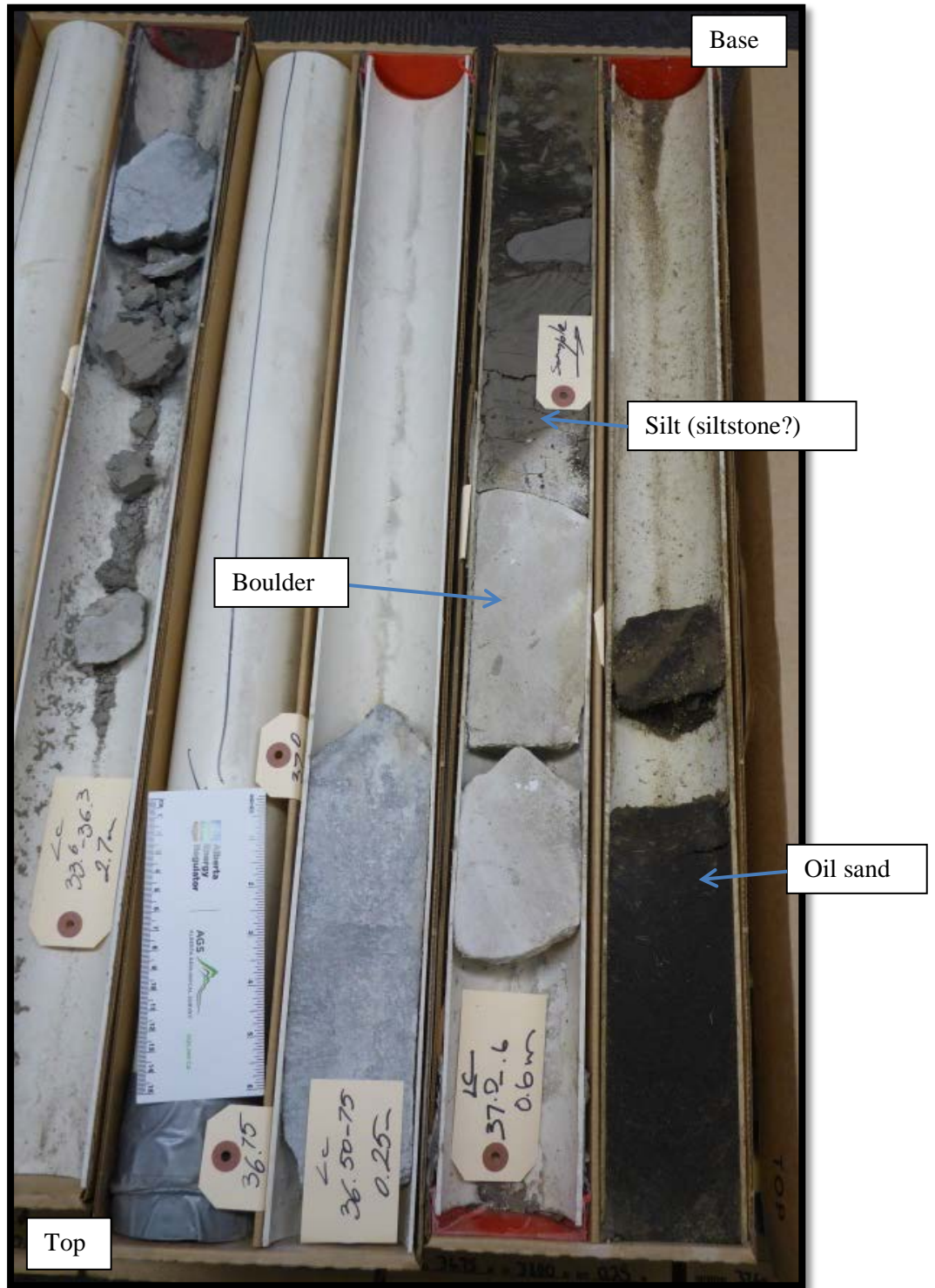


Figure 140. Photograph of core interval from well SUNCOR AUDET 9-15-98-6W4 (36.75–38.5 m depth, 322.85–321.1 m asl) showing boulders in till, with sharp contact to oil sand (light grey blebs within oil sand are siltstone rafts). Core boxes are 0.9 m long.

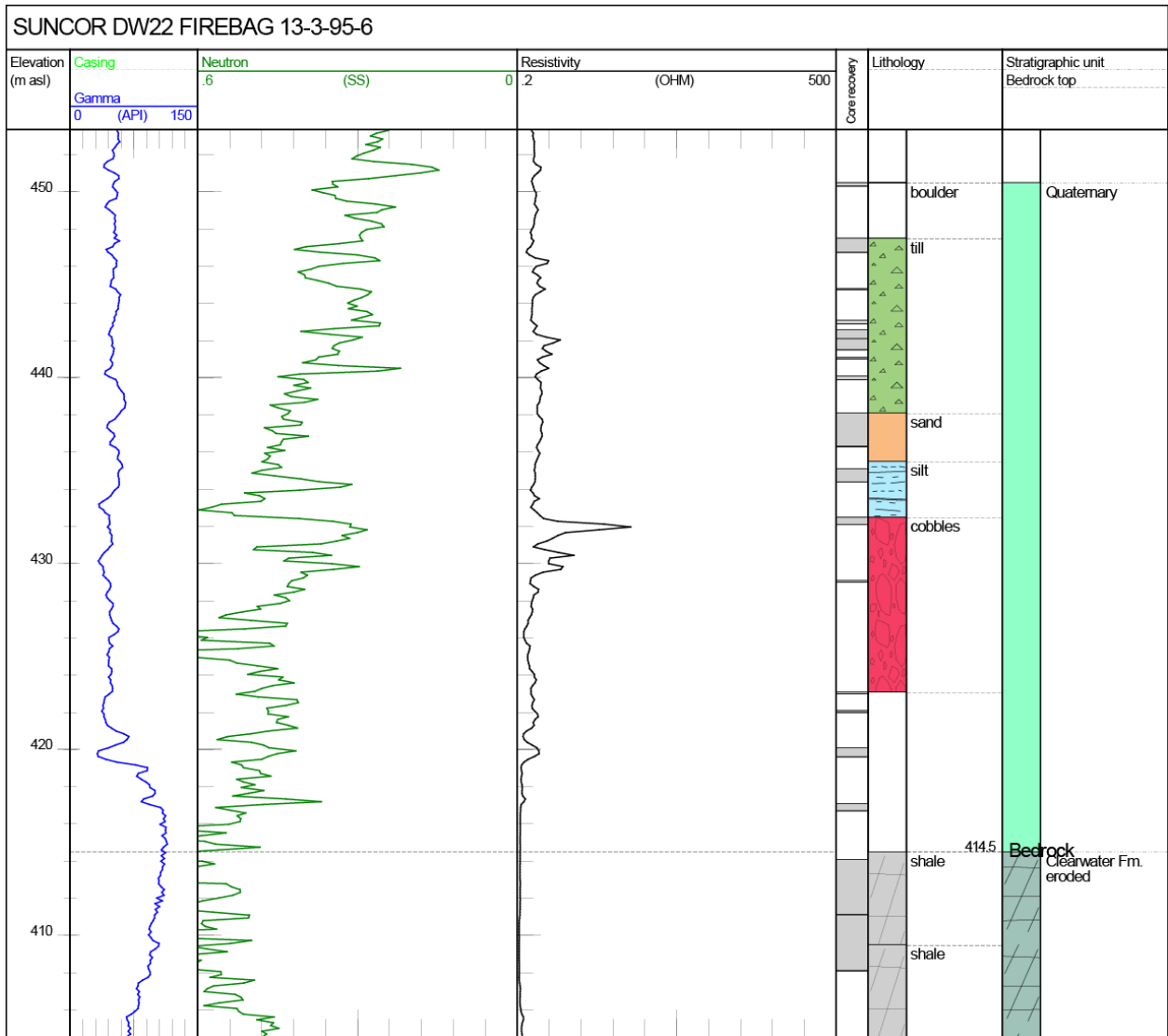


Figure 141. Logs for well SUNCOR DW22 FIREBAG 13-3-95-6W4. Litholog determined from examination of core. Poor recovery above reported bedrock top. Kelly bushing at 595.5 m asl and total depth at 131.5 m asl. Abbreviations: Gamma, gamma ray; Neutron, neutron porosity; OHM, ohm•m; SS, sandstone units.



Figure 142. Photograph of core interval from well SUNCOR DW22 FIREBAG 13-3-95-6W4 (153–154 m depth, 442.5–441.5 m asl) showing till. Core boxes are 0.9 m long.

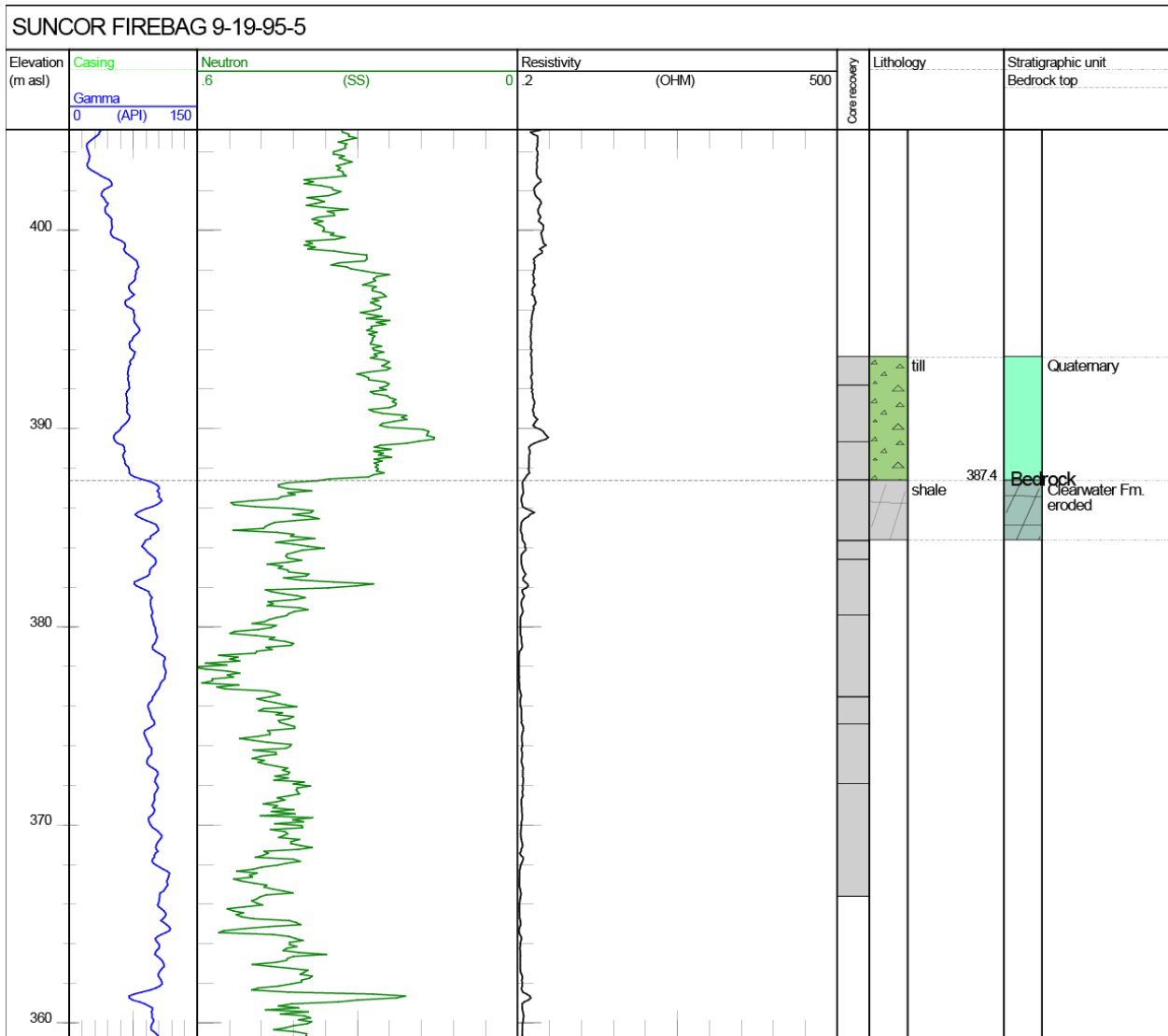


Figure 143. Logs for well SUNCOR FIREBAG 9-19-95-5W4. Litholog determined from examination of core. Kelly bushing at 589.4 m asl and total depth at 260.9 m asl. Abbreviations: Gamma, gamma ray; Neutron, neutron porosity; OHM, ohm·m; SS, sandstone units.

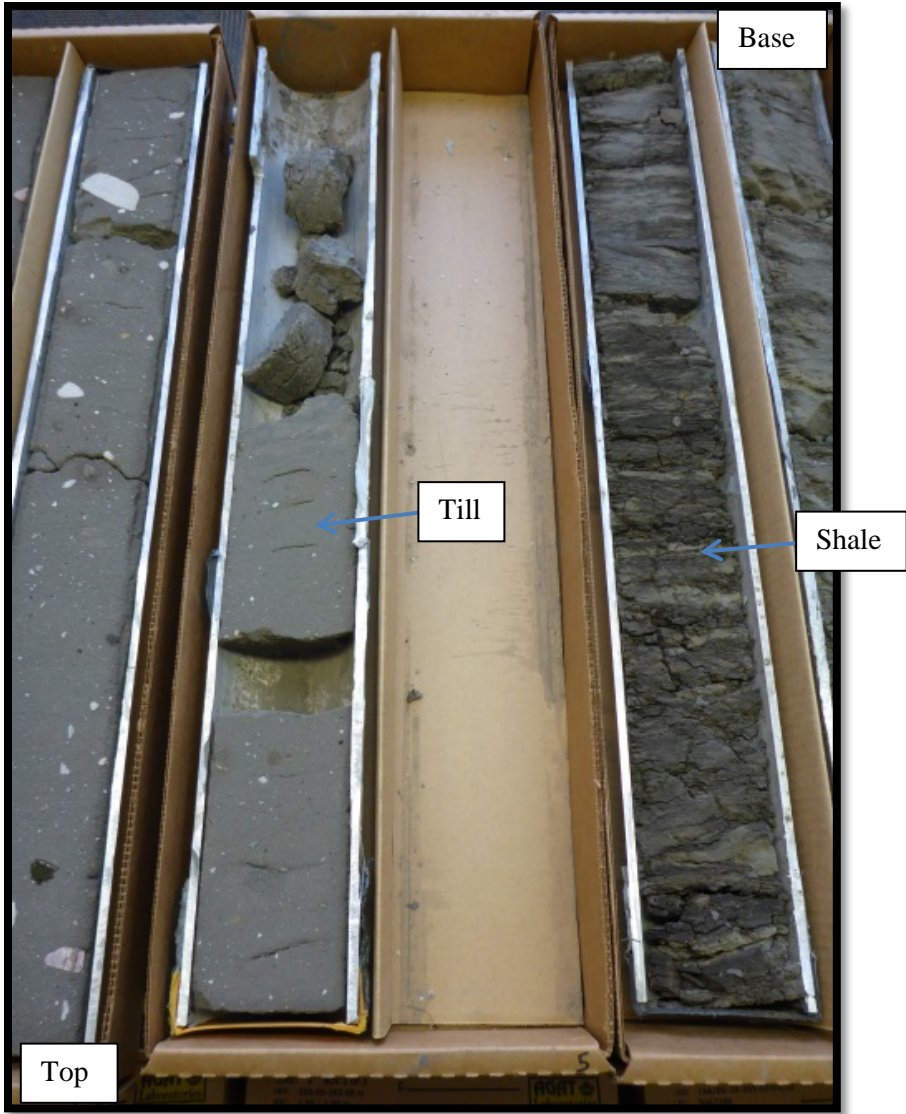


Figure 144. Photograph of core interval from well SUNCOR FIREBAG 9-19-95-5W4 (199–203 m depth, 390.4–386.4 m asl) showing till overlying bedrock. Core boxes are 0.9 m long.

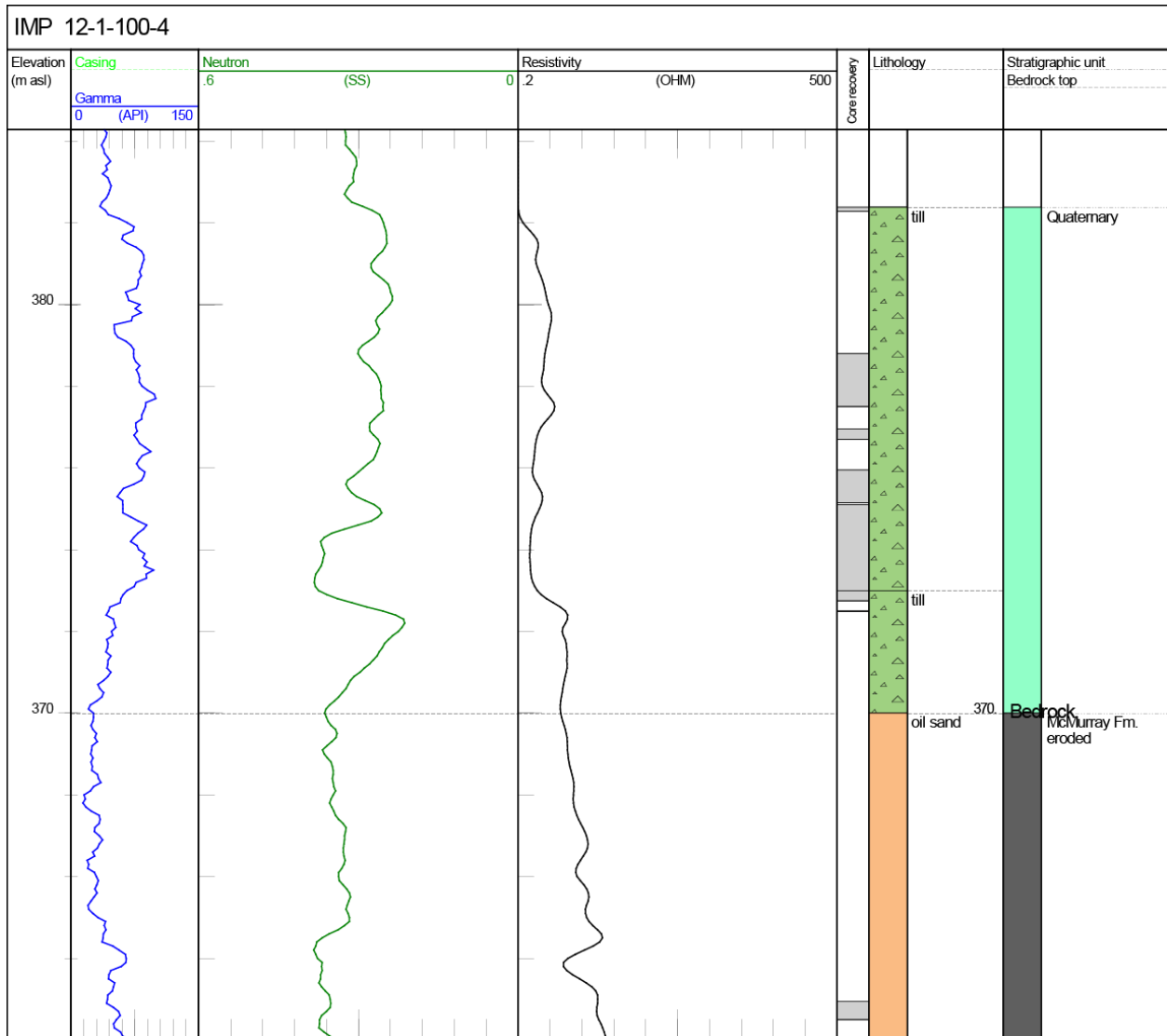


Figure 145. Logs for well IMP 12-1-100-4W4. Litholog determined from examination of core. Poor core recovery at bedrock top. Kelly bushing at 404.5 m asl and total depth at 320.5 m asl. Abbreviations: Gamma, gamma ray; Neutron, neutron porosity; OHM, ohm•m; SS, sandstone units.

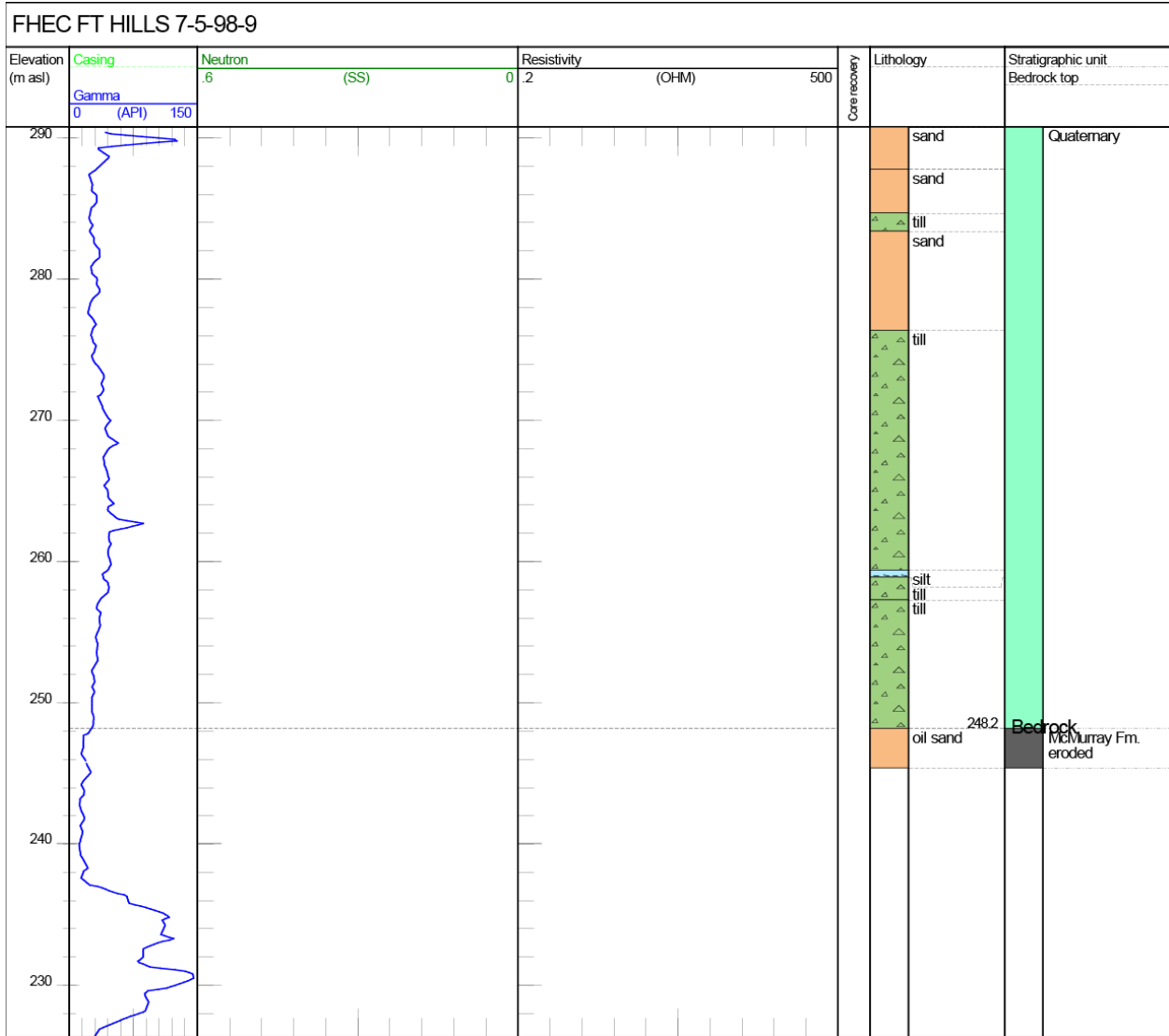


Figure 146. Logs for well FHEC FT HILLS 7-5-98-9W4. Litholog determined from examination of core. Neutron and resistivity data unavailable. Kelly bushing at 295.4 m asl and total depth at 195.1 m asl. Abbreviations: Gamma, gamma ray; Neutron, neutron porosity; OHM, ohm·m; SS, sandstone units.

Table 6. Examined cores that did not contain Quaternary sediments.

Corehole	Kelly Bushing (m asl)	Total Depth (m asl)	Comments
TLK 10-12-96-4W4	493.4	284.4	No Quaternary in core
SUNCOR AUDET 9-8-98-6W4	352.7	284.9	No Quaternary in core
SUNCOR AUDET 12-15-98-6W4	346.5	269.7	No Quaternary in core
SYNENCO 05-240 FIREBAG 12-10-99-6W4	300.0	253.4	No Quaternary in core
SYNENCO 20-33 FIREBAG 9-11-99-6W4	314.1	213.4	No Quaternary in core
SUNCOR AUDET 1-16-98-6W4	352.7	231.6	No Quaternary in core
IMP 2-10-100-4W4	356.1	306.2	Only oil sand in core
IMP 1024332 FIREBAG 10-14-99-4W4	395.4	305.7	Only bedrock in core
SILVERBIRCH 2-15-100-11W4	322.6	202.6	See Figure 46
SUNCOR FIREBAG 10-23-93-5W4	639.2	293.7	See Figure 52

Quaternary Sediments Examined in Drill Cuttings

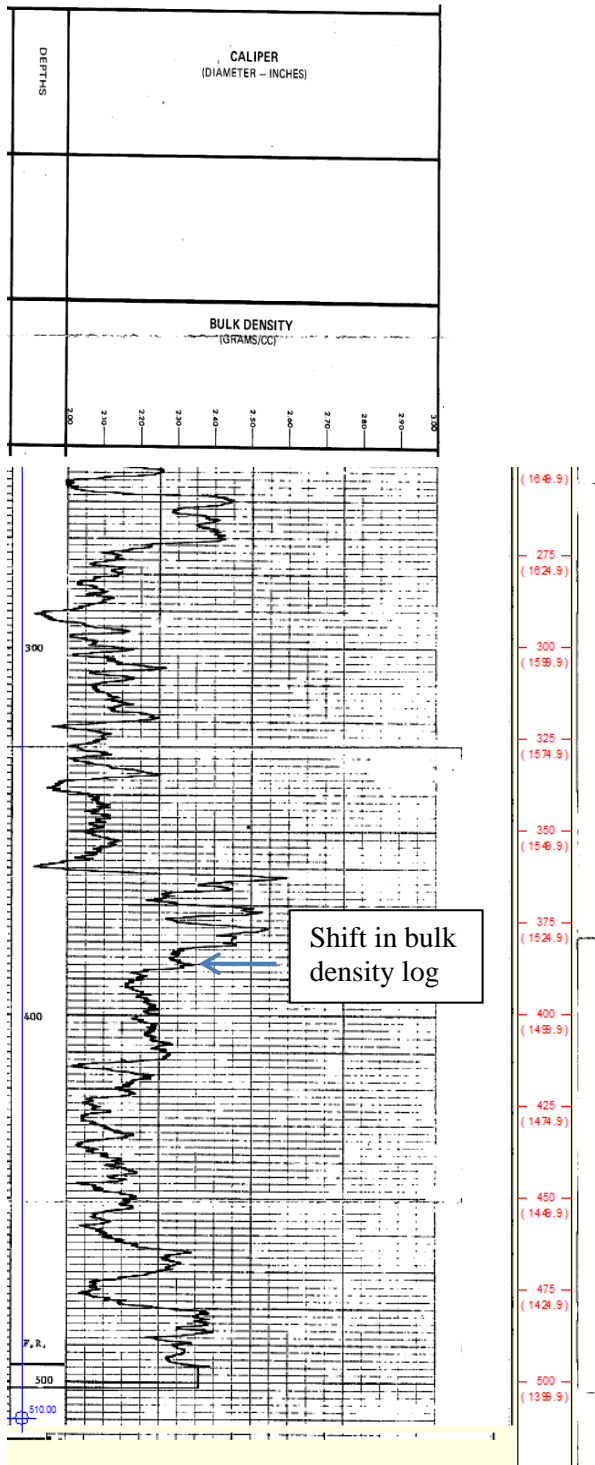


Figure 147. Portion of log at bedrock contact in well SHELL 16 ATHAE OV 10-16-98-2W4. Shift in bulk density log at 109.7–115.8 m asl (360–380 ft.), corresponds with a change from light to dark grains in the drill cuttings (Figure 148). Kelly bushing at 579.1 m asl (1899.9 ft.) and total depth at 175.6 m asl (576.1 ft.). Depth in m asl shown in red on right-hand side.



Shift to dark material.

Figure 148. Drill cuttings from well SHELL 16 ATHAE OV 10-16-98-2W4. Note the shift from light to dark grains, which corresponds to the shift in the bulk density values in the geophysical log (Figure 147).

AA/13-11-099-01W4/0

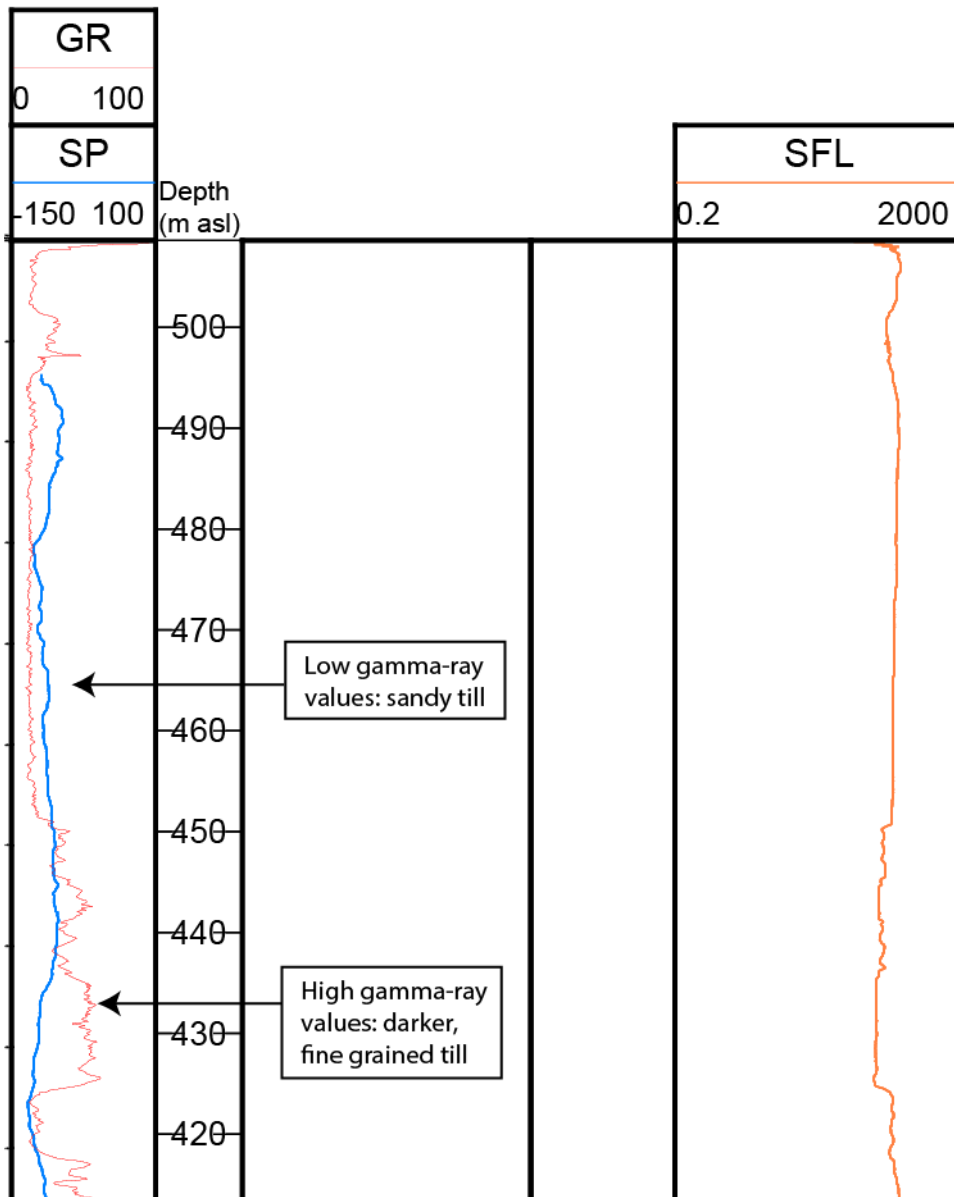
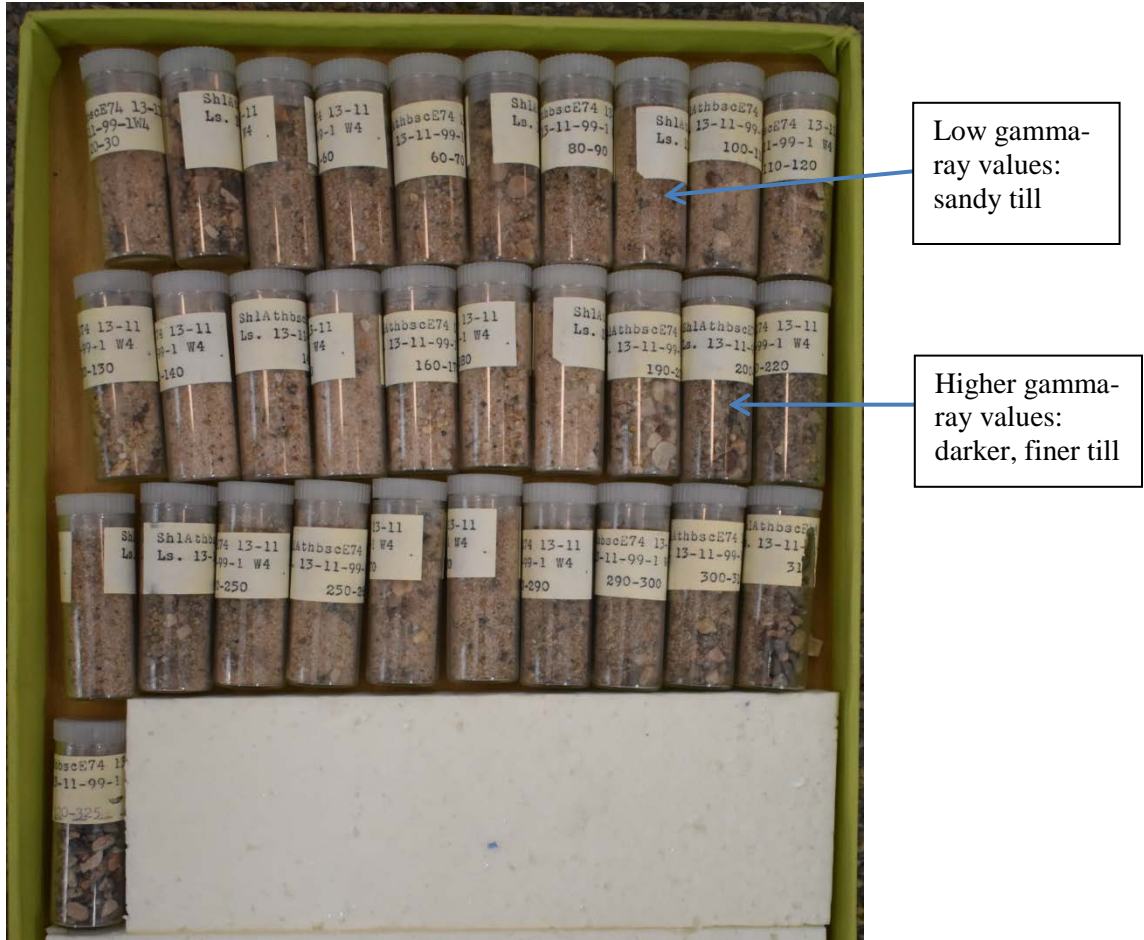


Figure 149. Portion of logs at bedrock contact in well SHELL 19 ATHAE OV 13-11-99-1W4. Shift in the gamma-ray log occurs at 61.0 m asl (200 ft. asl) and corresponds to a change to darker and apparently finer material. Kelly bushing at 510.5 m asl (1674.9 ft.) and total depth at 99.1 m asl (325.1 ft.). Abbreviations: GR, gamma ray in API units; SFL, spherically focused resistivity in ohm·m; SP, spontaneous potential in mV.



Low gamma-ray values:
sandy till

Higher gamma-ray values:
darker, finer till

Figure 150. Drill cuttings from well SHELL 19 ATHAE OV 13-11-99-1W4. Note the shift to darker and finer grains. This shift corresponds to a shift to higher gamma-ray values in the log (Figure 149), which is inferred to relate to finer grained material.

AA/02-03-099-01W4/0

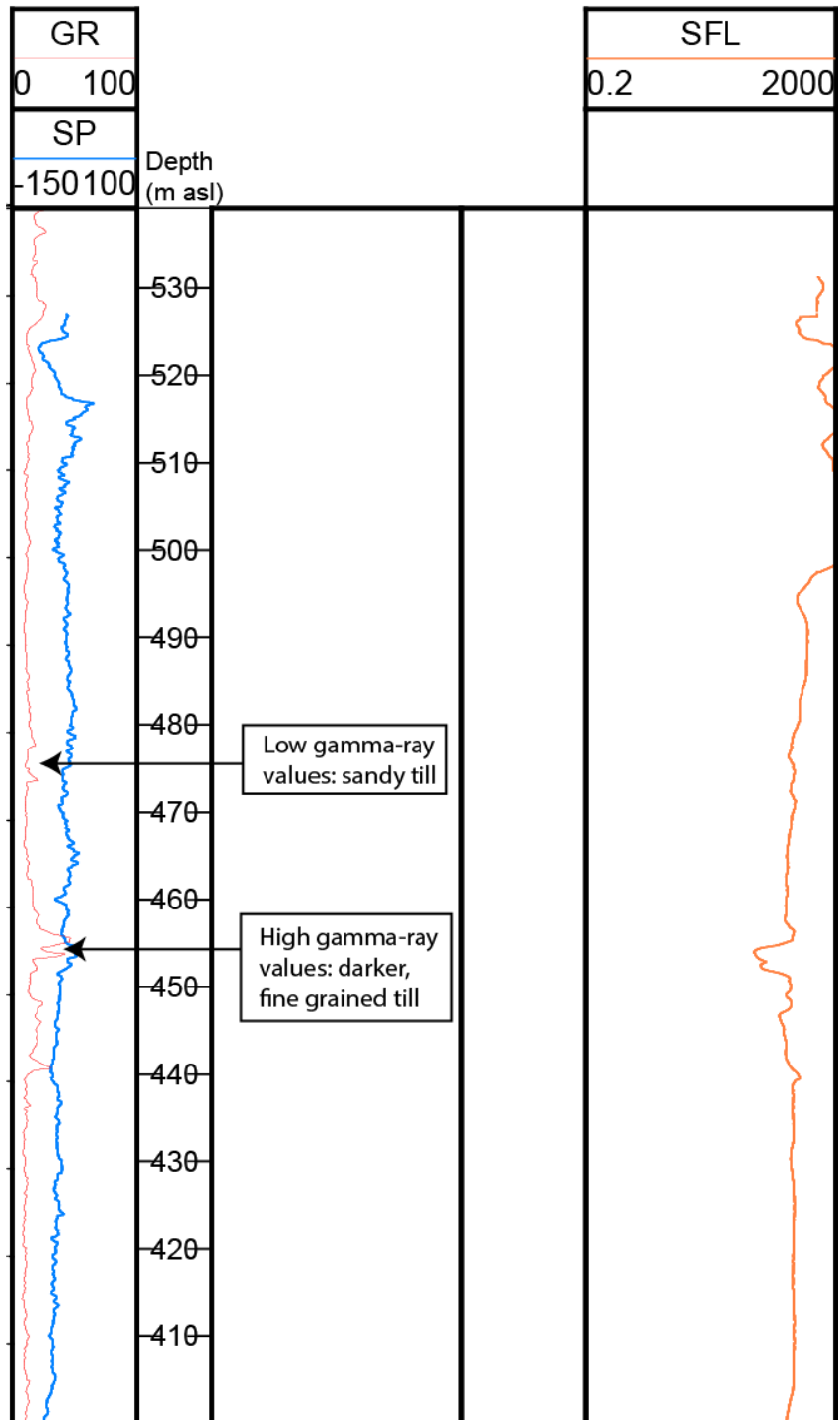


Figure 151. Portion of logs from well SHELL 18 ATHAE OV 2-3-99-1W4. The materials interpreted from the logs correspond to the materials in the drill cuttings (Figure 152). Kelly bushing at 541.0 m asl (1774.9 ft.) and total depth at 143.9 m asl (472.1 ft.). Abbreviations: GR, gamma ray in API units; SFL, spherically focused resistivity in ohm*m; SP, spontaneous potential in mV.



Figure 152. Drill cuttings from well SHELL 18 ATHAE OV 2-3-99-1W4. Note shift to darker and finer grains. This shift corresponds to a shift to higher gamma-ray values in the log (Figure 151), which is inferred to relate to finer grained material.

AA/01-13-098-01W4/0

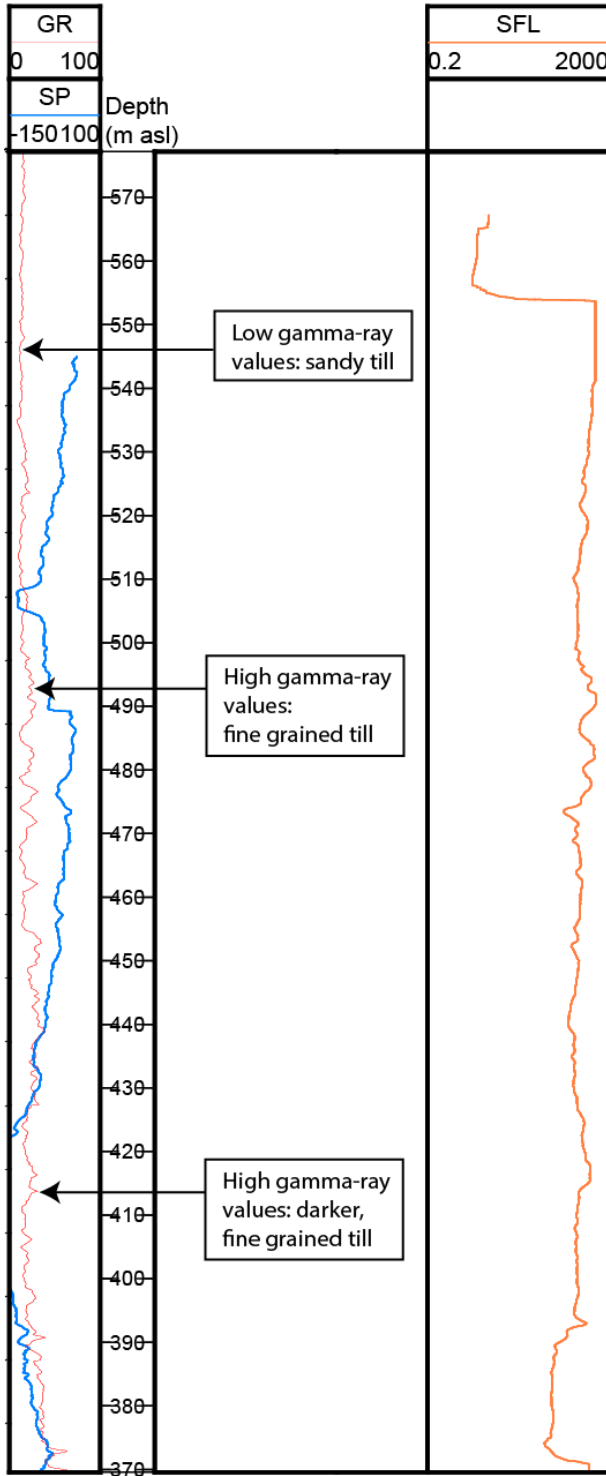


Figure 153. Portion of logs from well SHELL 15 ATHAE OV 1-13-98-1W4. The materials interpreted from the logs correspond to the materials in the drill cuttings (Figure 152). Kelly bushing at 579.1 m asl (1899.9 ft.) and total depth at 211.2 m asl (692.9 ft.). Abbreviations: GR, gamma ray in API units; SFL, spherically focused resistivity in ohm•m; SP, spontaneous potential in mV.



Figure 154. Drill cuttings from well SHELL 15 ATHAE OV 1-13-98-1W4. Note differing till types, which are interpreted to correspond to shifts on geophysical logs (Figure 153).